University of Alberta

Uncertainty Quantification of Dynamical Systems and Stochastic Symplectic Schemes

By

Jian Deng

A thesis submitted in partial fulfillment of the

requirements for the degree of

Doctor of Philosophy

in

Applied Mathematics

Department of Mathematical and Statistical Sciences

Spring 2013

Edmonton, Alberta

Abstract

It has been known that for some physical problems, a small change in the system parameters or in the initial/boundary conditions could leas to a significant change in the system response. Hence, it is of importance to investigate the impact of uncertainty on dynamical system in order to fully understand the system behavior. In this thesis, numerical methods used to simulate the effect of random/stochastic perturbation on dynamical systems are studied. In the first part of this thesis, an aeroelastic system model representing an oscillating airfoil in pitch and plunge with random variations in the flow speed, the structural stiffness terms and initial conditions are concerned. Two approaches, stochastic normal form and stochastic collocation method, are proposed to investigate the Hopf bifurcation and the secondary bifurcation behavior, respectively. Stochastic normal form allows us to study analytically the Hopf bifurcation scenario and to predict the amplitude and frequency of the limit cycle oscillation; while numerical simulations demonstrate the effectiveness of stochastic collocation method for long term computation and discontinuous problems. In the second part of this work, we focus the construction of efficient and robust computational schemes for stochastic system, and the stochastic symplectic schemes for stochastic Hamiltonian system are developed. A systematic procedure to construct symplectic numerical schemes for stochastic Hamiltonian systems is presented. The approach is an extension to the stochastic case of the methods based on generating functions. The idea is also extended to the symplectic weak scheme construction. Theoretical analysis of the convergence is reported for strong/weak symplectic integrators. The numerical simulations are carried out to confirm that the symplectic methods are efficient computational tools for long-term behaviors. Moreover, the coefficients of the generating function are invariant under permutations for the stochastic Hamiltonian system preserving Hamiltonian functions. As a consequence the high-order symplectic weak and strong methods have

simpler forms than the Taylor expansion schemes with the same order.

Acknowledgements

I am deeply indebted and appreciate to my supervisors Professor Yau Shu Wong and Professor Christina Adela Anton, for their excellent guidance and great encouragement and generous support during my study at Edmonton.

I am truly grateful to Department of Mathematical & Statistical Sciences, University of Alberta for its support through my doctor program.

I would like to thank many of my friends in Edmonton for their enthusiastic help on my study and living in Edmonton. I also want to thank my officemates, Menglu Che, for the many happy conversations and laughter we had.

Finally, I am greatly indebted to my parents. Without their constant and selfless love and support, I could not have the opportunity to have and enjoy such joyous and great life in Canada.

List of Tables

List of Figures

Notation and Symbols

a_h	non-dimensional distance from airfoil mid-chord to elastic axis
b	airfoil semi-chord
C_L	aerodynamic lift coefficient
C_M	pitching moment coefficient
c	chord
h	plunge displacement
m	airfoil mass
r_α	radius of gyration about the elastic axis
τ	time
U	free stream velocity
U^*	non-dimensional flow velocity ($= U/b\omega_\alpha$)
U_L^*	non-dimensional linear flutter speed
x_α	non-dimensional distance from elastic axis to center of mass
α	pitch angle
ε_1, ε_2	constants in Wagner's function
μ	airfoil-air mass ratio ($= m/\pi\rho b^2$)
ρ	density
τ	non-dimensional time ($= Ut/b$)
ω_α	natural frequencies of the uncoupled pitching modes
ω_ς	natural frequencies of the uncoupled plunging modes
$\tilde{\omega}$	frequency ratio ($= \omega_\varsigma/\omega_\alpha$)
ψ_1, ψ_2	constants in Wagner's function
ς,	non-dimensional displacement of the elastic axis
ζ_α	viscous pitch damping ratio
ζ_ς	viscous plunge damping ratio

$E[\cdot]$	expected value
$P(\cdot)$	probability

Abbreviation

UQ	uncertainty quantification
LCO	limit cycle oscillations
SHS	stochastic Hamiltonian system
DOF	degree-of-freedom
MCS	Monte Carlo simulations

Contents

Chapter 1

Introduction

A purpose of mathematical models is to describe and predict the future behaviors of physical systems. Although differential equations have been successfully used to explain and predict the responses of physical events, the accuracy of the predictions usually relies on the mathematical model, and correct estimation or the measurement of the values of system parameters, initial values or boundary conditions.

In recent years, there is a growing interest in the study of uncertainty quantification (UQ). The goal of UQ is to investigate the impact due to uncertainty in data or in the mathematical model, so that we could perform a more reliable prediction for the real physical problems.

The first part of my Ph.D work is concerned with the UQ of aeroelastic dynamical systems, which is a continuation of my master research program [6]. Unlike a deterministic model in which the governing mathematical formulation is given by a system of nonlinear differential equations, the present aeroelastic model is represented by nonlinear differential equations with random parameters, i.e., random differential equations.

Several UQ aeroelastic investigations focusing on limit cycle oscillations (LCO) and the bifurcation analysis are reported, such as Monte Carlo simulations (MCS) [15, 14, 4], polynomial chaos expansions [25, 5, 18, 17], perturbation techniques [11, 13] and so on. In the present study, two new approaches based on the stochastic normal form and stochastic collocation methods are proposed to analyze the effect of parameters uncertainty on the Hopf and secondary bifurcation, respectively [8, 9, 2].

In the second part of my thesis, I develop serval efficient and reliable numerical

methods for stochastic Hamiltonian systems. At present, Hamiltonian systems are already widely used in many diverse fields of applied and pure mathematics such as the optimal control, elasticity, KAM theory, quantum mechanics, etc. Hence it is of importance to derive efficient and reliable computational methods for solving Hamiltonian systems numerically.

After the initial work of Hamilton, which was developed further by Jacobi, the most significant progress of Hamiltonian formalism was made by Poincaré, resulting in symplectic geometry, which has become the natural language for the Hamiltonian system. Since the symplecticity is a characteristic property of Hamiltonian systems, it is desirable that numerical methods should preserve this property as much as possible. A natural way to achieve this is to work out numerical methods that share these property, so called the symplectic integration. The pioneering work on the symplectic integration is due to de Vogelaere [23], Ruth [22] and Feng [10]. The approach turned out to be fruitful and successful. Many simulations and applications show the significant advantage of the symplectic integration on accuracy of long time computation. Symplectic integration is one of the most important subjects in computational mathematics and scientific computing.

Inspired by the idea of the symplecticity invariance, Milstein et al. [21] [20] proposed symplectic numerical scheme to the stochastic Hamiltonian system (SHS). Since then, there is growing interesting and effort on the theoretical and numerical studies on special stochastic hamiltonian systems [12], [16]. The variational integrator method proposed by Wang et al. [24] is to construct the symplectic scheme on SHS. But the systematic research on stochastic symplectic methods is still rare and the construction of high order symplectic method is an open problem. In our research [7], we employ the properties of multiple stochastic integrals to derive a recursive formula for determining the coefficients of the generating function. Theoretically, this formula allows us to derive stochastic sympletic schemes of any order with corresponding conditions on the Hamiltonian functions. It is a non-trivial extension of the methods based on generating

functions from deterministic Hamiltonian systems to stochastic setting. Hence, the major contribution of our work is to present a framework to construct different types of stochastic symplectic schemes of any order.

Moreover, we extend the results to the symplectic weak schemes (in the sense of the convergence of expectation) by using the relation of Stratonovich multiple integrals and Ito multiple integrals [3]. So we are able to construct the second order weak stoachstic symplectic scheme for the general SHSs, which answers the open problem proposed by Milstein. et al [19].

Using the method based on generating functions, we construct computationally attractive high order symplectic schemes [1] for a special type of SHS preserving the hamiltonian functions. The developed symplectic schemes are efficient compared with the Taylor-Stratonovich expansion type scheme, because the laborious approximation of the multiple stochastic integrals is not required for the proposed high order symplectic scheme. Moreover, it only requires one random variable for each Brownian motion at each time step. Hence it provides subtantial saving in the computational time used to generate the quasi-random numbers.

This thesis is organized as follows. We first provide introduction about an aeroelastic system representing an oscillating airfoil in pitch and plunge in Chapter 2. The implementation of stochastic normal form and stochastic collocation method on aeroelastic system will be discussed in Chapter 3 and 4, respectively. Then, we will focus on the stochastic symplectic schemes. The definition of SHS and the construction of the strong symplectic schemes will be covered in Chapter 5. Chapter 6 presents the construction of weak stochastic symplectic schemes. The symplectic schemes for SHS preserving Hamiltonian functions are reported in Chapter 7. Finally, conclusions will be presented in Chapter 8.

It is worth noting that the works presented in Chapter 3 – 7 have been accepted/submitted for referred jounral publications. In particular,

Chapter 3 appeared as *Hopf bifurcation analysis of an aeroelastic model using*

stochastic normal form in *Journal of Sound and Vibration* in 2011.

Chapter 4 appeared as *Stochastic collocation method for secondary bifurcation of a nonlinear aeroelastic system* in *Journal of Sound and Vibration* in 2010.

Chapter 5 was submitted as *High-order symplectic schemes for stochastic Hamiltonian systems* to *Communications in Computational Physics* in 2012.

Chapter 6 was submitted as *Weak symplectic schemes for stochastic Hamiltonian equations* to *Journal of Computational and Applied Mathematics* in 2012.

Chapter 7 was submmited as *Symplectic numerical schemes for stochastic systems preserving Hamiltonian functions* to *International Journal of Numerical Analysis & Modeling* in 2012.

Bibliography

[1] C. Anton, J. Deng, and Y. S. Wong. Symplectic numerical schemes for stochastic systems preserving hamiltonian functions. *Submitted to International Journal of Numerical Analysis & Modeling*, 2012.

[2] C. Anton, J. Deng, and Y.S. Wong. Hopf bifurcation analysis of an aeroelastic model using stochastic normal form. *Journal of Sound and Vibration*, 331:3866 – 3886.

[3] C. Anton, J. Deng, and Y.S. Wong. Weak symplectic schemes for stochastic hamiltonian equations. *Submitted to Journal of Computational and Applied Mathematics.*

[4] P. J. Attar and E.H. Dowell. A stochastic analysis of the limit cycle behaviour of a nonlinear aeroelastic model using the response surface method. In *Proceedings of the 46th AIAA/ ASME/ ASCE/ AHS/ ASC/ Structures, Structural Dynamics, and Materials Conference*, 2005. AIAA Paper 2005-1986.

[5] P.S. Beran, C.L. Pettit, and D.R. Millman. Uncertainty quantification of limit-cycle oscillations. *Journal of Computational Physics*, 217:217–247, 2006.

[6] J. Deng. Stochastic collocation methods for aeroelastic system with uncertainty. Master's thesis, University of Alberta, Edmonton, AB,Canada, 2009.

[7] J. Deng, C. Anton, and Y.S. Wong. High-order symplectic schemes for stochastic hamiltonian systems. *Submitted to Communications in Computational Physics*.

[8] J. Deng, C. A. Popescu, and Y. S. Wong. Application of the stochastic normal form for a nonlinear aeroelastic model. In *Proceedings of the 52nd AIAA/ ASME/ ASCE/ AHS/ ASC/ Structures, Structural Dynamics, and Materials Conference*, Denver, U.S., 2011. 42-58.

[9] J. Deng, C. A. Popescu, and Y. S. Wong. Stochastic collocation method for secondary bifurcation of a nonlinear aeroelastic system. *Journal of Sound and Vibration*, 330:3006–3023, 2011.

[10] K. Feng. On difference schemes and symplectic geometry. In *Proceedings of the 5-th Intern. Symposium on differential geometry & differential equations*, Beijing, China, 1985. 42-58.

[11] M. Ghommem, M.R. Hajj, and A.H. Nayfeh. Uncertainty analysis near bifurcation of an aeroelastic ystem. *Journal of Sound and Vibrations*, 329:3335–3347, 2010.

[12] J. Hong, R. Scherer, and L. Wang. Predictorcorrector methods for a linear stochastic oscillator with additive noise. *Mathematical and Computer Modelling*, 46(5–6):738–764, 2007.

[13] D.G Liaw and H.T.Y. Yang. Reliality and nonlinear supesonic flutter of uncertain laminated plates. *AIAA Journal*, 31(12):2304–2311, 1993.

[14] N. Lindsley and P. Beran. Increased efficiency in the stochastic interrogation of an uncertain nonlinear aeroelastic system. In *Proceedings of the International on Aeroelasticity and Structural Dynamics*, Munich, Germany, 2005. IF-055.

[15] N. Lindsley, P. Beran, and C. Pettit. Effects of uncertainty on nonlinear plate aeroelastic response. 2002. AIAA paper AIAA-2002-1271.

[16] A.H.S. Melbo and D.J. Higham. Numerical simulation of a linear stochastic oscillator with additive noise. *Applied Numerical Mathematics*, 51(1):89–99, 2004.

[17] D.R. Millman, P.I. King, and P.S. Beran. Airfoil pitch-and-plunge bifurcation behavior with Fourier chaos expansions. *Journal of Aircraft*, 42(2):376–384, 2005.

[18] D.R. Millman, P.I. King, R.C. Maple, P.S. Beran, and L.K. Chilton. Uncertainty quantification with B-spline stochastic projection. *AIAA Journal*, 44(8):1845–1853, 2006.

[19] G. N. Milstein and M. V. Tretyakov. Quasi-symplectic methods for langevin-type equations. *IMA Journal of Numerical Analysis*, (23):593–626, 2003.

[20] G. N. Milstein, M. V. Tretyakov, and Y. M. Repin. Numerical methods for stochastic systems preserving symplectic structure. *SIAM Journal on Numerical Analysis*, 40:1583–1604, 2002.

[21] G. N. Milstein, M. V. Tretyakov, and Y. M. Repin. Symplectic integration of hamiltonian systems with additive noise. *SIAM Journal on Numerical Analysis*, 39:2066–2088, 2002.

[22] R.D. Ruth. A canonical integration technique. *IEEE Trans. Nuclear Science*, (30):2669–2671, 1983.

[23] R. de Vogelaere. Methods of integration which preserve the contact transformation property of the hamiltonian equations. Technical report, Report No. 4, Dept. Math., Univ. of Notre Dame, Notre Dame, Ind., 1956.

[24] L. Wang, J. Hong, R. Scherer, and F. Bai. Dynamics and variational integrators of stochastic hamiltonian systems. *International Journal of Numerical Analysis & Modeling*, 6(4):586–602, 2009.

[25] J. A. S. Witteveen and H. Bijl. Higher periodic stochastic bifurcation of nonlinear airfoil fluid-structure interaction. *Mathematical Problems in Engineering*, pages 1–26, 2009. Article ID 394387.

Part I

Uncertainty Quantification of Aeroelastic System

Chapter 2

Introduction to Aeroelastic Dynamical System

Nonlinear airfoil flutter is one of the important topics encountered in aerospace engineering. It is well-known that assuming a linear model for the structural components of the aircraft, will produce an inaccurate prediction for aging aircrafts and combat aircrafts that carry heavy external stores [3, 1]. In an aeroelastic system, structural nonlinearities arises from worn hinges or control surfaces. It has been reported that for some systems, small perturbations in the initial conditions and/or the system parameters could lead to significant changes in the nonlinear response [3]. Hence, in addition to studying the deterministic model, it is desirable to carry out an investigation that takes into account the effects due to uncertainty.

2.1 Mathematical model

The two-degree-of-freedom (DOF) dynamic model (see Fig. 1) simulating an airfoil oscillating in pitch and plunge can be expressed as a coupled system of two second-order nonlinear integro-differential equations, and the detail description can be found in [3]:

$$\begin{aligned} &\varsigma'' + x_\alpha \alpha'' + 2\zeta_\varsigma \frac{\tilde{\omega}}{U^*}\varsigma' + \left(\frac{\tilde{\omega}}{U^*}\right)^2 G(\varsigma) = -\frac{1}{\pi\mu}C_L(\tau) \\ &\frac{x_\alpha}{r_\alpha^2}\varsigma'' + \alpha'' + 2\frac{\zeta_\alpha}{U^*}\alpha' + \frac{1}{U^{*2}}M(\alpha) = \frac{2}{\pi\mu r_\alpha^2}C_M(\tau). \end{aligned} \tag{2.1}$$

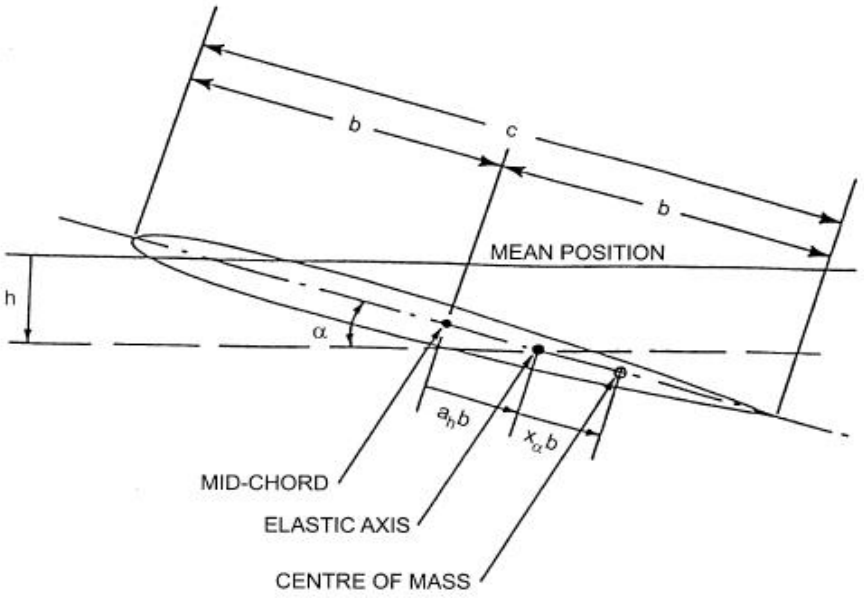

Figure 1: Two-degree-of-freedom airfoil motion

Here $\varsigma = h/b$ is the non-dimensional displacement of the elastic axis, $U^* = U/(b\omega_\alpha)$ is a non-dimensional velocity, ' denotes differentiation with respect to the non-dimensional time $\tau = Ut/b$, $\tilde{\omega} = \omega_\varsigma/\omega_\alpha$ is the ratio of the natural frequencies, r_α is the radius of gyration about the elastic axis, and ζ_ς, ζ_α are the damping ratios. $G(\varsigma)$ and $M(\alpha)$ are the nonlinear plunge and pitch stiffness terms, respectively, and the lift and pitching moment coefficients are denoted by $C_L(\tau)$ and $C_M(\tau)$. For subsonic flow, they are expressed as:

$$\begin{aligned} C_L(\tau) =& \pi(\varsigma'' - a_h\alpha'' + \alpha') + 2\pi\{\alpha(0) + \varsigma'(0) + [\frac{1}{2} - a_h]\alpha'(0)\}\phi(\tau) \\ &+ 2\pi\int_0^\tau \phi(\tau-\sigma)[\alpha'(\sigma) + \varsigma''(\sigma) + (\frac{1}{2} - a_h)\alpha''(\sigma)]\mathrm{d}\sigma, \end{aligned} \tag{2.2}$$

$$\begin{aligned} C_M(\tau) =& \pi(\frac{1}{2} + a_h)\{\alpha(0) + \varsigma'(0) + [\frac{1}{2} - a_h]\alpha'(0)\}\phi(\tau) \\ &+ \pi(\frac{1}{2} + a_h)\int_0^\tau \phi(\tau-\sigma)[\alpha'(\sigma) + \varsigma''(\sigma) + (\frac{1}{2} - a_h)\alpha''(\sigma)]\mathrm{d}\sigma \\ &+ \frac{\pi}{2}a_h(\varsigma'' - a_h\alpha'') - (\frac{1}{2} - a_h)\frac{\pi}{2}\alpha' - \frac{\pi}{16}\alpha'' \end{aligned} \tag{2.3}$$

where the Wagner function $\phi(\tau)$ is given by

$$\phi(\tau) = 1 - \psi_1 e^{-\varepsilon_1 \tau} - \psi_2 e^{-\varepsilon_2 \tau} \tag{2.4}$$

and the constants are $\psi_1 = 0.165$, $\psi_2 = 0.335$, $\varepsilon_1 = 0.0455$ and $\varepsilon_2 = 0.3$.

By introducing four new variables w_1, w_2, w_3, w_4:

$$w_1(\tau) = \int_0^\tau e^{-\varepsilon_1(\tau-\sigma)}\alpha(\sigma)\mathrm{d}\sigma$$

$$w_2(\tau) = \int_0^\tau e^{-\varepsilon_2(\tau-\sigma)}\alpha(\sigma)\mathrm{d}\sigma$$

$$w_3(\tau) = \int_0^\tau e^{-\varepsilon_1(\tau-\sigma)}\varsigma(\sigma)\mathrm{d}\sigma$$

$$w_4(\tau) = \int_0^\tau e^{-\varepsilon_2(\tau-\sigma)}\varsigma(\sigma)\mathrm{d}\sigma,$$

(2.1) can be rewritten as:

$$\begin{aligned}
&c_0\varsigma'' + c_1\alpha'' + c_2\varsigma' + c_3\alpha' + c_4\eta + c_5\alpha + c_6 w_1 + c_7 w_2 + c_8 w_3 + c_9 w_4 \\
&+ (\frac{\tilde{\omega}}{U^*})^2 G(\varsigma) = f(\tau) \\
&d_0\varsigma'' + d_1\alpha'' + d_2\varsigma' + d_3\alpha' + d_4\eta + d_5\alpha + d_6 w_1 + d_7 w_2 + d_8 w_3 + d_9 w_4 \\
&+ (\frac{1}{U^*})^2 M(\alpha) = g(\tau).
\end{aligned} \tag{2.5}$$

The coefficients of Eq. (2.5) are as follows:

$$c_0 = 1 + \frac{1}{\mu}, \quad c_1 = x_\alpha - \frac{a_h}{\mu}, \quad c_2 = 2\zeta_\varsigma \frac{\tilde{\omega}}{U^*} + \frac{2}{\mu}(1 - \psi_1 - \psi_2),$$

$$c_3 = \frac{1 + (1 - 2a_h)(1 - \psi_1 - \psi_2)}{\mu}, \quad c_4 = \frac{2}{\mu}(\psi_1\varepsilon_1 + \psi_2\varepsilon_2),$$

$$c_5 = \frac{2}{\mu}[(1 - \psi_1 - \psi_2) + (1/2 - a_h)(\psi_1\varepsilon_1 + \psi_2\varepsilon_2)],$$

$$c_6 = \frac{2}{\mu}\psi_1\varepsilon_1[1-(1/2-a_h)\varepsilon_1], \quad c_7 = \frac{2}{\mu}\psi_2\varepsilon_2[1-(1/2-a_h)\varepsilon_2],$$

$$c_8 = -\frac{2}{\mu}\psi_1\varepsilon_1^2, \quad c_9 = -\frac{2}{\mu}\psi_2\varepsilon_2^2,$$

$$d_0 = \frac{x_\alpha}{r_\alpha^2} - \frac{a_h}{\mu r_\alpha^2}, \quad d_1 = 1 + \frac{1+8a_h^2}{8\mu r_\alpha^2},$$

$$d_2 = 2\frac{\zeta_\varsigma}{U^*} + \frac{1-2a_h}{2\mu r_\alpha^2} - \frac{(1+2a_h)(1-2a_h)(1-\psi_1-\psi_2)}{2\mu r_\alpha^2},$$

$$d_3 = -\frac{(1+2a_h)(1-\psi_1-\psi_2)}{\mu r_\alpha^2} - \frac{(1+2a_h)(1-2a_h)(\psi_1\varepsilon_1+\psi_2\varepsilon_2)}{2\mu r_\alpha^2},$$

$$d_4 = -\frac{(1+2a_h)(1-\psi_1-\psi_2)}{\mu r_\alpha^2}, \quad d_5 = \frac{(1+2a_h)(1-2a_h)(\psi_1\varepsilon_1+\psi_2\varepsilon_2)}{2\mu r_\alpha^2},$$

$$d_6 = -\frac{(1+2a_h)\psi_1\varepsilon_1[1-(1/2-a_h)\varepsilon_1]}{\mu r_\alpha^2} \quad d_7 = -\frac{(1+2a_h)\psi_2\varepsilon_2[1-(1/2-a_h)\varepsilon_2]}{\mu r_\alpha^2},$$

$$d_8 = -\frac{(1+2a_h)\psi_1\varepsilon_1^2}{\mu r_\alpha^2}, \quad d_9 = -\frac{(1+2a_h)\psi_2\varepsilon_2^2}{\mu r_\alpha^2},$$

where $M(\alpha)$ is the nonlinear pitch stiffness term, $G(\varsigma)$ is the plunge stiffness term. The forcing terms $f(\tau)$ and $g(\tau)$ are expressed as follows:

$$f(\tau) = \frac{2}{\mu}((\frac{1}{2}-a_h)\alpha(0)+\varsigma(0))(\psi_1\varepsilon_1 e^{-\varepsilon_1\tau} + \psi_2\varepsilon_2 e^{-\varepsilon_2\tau}),$$

$$g(\tau) = -\frac{(1+2a_h)f(\tau)}{2r_\alpha^2}.$$

When τ is sufficiently large, the steady-state solutions are obtained, $f(\tau)$ and $g(\tau)$ converges to zero. Hence, we suppose $f(\tau)$ and $g(\tau)$ are zero in our study. Let $x_1 =$

$\alpha, x_2 = \alpha', x_3 = \varsigma, x_4 = \varsigma', x_5 = w_1, x_6 = w_2, x_7 = w_3$, and $x_8 = w_4$, we can rewrite (2.5) as the following system of eight-order ODEs:

$$\begin{aligned}
x_1' &= x_2 \\
x_2' &= (c_0\mathbf{A} - d_0\mathbf{B})/(d_0c_1 - c_0d_1) \\
x_3' &= x_4 \\
x_4' &= (c_1\mathbf{A} + d_1\mathbf{B})/(d_0c_1 - c_0d_1) \\
x_5' &= x_1 - \epsilon_1 x_5 \\
x_6' &= x_1 - \epsilon_2 x_6 \\
x_7' &= x_3 - \epsilon_1 x_7 \\
x_8' &= x_3 - \epsilon_2 x_8,
\end{aligned} \tag{2.6}$$

where

$$\mathbf{A} = d_3x_1 + d_2x_2 + d_5x_3 + d_4x_4 + d_6x_5 + d_7x_6 + d_8x_7 + d_9x_8 + (\frac{1}{U^*})^2 M(x_1) - g(\tau),$$

$$\mathbf{B} = c_5x_1 + c_3x_2 + c_4x_3 + c_2x_4 + c_6x_5 + c_7x_6 + c_8x_7 + c_9x_8 + (\frac{\tilde{\omega}}{U^*})^2 G(x_3) - f(\tau).$$

In this study, we assume that the non-linear plunge and pitch stiffness terms are polynomial functions. However, other representations, such as freeplay and hysteresis models, can also be used for $M(x_1)$ and $G(x_3)$.

2.2 Dynamical behavior

If the pitch stiffness term $M(\alpha)$ is given by a cubic polynomial model $M(x_1) = x_1 + k_3x_1^3$ and the plunge stiffness term is linear $G(x_3) = x_3$, the aeroelastic system undergoes a Hopf-bifurcation at the $U^* = U_L^*$, where U_L^* is called the linear flutter speed. Here, positive values of k_3 yields a supercritical Hopf bifurcation (see Fig. 2(a)) for which a stable LCO exists for $U^* > U_L^*$; negative values yields a subcritical bifurcation (see Fig. 2(b)) leading to unstable LCO for $U^* < U_L^*$.

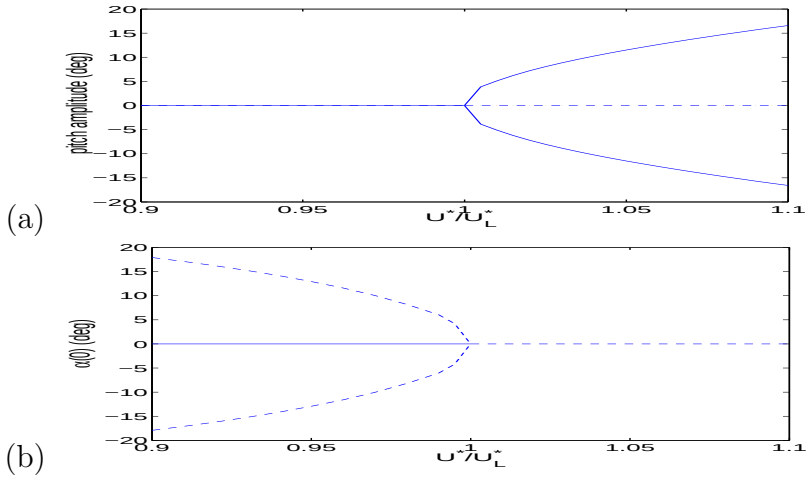

Figure 2: Hopf-bifurcation in the aeroelastic system: solid line: stable branch; dashed line: unstable branch; (a) supercritical bifurcation for $k_3 = 3$; (b) subcritical bifurcation for $k_3 = -3$

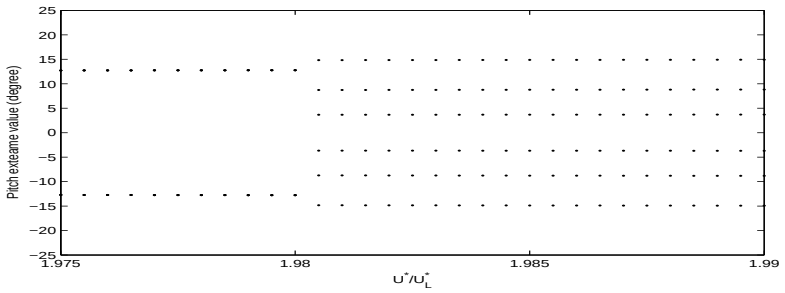

Figure 3: Secondary bifurcation in the aeroelastic system

When U^* increases further to about $2U_L^*$ and with a strong cubic nonlinearity for $k_3 > 0$, a jump phenomenon in the LCO amplitude and frequency is observed, and this is known as the secondary bifurcation (see Fig. 3). Lee et. al. [2] and Liu et. al. [4] investigated the aeroelastic behavior in the secondary bifurcation when the cubic nonlinearity in the pitch DOF is given by $M(x_1) = x_1 + k_3 x_1^3$ with $k_3 = 80$. They have noted that the flow velocity at which the secondary bifurcation occurs may depend on the initial conditions.

Bibliography

[1] C. M. Denegri Jr. Limit cycle oscillation flight test results of a fighter with external stores. *J. of Aircraft*, 37(5):761–769, 2000.

[2] B. H. K. Lee, L. Liu, and K. W Chung. Airfoil motion in subsonic flow with strong cubic nonlinear restoring forces. *Journal of Sound and Vibration*, 281(3-5):483–1245, 2004.

[3] B. H. K. Lee, S. J. Price, and Y. S. Wong. Nonlinear aeroelastic analysis of airfoils: bifurcation and chaos. *Progress in Aerospace Sciences*, 35:205–334, 1999.

[4] L. Liu and E. H. Dowell. The secondary bifurcation of an aeroelastic airfoil motion: Effect of high harmonics. *Nonlinear Dynamics*, 37:31–49, 2004.

Chapter 3

Hopf Bifurcation Analysis Using Stochastic Normal Form

The normal form for deterministic aeroelastic systems was developed in [9]. To extend these results to the stochastic case, we apply the stochastic normal form (Chapter 8 in [1]) to reduce the dimension of the system. We consider random parameters in the flow speed and in both the pitch and the plunge non-linear stiffness terms. Using the reduced model represented by the stochastic normal form, we confirm analytically the stochastic Hopf bifurcation scenario obtained numerically in [12]. We also obtain explicit formulas for the frequency and the amplitude of the LCOs.

When using various chaos expansions, it was observed [4, 6, 5] that the accuracy of the computed results is lower around the bifurcation point due to discontinuities in the parameter space. On the other hand, an analytical study based on the stochastic normal form gives the highest accuracy around the bifurcation point. Thus, the analytical study presented here can complement an approach based on chaos expansions because it is capable of providing explicit formulas for the amplitude and the frequency of the LCOs, and to determine the effects of parameters uncertainties near the Hopf bifurcation point.

3.1 Stochastic normal form

In this section, we assume that the non-linear plunge and pitch stiffness terms are given by $G(x_3) = \beta_1 x_3 + \beta_2 x_3^3$ and $M(x_1) = \beta_3 x_1 + \beta_4 x_1^3$, and consider random perturbations

of the coefficients of the cubic terms and the bifurcation parameter. Then we can rewrite (2.6) as follows:

$$\mathbf{X}^{'} = A\mathbf{X} + \delta B\mathbf{X} + (1-\delta)\mathbf{F}_1(\mathbf{X}), \tag{3.1}$$

where $\delta = 1 - (U_L^*/U^*)^2$ is the bifurcation parameter (with U_L^* the linear flutter velocity). The matrix A is the 8×8 Jacobian matrix evaluated at the equilibrium point $\mathbf{X} = \mathbf{0}$ and at the bifurcation value $\delta = 0$, and $\mathbf{F}_1(\mathbf{X})$ contains cubic terms in x_1 and x_3:

$$A = \begin{bmatrix} 1 & 0 & 0 & 0 & 0 & 0 & 0 & 0 \\ a_{21} - b_{21} & a_{22} & a_{23} - b_{23} & a_{24} & a_{25} & a_{26} & a_{27} & a_{28} \\ 0 & 0 & 0 & 1 & 0 & 0 & 0 & 0 \\ a_{41} - b_{41} & a_{42} & a_{43} - b_{43} & a_{44} & a_{45} & a_{46} & a_{47} & a_{48} \\ 1 & 0 & 0 & 0 & -\epsilon_1 & 0 & 0 & 0 \\ 1 & 0 & 0 & 0 & 0 & -\epsilon_2 & 0 & 0 \\ 0 & 0 & 1 & 0 & 0 & 0 & -\epsilon_1 & 0 \\ 0 & 0 & 1 & 0 & 0 & 0 & 0 & -\epsilon_2 \end{bmatrix},$$

$$B = \begin{bmatrix} 0 & 0 & 0 & 0 & \dots & 0 \\ b_{21} & 0 & b_{23} & 0 & \dots & 0 \\ 0 & 0 & 0 & 0 & \dots & 0 \\ b_{41} & 0 & b_{43} & 0 & \dots & 0 \\ 0 & \dots & \dots & \dots & \dots & 0 \\ \vdots & & & & & \vdots \\ 0 & \dots & \dots & \dots & \dots & 0 \end{bmatrix}, \quad F_1 = \begin{bmatrix} 0 \\ -b_{21}\frac{\beta_4}{\beta_3}x_1^3 + b_{23}\frac{\beta_2}{\beta_1}x_3^3 \\ 0 \\ b_{41}\frac{\beta_4}{\beta_3}x_1^3 - b_{43}\frac{\beta_2}{\beta_1}x_3^3 \\ 0 \\ \vdots \\ 0 \end{bmatrix}$$

Now consider random perturbations of the coefficients of the third order terms in x_1^3 and x_3^3, and the bifurcation parameter δ:

$$\tilde{\delta} = \delta + \sigma_1\eta_1, \quad \tilde{\beta_2} = \beta_2 + \sigma_2\eta_2, \quad \tilde{\beta_4} = \beta_4 + \sigma_3\eta_3, \tag{3.2}$$

where δ, β_2, β_4, $\sigma_1 \geq 0$, $\sigma_2 \geq 0$, $\sigma_3 \geq 0$ are constants, and $\eta_1(\cdot)$, $\eta_2(\cdot)$, and $\eta_3(\cdot)$ are independent random variable uniformly distributed on the interval $[-1, 1]$.

Thus, our random model is given by:

$$\mathbf{X}' = A\mathbf{X} + (\delta + \sigma_1\eta_1)B\mathbf{X} + (1 - \delta - \sigma_1\eta_1)\left(\mathbf{F}_1(\mathbf{X}) + \sum_{i=2}^{3} \sigma_i\eta_i\mathbf{F}_i(\mathbf{X})\right), \tag{3.3}$$

where $\mathbf{F}_i(\mathbf{X})$, $i = 1, 2, 3$ contain terms in x_1^3 and x_3^3. We use the same values of the parameters as in [9], so that the matrix A has one pair of purely imaginary eigenvalues $\lambda_{1,2} = \pm\omega_0$, one pair of complex eigenvalues with negative real parts $\lambda_{3,4} = b \pm ic$, and four negative real eigenvalues $\lambda_i < 0$, $i = 5, \ldots, 8$.

We first apply a deterministic transformation $\mathbf{Y} = P^{-1}\mathbf{X}$, where the matrix P is constructed from the eigenspace of A such that $P^{-1}AP = J$, with J the Jordan Canonical form of A:

$$J = \begin{bmatrix} J_c & 0 \\ 0 & J_s \end{bmatrix}, \quad J_c = \begin{bmatrix} 0 & \omega_0 \\ -\omega_0 & 0 \end{bmatrix}, \quad J_s = \begin{bmatrix} b & c & 0 & 0 & 0 & 0 \\ -c & b & 0 & 0 & 0 & 0 \\ 0 & 0 & \lambda_3 & 0 & 0 & 0 \\ 0 & 0 & 0 & \lambda_4 & 0 & 0 \\ 0 & 0 & 0 & 0 & \lambda_5 & 0 \\ 0 & 0 & 0 & 0 & 0 & \lambda_6 \end{bmatrix}. \tag{3.4}$$

In the new variable $\mathbf{Y} = (y_1, \ldots, y_8)^T = (\mathbf{Y}_c, \mathbf{Y}_s)^T$, with $\mathbf{Y}_c = (y_1, y_2)^T$, the system (3.3) can be rewritten as

$$\begin{aligned} \mathbf{Y}' = {} & J\mathbf{Y} + (\delta + \sigma_1\eta_1)P^{-1}BP\mathbf{Y} + (1 - \delta - \sigma_1\eta_1)\big(P^{-1}\mathbf{F}_1(P\mathbf{Y}) \\ & + \sum_{i=2}^{3} \sigma_i\eta_i P^{-1}\mathbf{F}_i(P\mathbf{Y})\big). \end{aligned} \tag{3.5}$$

Similar to the deterministic normal form, the stochastic normal form retains the essential characteristics of the system, but reduces the dimension of the original problem. In our case, since the system given in equations (3.5) contains both stable and critical modes, we now reduce the dimension from eight to two using the procedure

described in the proof of Theorem 8.4.3 in [1]. This method allows us to obtain simultaneously the center manifold and the stochastic normal form. We consider a small noise scenario, and suppose that the parameters $\mathbf{\Delta} = (\delta, \sigma_1, \sigma_2, \sigma_3)^T$ are all close to zero. So, to equation Eq. (3.5) we add four more equations:

$$\delta^{'} = 0, \quad \sigma_1^{'} = 0, \quad \sigma_2^{'} = 0, \quad \sigma_3^{'} = 0. \tag{3.6}$$

Let denote by $\mathbf{F}(\mathbf{Y}, \mathbf{\Delta})$ the random polynomial given by the right hand side of equation Eq. (3.5). Then a Taylor expansion of $\mathbf{F}$ gives

$$\mathbf{F}(\mathbf{Y}, \mathbf{\Delta}) = J\mathbf{Y} + \sum_{\substack{1 \leq p+q \leq 3 \\ 0 \leq r \leq 1}} \mathbf{F}_{pqr}(\mathbf{Y}, \mathbf{\Delta}) + O(|\mathbf{Y}|^4 + |\mathbf{\Delta}|^2), \tag{3.7}$$

where $\mathbf{F}_{pqr}$ is a random homogeneous polynomial of degree $p+q+r$, which is of degree p in $\mathbf{Y}_c$, of degree q in $\mathbf{Y}_s$, and of degree r in $\mathbf{\Delta}$, with values in R^8. More precisely, for any $1 \leq p+q \leq 3$, $0 \leq r \leq 1$, we have $\mathbf{F}_{pqr}(\mathbf{Y}, \mathbf{\Delta}) = (f_{1,pqr}, \ldots, f_{8,pqr})^T(\mathbf{Y}, \mathbf{\Delta})$ with

$$f_{i,pqr}(\mathbf{Y}, \mathbf{\Delta}) = \sum_{\substack{n_1+n_2=p \\ n_3+\cdots+n_8=q \\ r_1+\cdots+r_4=r}} f_{i,n_1,\ldots,n_8,r_1,\ldots,r_4} y_1^{n_1} \cdots y_8^{n_8} \delta^{r_1} \sigma_1^{r_2} \sigma_2^{r_3} \sigma_3^{r_4}, \tag{3.8}$$

where $f_{i,n_1,\ldots,n_8,r_1,\ldots,r_4}$, $i = 1, \ldots, 8$, are the random variables, but they are not time dependent. Notice that given the cubic form of the non-linearities considered here, we have no quadratic terms in the Taylor expansion (i.e. $\mathbf{F}_{pqr}(\mathbf{Y}, \mathbf{\Delta}) = 0$, for any $p+q = 2$ and any $0 \leq r \leq 1$).

Next, we find a near-identity random transformation

$$\begin{aligned} \mathbf{Y} \to \mathbf{Y} + \mathbf{H}(\mathbf{Y}, \mathbf{\Delta}) = \begin{bmatrix} \mathbf{Y}_c \\ \mathbf{Y}_s \end{bmatrix} + \begin{bmatrix} \sum_{\substack{1 \leq p+q \leq 3, 0 \leq r \leq 1, \\ (p+q,r) \neq (1,0)}} \mathbf{H}^c_{pqr}(\mathbf{Y}_c, \mathbf{Y}_s, \mathbf{\Delta}) \\ \sum_{\substack{1 \leq p+q \leq 3, 0 \leq r \leq 1, \\ (p+q,r) \neq (1,0)}} \mathbf{H}^s_{pqr}(\mathbf{Y}_c, \mathbf{Y}_s, \mathbf{\Delta}) \end{bmatrix} \\ + O(|\mathbf{Y}|^4 + |\mathbf{\Delta}|^2), \end{aligned} \tag{3.9}$$

where $\mathbf{H}^c_{pqr}$ and $\mathbf{H}^s_{pqr}$ are random homogeneous polynomials of degree $p+q+r$, which are of degree p in $\mathbf{Y}_c$, q in $\mathbf{Y}_s$ and r in $\mathbf{\Delta}$, with values in R^2 and R^6 respectively.

They have a similar representation with $\mathbf{F}_{pqr}$ shown above in Eq. (3.8). Applying the transformation (3.9) to (3.5),we get

$$\mathbf{Y}_c^{'} = J_c\mathbf{Y}_c + \sum_{\substack{1\leq n\leq 3, 0\leq r\leq 1,\\ (n,r)\neq(1,0)}} \mathbf{G}_{nr}^c(\mathbf{Y}_c, \mathbf{\Delta}) + O(|\mathbf{Y}_c|^4 + |\mathbf{\Delta}|^2) \tag{3.10}$$

$$\mathbf{Y}_s^{'} = J_s\mathbf{Y}_s + \sum_{\substack{1\leq p+q\leq 3, 0\leq r\leq 1,\\ q\geq 1, (p,r)\neq(0,0)}} \mathbf{G}_{pqr}^s(\mathbf{Y}_c, \mathbf{Y}_s, \mathbf{\Delta}) + O(|\mathbf{Y}|^4 + |\mathbf{\Delta}|^2), \tag{3.11}$$

where $\mathbf{G}_{nr}^c$ and $\mathbf{G}_{pqr}^s$ are random homogeneous polynomials with a similar representation with $\mathbf{F}_{pqr}$ (see Eq. (3.8)). $\mathbf{G}_{nr}^c$ is of degree $n+r$, such that it is of degree n in $\mathbf{Y}_c$ and r in $\mathbf{\Delta}$, with values in R^2. $\mathbf{G}_{pqr}^s$ is of degree $p+q+r$, such that it is of degree p in $\mathbf{Y}_c$, q in $\mathbf{Y}_s$, and r in $\mathbf{\Delta}$, with values in R^6. Similar to the deterministic cases, we try to solve the cohomological equations and to find the resonant terms that cannot be eliminated through the transformation given in Eq. (3.9), while making the polynomials $\mathbf{G}_{nr}^c$ and $\mathbf{G}_{pqr}^s$ as simple as possible.

To get the cohomological equations, we start from the following equation (see Eq. (8.4.7) in [1]):

$$\mathbf{F}(\mathbf{Y} + \mathbf{H}(\mathbf{Y}, \mathbf{\Delta})) = \mathbf{Y}^{'} + (D_{\mathbf{Y}_c}\mathbf{H})\mathbf{Y}_c^{'} + (D_{\mathbf{Y}_s}\mathbf{H})\mathbf{Y}_s^{'} + \frac{d}{dt}\mathbf{H}(\mathbf{Y}, \mathbf{\Delta}), \tag{3.12}$$

and replace $\mathbf{Y}^{'}$ with the formal Taylor expansions given on the right hand side of equations (3.10)-(3.11), $\mathbf{F}$ with the expansion (3.7), and $\mathbf{H}$ with the Taylor expansion given in Eq. (3.9). Equating the coefficients and separating the center and the stable components, we get the corresponding cohomological equations. Since we are mainly interested in the center equation of the truncated stochastic normal form (3.10), we focus on the corresponding cohomological equations (see also equations 8.4.17 and 8.4.18 in [1]):

$$\begin{aligned}&\frac{d}{dt}\mathbf{H}_{p0r}^c(\mathbf{Y}_c, \mathbf{\Delta}) - J_c\mathbf{H}_{p0r}^c(\mathbf{Y}_c, \mathbf{\Delta}) + D_{\mathbf{Y}_c}\mathbf{H}_{p0r}^c(\mathbf{Y}_c, \mathbf{\Delta})J_c\mathbf{Y}_c = -\mathbf{G}_{pr}^c(\mathbf{Y}_c, \mathbf{\Delta})\\ &+ \mathbf{R}_{p0r}^c(\mathbf{Y}_c, \mathbf{\Delta})\end{aligned} \tag{3.13}$$

$$\frac{d}{dt}\mathbf{H}_{p0r}^s(\mathbf{Y}_c, \mathbf{\Delta}) - J_s\mathbf{H}_{p0r}^s(\mathbf{Y}_c, \mathbf{\Delta}) + D_{\mathbf{Y}_s}\mathbf{H}_{p0r}^s(\mathbf{Y}_c, \mathbf{\Delta})J_c\mathbf{Y}_c = \mathbf{R}_{p0r}^s(\mathbf{Y}_c, \mathbf{\Delta}), \tag{3.14}$$

where $\mathbf{R}^c_{p0r}$ and $\mathbf{R}^s_{p0r}$ depend only on $\mathbf{F}_{p0r}$ and on $\mathbf{H}_{p+1,0,r'-1}$, $\mathbf{H}_{p',0,r'}$, $\mathbf{G}^c_{p'r'}$, $\mathbf{G}^s_{p'0r'}$, for $p' \leq p$, $r' \leq r$, and $p' + r' \leq p + r - 1$.

Since Eq. (3.13) is resonant, instead of trying to find stationary solutions, we let $\mathbf{H}^c_{p0r} = 0$ and thus $\mathbf{G}^c_{pr} = \mathbf{R}^c_{p0r}$. Eq. (3.14) is not resonant and we can find stationary solutions as in Chapter 8.4 in [1]. In fact, we do not even need to solve for the stationary solution of a general random differential equation because the cohomological equations (3.14) with $p = 2, 3$ and $r = 0$ are deterministic, and only some of the equations corresponding to $r = 1$ and $p = 1, 3$ contain the random terms. Moreover, since we consider uncertainties expressed by random variables (which do not depend on time), finding the stationary solutions reduces to finding the time independent solution of a system of linear equations.

To determine the coefficients of $\mathbf{H}^s_{p00}$ for each $p = 1, 2, 3, ,$ we solve 4 linear systems of $p + 1$ coupled equations, and one linear system of $2(p + 1)$ equations. When solving for the coefficients of $\mathbf{H}^s_{p01}$, we have 16 linear systems of $p + 1$ coupled equations, and four linear systems of $2(p + 1)$ equations. After extensive calculations using Maple, the approximate center manifold (up to the terms of order 3 in $\mathbf{Y}_c$ and order 1 in $(\delta, \sigma_1, \sigma_2, \sigma_3)$) is the graph:

$$
\begin{aligned}
&R^2 \times R^4 \ni (y_1, y_2, \delta, \sigma_1, \sigma_2, \sigma_3) \to \delta(\mathbf{H}^s_{101000} y_1 + \mathbf{H}^s_{011000} y_2) + \sigma_1 \eta_1(\cdot)(\mathbf{H}^s_{100100} y_1 \\
&+ \mathbf{H}^s_{010100} y_2) + \sum_{i+j=3, i\geq 0, j\geq 0} y_1^i y_2^j (\mathbf{H}^s_{ij0000} + \delta \mathbf{H}^s_{ij1000} + \sigma_1 \eta_1(\cdot) \mathbf{H}^s_{ij0100} \\
&+ \sigma_2 \eta_2(\cdot) \mathbf{H}^s_{ij0010} + \sigma_3 \eta_3(\cdot) \mathbf{H}^s_{ij0001}) \in R^6,
\end{aligned}
\tag{3.15}
$$

and the truncated center equation is

$$
\begin{aligned}
\mathbf{Y}_c' = &\begin{bmatrix} g^{c1}_{101000}\delta + g^{c1}_{100100}\sigma_1\eta_1 & -\omega_0 + g^{c1}_{011000}\delta + g^{c1}_{010100}\sigma_1\eta_1 \\ \omega_0 + g^{c2}_{101000}\delta + g^{c2}_{100100}\sigma_1\eta_1 & g^{c2}_{011000}\delta + g^{c2}_{010100}\sigma_1\eta_1 \end{bmatrix} \mathbf{Y}_c \\
&+ \sum_{i+j=3, i\geq 0, j\geq 0} y_1^i y_2^j \Bigg(\begin{bmatrix} g^{c1}_{ij0000} + \delta g^{c1}_{ij1000} + g^{c1}_{ij0100}\sigma_1\eta_1 \\ g^{c2}_{ij0000} + \delta g^{c2}_{ij1000} + g^{c2}_{ij0100}\sigma_1\eta_1 \end{bmatrix} + \sigma_2 \begin{bmatrix} g^{c1}_{ij0010} \\ g^{c2}_{ij0010} \end{bmatrix} \eta_2 \\
&+ \sigma_3 \begin{bmatrix} g^{c1}_{ij0001} \\ g^{c2}_{ij0001} \end{bmatrix} \eta_3 \Bigg).
\end{aligned}
\tag{3.16}
$$

Here, we have

$$\mathbf{H}^s_{p0r} = \sum_{\substack{i+j=p,k+l+n+m=r \\ i,j,k,l,n,m\geq 0}} \mathbf{H}^s_{ijklnm} y_1^i y_2^j \eta_1^l \eta_2^n \eta_3^m \delta^k \sigma_1^l \sigma_2^n \sigma_3^m \tag{3.17}$$

$$\mathbf{G}^c_{pr} = \begin{bmatrix} \sum_{\substack{i+j=p,k+l+n+m=r \\ i,j,k,l,n,m\geq 0}} (g^{c1}_{ijklnm} \eta_1^l \eta_2^n \eta_3^m) y_1^i y_2^j \delta^k \sigma_1^l \sigma_2^n \sigma_3^m \\ \sum_{\substack{i+j=p,k+l+n+m=r \\ i,j,k,l,n,m\geq 0}} (g^{c2}_{ijklnm} \eta_1^l \eta_2^n) y_1^i y_2^j \delta^k \sigma_1^l \sigma_2^n \sigma_3^m \end{bmatrix}. \tag{3.18}$$

Notice that from Eq. (3.5) and (3.8), we get $f_{i,n_1,\ldots,n_8,1,0,0,0} = f_{i,n_1,\ldots,n_8,0,1,0,0}$, for any $i = 1,\ldots,8$, and any non-negative integers $n_1,\ldots,n_8$. As a consequence, in the truncated normal form (3.16), we have $g^{c1}_{ij1000} = g^{c1}_{ij0100}$ and $g^{c2}_{ij1000} = g^{c2}_{ij0100}$, for any non-negative integers $i, j = 0,\ldots,3$.

We then reduce the number of terms in the center part of the truncated normal form (3.16) by proceeding as in [9], we bring the linear part to a diagonal form by applying the transformation $V = NP^{-1}\mathbf{Y}_c$, where

$$NP = \frac{1}{\sqrt{b_{12}^2 + \beta^2 + (\alpha - b_{11})^2}} \begin{bmatrix} 0 & b_{12} \\ \beta & \alpha - b_{11} \end{bmatrix}, \tag{3.19}$$

with $b_{11} = g^{c1}_{101000}\delta + g^{c1}_{100100}\sigma_1\eta_1$, $b_{12} = -\omega_0 + g^{c1}_{011000}\delta + g^{c1}_{010100}\sigma_1\eta_1$, $b_{21} = \omega_0 + g^{c2}_{101000}\delta + g^{c2}_{100100}\sigma_1\eta_1$, $b_{22} = g^{c2}_{011000}\delta + g^{c2}_{010100}\sigma_1\eta_1$, $\alpha = (b_{11}+b_{22})/2$, and $\beta = \sqrt{b_{11}b_{22} - b_{12}b_{21} - \alpha^2}$. In the next section, we show that for the values of the parameters corresponding to the aeroelastic system considered here and for values of δ and σ_1 close to zero, we have $b_{12} \neq 0$ and $b_{12} \neq b_{21}$, for any random value of $\eta_1 \in [-1, 1]$. In this case, since we can also write $\beta = \sqrt{b_{12}(b_{12} - b_{21})}$, using Eq. (3.19), we easily verify that the matrix NP is invertible for any random value of $\eta_1 \in [-1, 1]$.

The complex form of the transformed Eq. (3.16) is given by

$$Z' = \lambda(\delta, \sigma_1)Z + F_z(Z, \bar{Z}, \Delta), \tag{3.20}$$

where $\lambda(\delta, \sigma_1) = \alpha + i\beta$ and $Z = v_1 + iv_2$, $V = (v_1, v_2)^T$. Here, we consider $\mathbf{\Delta} = (\delta, \sigma_1, \sigma_2, \sigma_3)$ as small parameters. By adding four more equations $\delta' = 0$, $\sigma_1' = 0$,

$\sigma_2^{'} = 0$, $\sigma_3^{'} = 0$, we apply the same procedure as before to find simultaneously the stochastic normal form and the center manifold.

Using a Taylor expansion we rewrite Eq. (3.20) as

$$\begin{aligned} Z^{'} &= (\alpha_{01}\delta + \alpha_{01}\sigma_1\eta_1 + i(\beta_{00} + \beta_{01}\delta + \beta_{01}\sigma_1\eta_1))\, Z \\ &+ \sum_{\substack{1\le p+q\le 3, 0\le r\le 1,\\ (p+q,r)\neq(1,0)}} \sum_{k+l+n+m=r} f_{z,pqklmn} Z^p \bar{Z}^q \delta^k \sigma_1^l \sigma_2^m \sigma_3^n + O(|Z|^4 + |\mathbf{\Delta}|^2), \end{aligned} \tag{3.21}$$

where $\alpha_{01} = (g^{c1}_{101000} + g^{c2}_{011000})/2 = (g^{c1}_{100100} + g^{c2}_{010100})/2$. Note that given the cubic form of the non-linearities, we have $f_{z,pqklmn} = 0$ if $p + q = 2$, for any non-negative integers k, l, m, n. We now find a near-identity random transformation

$$Z \to Z + H_z(Z, \mathbf{\Delta}) = Z + \sum_{\substack{1\le p+q\le 3, 0\le r\le 1,\\ (p+q,r)\neq(1,0)}} H_{z,pqr}(Z, \bar{Z}, \mathbf{\Delta}) + O(|Z|^4 + |\mathbf{\Delta}|^2), \tag{3.22}$$

which transforms Eq. (3.21) into

$$\begin{aligned} Z^{'} &= (\alpha_{01}\delta + \alpha_{01}\sigma_1\eta_1 + i(\beta_{00} + \beta_{01}\delta + \beta_{01}\sigma_1\eta_1))\, Z \\ &+ \sum_{\substack{1\le p+q\le 3, 0\le r\le 1,\\ (p+q,r)\neq(1,0)}} G_{z,pqr}(Z, \bar{Z}, \mathbf{\Delta}) + O(|Z|^4 + |\mathbf{\Delta}|^2), \end{aligned} \tag{3.23}$$

where $H_{z,pqr}$ and $G_{z,pqr}$ are random homogeneous polynomials of degree $p+q+r$, such that they are of degree p in Z, q in $\bar{Z}$, and r in $\mathbf{\Delta}$:

Since η_1, η_2 and η_3 are random variables, they do not depend on time, and proceeding similar to the deterministic Hopf bifurcation case (see, for example, Chapter 11 in [11]) we can find stationary solutions $H_{z,pqr}$ of the cohomological equations and make $G_{z,pqr} = 0$ if $(p, q) \neq (2, 1)$, for any $1 \le p + q \le 3$, $0 \le r \le 1$, $(p + q, r) \neq (1, 0)$. Moreover, solving the cohomological equations, we get $H_{z,pqr} = 0$ if $p + q \neq 3$ and $H_{z,21r} = 0$. More exactly we have

$$H_{z,pqr} = \sum_{k+l+m+n=r,k,l,m,n\ge 0} H_{z,pqklmn} \eta_1^l \eta_2^m \eta_3^n Z^p \bar{Z}^q \delta_0^k \sigma_1^l \sigma_2^m \sigma_3^n, \tag{3.24}$$

$$G_{z,pqr} = \sum_{k+l+m+n=r,k,l,m,n\ge 0} G_{z,pqklmn} \eta_1^l \eta_2^m \eta_3^n Z^p \bar{Z}^q \delta_0^k \sigma_1^l \sigma_2^m \sigma_3^n, \tag{3.25}$$

where $H_{z,pqklmn}$ and $G_{z,pqklmn}$ are complex constants. From the formula in the right hand side of Eq. (3.5), we get $G_{z,pq10mn}= G_{z,pq01mn}$, for any non-negative integers p, q, m, n.

The truncated normal form up to the terms of order 3 in $(Z,\bar{Z})$ and order 1 in $(\delta, \sigma_1, \sigma_2, \sigma_3)$ can be expressed as

$$\begin{aligned} Z^{'} &= (\alpha_{01}\delta + \alpha_{01}\sigma_1\eta_1 + i(\beta_{00} + \beta_{01}\delta + \beta_{01}\sigma_1\eta_1))\, Z + Z^2\bar{Z}(G_{z,210000} \\ &\quad + G_{z,211000}\delta + G_{z,211000}\sigma_1\eta_1 + G_{z,210010}\sigma_2\eta_2 + G_{z,210001}\sigma_3\eta_3). \end{aligned} \tag{3.26}$$

If we write $Z = r(\tau)e^{i\theta(\tau)}$, we can express the truncated normal form (3.26) in polar coordinates:

$$\begin{aligned} r^{'} &= (\alpha_{01}\delta + \alpha_{01}\sigma_1\eta_1)r + r^3(\mathrm{Re}(G_{z,210000}) + \mathrm{Re}(G_{z,211000})\delta \\ &\quad + \mathrm{Re}(G_{z,211000})\sigma_1\eta_1 + \mathrm{Re}(G_{z,210010})\sigma_2\eta_2 + \mathrm{Re}(G_{z,210001})\sigma_3\eta_3) \end{aligned} \tag{3.27}$$

$$\begin{aligned} \theta^{'} &= \beta_{00} + \beta_{01}\delta + \beta_{01}\sigma_1\eta_1 + r^2(\mathrm{Im}(G_{z,210000}) + \mathrm{Im}(G_{z,211000})\delta \\ &\quad + \mathrm{Im}(G_{z,211000})\sigma_1\eta_1 + \mathrm{Im}(G_{z,210010})\sigma_2\eta_2 + \mathrm{Im}(G_{z,210001})\sigma_3\eta_3). \end{aligned} \tag{3.28}$$

Equations (3.27)-(3.28) can be solved analytically, and the result can be used to study the stochastic bifurcation and to analyze the effect of parameter uncertainties on the amplitude and the frequency of the limit cycle oscillations.

Remark 1 *Although the stochastic normal form was obtained under the restrictive assumption that the parameter uncertainties are expressed by random variables, the results can be extended to more complex types of noise. More precisely, a similar truncated normal form with the one given in Eq. (3.16) can be obtained if* η_1, η_2, *and* η_3 *are any stationary stochastic processes (also called real noise) or if they are white noises (Brownian motion/Wiener processes) (see [1, chap. 8] or [3] for a succinct presentation of stochastic normal form). To obtain the decoupled equations (3.27)-(3.28), we needed more restrictive conditions on the nature of the noises* η_1, η_2, *and* η_3. *If only uncertainties in the coefficients of the cubic terms are present* ($\sigma_1 = 0$), *then if* η_2 *and* η_3 *are real noises, a condition to determine stationary solutions for the*

cohomological equations is given in [2] in terms of the spectral density matrix. If η_2 and η_3 are Gaussian white noises, then it is not possible to reduce the normal form to the decoupled equations (3.27)-(3.28) because there are no stationary solutions for the corresponding stochastic differential equations (see [10]).

3.2 Stochastic bifurcation

To study the stochastic bifurcation, we notice that Eq. (3.27) can be solved independently of Eq. (3.28), and we have a bifurcation scenario in dimension one similar to the case represented in Eq. (17) in [13]. The solutions of system (3.27)-(3.28) define a local random dynamical system [13], $\Phi_\delta(\tau, \omega)$, but the bifurcation study in [13] cannot be applied directly because the noises η_i, $i = 1, 2, 3$ are random variables, so they are not ergodic processes. However, we can find the invariant measures following a similar approach.

3.2.1 Stochastic bifurcation in dimension one

Consider the random differential equation

$$x^{'} = (a + \xi_1(\omega))x + x^3(b + \xi_2(\omega)) \tag{3.29}$$

where ξ_1 and ξ_2 are random variables and a, b are constants. To study the stochastic bifurcation, we note that Eq. (3.29) can be solved analytically and we have a bifurcation in dimension one scenario similar with the case represented in Eq. (16) in [13].

First, using the transformation $y = 1/x^2$ in Eq. (3.29) and solving the linear equation in y, we obtain explicitly the solution $x(\tau, \omega, x_0)$ starting at $\tau = 0$ from $x_0 \neq 0$:

$$x(\tau, \omega, x_0) = \begin{cases} \dfrac{sign(x_0)e^{(a+\xi_1(\omega))\tau}}{\sqrt{\frac{1}{x_0^2} - \frac{b+\xi_2(\omega)}{a+\xi_1(\omega)}\left(e^{2(a+\xi_1(\omega))\tau} - 1\right)}} & \text{if } a + \xi_1(\omega) \neq 0 \\ \dfrac{sign(x_0)}{\sqrt{\frac{1}{x_0^2} - (b+\xi_2(\omega))\tau}} & \text{if } a + \xi_1(\omega) = 0 \end{cases} \tag{3.30}$$

Consequently the local random dynamical system [1] (RDS) $\phi(\tau,\omega)x_0 : D_\tau(\omega) \to R_\tau(\omega)$ generated by (3.29) is given by

$$0 \to 0$$
$$0 \neq x_0 \to \phi(\tau,\omega)x_0 = x(\tau,\omega,x_0),$$

where $x(\tau,\omega,x_0)$ is given in Eq. (3.30).

In general, there are two types of stochastic bifurcations [1]: phenomenological bifurcations regarding the structural changes of the stationary measures, and the dynamical bifurcations related to the invariant measures. For Eq. (3.29), the two types of bifurcations coincide because the noises ξ_1 and ξ_2 do not depend on time, and consequently any invariant measure ρ is also a stationary measure, i.e. for all $\tau > 0$ we have

$$\int P\left(\omega : (x(\tau,\omega,x_0)) \in B\right) \rho(d(x_0))) = \rho(B), \quad P - \text{almost sure.} \tag{3.31}$$

Lemma 2.3 in [13] is also true in our case and using Eq. (3.30), we can easily obtain a similar result given in Lemma 4.1 in [13]. Thus, we have:

$$D_\tau(\omega) = \begin{cases} (-\infty,\infty) & \text{if } c(\tau,\omega) \leq 0 \\ \left(-\frac{1}{\sqrt{c(\tau,\omega)}}, \frac{1}{\sqrt{c(\tau,\omega)}}\right) & \text{if } c(\tau,\omega) > 0 \end{cases} \tag{3.32}$$

$$R_\tau(\omega) = \begin{cases} (-\infty,\infty) & \text{if } c(\tau,\omega) \geq 0 \\ \left(-\frac{e^{(a+\xi_1(\omega))\tau}}{\sqrt{-c(\tau,\omega)}}, \frac{e^{(a+\xi_1(\omega))\tau}}{\sqrt{-c(\tau,\omega)}}\right) & \text{if } c(\tau,\omega) < 0 \end{cases} \tag{3.33}$$

where

$$c(\tau,\omega) = \begin{cases} \frac{b+\xi_2(\omega)}{a+\xi_1(\omega)}\left(e^{2(a+\xi_1(\omega))\tau} - 1\right) & \text{if } a + \xi_1(\omega) \neq 0 \\ (b+\xi_2(\omega))\tau & \text{if } a + \xi_1(\omega) = 0 \end{cases} \tag{3.34}$$

The set $A(\omega) = \bigcap_{\tau\in R} D_\tau(\omega)$ of the initial values at time $\tau = 0$ whose orbits never

explode can be explicitly determined as

$$A(\omega) = \begin{cases} (-\infty, \infty) & \text{if } b + \xi_2(\omega) = 0 \\ \{0\} & \text{if } \frac{a+\xi_1(\omega)}{b+\xi_2(\omega)} \geq 0 \\ \left[-\sqrt{-\frac{a+\xi_1(\omega)}{b+\xi_2(\omega)}}, \sqrt{-\frac{a+\xi_1(\omega)}{b+\xi_2(\omega)}}\right] & \text{if } \frac{a+\xi_1(\omega)}{b+\xi_2(\omega)} < 0 \end{cases} \tag{3.35}$$

Notice that $A(\omega)$ is a random interval, and proceeding as in [13] the nontrivial invariant measures are random Dirac measures sitting at the boundary points of $A(\omega)$. Obviously $x = 0$ is a stationary solution for Eq. (3.29) and the linearised equation at $x = 0$ is

$$x^{'} = (a + \xi_1(\omega))x. \tag{3.36}$$

It is easy to verify that

$$\phi(\tau, \omega)\left(\pm\sqrt{-\frac{a + \xi_1(\omega)}{b + \xi_2(\omega)}}\right) = \pm\sqrt{-\frac{a + \xi_1(\omega)}{b + \xi_2(\omega)}}, \tag{3.37}$$

and the linearised equation at $x = \pm\sqrt{-\frac{a+\xi_1(\omega)}{b+\xi_2(\omega)}}$ is

$$x^{'} = -2(a + \xi_1(\omega))x. \tag{3.38}$$

Using (3.35)-(3.38), we can prove a result similar with Theorem 4.4 and 4.5 stated in [13]:

Proposition 2 *1. If $b + \xi_2(\omega) < 0$ and $a + \xi_1(\omega) < 0$, then the Dirac measure δ_0 is the unique invariant measure and it is stable.*

2. If $b + \xi_2(\omega) > 0$ and $a + \xi_1(\omega) > 0$, then the Dirac measure δ_0 is the unique invariant measure and it is unstable.

3. If $b + \xi_2(\omega) < 0$ and $a + \xi_1(\omega) > 0$, then the Dirac measure δ_0 is unstable and we have two new stable Dirac measures $\delta_{\pm\sqrt{-\frac{a+\xi_1(\omega)}{b+\xi_2(\omega)}}}$

4. *If* $b+\xi_2(\omega) > 0$ *and* $a+\xi_1(\omega) < 0$, *then the Dirac measure* δ_0 *is stable and we also have the unstable invariant Dirac measures* $\delta_{\pm\sqrt{-\frac{a+\xi_1(\omega)}{b+\xi_2(\omega)}}}$.

These results can be applied to study the stochastic Hopf bifurcation for the following random differential equations in polar coordinates: Consider the random differential equations

$$r' = (a+\xi_1(\omega))r + r^3(b+\xi_2(\omega)) \tag{3.39}$$

$$\theta' = c+\xi_3(\omega) + r^2(d+\xi_4(\omega)) \tag{3.40}$$

where ξ_i, $i = 1,\ldots,4$, are random variables and a, b, c, d are constants. Using the transformation $y = 1/r^2$ and solving the linear equation in y, we obtain the solution of Eq. (3.39) explicitly. Replacing the formula for r in Eq. (3.40) and solving for θ, we obtain the following expression for the solution $(r(\tau,\omega,r_0),\theta(\tau,\omega,\theta_0,r_0))$ starting at $\tau = 0$ from (r_0,θ_0), $r_0 > 0$:

$$r = \begin{cases} \dfrac{e^{(a+\xi_1(\omega))\tau}}{\sqrt{\frac{1}{r_0^2} - \frac{b+\xi_2(\omega)}{a+\xi_1(\omega)}\left(e^{2(a+\xi_1(\omega))\tau}-1\right)}} & \text{if } a+\xi_1(\omega) \neq 0 \\ \dfrac{1}{\sqrt{\frac{1}{r_0^2} - (b+\xi_2(\omega))\tau}} & \text{if } a+\xi_1(\omega) = 0 \end{cases} \tag{3.41}$$

$$\theta = \begin{cases} \theta_0 \quad +(c+\xi_3(\omega))\tau - \frac{(d+\xi_4(\omega))}{2(b+\xi_2(\omega))}\ln\left|1 - r_0^2\frac{b+\xi_2(\omega)}{a+\xi_1(\omega)}\left(e^{2(a+\xi_1(\omega))\tau}-1\right)\right| \\ \qquad \text{if } a+\xi_1(\omega)\neq 0, b+\xi_2(\omega)\neq 0 \\ \theta_0 \quad +(c+\xi_3(\omega))\tau - \frac{(d+\xi_4(\omega))}{(b+\xi_2(\omega))}\ln|1 - r_0^2(b+\xi_2(\omega))\tau| \\ \qquad \text{if } a+\xi_1(\omega)= 0, b+\xi_2(\omega)\neq 0 \\ \theta_0 \quad +(c+\xi_3(\omega))\tau + \frac{(r_0(d+\xi_4(\omega)))}{(a+\xi_1(\omega))}e^{a+\xi_1(\omega)} \\ \qquad \text{if } a+\xi_1(\omega)\neq 0, b+\xi_2(\omega)= 0 \\ \theta_0 \quad +(c+\xi_3(\omega))\tau + r_0(d+\xi_4(\omega)) \\ \qquad \text{if } a+\xi_1(\omega)= 0, b+\xi_2(\omega)= 0 \end{cases} \tag{3.42}$$

As a consequence the local random dynamical system $\Phi(\tau,\omega)(r_0,\theta_0)$ associated with the system (3.39)-(3.40) is given by:

$$(0,0) \to (0,0)$$
$$(r_0,\theta_0) \to \Phi(\tau,\omega)(r_0,\theta_0) = (r(\tau,\omega,r_0),\theta(\tau,\omega,\theta_0,r_0)), r_0 \neq 0$$

where $r(\tau,\omega,r_0)$, $\theta(\tau,\omega,\theta_0,r_0)$ are given in equations (3.41)-(3.42).

To study the bifurcation scenario for the system given in equations (3.39)-(3.40), we define Leb(r) to be the normalized Lebesgue measure[13] on the circle $S(r) = \{x^2+y^2=r^2\}$ with radius r in R^2. We have the following result similar to Theorems 4.8 and 4.9 given in [13]:

Proposition 3 *1. If $b+\xi_2(\omega) < 0$ and $a+\xi_1(\omega) < 0$, then the Dirac measure δ_0 is the unique invariant measure and it is stable.*

2. If $b+\xi_2(\omega) < 0$ and $a+\xi_1(\omega) > 0$, then there are two invariant measures: the Dirac measure δ_0 and μ_ω =Leb$\left(\sqrt{-\frac{a+\xi_1(\omega)}{b+\xi_2(\omega)}}\right)$ Moreover, δ_0 is unstable and μ_ω is stable.

3. If $b+\xi_2(\omega) > 0$ and $a+\xi_1(\omega) > 0$, then the Dirac measure δ_0 is the unique invariant measure and it is unstable.

4. If $b+\xi_2(\omega) > 0$ and $a+\xi_1(\omega) < 0$, then there are two invariant measures: the Dirac measure δ_0 and μ_ω =Leb$\left(\sqrt{-\frac{a+\xi_1(\omega)}{b+\xi_2(\omega)}}\right)$. Moreover, the Dirac measure δ_0 is stable and μ_ω is unstable.

Proof:

The proof is similar with the proof of Theorem 3.7 in [13]. If $\frac{a+\xi_1(\omega)}{b+\xi_2(\omega)} > 0$, then analogously with Eq. (3.35), we can show that $A(\omega) = \{0\}$. Thus the only possible invariant measure for Φ is the Dirac measure δ_0.

If $\frac{a+\xi_1(\omega)}{b+\xi_2(\omega)} < 0$, then using formulas (3.41)-(3.42) and Proposition 1, we can easily show that

$$\begin{aligned}\Phi(\tau,\omega)\left(\sqrt{-\frac{a+\xi_1(\omega)}{b+\xi_2(\omega)}},\theta_0\right) = \Bigg(\sqrt{-\frac{a+\xi_1(\omega)}{b+\xi_2(\omega)}},\theta_0 + (c+\xi_3)\tau \\ - (d+\xi_4)\frac{a+\xi_1(\omega)}{b+\xi_2(\omega)}\Bigg)\end{aligned} \tag{3.43}$$

Consequently,

$$\Phi(\tau,\omega)S\left(\sqrt{-\frac{a+\xi_1(\omega)}{b+\xi_2(\omega)}}\right) = S\left(\sqrt{-\frac{a+\xi_1(\omega)}{b+\xi_2(\omega)}}\right), \quad \text{if } \frac{a+\xi_1(\omega)}{b+\xi_2(\omega)} < 0. \tag{3.44}$$

Thus the support of μ_ω is Φ invariant, so μ_ω is invariant.

To show the uniqueness, we suppose that there exists an invariant measure $\rho_\omega \neq \mu_\omega$, and we show that $\rho_\omega = \delta_0$. Since ρ_ω is invariant, we have $\Phi(\tau,\omega)\rho_\omega = \rho_\omega$. Thus for any function f continuous and bounded we have

$$\Phi(\tau,\omega)\rho_\omega(f) = \int f(\Phi(\tau,\omega)(r,\theta))\rho_\omega(d(r,\theta)) = \rho_\omega(f). \tag{3.45}$$

But $\int f(\Phi(\tau,\omega)(r,\theta))\rho_\omega(d(r,\theta)) \to f(0,0)$ because $\Phi(\tau,\omega)(r,\theta) \to (0,0)$ for all $r \neq \sqrt{-\frac{a+\xi_1(\omega)}{b+\xi_2(\omega)}}$. As a consequence, from Eq. (3.45), we get $\rho_\omega(f) = f(0,0) = \delta_0(f)$.

Finally, the stability can easily be proved using the linearized equations. □

3.2.2 Stochastic bifurcation of aeroelastic system

To simplify the notation let denote $G_{z,210000} = a_1 + ib_1$, $G_{z,211000} = a_2 + ib_2$, $G_{z,210010} = a_3 + ib_3$, and $G_{z,210001} = a_4 + ib_4$. Solving Eq. (3.27) explicitly, replacing the formula for r in Eq. (3.28), and solving for θ, we obtain the following expression for the solution $(r(\tau,\omega,r_0),\theta(\tau,\omega,\theta_0,r_0))$ starting at $\tau = 0$ from (r_0,θ_0), $r_0 > 0$ (see also equations

(3.41)-(3.42) in Subsection 3.2.1):

$$r(\tau,\omega,r_0)=\frac{e^{(\alpha_{01}\delta+\alpha_{01}\sigma_1\eta_1(\omega))\tau}}{\sqrt{\frac{1}{r_0^2}-\frac{a_1+a_2\delta+a_2\sigma_1\eta_1(\omega)+a_3\sigma_2\eta_2(\omega)+a_4\sigma_3\eta_3(\omega)}{\alpha_{01}\delta+\alpha_{01}\sigma_1\eta_1(\omega)}\left(e^{2(\alpha_{01}\delta+\alpha_{01}\sigma_1\eta_1(\omega))\tau}-1\right)}} \tag{3.46}$$

$$\begin{aligned}\theta(\tau,\omega,r_0,\theta_0)&=\theta_0+(\beta_{00}+\beta_{01}\delta+\beta_{01}\sigma_1\eta_1(\omega))\tau\\&-\frac{(b_1+b_2\delta+b_2\sigma_1\eta_1(\omega)+b_3\sigma_2\eta_2(\omega)+b_4\sigma_3\eta_3(\omega))}{2(a_1+a_2\delta_0+a_2\sigma_1\eta_1(\omega)+a_3\sigma_2\eta_2(\omega)+a_4\sigma_3\eta_3(\omega))}\ln\Bigg|1-r_0^2\\&\frac{a_1+a_2\delta_0+a_2\sigma_1\eta_1(\omega)+a_3\sigma_2\eta_2(\omega)+a_4\sigma_3\eta_3(\omega)}{\alpha_{01}\delta+\alpha_{01}\sigma_1\eta_1(\omega)}\left(e^{2(\alpha_{01}\delta+\alpha_{01}\sigma_1\eta_1(\omega))\tau}-1\right)\Bigg|\end{aligned} \tag{3.47}$$

To study the bifurcation scenario for the system given in equations (3.27)-(3.28), we define Leb(r) to be the normalized Lebesgue measure[13] on the circle with radius r in R^2. We can now prove results similar with Theorems 4.8 and 4.9 in [13] for the system (3.27)-(3.28) (see Proposition 2 in Section 3.2.1):

Case (a) If $a_1+a_2\delta+a_2\sigma_1\eta_1(\omega)+a_3\sigma_2\eta_2(\omega)+a_4\sigma_3\eta_3(\omega)<0$ and $\alpha_{01}\delta+\alpha_{01}\sigma_1\eta_1(\omega)<0$, then the Dirac measure δ_0 is the unique invariant measure and it is stable.

Case (b) If $a_1+a_2\delta+a_2\sigma_1\eta_1(\omega)+a_3\sigma_2\eta_2(\omega)+a_4\sigma_3\eta_3(\omega)<0$ and $\alpha_{01}\delta+\alpha_{01}\sigma_1\eta_1(\omega)>0$, then there are two invariant measures: the Dirac measure δ_0 and $\mu_\omega=$ Leb $\left(\sqrt{-\frac{\alpha_{01}\delta+\alpha_{01}\sigma_1\eta_1(\omega)}{a_1+a_2\delta+a_2\sigma_1\eta_1(\omega)+a_3\sigma_2\eta_2(\omega)+a_4\sigma_3\eta_3(\omega)}}\right)$. Moreover, δ_0 is unstable and μ_ω is stable.

Case (c) If $a_1+a_2\delta+a_2\sigma_1\eta_1(\omega)+a_3\sigma_2\eta_2(\omega)+a_4\sigma_3\eta_3(\omega)>0$ and $\alpha_{01}\delta+\alpha_{01}\sigma_1\eta_1(\omega)>0$, then the Dirac measure δ_0 is the unique invariant measure and it is unstable.

Case (d) If $a_1+a_2\delta+a_2\sigma_1\eta_1(\omega)+a_3\sigma_2\eta_2(\omega)+a_4\sigma_3\eta_3(\omega)>0$ and $\alpha_{01}\delta+\alpha_{01}\sigma_1\eta_1(\omega)<0$, then there are two invariant measures: the Dirac measure δ_0 and $\mu_\omega=$ Leb $\left(\sqrt{-\frac{\alpha_{01}\delta+\alpha_{01}\sigma_1\eta_1(\omega)}{a_1+a_2\delta+a_2\sigma_1\eta_1(\omega)+a_3\sigma_2\eta_2(\omega)+a_4\sigma_3\eta_3(\omega)}}\right)$. Moreover, the Dirac measure δ_0 is stable and μ_ω is unstable.

To explain our results, consider the case when $\alpha_{01}\delta+\alpha_{01}\sigma_1\eta_1(\omega)>0$ and $a_1+a_2\delta+a_2\sigma_1\eta_1(\omega)+a_3\sigma_2\eta_2(\omega)+a_4\sigma_3\eta_3(\omega)<0$. In the deterministic case (i.e. when

$\sigma_1 = \sigma_2 = \sigma_3 = 0$), we have a supercritical Hopf bifurcation when $\delta = 0$ representing a transition from a stationary solution to a limit cycle oscillation, namely for $\alpha_{01}\delta > 0$ and $a_1 + a_2\delta < 0$, we have a periodic solution on the circle with radius $\sqrt{-\alpha_{01}\delta/(a_1 + a_2\delta)}$. In the stochastic case, when the system is perturbed by noises with small intensities such that $a_1 + a_2\delta \leq -a_2\sigma_1\eta_1(\omega) - a_3\sigma_2\eta_2(\omega) - a_4\sigma_3\eta_3(\omega)$, then for $\alpha_{01}\delta + \alpha_{01}\sigma_1\eta_1(\omega) > 0$, the solution become a random process on a circle whose radius depends on the sample path. The support of the bifurcating invariant measure $\mu_\omega = \text{Leb}\Big(\sqrt{-\frac{\alpha_{01}\delta+\alpha_{01}\sigma_1\eta_1(\omega)}{a_1+a_2\delta+a_2\sigma_1\eta_1(\omega)+a_3\sigma_2\eta_2(\omega)+a_4\sigma_3\eta_3(\omega)}}\Big)$ is this "random" circle.

Since the noises η_i, $i = 1, 2, 3$ are not ergodic, the bifurcation diagrams depend on the sample path (i.e. on the random realization ω). However, for the values of the parameters corresponding to the aeroelastic model considered in this chapter and for small values for $|\delta| \ll 1$, $0 < \sigma_i \ll 1$, $i = 1, 2, 3$, because the noises η_i, $i = 1, 2, 3$ are uniformly distributed on $[-1, 1]$, the bifurcation diagram is in many cases independent on the sample path.

Cases studies

To illustrate the previous bifurcation scenarios, we consider three case studies representing aeroelastic models with cubic structural non-linearities. The values of the system parameters [9] are $\mu = 100$, $a_h = -0.5$, $x_\alpha = 0.25$, $\tilde{\omega} = 0.4$, $r_\alpha = -0.5$, $U_L = 5.23376$, $\zeta_\xi = 0$ and $\zeta_\alpha = 0$. We consider the combinations of the plunge and pitch coefficients of the stiffness terms β_1, β_2, β_3 and β_4 shown in Table. 1. For the deterministic aeroelastic dynamical system with the same parameters setting, Cases 1 and 2 were studied in [9], and Case 3 was studied in [8]. Recalling that $\delta = 1 - (U_L^*/U^*)^2$, for the deterministic system given in Eq. (2.1), we know that when $\delta < 0$ (i.e. $U^*/U_L < 1$) the dynamical system converges to a steady solution, and when $\delta > 0$ (i.e. $U^*/U_L > 1$), we have LCOs.

For Case 1, non-linearities are present in both pitch and plunge stiffness terms, and for Cases 2 and 3 cubic restoring forces are considered only in the pitch degree of

Table 1: Cases studies

Case	β_1	β_2	β_3	β_4
1	1	1	1	4
2	1	0	1	3
3	1	0	1	0.3

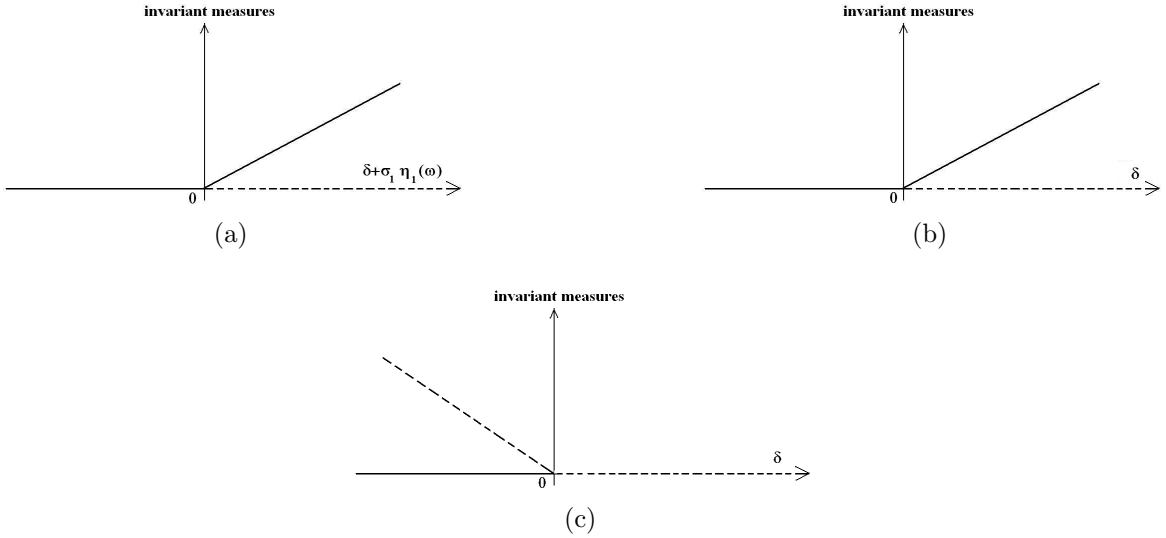

Figure 4: Stochastic bifurcation: (a) Case study 1 for $0 < \sigma_i \ll 1$, $i = 1, \ldots, 3$ (b) Cases studies 2 and 3 for $0 < \sigma_3 \ll 1$ (c)Case study 3 for $0.3 < \sigma_3 < 1$, $-0.00006117092055 - 0.000366081350\delta - 0.0002039030684\sigma_3\eta_3(\omega) > 0$.

freedom ($\beta_2 = 0$), so in these two cases only one random variable is included ($\sigma_1 = \sigma_2 = 0$). Small perturbations with $\sigma_2 \ll 1$ and $\sigma_3 \ll 1$ in the cubic coefficients do not lead to unstable motions for Cases 1 and 2, because we have strong structural non-linearities in the pitch degree of freedom ($\beta_4 > 1$), and the aeroelastic random dynamical system is restricted to the bifurcation diagrams in Fig. 4 (a) and (b). For Case 3, only a weak cubic non-linearity ($\beta_4 = 0.3$) is considered, and different types of random dynamical behavior can be expected for various values of the noise intensity $\sigma_3 \ll 1$.

For Case 1, the truncated center equation of the normal form corresponding to Eq.

(3.16) with $\mathbf{Y}_c = (y_1, y_2)^T$ is given by

$$\begin{aligned}
y_1^{'} &= (-0.11922586 - 0.107901555\delta - 0.10790155\sigma_1\eta_1)y_2 + (0.110675736\delta \\
&+ 0.11067573\sigma_1\eta_1)y_1 + (0.001459301 + 0.0006154173\eta_3\sigma_3 \\
&+ 0.00007900853\eta_2\sigma_2 - 0.014640646\delta - 0.01464064\sigma_1\eta_1){y_2}^3 \\
&+ (-0.003958199 - 0.001311882\eta_3\sigma_3 + 0.001289329\eta_2\sigma_2 - 0.017983576\delta \\
&- 0.01798357\sigma_1\eta_1)y_1{y_2}^2 + (0.003175896 + 0.0009321777\eta_3\sigma_3 \\
&- 0.0005528146\eta_2\sigma_2 + 0.023882116\delta + 0.02388211\sigma_1\eta_1){y_1}^2y_2 \\
&+ (-0.0008041554 - 0.0002207909\eta_3\sigma_3 + 0.00007900853\eta_2\sigma_2 \\
&- 0.025845396\delta - 0.02584539\sigma_1\eta_1)y_1^3,
\end{aligned} \tag{3.48}$$

$$\begin{aligned}
y_2^{'} &= (0.11922586 - 0.064798753\delta - 0.064798753\sigma_1\eta_1)y_1 + (0.081478506\delta \\
&+ 0.081478506\sigma_1\eta_1)y_2 + (-0.0009378495 - 0.00028533270\eta_3\sigma_3 \\
&+ 0.0002034812\eta_2\sigma_2 + 0.008750621\delta + 0.008750621\sigma_1\eta_1){y_2}^3 \\
&+ (0.002171234 + 0.0006082423\eta_3\sigma_3 - 0.0002617347\eta_2\sigma_2 + 0.007074308\delta \\
&+ 0.007074308\sigma_1\eta_1)y_1{y_2}^2 + (-0.001616561 - 0.0004321958\eta_3\sigma_3 \\
&+ 0.0001122217\eta_2\sigma_2 - 0.009777089\delta - 0.009777089\sigma_1\eta_1){y_1}^2y_2 \\
&+ (0.0003934322 + 0.0001023677\eta_3\sigma_3 - 0.00001603878\eta_2\sigma_2 \\
&+ 0.011959696\delta + 0.01195969\sigma_1\eta_1)y_1^3.
\end{aligned} \tag{3.49}$$

Thus, for the linear transformation defined in Eq. (3.19), we have $b_{12} = -0.11922586 - 0.10790155\delta - 0.10790155\sigma_1\eta_1$ and $b_{21} = 0.11922586 - 0.064798753\delta - 0.064798753\sigma_1\eta_1$. Since $\eta_1 \in [-1, 1]$, notice that for any value of δ very close to zero and for any $0 < \sigma_1 \ll 1$, $\sigma_1\eta_1 \neq -1.10495 - \delta$ and $\sigma_1\eta_1 \neq 5.532163 + \delta$. Consequently $b_{12} \neq 0$ and $b_{21} - b_{12} \neq 0$, the matrix NP given in Eq. (3.19) is invertible.

Transforming the truncated center equations into the normal form in polar coordinates, we obtain the following equations:

$$
\begin{aligned}
r' &= (0.096077122\delta + 0.096077122\sigma_1\eta_1)r + r^3(-0.00067504 - 0.0047343\delta \\
&\quad - 0.0047343\sigma_1\eta_1 - 0.00020390\sigma_2\eta_2 + 0.00014056\sigma_3\eta_3)
\end{aligned} \tag{3.50}
$$

$$
\begin{aligned}
\theta' &= (0.119225 + 0.02155514\delta + 0.0215514\sigma_1\eta_1) + r^2(-0.000262641 \\
&\quad + 0.00449096\delta + 0.00449096\sigma_1\eta_1 - 0.000116442\sigma_2\eta_2 + 0.000203129\sigma_3\eta_3).
\end{aligned} \tag{3.51}
$$

Since $\eta_i \in [-1, 1]$, $0 < \sigma_i \ll 1$, $i = 1, 2, 3$ and δ is very close to zero, the bifurcation diagram is the stochastic version of the supercritical Hopf bifurcation encountered in the deterministic case, and is given in Fig. 4 (a). More precisely, if $-0.06983 < \delta + \sigma_1\eta_1(\omega) < 0$, then $0.096077122\delta + 0.096077122\sigma_1\eta_1(\omega) < 0$ and $-0.00067504 - 0.0047343\delta - 0.0047343\sigma_1\eta_1(\omega) - 0.00020390\sigma_2\eta_2(\omega) + 0.00014056\sigma_3\eta_3(\omega) < 0$. Thus, we are in Case (a), and the Dirac measure δ_0 is the unique invariant measure, and it is stable. If $\delta + \sigma_1\eta_1(\omega) > 0$ then $0.096077122\delta + 0.096077122\sigma_1\eta_1(\omega) > 0$ and $-0.00067504 - 0.0047343\delta - 0.0047343\sigma_1\eta_1(\omega) - 0.00020390\sigma_2\eta_2(\omega) + 0.00014056\sigma_3\eta_3(\omega) < 0$. Thus, we are in Case (b) with two invariant measures: the Dirac measure δ_0, which is unstable, and the stable measure μ_ω which is the Lebesgue measure

$$
\text{Leb}\left(\sqrt{\frac{-0.096077(\delta + \sigma_1\eta_1)}{-0.000675 - 0.004734(\delta + \sigma_1\eta_1) - 0.000203\sigma_2\eta_2 + 0.00014\sigma_3\eta_3}}\right). \tag{3.52}
$$

In the deterministic case, the bifurcation point is $\delta = 0$, but from Fig. 4(a), we note that in the stochastic case it is $\delta = -\sigma_1\eta_1(\omega)$, so it shifts around zero depending on the random value $\eta_1(\omega)$. However, for any sample path the asymptotic state of the system is a limit cycle oscillation for any $\delta > \sigma_1$.

For Cases 2 and 3, we have non-linearities only in pitch, and we consider only one random variable ($\sigma_1 = \sigma_2 = 0$). Since the only uncertainty is in the coefficient of the cubic term in pitch, the linear transformation defined in Eq. (3.19) is no longer stochastic, For both cases, we can reduce the truncated center equation of the normal form to the form given in equations (3.27)-(3.28).

For Case 2, we obtain the following equations in polar co-ordinates:

$$r' = 0.096077122\delta r + r^3(-.0006117092055 - 0.00366081350\delta - 0.0002039030684\sigma_3\eta_3) \tag{3.53}$$

$$\theta' = (0.119225 + 0.0215514\delta) + r^2(-0.0003493282 + 0.0046860370\delta - 0.0001164427486\sigma_3\eta_3). \tag{3.54}$$

If $-0.1 < \delta < 0$, then $0.096077122\delta < 0$ and $-.0006117092055 - 0.00366081350\delta - 0.0002039030684\sigma_3\eta_3 < 0$ for any $\sigma_3 \ll 1$ and any random realization of $\eta_3 \in [-1, 1]$. Thus, the bifurcation corresponds to Case (a), and the Dirac measure δ_0 is the unique invariant measure which is stable. If $\delta > 0$, then $0.096077122\delta > 0$ and $-.0006117092055 - 0.00366081350\delta - 0.0002039030684\sigma_3\eta_3 < 0$ for any value $\sigma_3 \leq 3$, so we have two invariant measures (Case (b)): the Dirac measure δ_0 (which is unstable) and the stable measure

$$\mu_\omega = \text{Leb}\left(\sqrt{\frac{-0.096077122\delta}{-.0006117092055 - 0.00366081350\delta - 0.0002039030684\sigma_3\eta_3}}\right). \tag{3.55}$$

The bifurcation diagram is similar with the one corresponding to Case 1, but this time the bifurcation point is $\delta = 0$, the same as in the deterministic case (see Fig. 4 (b)).

For Case 3, only a weak cubic non-linearity is considered in the pitch stiffness term. The following stochastic normal form of the Hopf bifurcation is obtained

$$r' = 0.096077122\delta r + r^3(-0.00006117092055 - 0.000366081350\delta - 0.0002039030684\sigma_3\eta_3) \tag{3.56}$$

$$\theta' = (0.119225 + 0.0215514\delta) + r^2(-0.00003493282 + 0.0004686037\delta - 0.0001164427486\sigma_3\eta_3). \tag{3.57}$$

Here, even for small values of the noise intensity $\sigma_3 < 1$, we may have different stochastic bifurcation diagrams (see the stochastic diagrams in Fig. 4 (b), (c)). For lower noise intensity $\sigma_3 < 0.3$, we have $-0.00006117092055 - 0.0002039030684\sigma_3\eta_3 < 0$ for any random realization of $\eta_3 \in [-1, 1]$. Thus for $U^*/U_L > 1$ (i.e. $\delta > 0$), we have

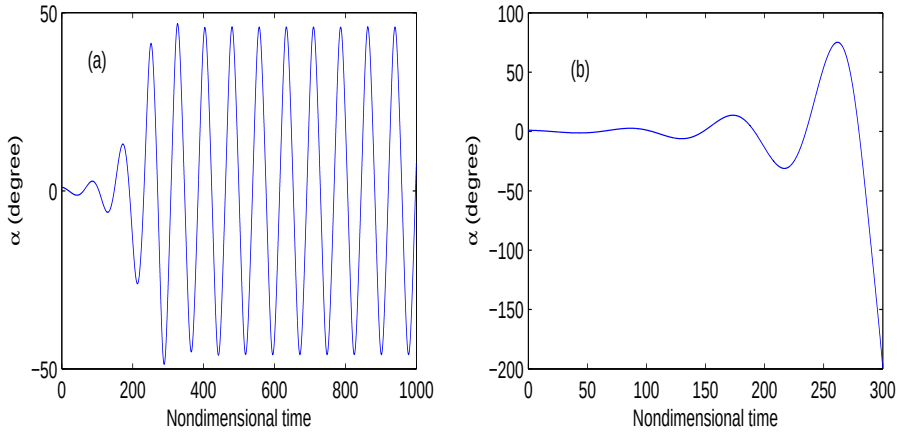

Figure 5: Pitch sample path for Case study 3 with (a) $\sigma_2 = 0.25, \eta_3 \approx 0.348$ and (b) $\sigma_2 = 0.4, \eta_3 \approx -0.823$.

stable LCOs with random amplitude and frequency (see Fig. 5(a)). Hence, bifurcation is in Case (b). For this case, we have two invariant measures, the unstable Dirac measure δ_0 and the stable measure

$$\mu_\omega = \text{Leb}\left(\sqrt{\frac{-0.096077122\delta}{-.00006117092055 - 0.000366081350\delta - 0.0002039030684\sigma_3\eta_3}}\right). \tag{3.58}$$

Thus, for very small values of $\sigma_3 \ll 1$, the bifurcation diagram is the same as shown for Case 2 (see Fig. 4 (b)).

However, if $0.3 < \sigma_3 \ll 1$ and $U^*/U_L > 1$ (i.e. $\delta > 0$), then there are sample paths for which $-0.00006117092055 - 0.000366081350\delta$ - $0.0002039030684\ \sigma_3\eta_3 > 0$. The unique invariant measure δ_0 is unstable, and we may have divergent solutions for some realizations of the random variable ϵ_2 (see Fig. 5(b)). For these sample paths, $-0.00006117092055 - 0.000366081350\delta - 0.0002039030684\sigma_3\eta_3 > 0$ and for $\delta < 0$, we have a transition from Case (d) to Case (c) when $\delta = 0$ (see the bifurcation digram in Fig. 4 (c)). In the deterministic case this would correspond to a transition from steady solutions to unstable solutions, and this sub-critical Hopf bifurcation behavior never occurs for the nonlinear deterministic system with this parameter setting.

3.3 Numerical simulations

In this section, we apply the stochastic normal to predict the frequency and amplitude of the LCOs. Since $r^{'} = 0$ and $\theta^{'} \neq 0$ corresponds to a periodic orbit in (3.27)- (3.28), the frequency of the LCOs is estimated by the relation below:

$$\theta = \beta_{00} + \beta_{01}\delta + \beta_{01}\sigma_1\eta_1 - \frac{(a_1 + a_2\delta + a_2\sigma_1\eta_1 + a_3\sigma_2\eta_2 + a_4\sigma_3\eta_3)}{b_1 + b_2\delta + b_2\sigma_1\eta_1 + b_3\sigma_2\eta_2 + b_4\sigma_3\eta_3})(\alpha_{01}\delta + \alpha_{01}\sigma_1\eta_1). \tag{3.59}$$

where a_i, b_i, $i = 1, \ldots, 4$ were defined at the beginning of Section 3.2.

To determine the pitch and plunge amplitudes of the LCOs, the following equations given by Lee et al. [7] are used

$$A = \frac{n_1^2 + s_1^2}{m_1^2 + (p_1 + q_1 r_\varsigma^2)^2}, \tag{3.60}$$

$$r_\varsigma^2 = AR_\alpha^2, \tag{3.61}$$

$$R_\alpha^2 = \frac{1}{q_2}(-s_2 \pm \sqrt{(p_2^2 + m_2^2)A - n_2^2}), \tag{3.62}$$

where r_ς and R_α denote the amplitude of the plunge motion ς and the pitch motion α, respectively, and $m_1, n_1, \ldots$ are functions of the system parameters and the frequency θ. The explicit definitions are given in [7].

Due to the presence of the random variables in equations (3.59) - (3.62), MCS are applied to provide the statistical information of the random frequency and amplitude of the LCOs. To verify the accuracy of these results obtained using the stochastic normal form, the frequency and amplitude predictions are compared with those obtained by the numerical simulation of the solutions of the random differential Eq. (3.3) with 10^4 samples, where for each sample the corresponding deterministic system is solved using an adaptive fourth order Runge-Kutta numerical scheme.

To demonstrate the validation of the stochastic normal form, we consider various combinations of the plunge and pitch stiffness terms coefficients β_1, β_2, β_3 and β_4 shown in the previous section in Table. 1.

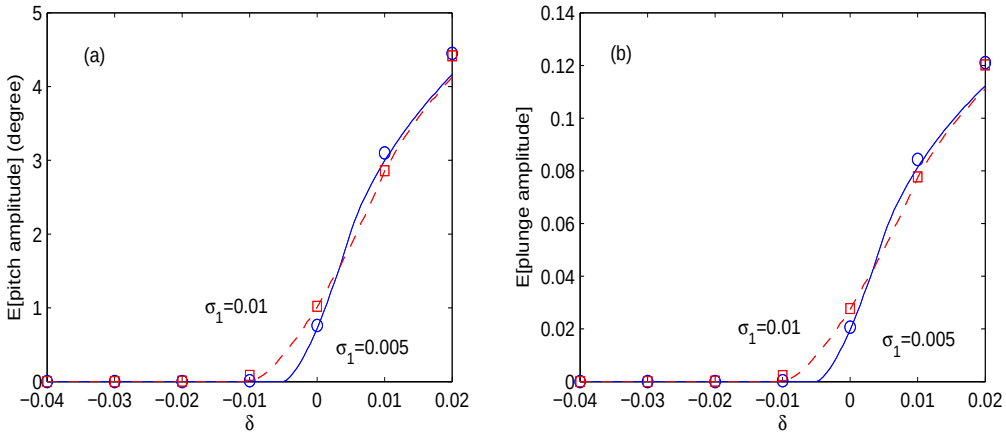

Figure 6: Expected dynamical response for Case study 1 with $\sigma_2 = 0.8$ and $\sigma_3 = 0.8$: line : stochastic norm form; circle or square: MCS.

Fig. 6 presents the expected dynamical response with different linear random perturbation for Case 1. In this case study, we have an aeroelastic system with cubic non-linearities in both the pitch and the plunge degrees of freedom, and the uncertainties in the cubic and the bifurcation parameters. The truncated normal form is given in equations (3.50)-(3.51), and the bifurcation diagram for this aeroelastic system is displayed in Fig. 4(a).

Fig. 6 shows that the stochastic norm form provides a good agreement with the expected pitch/plunge amplitude around the Hopf bifurcation. From the previous section, we know that the stochastic Hopf bifurcation point is shifted from the deterministic value $\delta = 0$ to $\delta = -\sigma_1\eta_1$. Thus the noise intensity, σ_1, influences the bifurcation position. We observe that the difference in the expected amplitude for various noise intensities, σ_1, is only noticeable around the Hopf bifurcation point; for some random realizations of η_1, the system convergences to a steady state, but not a LCO. However, for $\sigma_1 < \delta \ll 1$, the asymptotic state is a LCO for any sample path. Fig. 6 also shows that the expected dynamical response of the aeroelastic system becomes less sensitive to the small noise intensity σ_1. Actually, for $0.01 < \delta \ll 1$, the expected pitch amplitude (or the expected plunge amplitude) has almost the same values for $\sigma_1 = 0.005$ and $\sigma_1 = 0.01$.

In Case 2, we consider an aeroelastic system with structural non-linearity only in the pitch degree of freedom with one random variable ($\sigma_1 = \sigma_2 = 0$). The truncated normal form in polar coordinates is given in equations (3.53)-(3.54), and the bifurcation diagram is given in Fig. 4 (b). Recalling that $\delta = 1 - (U_L^*/U^*)^2$, since the influence of the parameter uncertainties on the amplitude and the frequency of the LCOs is of interest to the present study, we only investigate the performance of the stochastic normal form around $0 < \delta \ll 1$, i.e. when the speed U^* is slightly over the linear flutter speed $U_L = 5.23376$.

In Fig. 7, we display the predicted mean amplitudes and frequencies for the pitch motion corresponding to $\sigma_3 = 0.8$, 0.3, and 0.001. The estimated values are compared with the results obtained from MCS, and a good agreement in predicting the dynamical responses is shown.

To illustrate the influence of noise, the expected pitch amplitudes for various value of σ_3 are compared in Fig.8(a). It is clear that the expected value of the pitch amplitude increases only very slightly when σ_3 increases, $\sigma_3 < 1$. Moreover, the results displayed in Fig. 8(a) are very close to the results obtained for the deterministic dynamical system ($\sigma_3 = 0$), as reported in Fig. 2 in [9]. However, for larger values of $\sigma_3 > 1$, an increase in the expected value of the pitch amplitude has been observed [12]. The results displayed in Fig.8(b) indicate that there is no difference between the expected values of the LCOs frequencies for various values of σ_3.

To better investigate the influence of the random noise with small intensity on the LCO's amplitude, Fig.9 displays the probability density functions of the pitch amplitude at a fixed speed $U^* = 1.01U_L$. The estimations obtained using MCS and the stochastic normal form are very similar, and we can see that although there is almost no difference between the expected values of the pitch amplitudes, the range of the random pitch amplitude increases with the value of σ_3.

In Case 3, we have a weak cubic non-linearity in the pitch degree of freedom. The truncated normal form is given in equations (3.56)- (3.57). Depending on the

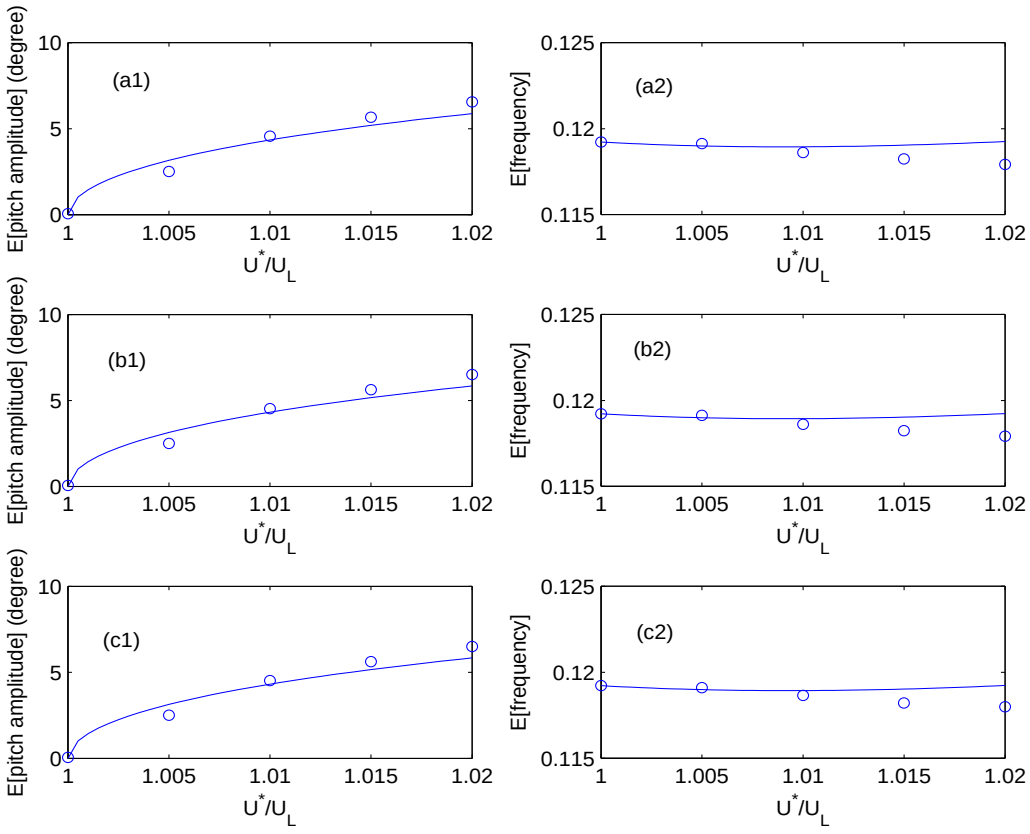

Figure 7: Expected dynamical response for Case study 2 with (a)$\sigma_3 = 0.8$; (b)$\sigma_3 = 0.3$; (c)$\sigma_3 = 0.001$: —, stochastic normal form; ∘ ∘ ∘, MCS.

noise intensity the bifurcation diagram shows supercritical (see Fig. 4 (b)) or unstable subcritical behaviors (see Fig. 4 (c)). Since we are interested in the influence of noise on the amplitude and frequency of the LCOs, in what follows we only consider values of $\sigma_3 < 0.3$ and U^* is slightly over the linear flutter speed $U_L = 5.23376$.

The expected values of the pitch amplitude and frequency obtained using the stochastic normal form and MCS are very similar (see Fig.10). Unlike the previous two cases, from the results displayed in Fig.11(a), we note that the expected value of the pitch amplitude obviously increases with the noise intensity σ_3, even for small values of $\sigma_3 < 0.3$.

From Figs. 8(b) and 11(b), we observe that the expected values of the frequency

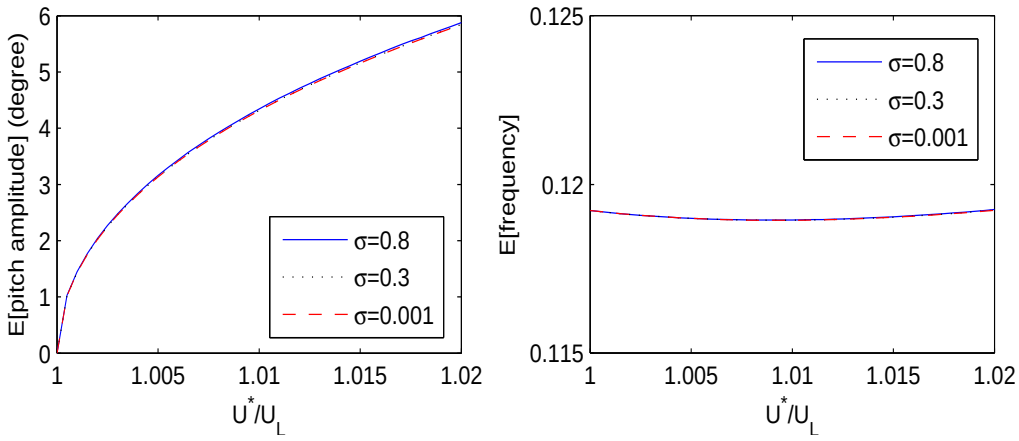

Figure 8: Expected values of (a) pitch amplitude and (b) frequency for Case study 2 estimated using stochastic normal form.

are almost the same in Case 2 and Case 3, and the noise intensity σ_3 has very little influence. The fact that the frequency variation with U^*/U_L is almost the same was also noticed [9] for the deterministic models corresponding to Cases 2 and 3, and it is a consequence of having the same values for the linear parameters, and having different values only for the values of the cubic parameters. To explain this analytically for the stochastic models corresponding to Cases 2 and 3, the frequency formula (3.59) is expressed explicitly in terms of β_4, δ, σ_3 and η_3

$$\begin{aligned}\theta = &\frac{0.0001164427486(\beta_4 - 0.001562012573\beta_4\delta + \sigma_3\eta_3)}{0.0002039030684(\beta_4 + 0.001220271180\beta_4\delta + \sigma_3\eta_3)} \\ &+ 0.119225 + 0.0215514\delta - 0.096077122\delta,\end{aligned} \tag{3.63}$$

where $\beta_4 = 3$ in Case 2 and $\beta_4 = 0.3$ in Case 3. Since η_3 is uniformly distributed on $[-1, 1]$, taking expectation we get the following estimation for the expected value of the frequency:

$$\begin{aligned}&\frac{0.532179\beta_4\delta^2}{\sigma_3}\ln\left(\frac{0.509758\beta_4 + 0.509758\sigma_3 + 3.050678\beta_4\delta}{0.509758\beta_4 - 0.509758\sigma_3 + 3.050678\beta_4\delta}\right) + 0.119225 \\ &- 0.033315\delta \approx 0.119225 - .033315\delta,\end{aligned} \tag{3.64}$$

for $0 < \delta, \sigma_3 << 1$. The approximation (3.64) provide an explanation of the fact that the cubic term and the noise intensity have very little influence on the expected value

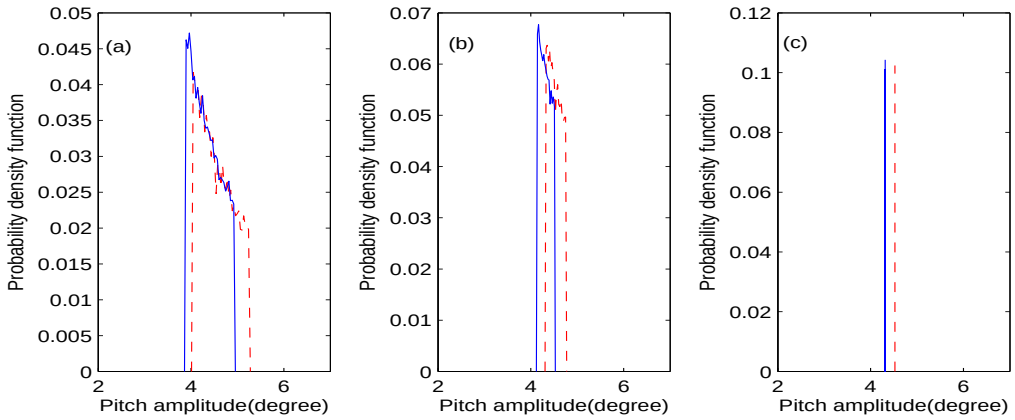

Figure 9: Probability density function of pitch amplitude of the aeroelastic system with (a)$\sigma_3 = 0.8$; (b)$\sigma_3 = 0.3$; (c)$\sigma_3 = 0.001$ for Case study 2 when $U^* = 1.010U_L$: —, stochastic normal form; - -, MCS.

of frequency around the Hopf bifurcation.

3.4 Conclusion

In this chapter, the stochastic normal form is presented and applied to an aeroelastic random dynamical system with uncertainties in the bifurcation parameter and the plunge and pitch non-linear terms. Using the stochastic normal form equations in polar coordinates, we are able to obtain analytically the stochastic bifurcation diagrams depending on the values of the noise intensities and the flow speed. Moreover, when the system behavior is characterized by limit cycles oscillations, the stochastic normal form can be used to study the influence of the noise on the limit cycle oscillation amplitudes and frequencies. After considering various combinations of values for the coefficients of the cubic terms in pitch and plunge, we conclude that the stochastic normal form gives accurate results for predicting the mean of the limit cycle oscillation amplitude and frequency for noise with small intensity.

The main effect of uncertainties in the deterministic bifurcation parameter is the shifting of the bifurcation point depending on the noise intensity and the sample path.

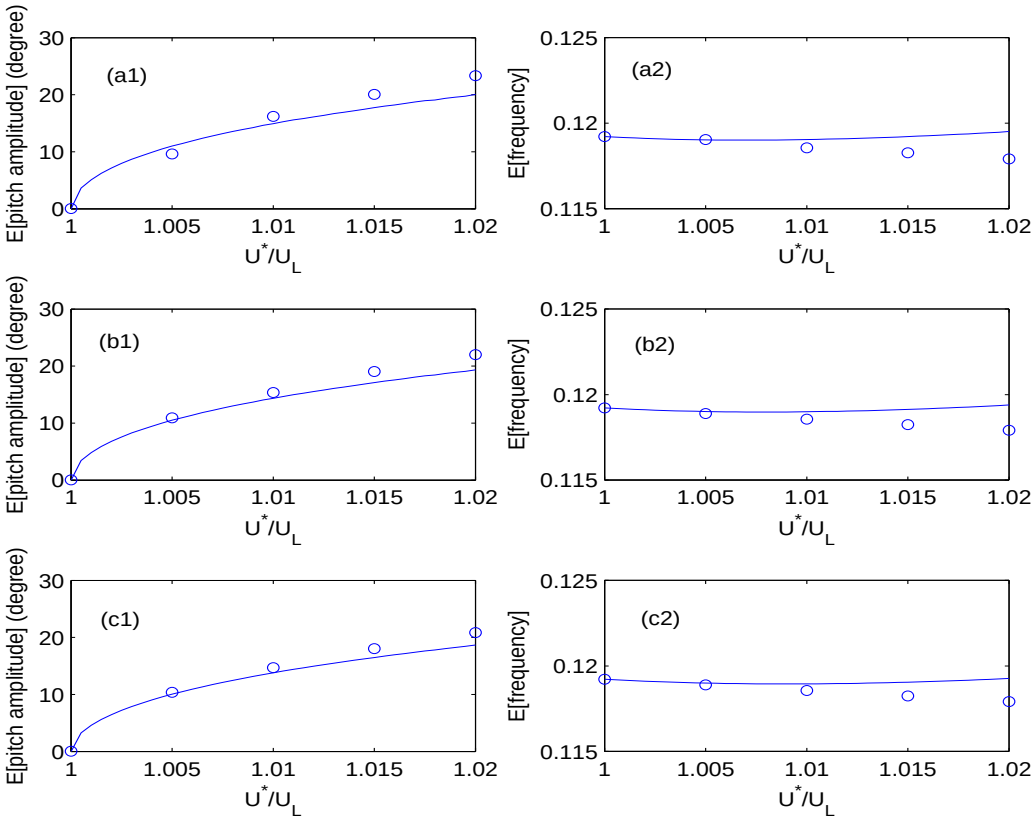

Figure 10: Expected dynamical response for Case study 3 with (a)$\sigma_2 = 0.25$; (b)$\sigma_2 = 0.2$; (c)$\sigma_2 = 0.1$: —, stochastic normal form; ∘ ∘ ∘, MCS.

Consequently, the onset of the limit cycle oscillations may occur at flow speeds less than the deterministic linear flutter speed.

When we have only one non-linearity in the pitch degree of freedom and using the stochastic normal form, we confirm the numerical results presented in [12]. Moreover, we provide a theoretical explanation why the noise with small intensity does not influence the limit cycle oscillation frequency. We also extend the study to aeroelastic systems with uncertainties in the coefficients of the cubic terms of both pitch and plunge, and notice again that the presence of noise with small intensity has very little effect on the mean frequency.

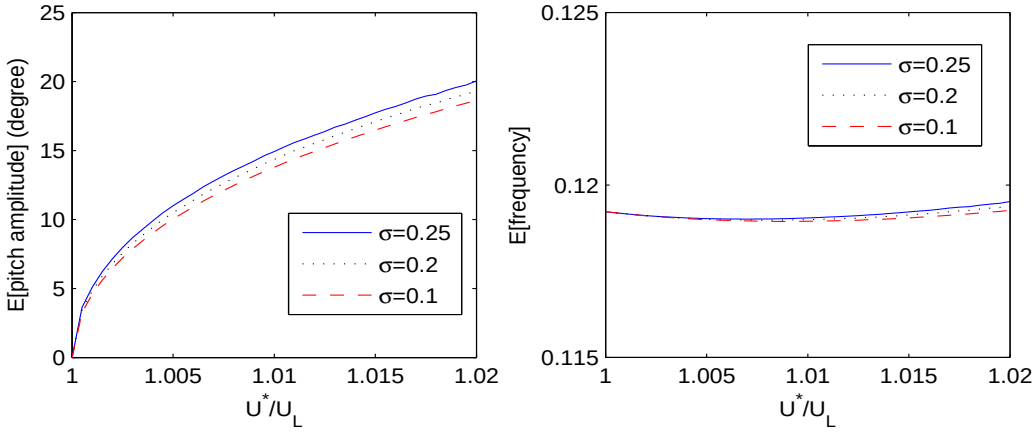

Figure 11: Expected values of (a) pitch amplitude and (b) frequency for Case study 3 estimated using stochastic normal form.

Previous numerical studies [12] show that the amplitude of the limit cycle oscillations increases with the noise intensity for aeroelastic systems with only one non-linearity in the pitch degree of freedom. We notice the same behavior for systems characterized by the noise with small intensity and weak structural non-linearities. Moreover, the study of the stochastic bifurcation shows that in this case the divergent solutions can happen for certain relatively small values of the noise intensity. On the other hand, for noise with small intensity and stronger cubic structural non-linearities, the effect on the limit cycle oscillation amplitude becomes small, and no divergent solution exists. Thus the effect of the noise on the behavior of the aeroelastic system is dependent on the strength of the structural non-linearity. Numerically this dependence can be illustrated by extensive simulations, but theoretically it can be easily analyzed using the stochastic bifurcation study presented in this chapter.

Bibliography

[1] L. Arnold. *Random Dynamical Systems*. Springer-Verlag, Berlin, 2003.

[2] L. Arnold, W. Hortsthemke, and J.W. Stucki. The influence of external real and

white noise on the Lotka-Volterra model. *Biom. Jounral.*, 21(5):451–471, 1979. Article ID 394387.

[3] L. Arnold, N.S. Namachchivaya, and K.R. Schenk-Hoppe. Toward an understanding of stochastic Hopf bifurcation: a case study. *International Journal of Bifurcation and Chaos*, 6(11):1947–1975, 1996. Article ID 394387.

[4] P.S. Beran, C.L. Pettit, and D.R. Millman. Uncertainty quantification of limit-cycle oscillations. *Journal of Computational Physics*, 217:217–247, 2006.

[5] J. Deng, C. Anton, and Y. S. Wong. Stochastic collocation method for secondary bifurcation of a nonlinear aeroelastic system. *Journal of Sound and Vibration*, 330:3006–3023, 2011.

[6] J. Deng, C. Anton, and Y. S. Wong. Uncertainty investigations in nonlinear aeroelastic systems. *Journal of Computational and Applied Mathematics*, 235:3910–3920, 2011.

[7] B. H. K. Lee, L. Y. Jiang, and Y. S. Wong. Flutter of an airfoil with a cubic nonlinear restoring force. *Journal of Fluids and Structures*, 13:75–101, 1999.

[8] B. H. K. Lee, S. J. Price, and Y. S. Wong. Nonlinear aeroelastic analysis of airfoils: bifurcation and chaos. *Progress in Aerospace Sciences*, 35:205–334, 1999.

[9] L. Liu, Y. S. Wong, and B. H. K. Lee. Application of the centre manifold theory in nonlinear aeroelasticity. *Journal of Sound and Vibration*, 234:641–659, 2000.

[10] S. Orey. Stationary solutions for linear systems with additive noise. *Stochastics*, 5:241–251, 1981. Article ID 394387.

[11] S. Wiggins. *Introduction to Applied Nonlinear Dynamical Systems and Chaos*. Springer-Verlag, Berlin, 1996.

[12] J. A. S. Witteveen and H. Bijl. Higher periodic stochastic bifurcation of nonlinear airfoil fluid-structure interaction. *Mathematical Problems in Engineering*, pages 1–26, 2009. Article ID 394387.

[13] K. Xu. Bifurcations of random differential equations in dimension one. *Random and Computational Dynamics*, 1(3):277–305, 1993.

Chapter 4

Secondary Bifurcation Analysis Using Stochastic Collocation Method

For an aeroelastic system modeling an airfoil oscillating in pitch and plunge, the uncertainties arise due to inexact values of the system parameters and/or the perturbations in the initial conditions. To perform a realistic simulation, we propose a mathematical model expressed as a system of random equations instead of the traditional formulation based on a deterministic system. A stochastic collocation method is developed to investigate the effect of the uncertainties in the aeroelastic model. In this study, particular attention is focused on the nonlinear behavior when a jump phenomenon between the Hopf and the secondary bifurcations occurs.

Several UQ aeroelastic investigations focusing on LCOs and the Hopf bifurcation analysis were reported. A special non-intrusive polynomial chaos formulation based on normalizing the oscillatory samples in terms of their phases was applied in Ref. [17]. The aeroelastic model is constructed starting from the same deterministic model as considered in our studies, but with uncertainty represented by a symmetric beta distribution in either the coefficient of the cubic pitch stiffness, or the initial pitch angle $\alpha(0)$, or the ratio of the natural frequencies $\bar{\omega}$. An intrusive polynomial chaos expansion and the method of multiple scales are used in Ref. [6] to determine the effect of the variations of the linear and nonlinear pitch and plunge coefficients on the stability near the Hopf bifurcation. In the series of papers [14, 12, 11, 1] different types of

chaos expansions are employed for a two DOF aeroelastic model, but with a structural nonlinearity in pitch represented by a fifth degree polynomial and the uncertainties expressed by Gaussian random variables included in the initial pitch angle $\alpha(0)$ and the coefficient of the cubic term in the pitch stiffness. Since the traditional polynomial chaos expansions produce inaccurate oscillatory motion for long time simulations [14], the dependence of the LCOs erupting from the Hopf bifurcations on random parameters was studied using other bases for the stochastic projection method, such as the Fourier chaos [11], the multivariate B-spline [12], and a local Wiener-Haar wavelet expansion [14, 1].

An alternative approach was proposed in our previous study [3] using a stochastic collocation method (SCM), in which the randomness is included through the interpolation of the corresponding solutions of the deterministic system computed at selected values of the uncertainty. The performance of the SCM was compared with various types of chaos expansions. For long time simulations and applications to discontinuous problems, the SCM gives more accurate results than the polynomial or the Fourier chaos expansions. Its performance is similar with the local Wiener-Haar wavelet expansion, but the attractive feature is that the implementation is straightforward because the SCM requires only the use of a deterministic solver [19].

The present study is a follow up investigation of our early work reported in [3], and the major contribution presented here is the application of the SCM for multidimensional UQ problems in the secondary bifurcation. To the best of our knowledge, only a few results are available for aeroelastic response with multidimensional uncertainties. Here, we extend the study presented in Ref. [17] for parameter uncertainty expressed by more than one random variable. We study the nonlinear response in the presence of two random variables due to uncertainties in the initial pitch angle and the coefficients of the nonlinear restoring force. We also analyze the influence of the parameter uncertainty expressed by a combination of five random variables on the LCO behavior. An

improved version of the SCM is presented, in which higher order schemes such as piecewise cubic interpolation and piecewise cubic spline interpolation are used. Moreover, in order to effectively deal with multidimensional random variables, the traditional approach based on a tensor product for interpolation in multidimensional spaces is now replaced by an efficient sparse grid strategy incorporating the Smolyak algorithm and a dimension adaptive approach [15, 19, 10, 13, 5].

In this section, we consider a linear plunge stiffness term $G(x_3) = x_3$, and the nonlinear pitch stiffness term $M(x_1)$ is defined as a cubic spring:

$$M(x_1) = x_1 + k_3 x_1^3, \tag{4.1}$$

where k_3 is a constant for the deterministic model.

We apply the stochastic collocation method to study three different models with uncertainties in the coefficient k_3 of the cubic term and the initial condition $\alpha(0)$. First we introduce a random perturbation in the cubic nonlinearity in the pitch restoring force,

$$k_3(\xi) = [k_3]_0 + [k_3]_1 \xi \tag{4.2}$$

where $[k_3]_0 = 80$, $[k_3]_1 = 8$ and ξ is a uniform random variable on $[-1, 1]$. For this model, we compare the performance of various implementations of the stochastic collocation based on different interpolation methods near the Hopf and the secondary bifurcation points. Since the onset of the secondary bifurcation depends on the initial condition [9], we also consider a model with randomness in both the cubic coefficient and the initial pitch angle:

$$\begin{aligned} \alpha_0 &= [\alpha_0]_0 + [\alpha_0]_1 \xi_1 \\ k_3(\xi_2) &= [k_3]_0 + [k_3]_1 \xi_2 \end{aligned} \tag{4.3}$$

where $[\alpha_0]_0 = 0°, [\alpha_0]_1 = 5°$, $[k_3]_0 = 80$, $[k_3]_1 = 8$, and ξ_1 and ξ_2 are two independent random variables, ξ_1 uniformly distributed on [0,1] and ξ_2 uniformly distributed on [-1,1]. Finally, to simulate a more realistic type of noise and to test the performance of the proposed stochastic collocation method for higher dimensional problems, we

express the nonlinear coefficient k_3 by a time dependent combination of five random variables:

$$k_3(\tau, \xi) = \overline{k_3} + \widetilde{k_3}(\tau, \xi). \tag{4.4}$$

where $\overline{k_3}$ is a constant and $\widetilde{k_3}(\tau, \xi)$ is the noise with the following expression:

$$\widetilde{k_3}(\tau, \xi) = \sigma \sum_{i=1}^{5} \frac{1}{i^2\pi^2} cos(2\pi i\tau)\xi^i \tag{4.5}$$

where $\xi^i, i = 1, 2, \ldots, 5$ are independent uniformly distributed random variables on $[-1, 1]$.

4.1 Stochastic collocation method

The collocation approach provides a procedure to predict the behavior of a given system at a fixed time by interpolation. To illustrate the numerical implementation of the SCM, we consider the following simple random dynamical system:

$$u' = -\alpha(\xi)u, \quad t > 0, \quad u(0) = u_0, \tag{4.6}$$

where the coefficient α is a function of the random variable ξ on the interval $[a, b]$ with the probability density function ρ [18].

Let $\Theta = \{\xi^{(i)}\}_{i=1}^{N} \in [a, b]$ be a set of nodes selected on the interval $[a, b]$ according to a distribution with density ρ, where N is the total number of nodes. Clearly, Eq. (4.6) has to be satisfied at each node for $k = 1, \ldots, N$, so we have the deterministic equations:

$$u'(t) = -\alpha(\xi^{(k)})u, \quad t > 0, \quad u(0) = u_0. \tag{4.7}$$

Solving the differential equation (4.7), we get a deterministic solution $u(t; \xi^{(k)})$ for each sample. Outside the nodal set Θ, the solution $u(t, \xi)$ is estimated by the interpolation based on $u(t; \xi^{(i)})$.

From the well-developed classical theory of univariate Lagrange polynomial interpolation, we know that the convergence of a high degree polynomial interpolation requires

certain degree of smoothness. However, for a problem exhibiting a jump phenomena, even the assumption of continuity may not be satisfied. When using high degree interpolation polynomials, the discontinuity of the predicted function could result in a slow convergence or even divergence (e.g. the Gibbs' phenomenon [16]). Consequently, for the SCM, piecewise interpolation methods are generally preferred.

Although the SCM is an effective numerical scheme for UQ problems, the implementation becomes difficult and inefficient for multidimensional cases, because computing the coefficients of Lagrange polynomials turns out to be a very challenging task. A simple way to overcome this difficulty is to use the tensor product [3]. Although its implementation is straightforward, this approach is not recommended because the number of nodes, and hence the computational time, increases exponentially. Alternatively, we can construct a more efficient multidimensional collocation method using a sparse grid algorithm developed by Smolyak [15]. The sparse grid strategy has been successfully implemented to study various engineering UQ problems [10, 13], and it has been demonstrated that in some applications, it can overcomes the difficulties due to the 'curse of dimensionality' [5].

Without loss of generality, we consider to approximate a function $f : [0.1]^d \to \mathbb{R}$ using the values of the function at some selected nodes. In the one-dimensional case ($d = 1$), the interpolation formula is given by

$$\mathcal{I}^i f = \sum_{x_j^i \in \mathbf{X}^i} f(x_j^i) \delta_{x_j^i}, \tag{4.8}$$

where $\mathbf{X}^i = \{x_j^i \in [0,1], j = 1, \ldots, m_i\}$ is the set of nodes, $i \in \{0\} \cup \mathbb{N}$ is the resolution level that controls the grid, and $\delta_{x_j^i}$ satisfies $\delta_{x_j^i}(x_j^i) = 1$ and $\delta_{x_j^i}(y) = 0$ for $y \neq x_j^i$, $y \in \mathbf{X}^i$. Similarly, using the tensor product, we construct an interpolation formula for multivariate cases ($d > 1$):

$$(\mathcal{I}^{i_1} \otimes \cdots \otimes \mathcal{I}^{i_d}) f = \sum_{x_{j_1}^{i_1} \in \mathbf{X}^{i_1}} \cdots \sum_{x_{j_d}^{i_d} \in \mathbf{X}^{i_d}} f(x_{j_1}^{i_1}, \ldots, x_{j_d}^{i_d}) (\delta_{x_{j_1}^{i_1}} \otimes \cdots \otimes \delta_{x_{j_d}^{i_d}}). \tag{4.9}$$

However, the tensor product produces a large number $m_{i_1} \cdots m_{i_d}$ of nodes, and the

nodal set $\mathbf{X} = \prod_{j=1}^{d} \mathbf{X}^{i_j}$ is referred as the full grid.

To reduce the number of nodes, Smolyak proposed a more flexible selection algorithm [15]. With $\mathcal{I}^0 = 0, \triangle^i = \mathcal{I}^{i+1} - \mathcal{I}^i$, $\mathbf{i} = (i_1, \ldots, i_d)$ $|\mathbf{i}| = i_1 + \cdots + i_d$, and $q \geq 0$, the Smolyak interpolation is presented in [15] as

$$\mathbf{A}_{q,d}(f) = \sum_{|\mathbf{i}| \leq q} (\triangle^{i_1} \otimes \cdots \otimes \triangle^{i_d})(f) = \mathbf{A}_{q-1,d}(f) + \sum_{|\mathbf{i}|=q} (\triangle^{i_1} \otimes \cdots \otimes \triangle^{i_d})(f). \quad (4.10)$$

Due to the recursive structure of Eq. (4.10), $\mathbf{A}_{q-1,d}(f)$, the interpolation results at resolution level $q-1$, are utilized in the construction of the Smolyak algorithm at the resolution level q. If the nodal set on each dimension is nested (i.e. $\mathbf{X}^{i_j-1} \subset \mathbf{X}^{i_j}$) in the construction of the Smolyak algorithm from the resolution level $q-1$ to q, it is only necessary to evaluate the function f on the nodal set $\triangle\mathbf{H}_{q,d}$, given by [4]

$$\triangle\mathbf{H}_{q,d} = \bigcup_{|\mathbf{i}|=q} \triangle X^{i_1} \bigotimes \cdots \bigotimes \triangle X^{i_d}. \quad (4.11)$$

where $\triangle X^0 = \mathbf{X}^0$, $\triangle X^{i_j} = \mathbf{X}^{i_j} \backslash \mathbf{X}^{i_j-1}$). Hence the sparse grid at resolution level q is constructed using the following set of nodes

$$\mathbf{H}_{q,d} = \bigcup_{l=0\ldots q} \triangle\mathbf{H}_{l,d} = \bigcup_{|\mathbf{i}| \leq q} \triangle X^{i_1} \bigotimes \cdots \bigotimes \triangle X^{i_d}. \quad (4.12)$$

Several sparse grid strategies have been reported, and the nested sparse grid with equidistant nodes [10] is used in the present study. Here, x_j^i are defined as

$$x_j^i = \begin{cases} (j-1)/(m_i - 1) & \text{for} \quad j = 1, \ldots, m_i \quad \text{if} \quad m_i > 1, \\ 1/2 & \text{for} \quad j = 1 \quad \text{if} \quad m_i = 1, \end{cases} \quad (4.13)$$

$$m_i = \begin{cases} 1 & \text{if} \quad i = 0, \\ 2^i + 1 & \text{if} \quad i > 0. \end{cases} \quad (4.14)$$

We illustrate the construction of the sparse grid for a two dimensional example ($d = 2$), with resolution levels, $q = 1$ and $q = 2$. At the resolution level $q = 1$, using Eqs. (4.11)-(4.12), we get $\mathbf{H}_{1,2} = \triangle\mathbf{H}_{0,2} \bigcup \triangle\mathbf{H}_{1,2}$, and $\triangle\mathbf{H}_{0,2} = \triangle X^0 \bigotimes \triangle X^0$,

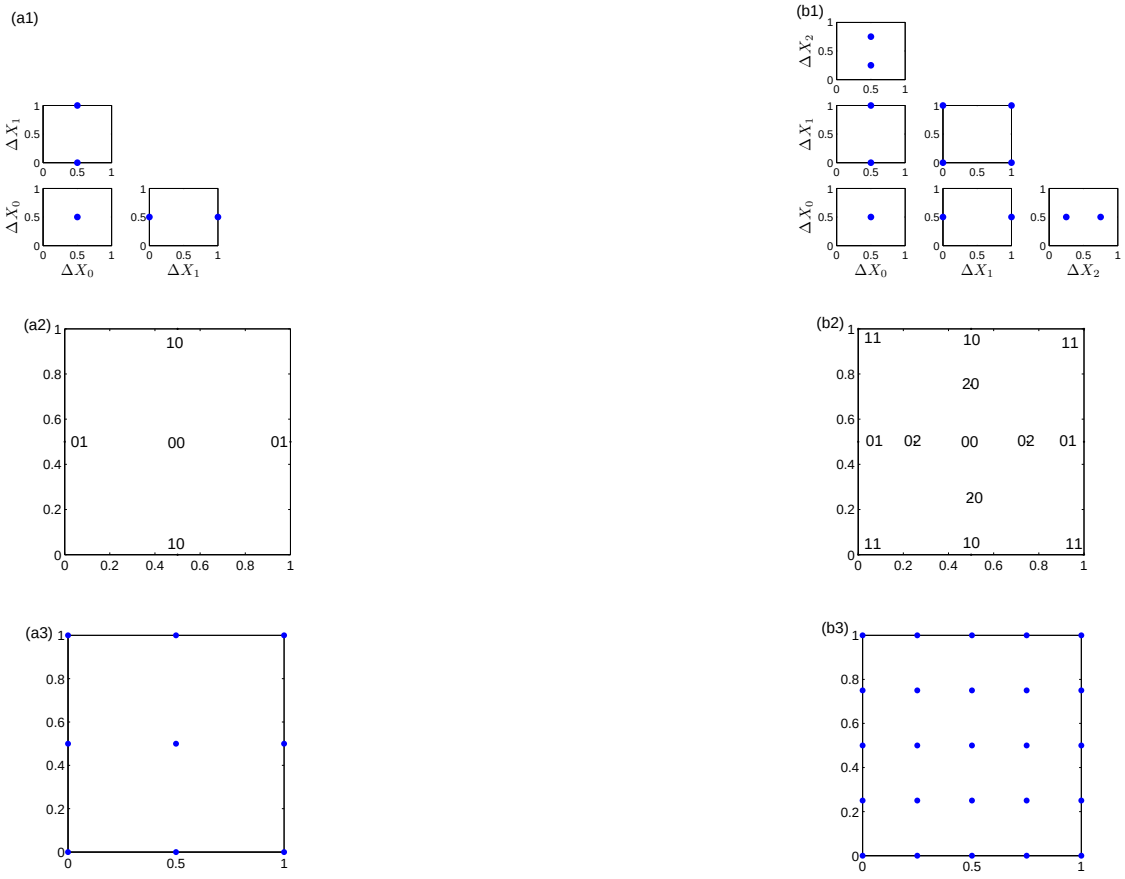

Figure 12: The hierarchical construction from $\mathbf{H}_{1,2}$ (a1, a2) to $\mathbf{H}_{2,2}$ (b1, b2), and the comparison of the nested sparse grid $\mathbf{H}_{1,2}$ (a2), $\mathbf{H}_{2,2}$ (b2) and full grid $\mathbf{X}^2 \bigotimes \mathbf{X}^2$ (a3, b3), where (a1) presents the decomposition of $\mathbf{H}_{1,2}$, (b1) presents the decomposition of $\mathbf{H}_{2,2}$

.

$\triangle\mathbf{H}_{1,2} = (\triangle X^0 \bigotimes \triangle X^1) \bigcup (\triangle X^1 \bigotimes \triangle X^0)$. Replacing i with 0 and 1 in Eqs. (4.13)-(4.14), for the equidistant nodes we have $\mathbf{X}^0 = \{x_1^0\} = \{1/2\}$ and $\mathbf{X}^1 = \{x_1^1, x_2^1, x_3^1\} = \{0, 1/2, 1\}$. Thus $\triangle X^0 = \{1/2\}$, $\triangle X^1 = \{0, 1\}$ and the two dimensional sparse grid at resolution level 1 is $\mathbf{H}_{1,2} = \triangle X^0 \bigotimes \triangle X^0 \bigcup \triangle X^1 \bigotimes \triangle X^0 \bigcup \triangle X^0 \bigotimes \triangle X^1$ (see Fig. 12 (a1 - a3) for the construction of $\mathbf{H}_{1,2}$ and a comparison with the full grid $X^1 \bigotimes X^1$). The two dimensional Smolyak interpolation with resolution level 1, $\mathbf{A}_{1,2}(f)$ in Eq. (4.10), is given by $(\triangle^0 \otimes \triangle^0)(f) + (\triangle^1 \otimes \triangle^0)(f) + (\triangle^0 \otimes \triangle^1)(f)$, where $\triangle^i = \mathcal{I}^{i+1} - \mathcal{I}^i$.

By the recursive structure of the sparse grid in Eq. (4.12), the construction of the sparse grid from resolution level 1 to 2 requires only the addition of the nodes on the

set $\triangle \mathbf{H}_{2,2} = \triangle X^0 \bigotimes \triangle X^2 \bigcup \triangle X^1 \bigotimes \triangle X^1 \bigcup \triangle X^2 \bigotimes \triangle X^0$ (see Fig. 12 (b1)). Making $i = 2$ in Eqs (4.13)-(4.14), for the equidistant nodes we have $\mathbf{X}^2 = \{x_1^2, x_2^2, x_3^2, x_4^2, x_5^2\} = \{0, 1/4, 1/2, 3/4, 1\}$ and $\triangle X^2 = \{1/4, 3/4\}$ (see Fig. 12 (b1, b2)). Hence the two dimensional Smolyak interpolation with resolution level 2 is given in the Eq. (4.10) as $\mathbf{A}_{2,2}(f) = \mathbf{A}_{1,2}(f) + (\triangle^0 \otimes \triangle^2)(f) + (\triangle^1 \otimes \triangle^1)(f) + (\triangle^2 \otimes \triangle^0)(f)$. Moreover from Fig. 12 (b2, b3) we observe that the two dimensional sparse grid $\mathbf{H}_{2,2} = \mathbf{H}_{1,2} \bigcup \triangle \mathbf{H}_{2,2}$ requires less nodal points than the full grid $\mathbf{X}^2 \bigotimes \mathbf{X}^2$. The amount of the nodes reduced by the sparse grid compared to the full grid with the same one dimensional nodes increases with the resolution level q, but the sparse grid consist of much smaller number of nodes than that of full grid [18]. For instance, $|H_{6,2}| = 321$, and $|\mathbf{X}^6 \bigotimes \mathbf{X}^6| = 4225$; $|H_{7,2}| = 705$, and $|\mathbf{X}^7 \bigotimes \mathbf{X}^7| = 16641$. Hence compared with the nodes in the full grid model, a significant reduction of 92% and 95% is achieved when the sparse grid with the resolution level 6 and 7 is used. Thus the Smolyak algorithm provides a more flexible high dimensional interpolation method.

Considering the discontinuity associated with the bifurcation behavior, we select the linear hat functions [10] as the basis functions $\delta_{x_j^i}(x)$:

$$\delta_{x_j^i}(x) = 1 \quad \text{for} \quad i = 1, \tag{4.15}$$

and for $i > 1$ and $j = 1, \ldots, m_i$

$$\delta_{x_j^i}(x) = \begin{cases} 1 - (m_i - 1)|x - x_j^i|, & \text{if} \quad |x - x_j^i| < 1/(m_i - 1), \\ 0, & \text{otherwise.} \end{cases} \tag{4.16}$$

If a d-variate function f has continuous mixed derivatives

$$\mathcal{D}^\alpha f = \frac{\partial^{|\alpha|} f}{\partial x_1^{\alpha_1} \cdots \partial x_d^{\alpha_d}}, \tag{4.17}$$

where $\alpha = (\alpha_1, \ldots, \alpha_d)$ with $\alpha_1, \ldots, \alpha_d$ positive integers less than or equal with 2, and $|\alpha| = \sum_{i=1}^d \alpha_i$, then according to [15], the piecewise linear Smolyak interpolation error is given by

$$\| f - \mathbf{A}_{q,d}(f) \|_\infty = \mathcal{O}(N^{-2} |\log_2 N|^{3(d-1)}), \tag{4.18}$$

with N denoting the number of nodes of this type of sparse grid. However, the piecewise linear interpolation error on the full grid with N nodes is only $\mathcal{O}(N^{(-2/d)})$ [5].

From Eq. (4.10), the interpolation in a standard sparse grid is constructed by the summation of $(\triangle^{i_1} \otimes \cdots \otimes \triangle^{i_d})(f)$ with the index set $|\mathbf{i}| \leq q$. The conventional sparse grid approach treats all dimensions equally, and thus gains no immediate advantage for problems in which dimensions are of different importance. A dimension adaptive method was developed by Gerstner et. al. [5] to adaptively assess the dimensions according to their importance. The idea of the adaptive algorithm is to find the most important dimensions and then construct a different index set depending on the different importance of each dimension.

In an adaptive algorithm, the index set is separated into two disjoint sets, called the active and the old index set. The active index set contains the indices $\mathbf{i}$, whose error has been estimated by the error estimator, but the error of the forward neighbors of $\mathbf{i}$ have not yet been calculated. Here, the forwards neighbors of an index $\mathbf{i}$ are defined as the d indices $\{\mathbf{i} + \mathbf{e_j}, 1 \leq j \leq d\}$, where $\mathbf{e_j}$ is the j-th unit vector. The old index set is formed by the other indices of the current index set. An adaptive process applied to a two dimensional example is presented by Gerstner et al. (see Fig. 2 in [5]). It is of interest to mention that the error estimator for the nested sets of nodes is given by

$$max\{w\frac{|\triangle Q_{\mathbf{i}} f|}{|\triangle Q_{\mathbf{1}} f|}, (1-w)\frac{1}{n_{\mathbf{i}}})\} \tag{4.19}$$

where $\triangle Q_{\mathbf{i}} f$ is the quadrature difference on the index $\mathbf{i}$, $n_{\mathbf{i}}$ is given by $n_{\mathbf{i}} = m_{i_1} \ldots m_{i_d}$, which is the number of nodes required for the computation of the quadrature difference $\triangle Q_{\mathbf{i}} f$, and $w \in [0, 1]$ is the control parameter [5]. Note that when $w = 0$, there is no adaptive process and the grid construction reverts to the classical sparse grid. If the estimated error for a given index is very small, then the index may stop any future refinement in its forwards neighbors. However, it is possible that the forward neighbors may have a large error and a refinement is required.

4.2 Numerical simulations

We now study the performance of the SCM for the 2 DOF aeroelastic system given in Eqs. (2.6). Following [8], [11] and [1], the system parameters are specified as: $\mu = 100, a_h = -0.5, x_\alpha = 0.25, \tilde{\omega} = 0.2, r_\alpha = -0.5, \zeta_\eta = 0$ and $\zeta_\alpha = 0$, while random variables are introduced in the coefficient k_3 and the initial pitch angle $\alpha(0)$.

In this section, the SCM is applied to study the secondary bifurcation by taking into account of the presence of uncertainties. Since the flow will not jump until U^* is close to $2U_L^*$, and the jump phenomenon occurs only at certain values of k_3, our simulations will focus on $U^*/U_L^* \approx 1.98$ and $k_3 \approx 80$. The effect of the uncertainties in the initial condition will also be examined. MCS reported here are based on 10,000 samples.

4.2.1 Simulations with one random variable

We first consider a model with a random variable in the cubic nonlinearity in the pitch restoring force,

$$k_3(\xi) = [k_3]_0 + [k_3]_1 \xi \tag{4.20}$$

where $[k_3]_0 = 80$, $[k_3]_1 = 8$ and ξ is a uniform random variable on $[-1, 1]$. The initial condition is deterministic, $\alpha(0) = 1.0°$, and all other initial values are set to zero. Near $U^*/U_L^* \approx 1.98$, we observe a jump phenomenon in the pitch motion similar to that reported by Liu et. al. [9]. However, to capture the correct aeroelastic behaviors, a very accurate solver must be employed for the deterministic aeroelastic system. Fig. 13 displays the pitch motions using Matlab ode45 algorithm, which is an adaptive 4th/5th-order Runge-Kutta scheme with an error checking. Clearly, the solutions depend on the tolerance specified in the ode45 algorithm, and the computed pitch motions are identical when the absolute error tolerances are set to be 10^{-11} and 10^{-13}. Thus, to ensure accurate numerical solutions for the deterministic system, we set the tolerance level to 10^{-11} in all calculations.

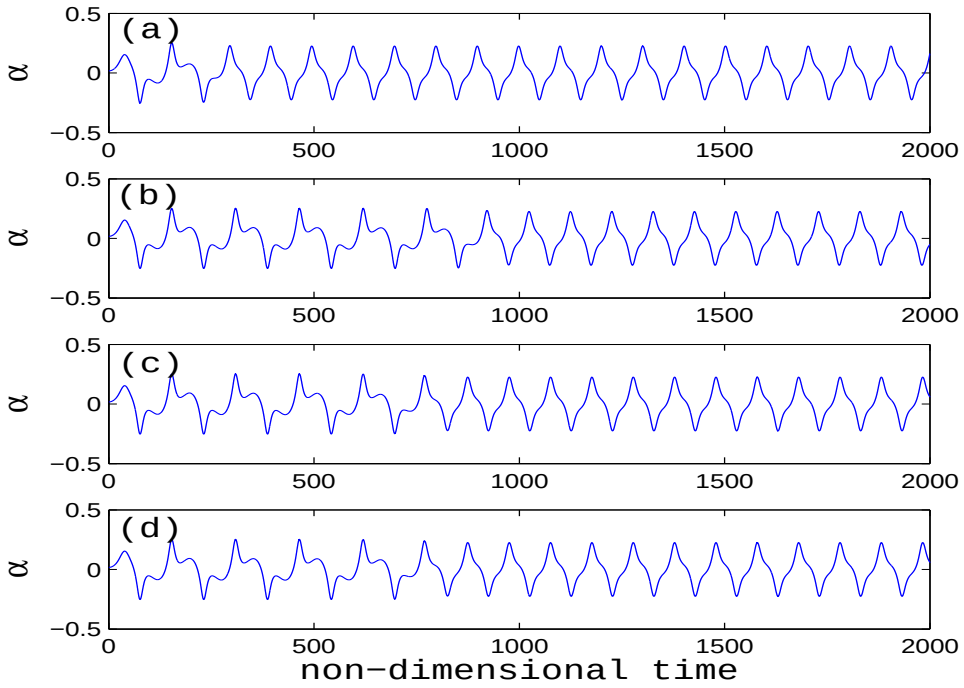

Figure 13: Pitch motions for $k_3 = 78$, $U^*/U_L^* = 1.9802$, with various relative and absolute error tolerance in ode45: (a)10^{-3}; (b)10^{-6}; (c)10^{-11}; (d)10^{-13}

Interpolation with piecewise linear functions

The results presented here are based on SCM using a piecewise linear interpolation. In Fig. 14, we show the LCO amplitude response at three different flow velocities. The values $U^*/U_L^* = 1.975$ and 1.985 are chosen, so that the jump phenomenon does not occur (see Fig.14(a)-(d)), and the pitch motion is restricted in either Hopf or secondary bifurcation. Notice that, the amplitude for $U^*/U_L^* = 1.985$ (i.e., in the secondary bifurcation) is higher than the amplitude for $U^*/U_L^* = 1.975$ (i.e., in the Hopf bifurcation). At $U^*/U_L^* = 1.9802$, we observe the occurrence of a jump phenomenon in the LCO amplitudes. In Fig. 14(e,f), the amplitude plot has two discontinuous parts, such that the lower part corresponds to the Hopf bifurcation and the upper part corresponds to the secondary bifurcation.

The SCM simulation displayed in Fig. 14(e,f) clearly indicates that there is a

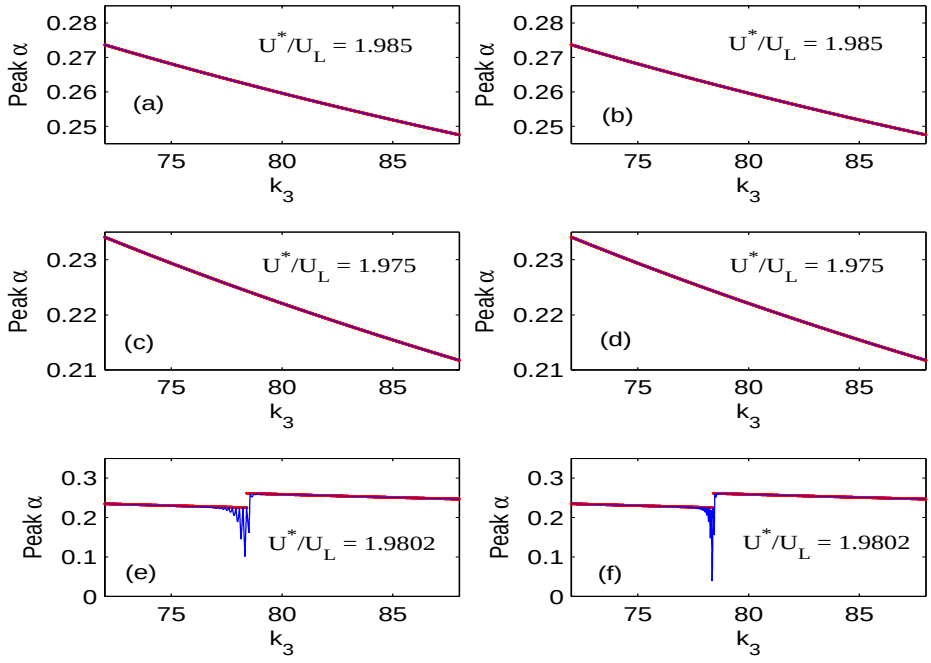

Figure 14: The amplitude response at various U^*/U_L values, where red dots: deterministic, blue dashed lines: SCM with 101 nodes in (a,c,e) and SCM with 201 nodes in (b,d,f)

significant decay of the LCO amplitudes near $k_3 = 78$ at which the jump phenomenon between the bifurcations occurs. The jump between the two bifurcations introduces the difficulty to accurately simulate the LCO amplitude using the SCM. However, if we compare Figs. 14 (e) and (f), we notice that some improvement around the discontinuity is obtained if more nodes are used in the SCM.

Fig. 15 shows the corresponding pitch motions at t=2000. Because the decay of the LCO amplitude is a result of the interpolation error in the random space, a significant error of the dynamical response is observed near $k_3 = 78$ (see Fig. 15 (e-f)), where the pitch motion is discontinuous in the random space. Thus the pictures presented in Fig. 15 reconfirm the simulation results reported in Fig. 14. Notice that for $U^*/U_L^* = 1.975$ and 1.985, when the pitch motion is entirely in the Hopf or the secondary bifurcation, there is no decay in the LCO amplitudes. Moreover for cases with no discontinuity the

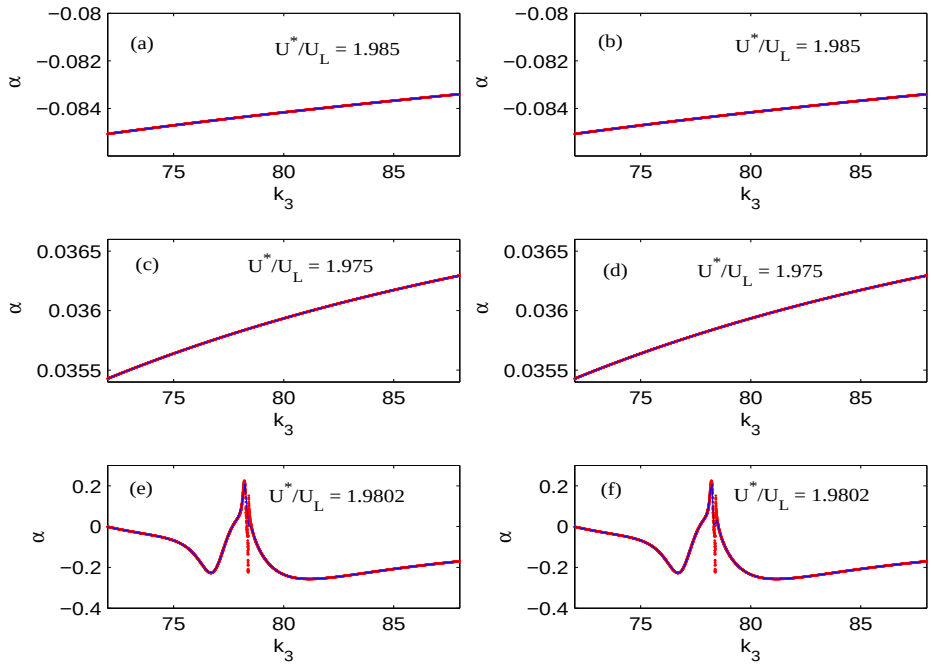

Figure 15: Pitch motion at t=2000 at various U^*/U_L values, where red dots: deterministic, blue dashed lines: SCM with 101 nodes in (a,c,e) and SCM with 201 nodes in (b,d,f)

SCM results using 101 or 201 nodes are essentially the same (see Fig. 14 (a-d) and Fig. 15 (a-d)).

Interpolation with high order basis functions

The previous results obtained using the SCM show that in order to accurately capture the discontinuity, we need to increase the number of nodes. Since the decay of the LCO amplitude is due to the interpolation error in the random space, a better alternative approach is to replace the piecewise linear interpolation with more accurate interpolation formulas, such as the piecewise cubic interpolation and the piecewise cubic spline interpolation. We select equidistant nodes, so that the total number of interpolating nodes remains unchanged.

Fig. 16 shows the probability density function (PDF) of the LCO amplitudes at

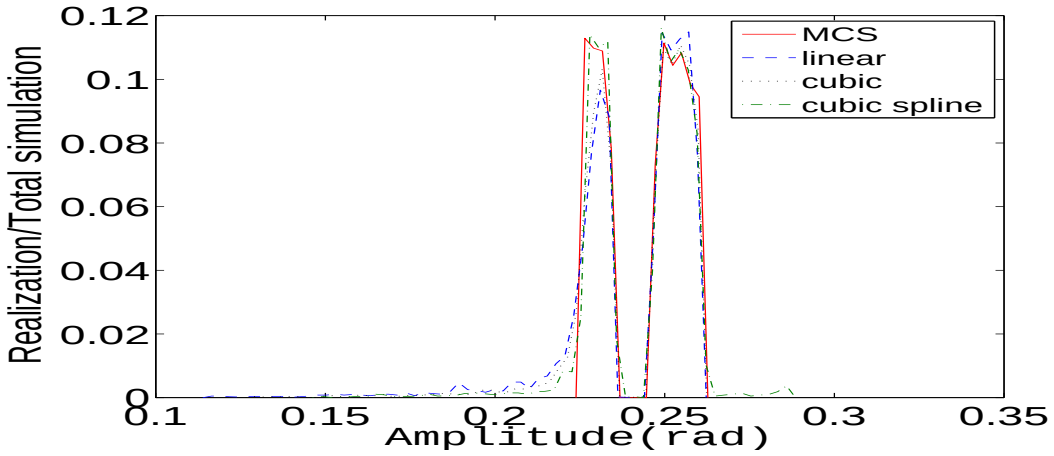

Figure 16: PDFs of the LCO amplitudes at $U^*/U_L^* = 1.9802$ by various interpolations with 151 nodes

$U^*/U_L^* = 1.9802$ using the SCM with various interpolation functions with 151 nodes and using a MCS. A small tail on the left side of the PDF is observed for the SCM results. We note that the SCM with the cubic spline interpolation has the smallest tail, and it produces an excellent agreement with the MCS. However, a small tail in the PDF generated by the cubic spline interpolation is also observed on the right side of PDF. This implies that the SCM with the cubic spline interpolation overestimates the LCO amplitude.

In Fig. 17 we compare the convergence of the SCM using various interpolations methods. The mean square error is defined by

$$E[(\alpha^{max}(\xi) - \hat{\alpha}^{max}(\xi))^2] = \int (\alpha^{max}(\xi) - \hat{\alpha}^{max}(\xi))^2 \rho(\xi) \mathrm{d}\xi \tag{4.21}$$

where $\alpha^{max}(\xi)$ is the exact LCO amplitude for the random variable ξ, $\hat{\alpha}^{max}$ is the LCO amplitude simulated by the SCM, and $\rho(\xi)$ is the probability density function of ξ (i.e. the uniform density on $[-1, 1]$)). The comparison in Fig. 17 also indicates that the best convergence rate is given by the SCM with a cubic spline interpolation. The SCM mean square error using a cubic spline interpolation with 61 nodes is about the same as that using a linear interpolation with 301 nodes. It should be noted that in a typical SCM simulation with 500 nodes, the computing time used for the interpolation is less

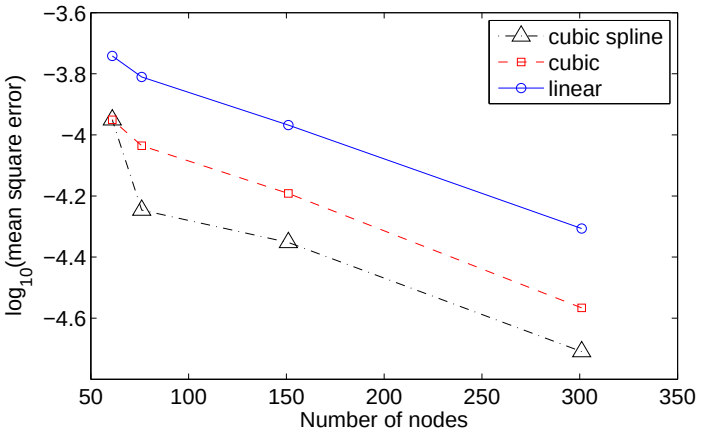

Figure 17: Comparison of mean square errors generated by various interpolations

that one percent of the overall computing time. Hence, for accurate simulation results, high order interpolation methods should be used.

4.2.2 Simulations with two random variables

In this section, we consider a model with uncertainties in the cubic nonlinearity term k_3 and the initial pitch angle α_0. The randomness are introduced as follows:

$$\begin{aligned} \alpha_0 &= [\alpha_0]_0 + [\alpha_0]_1 \xi_1, \\ k_3(\xi_2) &= [k_3]_0 + [k_3]_1 \xi_2 \end{aligned} \tag{4.22}$$

where $[\alpha_0]_0 = 0$, $[\alpha_0]_1 = 5$, $[k_3]_0 = 80$, $[k_3]_1 = 8$, ξ_1 is a uniform variables on [0,1], ξ_2 is a uniform variables on [-1,1], and ξ_1 and ξ_2 are independent. Here, $(\alpha_0, 0, 0, 0, 0, 0, 0, 0)$ represents the initial condition of the aeroelastic system given in Eq. (2.6). Hence only the nonnegative initial pitch angle is considered.

Particular attention is given to cases when $U^*/U_L^* = 1.98$ and 1.985, for which the pitch motion changes from the LCO corresponding to the Hopf bifurcation to the LCO corresponding to the secondary bifurcation. Here, the Smolyak algorithm is implemented using the Matlab Sparse Grid Interpolation Toolbox developed by Klimke [7].

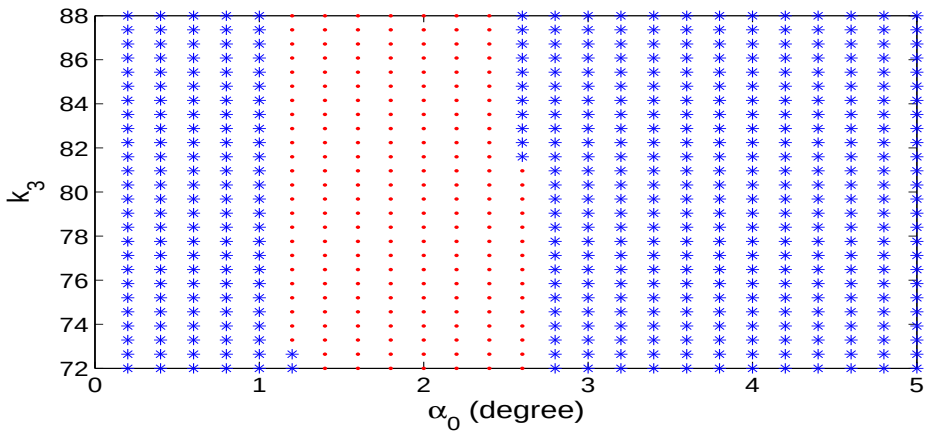

Figure 18: The amplitude response surface for $U^*/U_L^* = 1.98$. secondary bifurcation (red $\cdot$), Hopf bifurcation (blue *), where $\alpha_0 = 0^\circ$ is a singularity

Figs. 18 and 19 display the amplitude response surface for $U^*/U_L^* = 1.98$ and 1.985. Clearly, jump phenomena between the Hopf and secondary bifurcations exist at these flow velocities. In stochastic analysis, the jump phenomena lead to discontinuities in the random spaces, and consequently, to larger numerical errors for the SCM. In Figs. 18 and 19, the regions with different behavior are presented as bands. In the response surface, the x-axis corresponds to the random variables associated with α_0, and the y-axis with random variables in k_3. It is interesting to note that the responses are almost parallel to the k_3 axis. Hence, for the aeroelastic UQ problem, the initial value of the pitch angle is more critical than the cubic coefficient k_3. The simulation results are also confirmed by the bi-modal PDFs displayed in Fig. 20. The left peak on the PDFs is related to the amplitude of the LCO in the Hopf bifurcation, and the right peak corresponds to the amplitude of the LCO in the secondary bifurcation.

To demonstrate the effectiveness of the Smolyak algorithm, Fig. 20 reports the SCM performances using various grid strategies. Here, we simulate the PDFs of the amplitude of the LCOs generated by the piecewise linear SCM using 51×21 full grid (i.e., 51 nodes in α_0-dimension and 21 nodes in k_3-dimension), 21×51 full grid, and sparse grid with level 7 resolution (i.e., 705 nodes). Although the tensor product

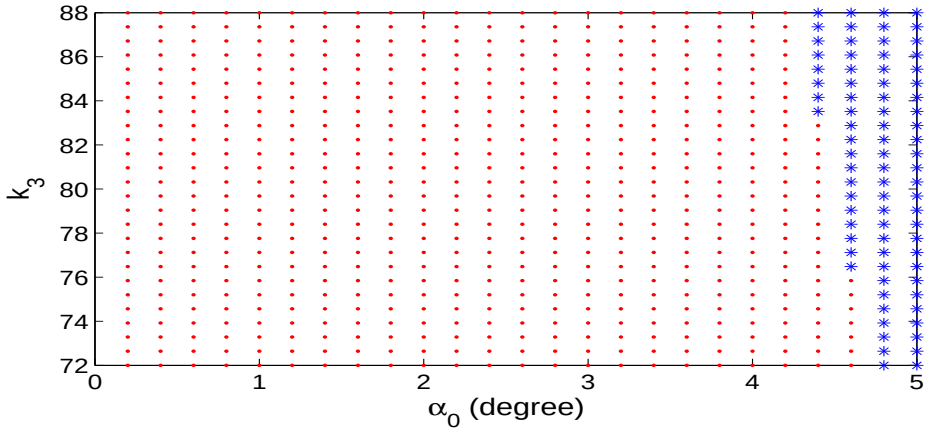

Figure 19: The amplitude response surface for $U^*/U_L^* = 1.985$. secondary bifurcation (red $\cdot$), Hopf bifurcation (blue *), where $\alpha_0 = 0^\circ$ is a singularity

produces the same number of nodes for the SCM, Fig 20 clearly shows that the PDFs with 51×21 full-grid is in better agreement with the MCS than that using 21×51 full grid. This is reasonable since the behavior is more sensitive to the initial pitch angle than the cubic nonlinear term. Among various grid methods, the SCM with the sparse grid gives the best approximation. Even though only 705 nodes are employed in the sparse grid with the resolution level 7, the results are in better agreement with the MCS than the results obtained using the full grid with 1071 nodes. This demonstrates that the Smolyak's sparse grid algorithm with a smaller number of nodes produces more accurate results than the interpolation based on the full grid (see also the interpolation error in Eq.(4.18)).

Fig. 21 displays the mean square error of the LCO amplitude using various grids: full grid with 21×21, 21×51, 21×101 nodes (i.e., increasing the number of nodes in k_3); full grid with 21×21, 51×21, 101×21 nodes (i.e., increasing the nodes in α_0); full grid with 21×21, 25×25, 51×51 nodes (i.e., increasing the nodes in both k_3 and α_0); and the sparse grids with resolution level from 1 (5 nodes) to 8 (1537 nodes). From the results presented here, we conclude that although increasing the nodes in the α_0-dimension improves the convergence when using full grid, the SCM with a sparse

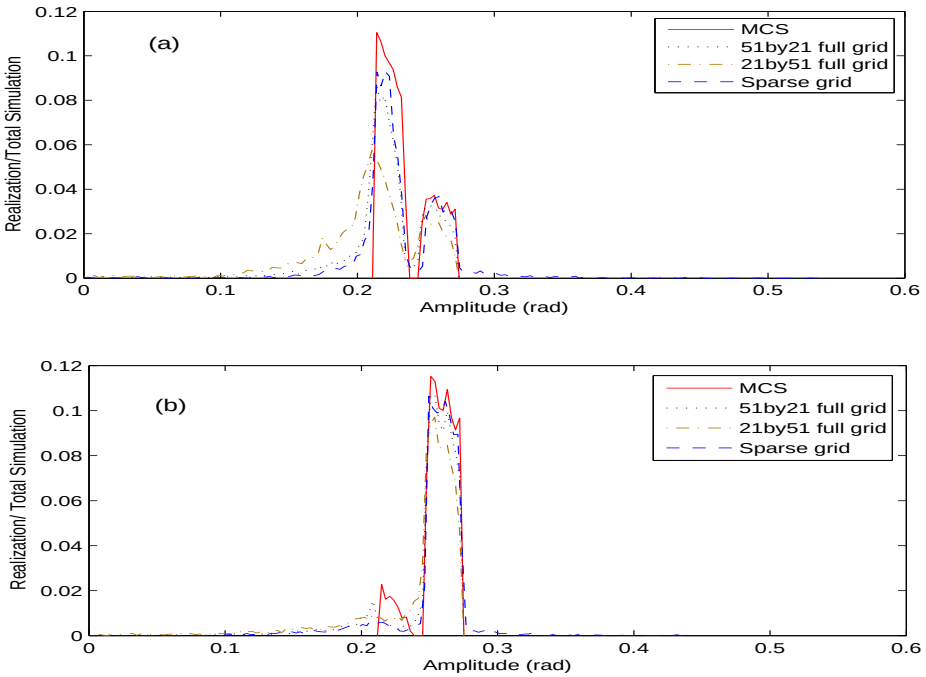

Figure 20: PDFs generated by various methods on $[0°, 5°]\times[72, 88]$ for (a) $U^*/U_L^* = 1.98$ and (b) $U^*/U_L^* = 1.985$

grid is clearly more efficient and produces a smaller error than those based on full grids (see Fig. 21).

4.2.3 Simulations with five random variables

In order to further evaluate the performance of the proposed SCM, we consider the aeroelastic system given in Eq. (2.6) with a fixed initial value for $\alpha = 1°$, but more random variables are now introduced in the nonlinear coefficient k_3. Since k_3 plays a crucial role in the onset of the Hopf and the secondary bifurcations [8], it is important to investigate the effects due to the presence of randomness in the nonlinear pitch stiffness. Here, we consider a time dependent process instead of a random variable. An aeroelastic model perturbed by a time dependent noise was also considered in [2], and the stochastic bifurcation was studied using a stochastic averaging.

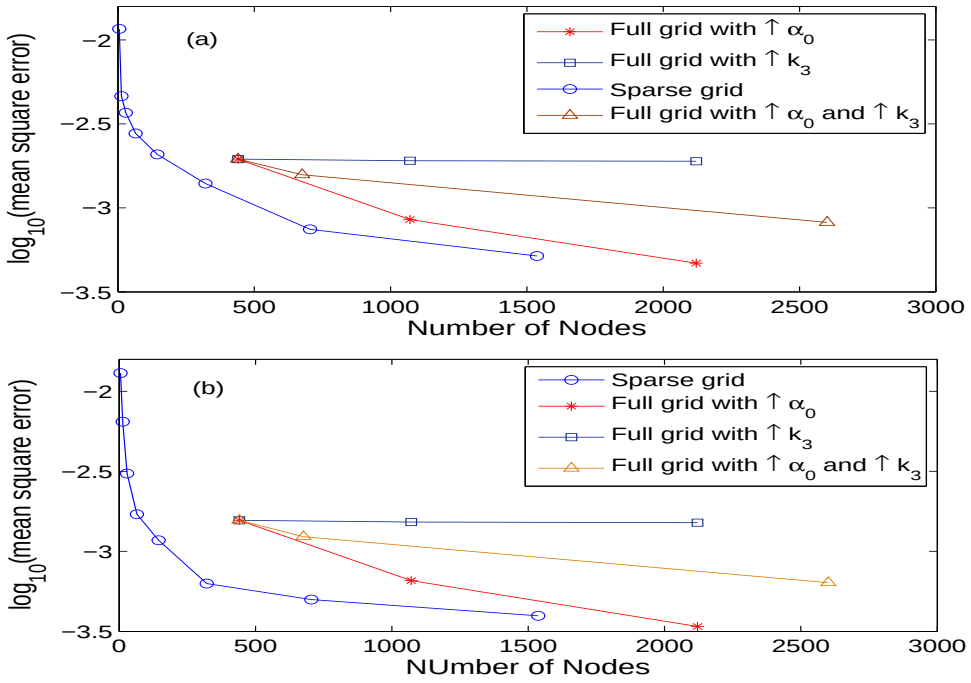

Figure 21: Comparison of mean square errors generated by various methods on $[0°, 5°]\times[72, 88]$ for (a) $U^*/U_L^* = 1.98$ and (b) $U^*/U_L^* = 1.985$

Let

$$k_3(t,\xi) = \overline{k_3} + \widetilde{k_3}(t,\xi). \tag{4.23}$$

where $\overline{k_3}$ is a constant and $\widetilde{k_3}(t,\xi)$ is the noise with the following expression:

$$\widetilde{k_3}(t,\xi) = \sigma \sum_{i=1}^{M} \frac{1}{i^2\pi^2} cos(2\pi it)\xi^i \tag{4.24}$$

where $\xi^i, i = 1, 2, \ldots, M$ are independent uniformly distributed random variables on $[-1, 1]$. The form given in Eq. (4.24) has been used to simulate noise in [19], and it represents a truncated expression of the Karhunen-Loeve (KL) expansion of a stochastic process. The series (4.24) converges as $M \longrightarrow \infty$, and

$$E(k_3(t,\xi)) = \overline{k_3}, \quad \overline{k_3} - \frac{\sigma}{6} < k_3(t,\xi) < \overline{k_3} + \frac{\sigma}{6}. \tag{4.25}$$

In this study, the number M of random variables is set to five. Numerical simulations are carried out at the flow velocity $U^*/U_L^* = 1.9802$, with $\overline{k_3} = 80$ and $\sigma = 48$.

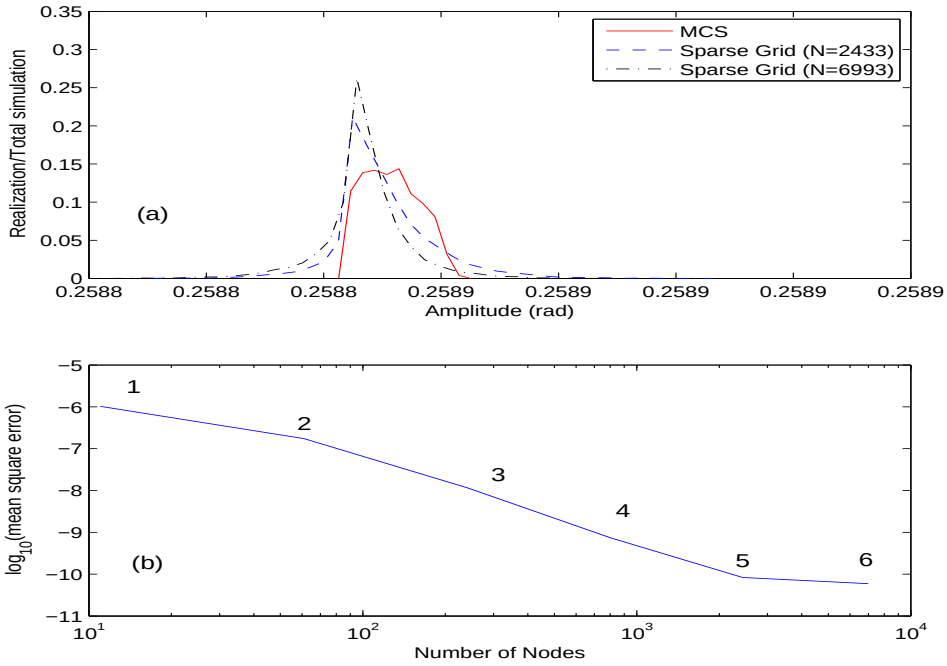

Figure 22: Comparison of PDFs and the SCM mean square error for $\overline{k_3} = 80$

The truncated KL expansion (4.24) is strictly positive for any positive integer M and it is bounded by [72, 88]. Here, we particularly focus on the comparisons of the simulation results using the Monte-Carlo method with 20,000 samples and the SCM with sparse grid.

The PDFs generated by the MCS and the SCM are shown in Fig. 22(a). Although $\overline{k_3} = 80$ is near the value where the jump phenomenon occurs (see Fig. 14), the range of the PDFsrs (see Fig. 14), the range of the PDFs is around 0.2588, and only one peak is displayed. Hence, from the LCO amplitude, we conclude that the aeroelastic system is in the secondary bifurcation. Fig. 22(b) shows that the SCM mean square error is decreasing as the resolution level increases in the sparse grid. Since no jump phenomenon occurs, the SCM produces accurate predictions. This is confirmed in Fig. 23 by comparing the time histories of the expected values of the pitch motion computed by MCS and the SCM with level $q = 5$ (see Eqs. (4.10)).

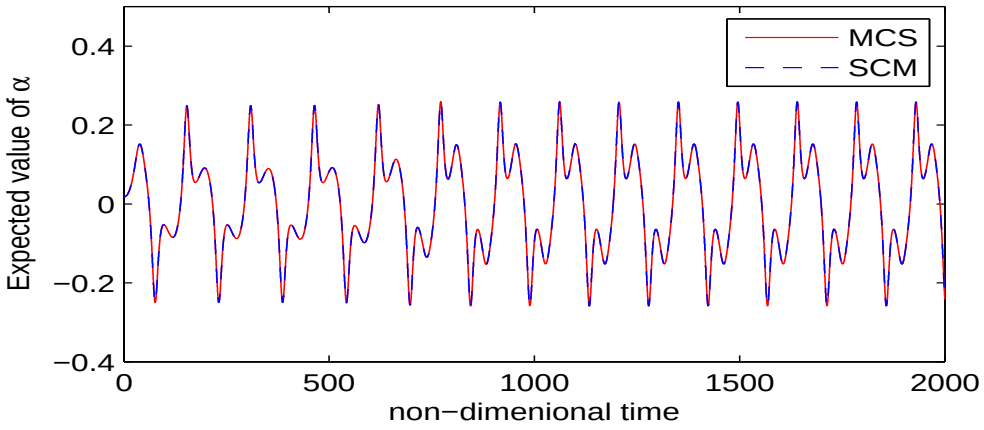

Figure 23: Expected value of the pitch motion calculated using the MCS and the SCM with level $q = 5$

To investigate a challenging case with discontinuity, we keep $M = 5$, but the expected value of cubic coefficient is shifted to $\overline{k_3} = 78$, a value around which a jump phenomenon occurs. Moreover, to extend the range of the expansion, we set σ to 60 . Hence, k_3 is bounded by $[68, 88]$.

Fig. 24(a) shows a bimodal PDF generated by the MCS, and the shape indicates that the random aeroelastic system converges to two types of LCOs. The left peak of the PDF corresponds to a smaller amplitude of the LCO for the Hopf bifurcation, and the right peak represents the LCOs in the secondary bifurcation. The jump phenomenon from the Hopf bifurcation to the secondary bifurcation produces the discontinuous behavior in the five dimensional random spaces. The corresponding PDFs obtained using sparse grid at different resolution levels are displayed in Fig. 24 (b)-(d). Clearly, better agreements are achieved as the resolution level q increases, and the bimodal shapes with the correct peak locations are obtained when $q \geq 4$.

The discontinuous behavior is also shown in the plot of the expected value of α displayed in Fig. 25. Note that when the non-dimensional time is around 800, a change of amplitude of the expected value of pitch happens. The expected value of α based on the SCM with level $q = 5$ has a good agreement with the results obtained using the MCS. However, unlike the previous case when an almost prefect match was

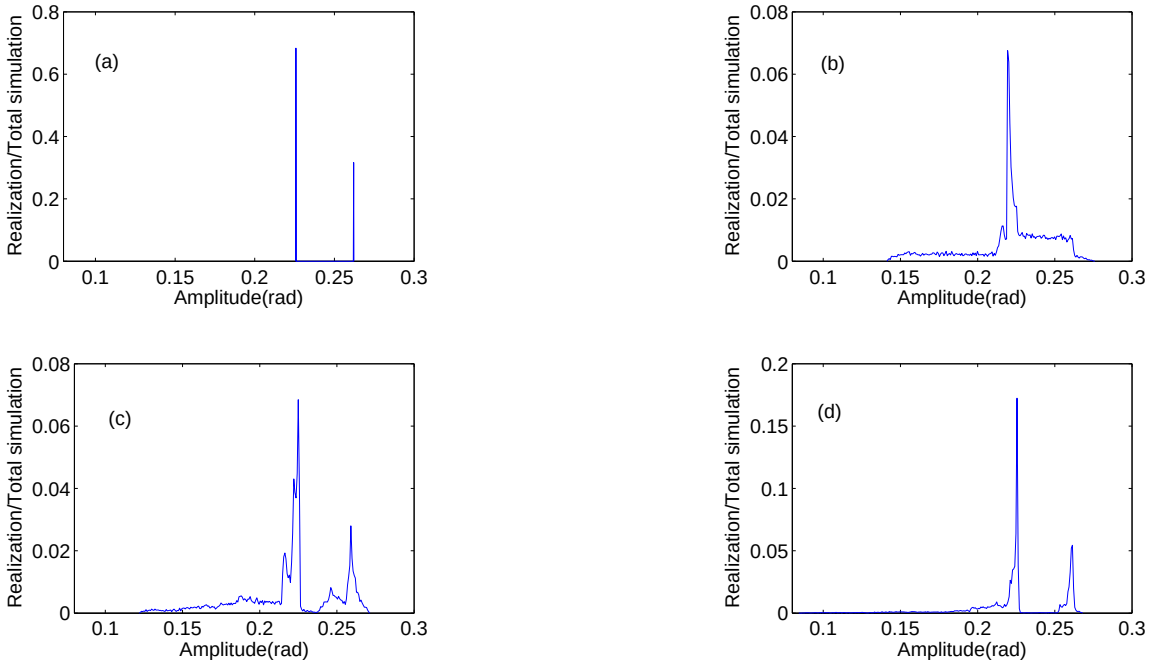

Figure 24: Comparison of PDFs from the MCS(a) and the SCM with sparse grid and $q =$ 3(b), 4(c) and 5(d)

shown in Fig. 23, a small discrepancy is observed in Fig. 25. The difficulty is generated by the presence of discontinuity, and it can also be seen by checking the mean square error plotted in Fig. 26. Compared with the errors shown in Fig. 22 (b), we note that when a discontinuity exits in the UQ problem, increasing the level (i.e., using more nodes) does not guarantee the reduction of the error.

Although we can achieve more accurate SCM results by increasing the resolution level in the Smolyak algorithm, this strategy is not recommended when dealing with high dimensional UQ problems because of the enormous increase in computing time. An effective way to improve the efficiency of the Smolyak algorithm is to incorporate the dimension adaptive method proposed in [5].

For the problem under consideration, the uncertainty is given in Eq. (4.24). Since the random variable ξ_i is scaled by $1/(i^2\pi^2)$, the effect of ξ_i is controlled by the index i. For this reason, the first random variable ξ_1 plays the essential role in the 'noise'. Hence, the resolution level in each dimension should be set according to the effect of

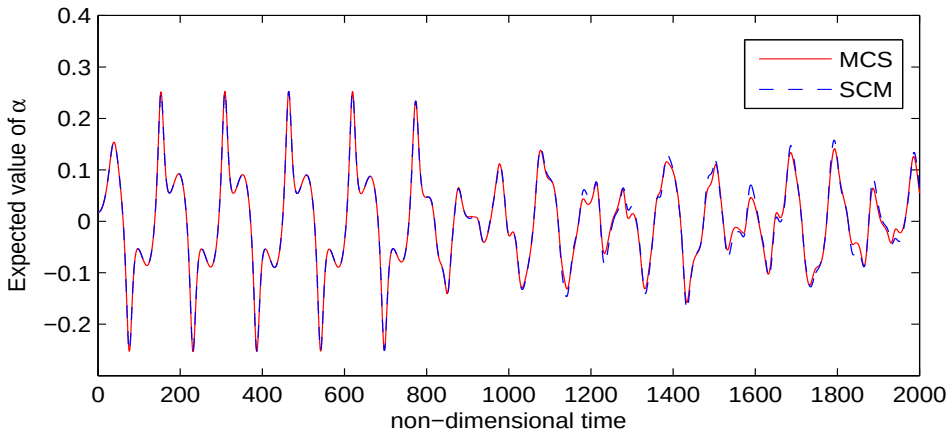

Figure 25: The expected value of the pitch motion calculated using the MCS and the SCM with level $q = 5$

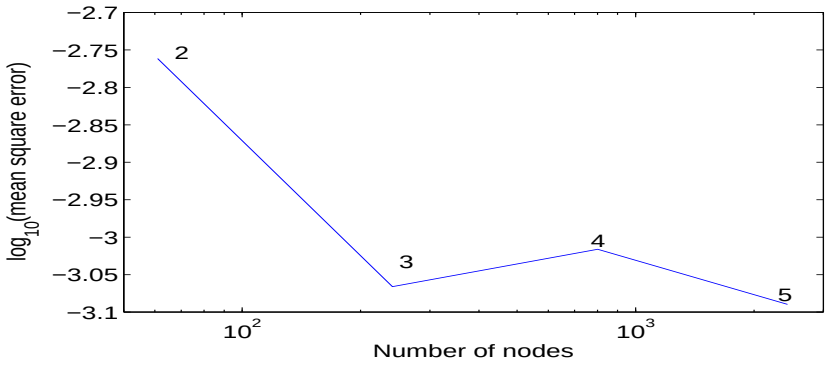

Figure 26: SCM mean square error with various levels

each random variable instead of treating all dimensions equally. In the implementation of this dimension adaptive approach, the iterative adaptive process is terminated once the number of accumulated nodes becomes greater than 1000.

Fig. 27 shows the PDFs generated by the MCS and the SCM with the dimension adaptive algorithm with $w = 0, 0.5, 1$. When the control parameter $w = 1$, the first dimension has the maximum resolution level implying that the random variable ξ_1 has a major contribution in the perturbation. As shown in Fig. 27, the SCM with adaptive sparse grid produces the bimodal shapes of the PDFs. The locations of the two peaks are in good agreement with those found using the MCS. Moreover, from the SCM

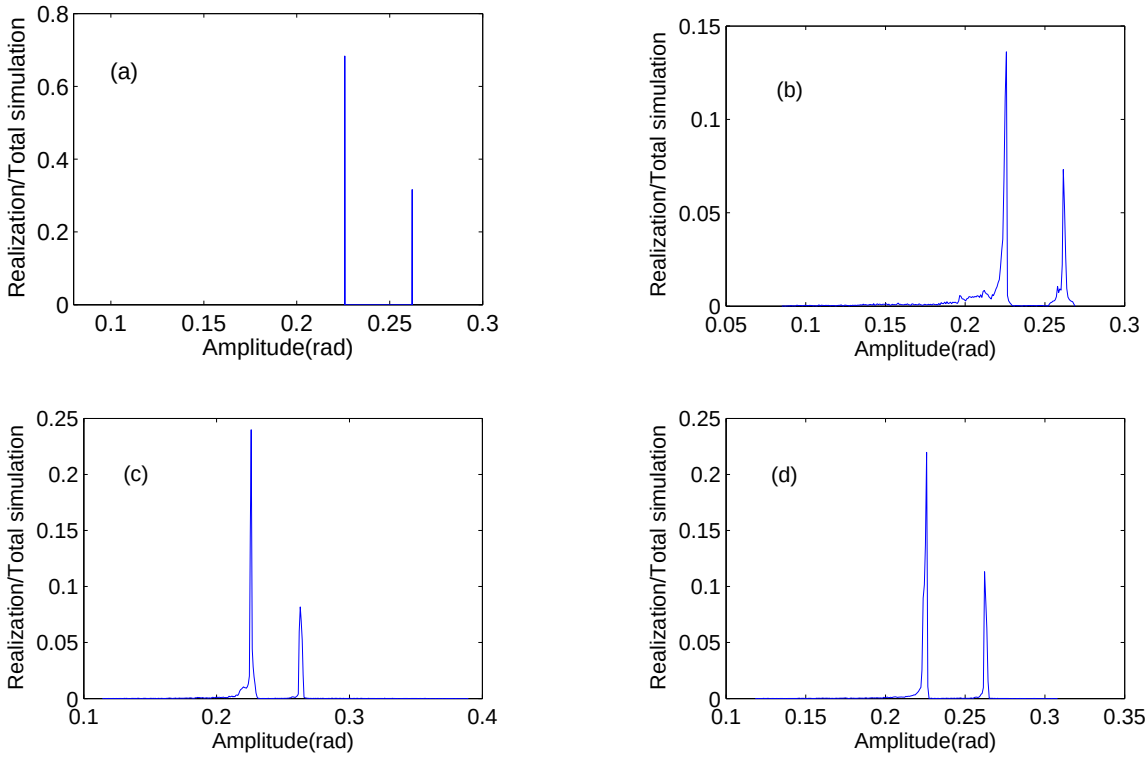

Figure 27: Comparison of PDFs from the MCS(a) and the SCM with the dimension adaptive approach with (b)$w = 0$, where the number of nodes = 1001, max resolution level on each dimension = [5 5 4 4 4]; (c)$w = 0.5$, where the number of nodes = 1025, max resolution level on each dimension = [8 4 4 4 4]; (d)$w = 1$, where the number of nodes = 1035, max resolution level on each dimension = [9 2 1 1 1]

mean square errors for various values of w illustrated in Fig. 28, it is clear that error reduction is achieved when the dimension adaptive method is applied (i.e., $w \neq 0$). For the problem considered here, $w = 1$ gives the best numerical simulation.

4.3 Conclusion

Interpolation schemes based on piecewise linear, piecewise cubic and piecewise cubic spline basis functions are examined, and the advantage of using a high order interpolation in the stochastic collocation method is demonstrated. For aeroelastic systems with multidimensional random variables, the efficiency of the stochastic collocation method

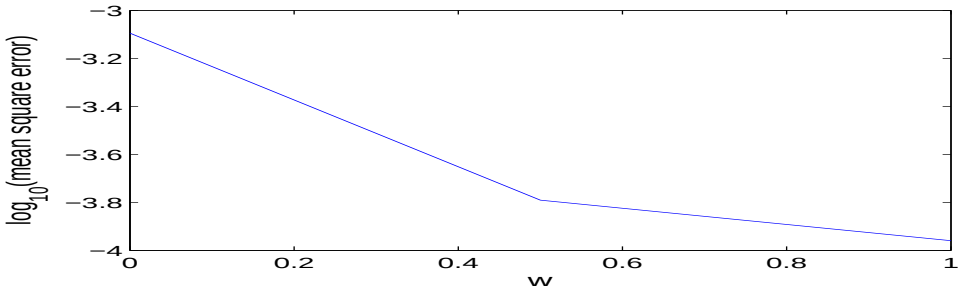

Figure 28: The SCM mean square error with the dimension adaptive algorithm at various values of the control parameter w

can be enhanced by incorporating a sparse grid and a dimension adaptive strategy. The stochastic collocation method performs well for the random aeroelastic model, and the results are in good agreement with those obtained by the Monte Carlo simulations. However, more work is needed in order to develop an effective stochastic collocation method which is capable of producing accurate simulations for the aeroelastic behavior when discontinuity exists in the random space.

Bibliography

[1] P.S. Beran, C.L. Pettit, and D.R. Millman. Uncertainty quantification of limit-cycle oscillations. *Journal of Computational Physics*, 217:217–247, 2006.

[2] S. Choi and N.S. Namachchivaya. Stochastic dynamics of a nonlinear aeroelastic system. *AIAA Journal*, 44(9):1921–1931, 2006.

[3] J. Deng, C. A. Popescu, and Y. S. Wong. Uncertainty investigations in nonlinear aeroelastic systems. *Journal of Computational and Applied Mathematics*.

[4] T. Gerstner and M. Griebel. Numerical integration using sparse grids. *Numer. Algorithms*, 18:209–232, 1998.

[5] T. Gerstner and M. Griebel. Dimension–adaptive tensor–product quadrature. *Computing*, 71(1):65–87, 2003.

[6] M. Ghommem, M.R. Hajj, and A.H. Nayfeh. Uncertainty analysis near bifurcation of an aeroelastic ystem. *Journal of Sound and Vibrations*, 329:3335–3347, 2010.

[7] A. Klimke. *Sparse Grid Interpolation Toolbox - User's Guide*, 2006.

[8] B. H. K. Lee, S. J. Price, and Y. S. Wong. Nonlinear aeroelastic analysis of airfoils: bifurcation and chaos. *Progress in Aerospace Sciences*, 35:205–334, 1999.

[9] L. Liu and E. H. Dowell. The secondary bifurcation of an aeroelastic airfoil motion: Effect of high harmonics. *Nonlinear Dynamics*, 37:31–49, 2004.

[10] X. Ma and N. Zabaras. An adaptive hierarchical sparse grid collocation algorithm for the solution of stochastic differential equations. *Journal of Computational Physics*, 228(8):3084–3113, 2009.

[11] D.R. Millman, P.I. King, and P.S. Beran. Airfoil pitch-and-plunge bifurcation behavior with Fourier chaos expansions. *Journal of Aircraft*, 42(2):376–384, 2005.

[12] D.R. Millman, P.I. King, R.C. Maple, P.S. Beran, and L.K. Chilton. Uncertainty quantification with B-spline stochastic projection. *AIAA Journal*, 44(8):1845–1853, 2006.

[13] F. Nobile, R. Tempone, and C. G. Webster. An anisotropic sparse grid stochastic collocation method for partial differential equations with random input data. *SIAM Journal on Numerical Analysis*, 46(5):2411–2442, 2008.

[14] C.L. Pettit and P.S. Beran. Spectral and multiresolution Wiener expansions of oscillatory stochastic processes. *Journal of Sound and Vibration*, 294(4–5):752–779, 2006.

[15] S. A. Smolyak. Quadrature and interpolation formulas for tensor product of certain calsses of functions. *Soviet Math. Dokl.*, 4:240–243, 1963.

[16] C. W. Ueberhuber. *Numerical Computation Methods, Software, and Analysis*. Springer, 1995.

[17] J. A. S. Witteveen and H. Bijl. Higher period stochastic bifurcation of nonlinear airfoil fluid-structure interaction. *Mathematical Problems in Engineering*, 2009(1), 2009.

[18] D. Xiu. Fast numerical methods for stochastic computations: A review. *Commum. Comput. Phys.*, 5(2-4):242–272, 2009.

[19] D. Xiu and J. S. Hesthaven. High-order collocation methods for differential equation with random inputs. *SIAM J.Sci.Comput.*, 27(3):1118–1139, 2005.

Part II

Stochastic Symplectic Schemes

Chapter 5

Construction High Order Strong Stochastic Sympletic Scheme

The symplectic integration is a special type of numerical method which is capable of preserving the symplecticity properties of the Hamiltonian system. The pioneering work on the symplectic integration is due to de Vogelaere [14], Ruth [13] and Feng [3]. Symplectic methods have been applied successfully to deterministic Hamiltonian systems, and numerical simulations consistently show that the most important feature of this approach is that the accuracy of the computed solution is guaranteed even for long term computation. In this chapter, we extend the approach to stochastic Hamiltonian systems (SHS), and we propose a systemic procedure to generate symplectic numerical schemes of any desired order for stochastic Hamiltonian systems.

There are growing interests and efforts on the theoretical study and computational implementation of numerical methods for SHS [12], [11], [9], [5], [15]. Milstein et al. [12] [11] introduced the symplectic numerical schemes to SHS, and demonstrated the superiority of the symplectic methods for long time computation. Here, we follow the rigorous approach presented in [2], and employ the properties of multiple stochastic integrals to derive a recursive formula for determining the coefficients of the generating function. Theoretically, this formula allow us to construct stochastic sympletic stochastic schemes of arbitrary high order with corresponding conditions on the Hamiltonian functions. Hence, the major contribution of the work reported here is to present a framework to construct different types of stochastic symplectic schemes of any order. Since the computation complexity increases with the order of the numerical schemes,

we mainly focus on the symplectic schemes with mean square order 1 for which we also present the convergence analysis. Moreover, for special types of SHSs, such as SHSs with additive noise, SHSs with separable Hamiltonians, or SHS preserving the Hamiltonian functions, using the method based on generating functions we construct computationally attractive symplectic schemes of mean square order 2. The study of high order stochastic symplectic scheme for the general SHS (5.1) can lead to more efficient construction of high order Runge-Kutta type schemes that avoid the need of higher order derivatives.

5.1 Stochastic Hamiltonian systems and symplecticity

Consider the stochastic differential equations (SDEs) in the sense of the Stratonovich:

$$\begin{aligned} dP_i &= -\frac{\partial H^{(0)}(P,Q)}{\partial Q_i}dt - \sum_{r=1}^{m}\frac{\partial H^{(r)}(P,Q)}{\partial Q_i}\circ dw_t^r, \quad P(t_0)=p, \\ dQ_i &= \frac{\partial H^{(0)}(P,Q)}{\partial P_i}dt + \sum_{r=1}^{m}\frac{\partial H^{(r)}(P,Q)}{\partial P_i}\circ dw_t^r, \quad Q(t_0)=q, \end{aligned} \tag{5.1}$$

where P, Q, p, q are n-dimensional vectors with components $P_i, Q_i, p_i, q_i, i = 1, \ldots, n$, and $w_t^r, r = 1, \ldots, m$ are independent standard Wiener Processes. The SDEs (5.1) are called the Stochastic Hamiltonian System (SHS) ([12]). The SHS (5.1) includes both Hamiltonian systems with additive or multiplicative noise.

A non-autonomous SHS is given by time-dependent Hamiltonian functions $H^{(r)}(t, P, Q)$, $r = 0, \ldots, m$. However, it can be rewritten as an autonomous SHS by introducing new variables e_k and f_k. Let $df_r = dt$, $de_r = -\frac{\partial H^{(r)}(t,P,Q)}{\partial t}\circ dw_t^r$, (where $dw_t^0 := dt$), with the initial condition $e_r(t_0) = -H^{(r)}(t_0, p, q)$ and $f_r(t_0) = t_0$, $r = 0, \ldots, m$. Then the new Hamiltonian functions $\bar{H}^{(r)}(\bar{P}, \bar{Q}) = H^{(r)}(f_r, P, Q)$, $r = 1, \ldots, m$, and $\bar{H}^{(0)}(\bar{P}, \bar{Q}) = H^{(0)}(f_r, P, Q) + e_0 + \cdots + e_m$, define an autonomous SHS with $\bar{P} = (P^T, e_0, \ldots, e_m)^T$

and $\bar{Q} = (Q^T, f_0, \ldots, f_m)^T$. Hence, in this study, we will only investigate the autonomous case as given in (5.1)

We denote the solution of the SHS (5.1) by $X(t; t_0, x_0; \omega) = \big(P^T(t; t_0, p, q; \omega), Q^T(t; t_0, p, q; \omega)\big)^T$, where $t_0 \leq t \leq t_0 + T$, and ω is an elementary event. It is known that if $H^{(j)}$, $j = 0, \ldots, m$ are sufficiently smooth, then $X(t; t_0, x_0; \omega)$ is a phase flow (diffeomorphism) for almost any ω ([7]). To simplify the notation, we will remove any mentioning of the dependence on ω unless it is absolutely necessary to avoid confusions, and we make the convention to understand that all the equations involving the solution of the SHS (5.1) are true for almost any ω.

In differential geometry, the differential 1-form of a function $f : \mathbb{R}^{2n} \to \mathbb{R}$ on $\xi \in \mathbb{R}^{2n}$ is defined as:

$$df(\xi) := \sum_{i=1}^{2n} \frac{\partial f}{\partial z_i} \xi_i. \tag{5.2}$$

The exterior product $df \wedge dg$ of $\xi, \eta \in \mathbb{R}^{2n}$ is given by $df \wedge dg(\xi, \eta) = df(\xi)dg(\eta) - df(\eta)dg(\xi)$, and represents the oriented area of the image of the parallelogram with sides $df(\xi)$ and $dg(\eta)$ on the $df(\xi), dg(\eta)$-plane.

The stochastic flow $(p, q) \longrightarrow (P, Q)$ of the SHS (5.1) preserves symplectic structure (Theorem 2.1 in [12]) as follows:

$$dP \wedge dQ = dp \wedge dq, \tag{5.3}$$

i.e. the sum over the oriented areas of its projections onto the two dimensional plane (p_i, q_i) is invariant. Here we consider the differential 2-form

$$dp \wedge dq = dp_1 \wedge dq_1 + \cdots + dp_n \wedge dq_n, \tag{5.4}$$

and the differentiation in (5.1) and (5.3) have different meanings: in (5.1) p, q are fixed parameters and differentiation is done with respect to time t, while in (5.3) differentiation is carried out with respect to the initial data p, q. We say that a method based on the one step approximation $\bar{P} = \bar{P}(t + h; t, p, q)$, $\bar{Q} = \bar{Q}(t + h; t, p, q)$ preserves symplectic structure if

$$d\bar{P} \wedge d\bar{Q} = dp \wedge dq. \tag{5.5}$$

Here, we introduce another definition of symplecticity. A random map $\varphi(\omega, x)$ is a map with the property that for any fixed $x \in \mathbb{R}^{2n}$, $\varphi(\cdot, x)$ is a random variable. We denote $\varphi_\omega(\cdot) = \varphi(\omega, \cdot)$.

Definition 5.1 (symplecticity:) *A differentiable random map $\varphi_\omega : U \to \mathbb{R}^{2n}$ (where $U \subset \mathbb{R}^{2n}$ is an open set) is called symplectic if the Jacobian matrix φ'_ω satisfies*

$$\varphi'_\omega(p,q)^T J \varphi'_\omega(p,q) = J \quad \textit{with} \quad J = \begin{bmatrix} 0 & I \\ -I & 0 \end{bmatrix} \tag{5.6}$$

for almost any ω and any $p, q \in \mathbb{R}^n$, $(p,q)^T \in U$, where I is the identity matrix of dimension n.

The two definitions of symplecticity are equivalent, as stated in the following theorem:

Theorem 5.2 *A random differentiable map $\varphi_\omega : (p,q) \to (P,Q)$ is symplectic if and only if $dP \wedge dQ = dp \wedge dq$ almost surely (a.s.).*

Proof: For any ξ, $\eta \in \mathbb{R}^n$ and for the $2n \times 1$ vectors $\zeta_1 = (dp_\xi, dq_\xi)^T$ and $\zeta_2 = (dp_\eta, dq_\eta)^T$, we have

$$\zeta_1^T J \zeta_2 = (dp_\xi, dq_\xi) J (dp_\eta, dq_\eta)^T = \sum_{i=1}^{n} (dp_{\xi_i} dq_{\eta_i} - dq_{\xi_i} dp_{\eta_i}) = \sum_{i=1}^{n} dp_i \wedge dq_i = dp \wedge dq(\xi, \eta). \tag{5.7}$$

If Φ is the Jacobian of φ_ω, then $(dP, dQ)^T = \Phi (dp, dq)^T$, and proceeding as in (5.7), we have

$$dP \wedge dQ(\xi, \eta) = (dp_\xi, dq_\xi) \Phi^T J \Phi (dp_\eta, dq_\eta)^T. \tag{5.8}$$

Thus, we get $\Phi^T J \Phi = J$ a.s. if and only if $dP \wedge dQ = dp \wedge dq$ a.s.. □

5.2 Generating function and stochastic Hamiltonian-Jacobi partial differential equation

In the deterministic case, generating functions are powerful tools to study symplectic transformations. The next lemma introduces the generating functions S_ω, S^i_ω, $i = 1, 2, 3$ in the stochastic case.

Lemma 5.3 *Let $\varphi_\omega : (p, q) \to (P, Q)$ be a smooth random map from $\mathbb{R}^{2n}$ to $\mathbb{R}^{2n}$. Then φ_ω is symplectic if any of the following statements is true:*

1. *There exists locally a smooth random map S_ω from $\mathbb{R}^{2n}$ to $\mathbb{R}^{2n}$ such that $\partial(S_\omega)/\partial q\partial Q$ is invertible a.s. and we have*

$$P_i = \frac{\partial S}{\partial Q_i}(q, Q), \quad p_i = -\frac{\partial S}{\partial q_i}(q, Q), \quad i = 1, \ldots, n. \tag{5.9}$$

2. *There exists locally a smooth random map S^1_ω from $\mathbb{R}^{2n}$ to $\mathbb{R}^{2n}$ such that $\partial(P^T q + S^1_\omega)/\partial P\partial q$ is invertible a.s., and we have*

$$p_i = P_i + \frac{\partial S^1_\omega}{\partial q_i}(P, q), \quad Q_i = q_i + \frac{\partial S^1_\omega}{\partial P_i}(P, q), \quad i = 1, \ldots, n. \tag{5.10}$$

3. *There exists locally a smooth random map S^2_ω from $\mathbb{R}^{2n}$ to $\mathbb{R}^{2n}$ such that $\partial(p^T Q + S^2_\omega)/\partial p\partial Q$ is invertible a.s., and we have*

$$q_i = Q_i + \frac{\partial S^2_\omega}{\partial p_i}(p, Q), \quad P_i = p_i + \frac{\partial S^2_\omega}{\partial Q_i}(p, Q), \quad i = 1, \ldots, n. \tag{5.11}$$

4. *There exists locally a smooth random map S^3_ω from $\mathbb{R}^{2n}$ to $\mathbb{R}^{2n}$ such that $\partial((P + p)^T(Q - q) - 2S^3_\omega)/\partial Y\partial y$ is invertible a.s., and we have*

$$Y = y - J\nabla S^3_\omega((y + Y)/2), \tag{5.12}$$

where $Y = (P^T, Q^T)^T$, $y = (p^T, q^T)^T$.

Proof:

The proof can be completed easily by adapting the proof of Theorem 3.1 in [11]. For example, to prove that the first statement implies that φ_ω is symplectic, we calculate

$$\sum_{i=1}^{n} dP_i \wedge dQ_i = \sum_{i=1}^{n} \left(\sum_{j=1}^{n} \frac{\partial^2 S_\omega}{\partial Q_i \partial Q_j} dQ_j + \sum_{j=1}^{n} \frac{\partial^2 S_\omega}{\partial Q_i \partial q_j} dq_j \right) \wedge dQ_i$$
$$= \sum_{i=1}^{n} \sum_{j=1}^{n} \frac{\partial^2 S_\omega}{\partial Q_i \partial Q_j} dQ_j \wedge dQ_i + \sum_{i=1}^{n} \sum_{j=1}^{n} \frac{\partial^2 S_\omega}{\partial Q_i \partial q_j} dq_j \wedge dQ_i,$$

where everwhere the arguments are Q, q. Since $dQ_i \wedge dQ_j = -dQ_j \wedge dQ_i$, we get

$$\sum_{i=1}^{n} dP_i \wedge dQ_i = \sum_{i=1}^{n} \sum_{j=1}^{n} \frac{\partial^2 S_\omega}{\partial Q_i \partial q_j} dq_j \wedge dQ_i. \tag{5.13}$$

Similarly, using the second equation in (5.9) and $dq_i \wedge dq_j = -dq_j \wedge dq_i$, we have

$$\sum_{i=1}^{n} dp_i \wedge dq_i = \sum_{i=1}^{n} \sum_{j=1}^{n} -\frac{\partial^2 S_\omega}{\partial q_i \partial Q_j} dQ_j \wedge dq_i. \tag{5.14}$$

From (5.13), (5.14) and $dq_i \wedge dQ_j = -dQ_j \wedge dq_i$, we get $dP \wedge dQ = dp \wedge dq$ a.s., so φ_ω is symplectic. □

The previous lemma gives us a powerful tool to analyze the symplectic structure and to construct symplectic methods. For instance, for the SHS (5.1), if in the relation (5.10) we let

$$S_\omega^1 = hH^{(0)}(P,q) + \frac{h}{2} \sum_{r=1}^{m} \sum_{j=1}^{n} \frac{\partial H^{(r)}}{\partial q_j}(P,q) \frac{\partial H^{(r)}}{\partial P_j}(P,q) + \sum_{r=1}^{m} \sqrt{h} \xi_r H^{(r)}(P,q) \tag{5.15}$$

where h is the time step and ξ_r are independent bounded random variables such that $E(\xi_r - \xi)^2 \leq h$, with $\xi \sim N(0,1)$, then we obtain the symplectic Euler scheme proposed by Milstein et al. [12] [11]. Lemma 5.3 guarantees that the numerical scheme is symplectic. Moreover the implicit midpoint scheme in [11] is obtained by setting

$$S_\omega^3 = hH^{(0)}((y+Y)/2) + \sum_{r=1}^{m} \sqrt{h} \xi_r H^{(r)}((y+Y)/2) \tag{5.16}$$

in relation (5.12).

The stochastic Hamilton-Jacobi partial differential equation associated with the SHS (5.1) follows the rigorous approach from [2]. We want to consider the effect of time in the generating function S_ω, so let $S_\omega(x,t)$ be a family of real valued processes with parameters $x \in \mathbb{R}^{2n}$. We can regard it as a random field with double parameters x and t. If $S_\omega(x,t)$ is a $\mathcal{C}^\infty$ function of x for almost all ω for any t, we can regard $S_\omega(x,t)$ as a $\mathcal{C}^\infty$ value process [8].

Let assume that the Hamiltonian function $H^{(r)}$ for $r = 0, \ldots, m$ in (5.1) belong to $\mathcal{C}^\infty$. In addition, we also suppose that:

$$\sum_{r=0}^{m}(|\nabla_p H^{(r)}(P,Q) - \nabla_p H^{(r)}(p,q)| + |\nabla_q H^{(r)}(P,Q) - \nabla_q H^{(r)}(p,q)|) \leq L_1(|P-p| + |Q-q|) \tag{5.17}$$

and

$$\sum_{r=0}^{m}(|\nabla_p H^{(r)}(p,q)| + |\nabla_q H^{(r)}(p,q)|) \leq L_2(1 + |p| + |q|) \tag{5.18}$$

So the Lipschitz condition (5.17) and linear growth bound (5.18) guarantees the local existence and uniqueness of the solution $\left(P(t,\omega)^T, Q(t,\omega)^T\right)^T$ of the SHS (5.1). Moreover, it is known that $X(t;t_0,x_0;\omega) = \left(P^T(t;t_0,p,q;\omega),\, Q^T(t;t_0,p,q;\omega)\right)^T$, where $t_0 \leq t \leq t_0 + T$ is a diffeomorphism a.s.[7]. Thus the generating function, which is a random mapping, becomes a stochastic process $S(q,Q,t,\omega)$, and through equations (5.9), this stochastic process generates the symplectic map $(p,q) \to (P(t,\omega), Q(t,\omega))$ of the flow of the SHS.

For the sake of simplification, let us keep the notation S_ω for the stochastic process $S(q,Q,t,\omega)$. The generating function S_ω is connected with the SHS (5.1) by the Hamilton-Jacobi partial differential equation (HJ PDE) (see Theorem 6.14 in [2]):

$$dS_\omega = -H^{(0)}(\frac{\partial S_\omega}{\partial Q_1}, \ldots, \frac{\partial S_\omega}{\partial Q_n}, Q_1, \ldots, Q_n)dt - \sum_{r=1}^{m} H^{(r)}(\frac{\partial S_\omega}{\partial Q_1}, \ldots, \frac{\partial S_\omega}{\partial Q_n}, Q_1, \ldots, Q_n) \circ dw_t^r, \tag{5.19}$$

with the initial condition $S_\omega(q,Q,0) = j(q,Q)$, where j is a C^∞ function. Starting from the flow $X(t;t_0,x_0;\omega)$ of the SHS (5.1) and using the method of characteristics, in Theorem 6.14 and its corollary in [2] it is shown that for any initial point x_0 there

exists a stopping time $\tau > t_0$ a.s and a local solution $S_\omega(q, Q, t)$, $t_0 \leq t < \tau$ of (5.19) for which we have the equations given in (5.9). Moreover, almost sure the flow $X(t; t_0, x_0; \omega)$ is a local Stratonovich semi-martingale, and $S_\omega(q, Q, t)$, $\partial S_\omega(q, Q, t)/\partial Q$ and $\partial S_\omega(q, Q, t)/\partial q$ are local Stratonovich semi-martingale, continuous on (q, Q, t), and $\mathcal{C}^\infty$ value processes (see also Theorem 6.1.5 in [8]).

Theorem 5.4 *Let $S_\omega(q, Q, t)$ be a local solution of the HJ PDE (5.22) with initial values satisfying $\frac{\partial j}{\partial q_i}(q, q) + \frac{\partial j}{\partial Q_i}(q, q) = 0$, $i = 1, \ldots, n$, and such that almost sure $S_\omega(q, Q, t)$, $\partial S_\omega(q, Q, t)/\partial Q$ and $\partial S_\omega(q, Q, t)/\partial q$ are local Stratonovich semi-martingale, continuous on (q, Q, t), and $\mathcal{C}^\infty$ value processes. If there exists a stopping time $\tau' > t_0$ a.s. such that the matrix $(\partial^2(S_\omega)/\partial q \partial Q)$ is a.s. invertible for $t_0 \leq t < \tau'$, then the map $(p, q) \to (P(t, \omega), Q(t, \omega))$, $t_0 \leq t < \tau'$, defined by (5.9) is the flow of the SHS (5.1).*

Proof: The mapping $(p, q) \to (P_\omega, Q_\omega)$ is well defined by (5.9) because of the invertibility of the matrix $(\partial^2(S_\omega)/\partial q \partial Q)$ for $t_0 \leq t < \tau'$, and the implicit function theorem.

Differentiation of the second equation of (5.9) (see Theorem 3.3.2 in [8]) yields

$$d(\frac{\partial S_\omega}{\partial q_i}) + \sum_{j=1}^{n} \frac{\partial^2 S_\omega}{\partial q_i \partial Q_j} dQ_j = 0. \tag{5.20}$$

Recalling that S_ω is the solution of the stochastic HJ PDE (5.19), the following equation holds by differentiating (5.19) with respect to q_i (see the corollary of Theorem 6.14 in [2]).

$$d(\frac{\partial S_\omega}{\partial q_i}) + \sum_{j=1}^{n} \frac{\partial H^{(0)}}{\partial P_j} \frac{\partial^2 S_\omega}{\partial q_i \partial Q_j} dt + \sum_{r=1}^{m} \sum_{j=1}^{n} \frac{\partial H^{(r)}}{\partial P_j} \frac{\partial^2 S_\omega}{\partial q_i \partial Q_j} \circ dw_t^r = 0. \tag{5.21}$$

Comparing equations (5.20) and (5.21) and using the invertibility of the matrix $(\frac{\partial^2 S_\omega}{\partial q_i \partial Q_j})$, we have the second equation of (5.1).

The first equation of (5.1) can be obtained using a similar procedure as reported above, i.e., by differentiating the first relation of (5.9) and the HJ PDE with respect

to Q_i, then subtracting the obtained equations. Also the initial values guarantee that $(P(t_0,\omega),Q(t_0,\omega)) = (p,q)$. □

The HJ PDEs for the coordinate transformations (2) and (4) in Lemma 5.3 can be expressed as

$$S^1_\omega(t,P,q) = \int_{t_0}^{t} H^{(0)}(P, q+\nabla_P S^1_\omega(s,P,q))ds + \int_{t_0}^{t}\sum_{r=1}^{m} H^{(r)}(P, q+\nabla_P S^1_\omega(s,P,q))\circ dw^r_s, \tag{5.22}$$

$$S^3_\omega(t,w) = \int_{t_0}^{t} H^{(0)}(w+\frac{1}{2}J^{-1}\nabla S^3_\omega(s,w))ds + \int_{t_0}^{t}\sum_{r=1}^{m} H^{(r)}(w+\frac{1}{2}J^{-1}\nabla S^3_\omega(s,w))\circ dw^r_s, \tag{5.23}$$

where $w \in \mathbb{R}^{2n}$, and we consider $S^1_\omega|_{t=t_0} = 0$ and $S^3_\omega|_{t=t_0} = 0$. It is straightforward to obtain the HJ PDE for the generating function (3) in Lemma 5.3, as it is just the adjoint case of (2).

5.3 Constructing high-order symplectic schemes

For deterministic problems, the construction of high-order symplectic schemes via generating functions was first proposed by Feng et al [3], [4]. The key idea is to obtain an approximation of the solution of the HJ PDE, and then to construct the symplectic numerical scheme through the relations (5.10) - (5.12).

Following this idea, we now seek an expansion which reflects the stochastic properties of the generating function. Due to the Ito representation theorem, the relation between the Ito integral, the Stratonovich integral and the stochastic Taylor-Stratonovich expansion, it is reasonable to assume that the generating function can be expressed by the following expansion locally:

$$S^1(P,q,t,\theta(t)\omega) = G^1_{(0)}(P,q)J_{(0)} + G^1_{(1)}(P,q)J_{(1)} + G^1_{(0,1)}(P,q)J_{(0,1)} + \cdots = \sum_\alpha G^1_\alpha J_\alpha, \tag{5.24}$$

where $\alpha = (j_1, j_2, \ldots, j_l), j_i \in \{0, 1, \ldots, m\}$, $i = 1, \ldots, l$ is a multi-index of length l, and J_α is the multiple Stratonovich integral

$$J_\alpha = \int_0^t \int_0^{s_l} \ldots \int_0^{s_2} \circ dw_{s_1}^{j_1} \cdots \circ dw_{s_{l-1}}^{j_{l-1}} \circ dw_{s_l}^{j_l}. \tag{5.25}$$

For convenience, ds is denoted by dw_s^0. Similarly, the multiple Ito stochastic integral I_α is given by

$$I_\alpha = \int_0^t \int_0^{s_l} \ldots \int_0^{s_2} dw_{s_1}^{j_1} \ldots dw_{s_{l-1}}^{j_{l-1}} dw_{s_l}^{j_l}. \tag{5.26}$$

5.3.1 Properties of multiple stochastic integrals

To prepare for the derivation of the symplectic numerical schemes, we present some properties of the multiple stochastic integrals. First, we define operations for multi-indexes.

If the multi-index $\alpha = (j_1, j_2, \ldots, j_l)$ with $l > 1$ then $\alpha- = (j_1, j_2, \ldots, j_{l-1})$, i.e. the last component is deleted. For instance, $(1, 3, 0)- = (1, 3)$. For any two multi-indexes $\alpha = (j_1, j_2, \ldots, j_l)$ and $\alpha' = (j_1', j_2', \ldots, j_{l'}')$, we define the concatenation operation $'*'$ as $\alpha * \alpha' = (j_1, j_2, \ldots, j_l, j_1', j_2', \ldots, j_{l'}')$. For example, $(1, 3, 0) * (1, 4) = (1, 3, 0, 1, 4)$. The concatenation of a collection Λ of multi-indexes with the multi-index α gives the collection formed by concatenating each element of the collection Λ with the multi-index α, i.e., $\Lambda * \alpha = \{\alpha' * \alpha | \alpha' \in \Lambda\}$. For example, if $\Lambda = \{(1, 1), (0, 1, 2), (1, 1)\}$ and $\alpha = (0)$, then $\Lambda * \alpha = \{(1, 1, 0), (0, 1, 2, 0), (1, 1, 0)\}$.

Proposition 5.5

$$J_\alpha J_{\alpha'} = \sum_{\beta \in \Lambda_{\alpha,\alpha'}} J_\beta \tag{5.27}$$

where $\alpha = (j_1, j_2, \ldots, j_l)$, $\alpha' = (j_1', j_2', \ldots, j_{l'}')$ *and* $\Lambda_{\alpha,\alpha'}$ *is the collection of multi-indexes*

depending on α and α' and given by the following recurrence relation:

$$\Lambda_{\alpha,\alpha'} = \begin{cases} \{(j_1, j'_1), (j'_1, j_1)\}, & \text{if} \quad l = 1 \text{and } l' = 1 \\ \{\Lambda_{(j_1),\alpha'-} * (j'_{l'}), \alpha' * (j_l)\}, & \text{if} \quad l = 1 \text{and } l' \neq 1 \\ \{\Lambda_{\alpha-,(j'_1)} * (j_l), \alpha * (j'_l)\}, & \text{if} \quad l \neq 1 \text{and } l' = 1 \\ \{\Lambda_{\alpha-,\alpha'} * (j_l), \Lambda_{\alpha,\alpha'-} * (j'_{l'})\}, & \text{if} \quad l \neq 1 \text{and } l' \neq 1 \end{cases} \tag{5.28}$$

Proof: Let consider two stochastic processes

$$X_t^1 = \int_0^t b_1(X_s) \circ dw_s^{j_l} \quad \text{and } X_t^2 = \int_0^t b_2(X_s) \circ dw_s^{j'_{l'}}. \tag{5.29}$$

Then, for the Stratonovich integrals, we have

$$X_t^1 X_t^2 = \int_0^t X_s^2 b_1(X_s) \circ dw_s^{j_l} + \int_0^t X_s^1 b_2(X_s) \circ dw_s^{j'_{l'}}. \tag{5.30}$$

If $l > 1$ and $l' > 1$, let $b_1(X_s) = J_{\alpha-}$ and $b_2(X_s) = J'_{\alpha'-}$, such that $X_t^1 = J_\alpha$ and $X_t^2 = J_{\alpha'}$. The product rule (5.30) of the stochastic integrals yields

$$J_\alpha J_{\alpha'} = \int_0^t J_{\alpha'} J_{\alpha-} \circ dw_s^{j_l} + \int_0^t J_\alpha J_{\alpha'-} \circ dw_s^{j'_{l'}}. \tag{5.31}$$

This implies the fourth relation in (5.28).

If $l = 1$ (or $l' = 1$), the second (or third) relation in the recurrence (5.28) is obtained for $b_1(X_s) = 1$ and $b_2(X_s) = J'_{\alpha'-}$ (or $b_1(X_s) = J_{\alpha-}$ and $b_2(X_s) = 1$). For the first relation, we take $b_1(X_s) = 1$ and $b_2(X_s) = 1$. □

For instance, since

$$\begin{aligned} \Lambda_{(2,0),(0,1)} &= \{\Lambda_{(2),(0,1)} * (0), \Lambda_{(2,0),(0)} * (1)\} \\ &= \{\{\Lambda_{(2),(0)} * (1), (0,1,2)\} * (0)\}, \{\Lambda_{(2),(0)} * (0), (2,0,0)\} * (1)\} \\ &= \{\{(2,0,1), (0,2,1), (0,1,2)\} * (0), \{(0,2,0), (2,0,0), (2,0,0)\} * (1)\} \\ &= \{(2,0,1,0), (0,2,1,0), (0,1,2,0), (0,2,0,1), (2,0,0,1), (2,0,0,1)\}, \end{aligned} \tag{5.32}$$

then we have $J_{(2,0)} J_{(0,1)} = J_{(2,0,1,0)} + J_{(0,2,1,0)} + J_{(0,1,2,0)} + J_{(0,2,0,1)} + 2J_{(2,0,0,1)}$

Remark 5.6 *From the recurrence (5.28), we can see that* $\Lambda_{\alpha,\alpha'} = \Lambda_{\alpha',\alpha}$*, and the length of the multi indexes in* $\Lambda_{\alpha,\alpha'}$ *is the summation of the lengths of* α *and* α'*, i.e. if* $\beta \in \Lambda_{\alpha,\alpha'}$*, then* $l(\beta) = l(\alpha) + l(\alpha')$*. This will be used to determine the coefficients of the generating function in the next subsection.*

Corollary 5.7 *For* $\alpha = (j_1, j_2, \ldots, j_l)$*,*

$$w_t^j J_\alpha = \sum_{i=0}^{l} J_{(j_1,\ldots,j_i,j,j_{i+1},\ldots,j_l)}. \tag{5.33}$$

Proof: The proof follows by repeatedly applying the second recurrence of (5.28). □

Similarly, we can show that the multiplication of a finite sequence of multiple-indexes can be expressed by the following summation:

$$\prod_{i=1}^{n} J_{\alpha_i} = \sum_{\beta \in \Lambda_{\alpha_1,\ldots,\alpha_n}} J_\beta, \tag{5.34}$$

where the collection $\Lambda_{\alpha_1,\ldots,\alpha_n}$ can be defined recursively by $\Lambda_{\alpha_1,\ldots,\alpha_n} = \{\Lambda_{\beta,\alpha_n} | \beta \in \Lambda_{\alpha_1,\ldots,\alpha_{n-1}}\}$, $n \geq 3$. For example, $\Lambda_{(1),(0),(0)} = \{\Lambda_{\beta,(0)} | \beta \in \Lambda_{(1),(0)}\} = \{\Lambda_{(0,1),(0)}, \Lambda_{(1,0),(0)}\}$ $= \{(0,0,1),(0,0,1),(0,1,0),(1,0,0),(0,1,0),(1,0,0)\}$. Thus $J_{(1)}J_{(0)}^2 = 2J_{(0,0,1)} + 2J_{(1,0,0)} + 2J_{0,1,0)}$.

In addition to the recurrence relation (5.28), we also propose an explicit way to calculate the collection $\Lambda_{\alpha,\alpha'}$. For any multi-index $\alpha = (j_1, j_2, \ldots, j_l)$ with no duplicated elements (i.e., $j_m \neq j_n$ if $m \neq n$, $m, n = 1, \ldots, l$), we define the set $R(\alpha)$ to be the empty set $R(\alpha) = \Phi$ if $l = 1$ and $R(\alpha) = \{(j_m, j_n) | m < n, m, n = 1, \ldots, l\}$ if $l \geq 2$. $R(\alpha)$ defines a partial order on the set formed with the numbers included in the multi-index α, defined by $i \prec j$ if and only if $(i, j) \in R(\alpha)$. We suppose that there are no duplicated elements in or between the multi-indexes $\alpha = (j_1, j_2, \ldots, j_l)$ and $\alpha' = (j'_1, j'_2, \ldots, j'_{l'})$.

Lemma 5.8 *If there are no duplicated elements in or between the multi-indexes* $\alpha = (j_1, j_2, \ldots, j_l)$ *and* $\alpha' = (j'_1, j'_2, \ldots, j'_{l'})$*, then*

$$\begin{aligned} \Lambda_{\alpha,\alpha'} = \{\beta \in \mathcal{M} | & l(\beta) = l(\alpha) + l(\alpha'), R(\alpha) \cup R(\alpha') \subseteq R(\beta) \\ & \textit{and } \beta \textit{ has no duplicated elements}\} \end{aligned} \tag{5.35}$$

where $\mathcal{M} = \{(\hat{j}_1, \hat{j}_2, \ldots, \hat{j}_{l+l'}) | \hat{j}_i \in \{j_1, j_2, \ldots, j_l, j'_1, j'_2, \ldots, j'_{l'}\}, i = 1, \ldots, l+l'\}$

Proof: Let denote $\Lambda'_{\alpha,\alpha'} = \{\beta \in \mathcal{M} | l(\beta) = l(\alpha) + l(\alpha'),\ R(\alpha) \cup R(\alpha') \subseteq R(\beta)$ and β has no duplicated elements $\}$. Since there are no duplicated elements in β and $l(\beta) = l(\alpha) + l(\alpha')$, each element of $\{j_1, j_2, \ldots, j_l, j'_1, j'_2, \ldots, j'_{l'}\}$ must appear in β only once.

We prove that $\Lambda_{\alpha,\alpha'} = \Lambda'_{\alpha,\alpha'}$ by induction on $l(\alpha) + l(\alpha')$. If $l(\alpha) + l(\alpha') = 2$, then $l(\alpha) = l(\alpha') = 1$ and $R(\alpha) = R(\alpha') = \Phi$. Hence $R(\beta)$ contains any pair with distinct components from $\mathcal{M} = \{(\hat{j}_1, \hat{j}_2) | \hat{j}_1, \hat{j}_2 \in \{j_1, j'_1\}\}$, so $\Lambda'_{\alpha,\alpha'} = \{(j_1, j'_1), (j'_1, j_1)\}$, and from the first equation in the recurrence (5.28), $\Lambda'_{\alpha,\alpha'} = \Lambda_{\alpha,\alpha'}$.

We suppose that $\Lambda_{\alpha,\alpha'} = \Lambda'_{\alpha,\alpha'}$ for any multi-indexes α and α' such that $l(\alpha)+l(\alpha') < k$ and we prove that $\Lambda_{\alpha,\alpha'} = \Lambda'_{\alpha,\alpha'}$ for any multi-indexes α and α' with $l(\alpha) + l(\alpha') = k$

First, we prove that $\Lambda'_{\alpha,\alpha'} \subseteq \Lambda_{\alpha,\alpha'}$. For any element $\beta = \{\hat{j}_1, \hat{j}_2, \ldots, \hat{j}_k\}$ in $\Lambda'_{\alpha,\alpha'}$, because j_l is the largest element with respect to the partial order defined by $R(\alpha)$, and $j'_{l'}$ is the largest element with respect to the partial order defined by $R(\alpha')$, then $\hat{j}_k$ can only be j_l or $j'_{l'}$. This leads to the following cases:

1. If $\hat{j}_k = j_l$ and $l = 1$, then $\beta = \alpha' * j_1 \in \Lambda_{\alpha,\alpha'}$, by the second equation in recurrence (5.28).

2. If $\hat{j}_k = j_l$ and $l > 1$, then $\beta- \in \Lambda'_{\alpha-,\alpha'} = \Lambda_{\alpha-,\alpha'}$ by the induction assumption because $l(\alpha-) + l(\alpha') = k - 1 < k$. Hence $\beta = \beta - *(j_l) \in \Lambda_{\alpha-,\alpha'} * (j_l)$, and from the fourth equation in recurrence (5.28) we get $\beta \in \Lambda_{\alpha,\alpha'}$.

3. If $\hat{j}_k = j_{l'}$ and $l' = 1$, then $\beta = \alpha * j'_1 \in \Lambda_{\alpha,\alpha'}$, by the third equation in recurrence (5.28).

4. If $\hat{j}_k = j_{l'}$ and $l' > 1$, then $\beta- \in \Lambda'_{\alpha,\alpha'-} = \Lambda_{\alpha,\alpha'-}$. Hence $\beta = \beta - *(j'_l) \in \Lambda_{\alpha,\alpha'-} * (j'_l)$, and from the fourth equation in recurrence (5.28) we get $\beta \in \Lambda_{\alpha,\alpha'}$.

Similarly, using the recurrence (5.28), we can prove that $\Lambda_{\alpha,\alpha'} \subseteq \Lambda'_{\alpha,\alpha'}$. Thus $\Lambda_{\alpha,\alpha'} = \Lambda'_{\alpha,\alpha'}$ and the lemma is proved. □

The lemma can be easily extended to determine the collection $\Lambda_{\alpha_1,\ldots,\alpha_n}$.

Lemma 5.9 *If there are no duplicated elements in or between any of the multi-indexes* $\alpha = (j_1^{(1)}, j_2^{(1)}, \ldots, j_{l_1}^{(1)})$, $\ldots$, $\alpha_n = (j_1^{(n)}, j_2^{(n)}, \ldots, j_{l_n}^{(n)})$, *then*

$$\begin{aligned}\Lambda_{\alpha_1,\ldots,\alpha_n} = \{\beta \in \mathcal{M} | l(\beta) = \sum_{k=1}^{n} l(\alpha_k) \textit{and } \cup_{k=1}^{n} R(\alpha_k) \subseteq R(\beta) \\ \textit{and there are no duplicated elements in } \beta\},\end{aligned} \tag{5.36}$$

where $\mathcal{M} = \{(\hat{j}_1, \hat{j}_2, \ldots, \hat{j}_{\hat{l}}) | \hat{j}_i \in \{j_1^{(1)}, j_2^{(1)}, \ldots, j_{l_1}^{(1)}, \ldots j_1^{(n)}, j_2^{(n)}, \ldots, j_{l_n}^{(n)}\}, i = 1, \ldots, \hat{l}, \hat{l} = l_1 + \cdots + l_n\}$.

To extend the previous two lemmas to multi-indexes with duplicated elements, we just need to assign a different subscript to each duplicated element, for example, $\Lambda_{(2,0),(0,1)} = \Lambda_{(2,0_1),(0_2,1)} = \{(2, 0_2, 1, 0_1), (0_2, 2, 1, 0_1), (0_1, 1, 2, 0_2), (0_2, 2, 0_1, 1), (2, 0_1, 0_2, 1), (2, 0_2, 0_1, 1)\}$.

5.3.2 Higher order symplectic scheme

Inserting (5.24) into the HJ PDE (5.22), and using the proposition (5.5), we get

$$\begin{aligned}
S_\omega^1 &= \int_0^t H^{(0)}(P, q + \sum_\alpha \frac{\partial G_\alpha^1}{\partial P} J_\alpha) ds + \sum_{r=1}^{m} \int_0^t H^{(r)}(P, q + \sum_\alpha \frac{\partial G_\alpha^1}{\partial P} J_\alpha) \circ dw_s^r \\
&= \sum_{r=0}^{m} \int_0^t H^{(r)}(P, q + \sum_\alpha \frac{\partial G_\alpha^1}{\partial P} J_\alpha) \circ dw_s^r \\
&= \sum_{r=0}^{m} \int_0^t \sum_{i=0}^{\infty} \frac{1}{i!} \sum_{k_1,\ldots,k_i=1}^{n} \frac{\partial^i H^{(r)}}{\partial q_{k_1} \ldots \partial q_{k_i}} (\sum_\alpha \frac{\partial G_\alpha^1}{\partial P} J_\alpha)_{k_1} \ldots (\sum_\alpha \frac{\partial G_\alpha^1}{\partial P} J_\alpha)_{k_i} \circ dw_s^r \\
&= \sum_{r=0}^{m} \sum_{i=0}^{\infty} \frac{1}{i!} \sum_{k_1,\ldots,k_i=1}^{n} \frac{\partial^i H^{(r)}}{\partial q_{k_1} \ldots \partial q_{k_i}} \sum_{\alpha_1,\ldots,\alpha_i} \frac{\partial G_{\alpha_1}^1}{\partial P_{k_1}} \cdots \frac{\partial G_{\alpha_i}^1}{\partial P_{k_i}} \int_0^t \prod_{k=1}^{i} J_{\alpha_k} \circ dw_s^r \\
&= \sum_{r=0}^{m} \sum_{i=0}^{\infty} \frac{1}{i!} \sum_{k_1,\ldots,k_i=1}^{n} \frac{\partial^i H^{(r)}}{\partial q_{k_1} \ldots \partial q_{k_i}} \sum_{\alpha_1,\ldots,\alpha_i} \frac{\partial G_{\alpha_1}^1}{\partial P_{k_1}} \cdots \frac{\partial G_{\alpha_i}^1}{\partial P_{k_i}} \sum_{\beta \in \Lambda_{\alpha_1,\ldots\alpha_i}} J_{\beta * (r)} \\
&= \sum_{r=0}^{m} \sum_{i=0}^{\infty} \sum_{k_1,\ldots,k_i=1}^{n} \sum_{\alpha_1,\ldots,\alpha_i} \sum_{\beta \in \Lambda_{\alpha_1,\ldots\alpha_i}} \frac{1}{i!} \frac{\partial^i H^{(r)}}{\partial q_{k_1} \ldots \partial q_{k_i}} \frac{\partial G_{\alpha_1}^1}{\partial P_{k_1}} \cdots \frac{\partial G_{\alpha_i}^1}{\partial P_{k_i}} J_{\beta * (r)}
\end{aligned} \tag{5.37}$$

where $(\sum_\alpha \frac{\partial G^1_{\alpha_i}}{\partial P})_{k_i}$ is the k_i-th component of the column vector $\sum_\alpha \frac{\partial G^1_{\alpha_i}}{\partial P}$. Equating the coefficients of J_α in (5.24) and (5.37), we get the recurrence formula for determining G^1_α.

For instance, for the SHS (5.1) with $m = 1$, we have

$$G^1_{(0)} = H^{(0)}, \qquad G^1_{(1)} = H^{(1)}. \tag{5.38}$$

To find $G^1_{(0,0)}$, since $l((0,0))$ =2 we only need to consider the values $i = 1$, $\alpha = (0)$ and $r = 0$, so that

$$G^1_{(0,0)} = \sum_{k=1}^{n} \frac{\partial H^{(0)}}{\partial q_k} \frac{\partial G^1_{(0)}}{\partial P_k} = \sum_{k=1}^{n} \frac{\partial H^{(0)}}{\partial q_k} \frac{\partial H^{(0)}}{\partial P_k}. \tag{5.39}$$

Similarly, using $i = 1$, $\alpha = (1)$ and $r = 0$ for $G^1_{(1,0)}$, $i = 1$, $\alpha = (0)$ and $r = 1$ for $G^1_{(0,1)}$, and $i = 1$, $\alpha = (1)$ and $r = 1$ for $G^1_{(1,1)}$ we obtain

$$G^1_{(1,1)} = \sum_{k=1}^{n} \frac{\partial H^{(1)}}{\partial q_k} \frac{\partial H^{(1)}}{\partial P_k}, \quad G^1_{(1,0)} = \sum_{k=1}^{n} \frac{\partial H^{(0)}}{\partial q_k} \frac{\partial H^{(1)}}{\partial P_k}, \quad G^1_{(0,1)} = \sum_{k=1}^{n} \frac{\partial H^{(1)}}{\partial q_k} \frac{\partial H^{(0)}}{\partial P_k}. \tag{5.40}$$

Because $l((0,0,0)) = 3$, the cases $i = 1$, $\alpha = (0,0)$, $r = 0$ and $i = 2$, $\alpha_1 = (0)$, $\alpha_2 = (0)$, $r = 0$ both contribute to the coefficient of $J_{(0,0,0)}$:

$$\begin{aligned} G^1_{(0,0,0)} &= \sum_{k_1=1}^{n} \frac{\partial H^{(0)}}{\partial q_{k_1}} \frac{\partial G^1_{(0,0)}}{\partial P_{k_1}} + \sum_{k_1,k_2=1}^{n} \frac{1}{2} \frac{\partial^2 H^{(0)}}{\partial q_{k_1} \partial q_{k_2}} 2 \frac{\partial G^1_{(0)}}{\partial P_{k_1}} \frac{\partial G^1_{(0)}}{\partial P_{k_2}} \\ &= \sum_{k_1,k_2=1}^{n} \left(\frac{\partial^2 H^{(0)}}{\partial q_{k_1} \partial q_{k_2}} \frac{\partial H^{(0)}}{\partial P_{k_1}} \frac{\partial H^{(0)}}{\partial P_{k_2}} + \frac{\partial H^{(0)}}{\partial q_{k_1}} \frac{\partial H^{(0)}}{\partial P_{k_2}} \frac{\partial^2 H^{(0)}}{\partial q_{k_2} \partial P_{k_1}} + \frac{\partial H^{(0)}}{\partial q_{k_1}} \frac{\partial H^{(0)}}{\partial q_{k_2}} \frac{\partial^2 H^{(0)}}{\partial P_{k_1} \partial P_{k_2}} \right). \end{aligned} \tag{5.41}$$

Similarly,

$$
\begin{aligned}
G^1_{(1,1,1)} &= \sum_{k_1,k_2=1}^{n} \left(\frac{\partial^2 H^{(1)}}{\partial q_{k_1}\partial q_{k_2}} \frac{\partial H^{(1)}}{\partial P_{k_1}} \frac{\partial H^{(1)}}{\partial P_{k_2}} + \frac{\partial H^{(1)}}{\partial q_{k_1}} \frac{\partial H^{(1)}}{\partial P_{k_2}} \frac{\partial^2 H^{(1)}}{\partial q_{k_2}\partial P_{k_1}} + \frac{\partial H^{(1)}}{\partial q_{k_1}} \frac{\partial H^{(1)}}{\partial q_{k_2}} \frac{\partial^2 H^{(1)}}{\partial P_{k_1}\partial P_{k_2}} \right), \\
G^1_{(1,1,0)} &= \sum_{k_1,k_2=1}^{n} \left(\frac{\partial^2 H^{(0)}}{\partial q_{k_1}\partial q_{k_2}} \frac{\partial H^{(1)}}{\partial P_{k_1}} \frac{\partial H^{(1)}}{\partial P_{k_2}} + \frac{\partial H^{(0)}}{\partial q_{k_1}} \frac{\partial H^{(1)}}{\partial P_{k_2}} \frac{\partial^2 H^{(1)}}{\partial q_{k_2}\partial P_{k_1}} + \frac{\partial H^{(0)}}{\partial q_{k_1}} \frac{\partial H^{(1)}}{\partial q_{k_2}} \frac{\partial^2 H^{(1)}}{\partial P_{k_1}\partial P_{k_2}} \right), \\
G^1_{(1,0,1)} &= \sum_{k_1,k_2=1}^{n} \left(\frac{\partial^2 H^{(1)}}{\partial q_{k_1}\partial q_{k_2}} \frac{\partial H^{(0)}}{\partial P_{k_1}} \frac{\partial H^{(1)}}{\partial P_{k_2}} + \frac{\partial H^{(1)}}{\partial q_{k_1}} \frac{\partial H^{(1)}}{\partial P_{k_2}} \frac{\partial^2 H^{(0)}}{\partial q_{k_2}\partial P_{k_1}} + \frac{\partial H^{(1)}}{\partial q_{k_1}} \frac{\partial H^{(0)}}{\partial q_{k_2}} \frac{\partial^2 H^{(1)}}{\partial P_{k_1}\partial P_{k_2}} \right), \\
G^1_{(0,1,1)} &= \sum_{k_1,k_2=1}^{n} \left(\frac{\partial^2 H^{(1)}}{\partial q_{k_1}\partial q_{k_2}} \frac{\partial H^{(1)}}{\partial P_{k_1}} \frac{\partial H^{(0)}}{\partial P_{k_2}} + \frac{\partial H^{(1)}}{\partial q_{k_1}} \frac{\partial H^{(0)}}{\partial P_{k_2}} \frac{\partial^2 H^{(1)}}{\partial q_{k_2}\partial P_{k_1}} + \frac{\partial H^{(1)}}{\partial q_{k_1}} \frac{\partial H^{(1)}}{\partial q_{k_2}} \frac{\partial^2 H^{(0)}}{\partial P_{k_1}\partial P_{k_2}} \right).
\end{aligned}
\tag{5.42}
$$

For $m \geq 1$, we apply lemma 5.9 to obtain a recurrence formula for G^1_α. If $\alpha = (r)$, $r = 1, \ldots, m$ then $G^1_\alpha = H^{(r)}$. If $\alpha = (i_1, \ldots, i_{l-1}, r)$, $l > 1$, $i_1, \ldots, i_{l-1}, r = 1, \ldots, m$ has no duplicates then

$$
G^1_\alpha = \sum_{i=1}^{l(\alpha)-1} \frac{1}{i!} \sum_{k_1,\ldots,k_i=1}^{n} \frac{\partial^i H^{(r)}}{\partial q_{k_1} \ldots \partial q_{k_i}} \sum_{\substack{l(\alpha_1)+\cdots+l(\alpha_i)=l(\alpha)-1 \\ R(\alpha_1)\cup\cdots\cup R(\alpha_i)\subseteq R(\alpha-)}} \frac{\partial G^1_{\alpha_1}}{\partial P_{k_1}} \cdots \frac{\partial G^1_{\alpha_i}}{\partial P_{k_i}}. \tag{5.43}
$$

If the multi-index α contains any duplicates, then we apply formula (5.43) after associating different subscripts to the repeating numbers.

We can use the same approach, but for the HJPDE (5.23). For example, for the SHS (5.1) with $m = 1$, for S^3_ω we get

$$
\begin{aligned}
&G^3_{(0)} = H^{(0)}, \qquad G^3_{(1)} = H^{(1)}, \qquad G^3_{(0,0)} = 0, \qquad G^3_{(1,1)} = 0 \\
&G^3_{(1,0)} = \frac{1}{2}(\nabla H^{(0)})^T J^{-1} \nabla H^{(1)}, \qquad G^3_{(0,1)} = \frac{1}{2}(\nabla H^{(1)})^T J^{-1} \nabla H^{(0)} \\
&\quad G^3_{(0,0,0)} = \frac{1}{4}(J^{-1}\nabla H^{(0)})^T \nabla^2 H^{(0)} (J^{-1}\nabla H^{(0)}), \qquad \ldots
\end{aligned}
\tag{5.44}
$$

Proceeding as for S^1_ω, we can obtain a general recurrence for finding the coefficients G^3_α of S^3_ω. Hence, if $\alpha = (r)$, $r = 1, \ldots, d$ then $G^3_\alpha = H_r$. If $\alpha = (i_1, \ldots, i_{l-1}, r)$, $l > 1$,

$i_1, \ldots, i_{l-1}, r = 1, \ldots, d$ has no duplicates then

$$G^3_\alpha = \sum_{i=1}^{l(\alpha)-1} \frac{1}{i!} \sum_{k_1,\ldots,k_i=1}^{2n} \frac{\partial^i H_r}{\partial y_{k_1} \ldots \partial y_{k_i}} \sum_{\substack{l(\alpha_1)+\cdots+l(\alpha_i)=l(\alpha)-1 \\ R(\alpha_1)\cup\cdots\cup R(\alpha_i)\subseteq R(\alpha-)}} (\frac{1}{2} J^{-1}\nabla G^3_{\alpha_1})_{k_1} \ldots (\frac{1}{2} J^{-1}\nabla G^3_{\alpha_i})_{k_i} \tag{5.45}$$

where $(J^{-1}\nabla G^3_{\alpha_i})_{k_i}$ is the k_i-th component of the column vector $J^{-1}\nabla G^3_{\alpha_i}$. If the multi-index α contains any duplicates, then we apply formula (5.45) after we associate different subscripts to the repeating numbers.

Using (5.10) and a truncated series for S^1_ω, or using (5.12) and a truncated series for S^3_ω, we obtain various symplectic schemes for the SHS (5.1). In this Chapter, we study only the strong schemes, but a similar approach can be applied to construct the weak schemes, and it will be reported in the next Chapter. Let define $\mathcal{A}_\gamma = \{\alpha : l(\alpha) + n(\alpha) \leq 2\gamma\}$ and $\mathcal{B}_\gamma = \{\alpha : l(\alpha) + n(\alpha) \leq 2\gamma \text{ or } l(\alpha) = n(\alpha) = \gamma + 0.5\}$, where $n(\alpha)$ is the number of zero components of the multi-index α (e.g. $n((0,0,1)) = 2$).

The implicit midpoint scheme in [12] is the numerical scheme of order 1 obtained from (5.12) using the truncated series $S^3_\omega \approx \sum_{\alpha\in\mathcal{A}_1} G^3_\alpha J_\alpha = \sum_{r=1}^m G^3_{(r)} J_{(r)}$ (see also Eq. (5.16) where bounded random variables are used to approximate $J_{(r)}$ because the scheme is implicit). A first order symplectic implicit scheme is also obtained if we truncate the Stratonovich expansion for S^1_ω according to $\mathcal{A}_1$:

$$S^1_\omega \approx G^1_{(0)} J_{(0)} + \sum_{r=1}^m \left(G^1_{(r)} J_{(r)} + G^1_{(r,r)} J_{(r,r)} \right) + \sum_{i,j=1, i\neq j}^m G^1_{(i,j)} J_{(i,j)}. \tag{5.46}$$

In the next section, we study the convergence and we prove the first order mean square convergence for the scheme based on the generating function given in (5.46).

To obtain the symplectic Euler scheme of order 0.5 in [11], we use the relation of the Ito stochastic multiple integrals and the Stratonovich stochastic multiple integrals ([6]), and we replace in the expansion (5.24) of S^1_ω each Stratonovich integral in terms of Ito integrals I_α. We truncate the series by keeping only terms corresponding to Ito

integrals I_α with $\alpha \in \mathcal{B}_{0.5}$, and for $m = 1$ we have

$$S^1_\omega \approx G^1_{(1)} I_{(1)} + (G^1_{(0)} + \frac{1}{2} G^1_{(1,1)}) I_{(0)}. \tag{5.47}$$

Notice that the generating function in (5.15) was obtained from the previous equation, using (5.38)-(5.39) and bounded random variables to approximate $I_{(1)}$.

For the 1.5 order scheme, we truncate according to $\mathcal{B}_{1.5}$, so, for $m = 1$ we get :

$$S^1_\omega \approx G^1_{(1)} I_{(1)} + \left(G^1_{(0)} + \frac{1}{2} G^1_{(1,1)} \right) I_{(0)} + \left(G^1_{(0,1)} + \frac{1}{2} G^1_{(1,1,1)} \right) I_{(0,1)} + \left(G^1_{(1,0)} + \frac{1}{2} G^1_{(1,1,1)} \right)$$
$$I_{(1,0)} + G^1_{(1,1)} I_{(1,1)} + \left(G^1_{(0,0)} + \frac{1}{2} (G^1_{(0,1,1)} + G^1_{(1,1,0)}) + \frac{1}{4} G^1_{(1,1,1,1)} \right) I_{(0,0)} \tag{5.48}$$

The formulas for the coefficients G^1_α included in (5.48) are given in (5.38)-(5.42), and the Ito integrals $I_{(0,1)}$, $I_{(1,0)}$, and $I_{(1,1)}$ should be approximated using bounded random variables ([11], [6]).

Remark 5.10 *If we consider the deterministic cases, i.e., $m = 0$, then $J_\alpha = \frac{1}{n!} t^n$ with $l(\alpha) = n$. The coefficients (5.39) - (5.41) and (5.44) of the approximations of the generating function proposed here, are consistent with those of Type (II) and Type (III) generating functions in [4]. In other words, the proposed construction of the stochastic symplectic numerical schemes via generating function is an extension of the methods introduced by Feng [4].*

5.4 Convergence analysis

In this section, we study the convergence of the first order symplectic implicit scheme constructed using the generating function given in (5.46). As we have mentioned early, since this is an implicit scheme we need to use bounded random variables. To keep the notation simple, we consider the SHS (5.1) with $n = 1$ and $m = 1$, but the same approach can be easily extended to the general case. Also for notation convenience, $\frac{\partial H}{\partial p}$ and $\frac{\partial H}{\partial q}$ are denoted as H_p and H_q, respectively.

As in [11], for the proposed implicit schemes with time step $h < 1$, we replace the random variable $\xi \sim N(0,1)$ with the bounded random variables ξ_h:

$$\xi_h = \begin{cases} -A_h & \text{if } \xi < -A_h \\ \xi & \text{if } |\xi| \le A_h \\ A_h & \text{if } \xi > A_h, \end{cases} \tag{5.49}$$

where $A_h = 2\sqrt{|\ln h|}$. From [11], we know that

$$E(\xi - \xi_h)^2 \le h^2, \tag{5.50}$$

$$0 \le E(\xi^2 - \xi_h^2) \le (1 + 4\sqrt{|\ln h|})h^2 \le 5h^{3/2}. \tag{5.51}$$

Carrying out similar calculations, we get

$$\begin{aligned} E(\xi^2 - \xi_h^2)^2 &= \frac{2}{\sqrt{2\pi}} \int_{A_h}^{\infty} (x^2 - A_h^2)^2 e^{-x^2/2} dx = \frac{2}{\sqrt{2\pi}} \int_0^{\infty} (y^2 + 2A_h y)^2 \\ e^{-\frac{(y+A_h)^2}{2}} dy &\le \frac{2e^{-\frac{A_h^2}{2}}}{\sqrt{2\pi}} \int_0^{\infty} (y^2 + 2A_h y)^2 e^{-\frac{y^2}{2}} dy = e^{-\frac{A_h^2}{2}} \left(3 + 4A_h^2 + \frac{8A_h}{\sqrt{2\pi}}\right) \\ &\le 27h. \end{aligned} \tag{5.52}$$

From (7.20), for any non-negative integer k, we can easily verify

$$E(\xi_h^{2k+1}) = E(\xi^{2k+1}) = 0, \quad E(|\xi_h|^k) \le E(|\xi|^k) < \infty. \tag{5.53}$$

Using (5.10) and (5.46), for the SHS (5.1) with $n = 1$ and $m = 1$, we construct an implicit symplectic scheme corresponding to the following one step approximation :

$$\begin{aligned} P &= p - (H_q^{(0)}(P,q)J_{(0)} + H_q^{(1)}(P,q)J_{(1)}^h + (H_p^{(1)}(P,q)H_q^{(1)}(P,q))_q J_{(1,1)}^h), \\ Q &= q + (H_p^{(0)}(P,q)J_{(0)} + H_p^{(1)}(P,q)J_{(1)}^h + (H_p^{(1)}(P,q)H_q^{(1)}(P,q))_p J_{(1,1)}^h), \end{aligned} \tag{5.54}$$

where $J_{(0)} = h$, $J_{(1)}^h = \sqrt{h}\xi_h$ and $J_{(1,1)}^h = \frac{1}{2}\xi_h^2$

We suppose that the Hamiltonian functions $H^{(0)}$ and $H^{(1)}$ and their partial derivatives up to order four are continuous, and the following inequalities hold for some

positive constants L_i, $i = 1, \ldots, 5$

$$\sum_{r=0}^{1}(|H_p^{(r)}(P,Q) - H_p^{(r)}(p,q)| + |H_q^{(r)}(P,Q) - H_q^{(r)}(p,q)|) \leq L_1(|P-p| + |Q-q|), \tag{5.55}$$

$$\sum_{r=0}^{1}(|H_p^{(r)}(p,q)| + |H_q^{(r)}(p,q)|) \leq L_2(1 + |p| + |q|), \tag{5.56}$$

$$\sum_{r=0}^{1}(|H_{pp}^{(r)}(p,q)| + |H_{pq}^{(r)}(p,q)| + |H_{qq}^{(r)}(p,q)|) \leq L_3, \tag{5.57}$$

$$\sum_{r=0}^{1}(|H_{ppq}^{(r)}(p,q)| + |H_{pqq}^{(r)}(p,q)| + |H_{ppp}^{(r)}(p,q)|) \leq \frac{L_4}{1 + |p| + |q|}, \tag{5.58}$$

$$|H_{pppq}^{(1)}(p,q)| + |H_{ppqq}^{(1)}(p,q)| + |H_{pppp}^{(1)}(p,q)| \leq \frac{L_5}{(1 + |p| + |q|)^2}. \tag{5.59}$$

$$\begin{aligned}&(|(H_p^{(1)}H_q^{(1)})_p(P,Q) - (H_p^{(1)}H_q^{(1)})_p(p,q)| \\ &+ |(H_p^{(1)}H_q^{(1)})_q(P,Q) - (H_p^{(1)}H_q^{(1)})_q(p,q)|) \leq L_1(|P-p| + |Q-q|),\end{aligned} \tag{5.60}$$

The first equation in (5.54) is implicit, so in the following lemma we show that the scheme (5.54) is well-defined.

Lemma 5.11 *There exists constants $K_0 > 0$ and $h_0 > 0$, such that for any $h < h_0$ the first equation in (5.54) has a unique solution P which satisfies*

$$|P - p| \leq K_0(1 + |p| + |q|)\left(|\xi_h|\sqrt{h} + h + \frac{1}{2}\xi_h^2 h\right), k = 1, 2, \ldots \tag{5.61}$$

Proof: The proof can be completed similarly with the proof of Lemma 2.4 in [11], using the assumptions (6.9)-(5.60) and the contraction principle. □

Corollary 5.12 *There exists constants $K > 0$ and $h_0 > 0$, such that for any $h < h_0$, we have*

$$E(|P-p|^i + |Q-q|^i) \leq K(1 + |p| + |q|)^i h^{\frac{i}{2}}, i = 1, 2, \ldots \tag{5.62}$$

To prove the first order mean square convergence for the scheme based on the one step approximation (5.54), we apply the following general result (Theorem 1.1 in [10]):

Theorem 5.13 *Let $\bar{X}_{t,x}(t+h)$ be a one step approximation for the solution $X_{t,x}(t+h)$ of the SHS (5.1). If for arbitrary $t_0 \le t \le t_0+T-h$, $x \in R^{2n}$ the following inequalities hold:*

$$\left|E\left(X_{t,x}(t+h) - \bar{X}_{t,x}(t+h)\right)\right| \le K(1+|x|^2)^{1/2}h^{p_1}, \tag{5.63}$$

$$\left[E\left|X_{t,x}(t+h) - \bar{X}_{t,x}(t+h)\right|^2\right]^{1/2} \le K(1+|x|^2)^{1/2}h^{p_2}, \tag{5.64}$$

with $p_2 \ge 1/2$ and $p_1 \ge p_2+1/2$, then the mean square order of accuracy of the method constructed using the one step approximation $\bar{X}_{t,x}(t+h)$ is $p_2 - 1/2$.

Before proving the main convergence theorem, we include some preliminary results in the following lemma.

Lemma 5.14 *There exists constants $K_1, K_2, K_3 > 0$ and $h_0 > 0$, such that for any $h < h_0$, we have*

$$|E(P-p)| + |E(Q-q)| \le K_1(1+|p|+|q|)h, \tag{5.65}$$

$$|E((P-p)J^h_{(11)})| + |E((Q-q)J^h_{(11)})| \le K_2(1+|p|+|q|)h^2, \tag{5.66}$$

$$|E((P-p)^2J^h_{(1)})| + |E((Q-q)^2J^h_{(1)})| \le K_3(1+|p|+|q|)^2h^{5/2}. \tag{5.67}$$

Proof: For $r = 0, 1$, $z = p$ or q, and with sufficiently small h, from (5.56) and (5.61), we have

$$\begin{aligned} |H^{(r)}_z(P,q)| &\le |H^{(r)}_z(P,q) - H^{(r)}_z(p,q)| + |H^{(r)}_z(p,q)| \le L_1|P-p| + |H^{(r)}_z(p,q)| \\ &\le (1+|p|+|q|)\left(K|\xi_h|\sqrt{h} + Kh + K\frac{1}{2}\xi_h^2 h + L_3\right). \end{aligned} \tag{5.68}$$

Hence, using (5.53) we show that there exist constants $KC_i > 0$, $i = 1, 2, \ldots$ such that

$$E|H^{(r)}_z(P,q)|^i \le KC_i(1+|p|+|q|)^i, \quad i = 1, 2, \ldots. \tag{5.69}$$

Using the Taylor expansion, we rewrite the first relation of (5.54) as $P - p = -H^{(1)}_q(p,q)J^h_{(1)} + R_1$ with $R_1 = -H^{(0)}_q(P,q)J_{(0)} - H^{(1)}_{qp}(\bar{p}_1, q)(P-p)J^h_{(1)} - (H^{(1)}_p(P,q)$ $H^{(1)}_q(P,q))_q J^h_{(1,1)}$ where $\bar{p}_1$ is between p and P. Hence, using the Cauchy-Schwarz

inequality, (5.56), (5.57), (5.62), and (5.69) imply that there is a constant $K_1 > 0$, such that

$$|E(R_1)| \leq E|R_1| \leq E|H_q^{(0)}(P,q)|J_{(0)} + L_3\sqrt{E|P-p|^2}\sqrt{E|J_{(1)}^h|^2} + \left(\sqrt{E|H_q^{(1)}(P,q)|^2} + \sqrt{E|H_p^{(1)}(P,q)|^2}\right) L_3\sqrt{E|J_{(11)}^h|^2} \leq \frac{K_1}{2}(1+|p|+|q|)h. \tag{5.70}$$

Moreover, since we have

$$R_1^2 \leq 2\Bigg((H_q^{(0)}(P,q))^2(J_{(0)})^2 + (H_{qp}^{(1)}(\bar{p}_1,q))^2(P-p)^2(J_{(1)}^h)^2 + \left((H_p^{(1)}(P,q))^2(H_{qq}^{(1)}(P,q))^2 + (H_{pq}^{(1)}(P,q))^2(H_q^{(1)}(P,q))^2\right)(J_{(1,1)}^h)^2\Bigg),$$

proceeding similarly we can show that there exists constants $K_2 > 0$ and $K_3' > 0$, such that

$$E(R_1^2) \leq \frac{1}{3}K_2^2(1+|p|+|q|)^2h^2, \quad |E(R_1^2J_{(1)}^h)| \leq K_3'(1+|p|+|q|)^2h^{5/2} \tag{5.71}$$

$$E(R_1^2(J_{(1)}^h)^2) \leq K_3'(1+|p|+|q|)^2h^3 \tag{5.72}$$

Using the Cauchy-Schwarz inequality, (5.70), (5.71) and (5.53) imply that there exists a constant $K_3 > 0$ such that:

$$|E(P-p)| \leq \left|H_q^{(1)}(p,q)E(J_{(1)}^h)\right| + |E(R_1)| \leq \frac{K_1}{2}(1+|p|+|q|)h, \tag{5.73}$$

$$|E((P-p)J_{(11)}^h)| \leq \left|H_q^{(1)}(p,q)E(J_{(1)}^hJ_{(11)}^h)\right| + |E(R_1J_{(11)}^h)| \leq \sqrt{E(R_1^2)E|J_{(11)}^h|^2}$$
$$\leq \frac{K_2}{2}(1+|p|+|q|)h^2 \tag{5.74}$$

$$|E((P-p)^2J_{(1)}^h)| \leq (H_q^{(1)}(p,q))^2\left|E((J_{(1)}^h)^3)\right| + |E(R_1^2J_{(1)}^h)| + 2\left|H_q^{(1)}(p,q)E(R_1(J_{(1)}^h)^2)\right|$$
$$\leq K_3'(1+|p|+|q|)^2h^{5/2} + 2\left|H_q^{(1)}(p,q)\right|\sqrt{E(R_1^2)E|J_{(1)}^h|^4} \leq \frac{K_3}{2}(1+|p|+|q|)^2h^{5/2} \tag{5.75}$$

Similarly, $|E(Q-q)| \leq \frac{K_1}{2}(1+|p|+|q|)h$, $|E((Q-q)J_{(11)}^h)| \leq \frac{K_2}{2}(1+|p|+|q|)h^2$, and $|E((Q-q)^2J_{(1)}^h)| \leq \frac{K_3}{2}(1+|p|+|q|)^2h^{5/2}$ so (5.65)- (5.67) are proved.

□

Remark 5.15 *Notice that for h sufficiently small, using Taylor expansions, inequalities (5.56)-(5.58), (5.62) and the characterization of the moments in (5.53), we can also show that there exists a constant $K_4 > 0$, such that*

$$
\begin{aligned}
&|E(R_1 J^h_{(1)})| \leq \left|E\left(\left(H^{(0)}_q(p,q)J_{(0)} + (H^{(1)}_p H^{(1)}_q)_q(p,q)J_{(1,1)}\right)J^h_{(1)}\right)\right| \\
&+ E\left|J^h_{(1)} H^{(0)}_{pq}(\bar{p}_0, q)J_{(0)}(P-p)\right| + E\left|J^h_{(1)}(H^{(1)}_p H^{(1)}_q)_{pq}(\bar{p}_{11}, q))J^h_{(1,1)}(P-p)\right| \\
&+ |E\left(J^h_{(1)} H^{(1)}_{pq}(\bar{p}_1, q)J^h_{(1)}(P-p)\right)| \leq L_3 K(1+|p|+|q|)h^2 + (3L_4L_2 + L_3^2)(1+|p|+|q|)h^2 \\
&+ 2|H^{(1)}_{pq}(p,q)||E(J^h_{(11)}(P-p))| + E|J^h_{(1)} H^{(1)}_{ppq}(\hat{\bar{p}}_1, q)J^h_{(1)}(\bar{p}_1 - p)(P-p)| \\
&\leq L_3 K(1+|p|+|q|)h^2 + (3L_4L_2 + L_3^2)(1+|p|+|q|)h^2 + 2K_2L_3(1+|p|+|q|)h^2 \\
&+ L_4(1+|p|+|q|)h^2 \leq K_4(1+|p|+|q|)h^2,
\end{aligned}
\tag{5.76}
$$

where $\bar{p}_0$, $\bar{p}_1$ and $\bar{p}_{11}$ are values between P and p, and $\hat{\bar{p}}_1$ is a value between $\bar{p}_1$ and p. Here we have also used $2J^h_{(11)} = (J^h_{(1)})^2$ and the fact that for sufficiently small h, Lemma 5.11 implies that there exists positive constants C_1 and C_2 such that

$$1 + |\bar{p}| + |q| \leq 1 + |P-p| + |p| + |q| \leq C_1(1+|p|+|q|), \tag{5.77}$$

$$\frac{1}{1+|\bar{p}|+|q|} \leq \frac{1}{1+|p|-|\bar{p}-p|+|q|} \leq \frac{1}{1+|p|-|P-p|+|q|} \leq \frac{C_2}{1+|p|+|q|} \tag{5.78}$$

for any $\bar{p}$ between P and p.

Theorem 5.16 *If the conditions (6.9) - (5.58) are satisfied, the scheme (5.54) converges with the mean square order 1.*

Proof: Applying Taylor expansions, for the first part of the one step approximation

(5.54), we have

$$\begin{aligned}
P-p &= -H_q^{(0)}(p,q)J_{(0)} - H_q^{(1)}(p,q)J_{(1)}^h - (H_p^{(1)}H_q^{(1)})_q(p,q)J_{(1,1)}^h \\
&- H_{pq}^{(0)}(p,q)J_{(0)}(P-p) - (H_p^{(1)}H_q^{(1)})_{pq}(p,q)J_{(1,1)}^h(P-p) \\
&- H_{pq}^{(1)}(p,q)(P-p)J_{(1)}^h - \frac{1}{2}H_{ppq}^{(0)}(\bar{p}_{00},q)(P-p)^2J_{(0)}^h \\
&- \frac{1}{2}H_{ppq}^{(1)}(p,q)(P-p)^2J_{(1)}^h - \frac{1}{2}(H_p^{(1)}H_q^{(1)})_{ppq}(\bar{p}_{011},q)(P-p)^2J_{(11)}^h \\
&- \frac{1}{6}H_{pppq}^{(1)}(\bar{p}_{01},q)(P-p)^3J_{(1)}^h \\
&= -H_q^{(0)}(p,q)J_{(0)} - H_q^{(1)}(p,q)J_{(1)}^h - (H_p^{(1)}(p,q)H_q^{(1)}(p,q))_qJ_{(1,1)}^h \\
&- H_{pq}^{(1)}(p,q)(P-p)J_{(1)}^h + R_2,
\end{aligned} \tag{5.79}$$

where $\bar{p}_{00}$, $\bar{p}_{01}$ and $\bar{p}_{011}$ are values between P and p. Since

$$\begin{aligned}
R_2^2 &\le 2(H_{pq}^{(0)}(p,q))^2(J_{(0)})^2(P-p)^2 + 2\left((H_p^{(1)}H_q^{(1)})_{pq}(p,q)\right)^2(J_{(1,1)}^h)^2(P-p)^2 \\
&+ \frac{1}{2}\left(H_{ppq}^{(0)}(\bar{p}_{00},q)\right)^2(P-p)^4(J_{(0)}^h)^2 + \frac{1}{2}\left(H_{ppq}^{(1)}(p,q)\right)^2(P-p)^4(J_{(1)}^h)^2 \\
&+ \frac{1}{2}\left((H_p^{(1)}H_q^{(1)})_{ppq}(\bar{p}_{011},q)\right)^2(P-p)^4(J_{(11)}^h)^2 + \frac{1}{18}\left(H_{pppq}^{(1)}(\bar{p}_{01},q)\right)^2(P-p)^6\left(J_{(1)}^h\right)^2
\end{aligned} \tag{5.80}$$

the assumptions (5.56) -(5.59), Cauchy-Schwarz inequality, inequalities (5.62), Lemma 5.14, and the characterization of the moments in (5.53) implies that for h sufficiently small there exists a positive constant K_6 such that

$$|E(R_2)| \le K_6(1+|p|+|q|)h^2, \quad E|R_2|^2 \le K_6(1+|p|+|q|)^2h^3. \tag{5.81}$$

Substituting $P-p = H_q^1(p,q)J_{(1)}^h + R_1$, where R_1 is defined in the proof of Lemma 5.14, into $H_{pq}^{(1)}(p,q)(P-p)J_{(1)}^h$, we obtain

$$\begin{aligned}
P-p &= -H_q^{(0)}(p,q)J_{(0)} - H_q^{(1)}(p,q)J_{(1)}^h - (H_p^{(1)}(p,q)H_q^{(1)}(p,q))_qJ_{(1,1)}^h \\
&- H_{pq}^{(1)}(p,q)H_q^1(p,q)(J_{(1)}^h)^2 - H_{pq}^{(1)}(p,q)J_{(1)}^hR_1 + R_2.
\end{aligned} \tag{5.82}$$

It is easy to verify that assumption (5.56) and inequalities (5.72), (5.76) and (5.81) imply that there exists a positive constant K_7 such that

$$\left|E(H_{pq}^{(1)}(p,q)J_{(1)}^hR_1 - R_2)\right| \le K_7(1+|p|+|q|)h^2, \tag{5.83}$$

$$E\left(H_{pq}^{(1)}(p,q)J_{(1)}^hR_1 - R_2\right)^2 \le K_7(1+|p|+|q|)^2h^3. \tag{5.84}$$

Recall that the Milstein scheme [6] for the stochastic Hamiltonian system (5.1) satisfying conditions (5.55) - (5.59) has the mean square order 1 and satisfies the inequalities (5.63)-(5.64) with $p_1 = 2$, $p_2 = 1.5$. The one step approximation corresponding to the Milstein scheme is given by

$$\begin{aligned}\tilde{P} &= p - H_q^{(0)}(p,q)J_{(0)} - H_q^{(1)}(p,q)J_{(1)} + (H_{pq}^{(1)}(p,q)H_q^{(1)}(p,q) - H_{qq}^{(1)}(p,q)H_p^{(1)}(p,q))J_{(1,1)} \\ \tilde{Q} &= q + H_p^{(0)}(p,q)J_{(0)} + H_p^{(1)}(p,q)J_{(1)} + (H_{pq}^{(1)}(p,q)H_p^{(1)}(p,q) - H_{pp}^{(1)}(p,q)H_q^{(1)}(p,q))J_{(1,1)}.\end{aligned} \tag{5.85}$$

Comparing the one step approximation corresponding to the Milstein scheme with (5.54), we obtain

$$\begin{aligned}P - \tilde{P} &= H_q^{(1)}(p,q)(J_{(1)} - J_{(1)}^h) + (H_{pq}^{(1)}(p,q)H_q^{(1)}(p,q) - H_{qq}^{(1)}(p,q)H_p^{(1)}(p,q))(J_{(1,1)} - J_{(1,1)}^h) \\ &\quad - H_{pq}^{(1)}(p,q)J_{(1)}^h R_1 + R_2.\end{aligned} \tag{5.86}$$

Thus, from (5.50)-(5.53), assumptions (5.56), (5.57), and(5.83), (5.84), we get

$$\begin{aligned}E(P - \tilde{P})^2 &\leq (1 + |p| + |q|)^2 h^3 \left(2L_2^2 + 54L_3^2 L_2^2 + K_7\right), \\ |E(P - \tilde{P})| &\leq (1 + |p| + |q|)h^2 \left(L_3 L_2 h^{\frac{1}{2}} + K_7\right).\end{aligned} \tag{5.87}$$

The proof for the $Q - \tilde{Q}$ follows similarly by repeating the same procedure for the second relation of (5.54), so the scheme corresponding to the one step approximation (5.54) satisfies the inequalities (5.63)-(5.64) with $p_1 = 2$, $p_2 = 1.5$ □

Remark 5.17 *Using the same approach, we were able to prove that the symplectic schemes based on truncations of S_ω^1 or S_ω^3 for multi-indexes $\alpha \in \mathcal{B}_k$ or $\alpha \in \mathcal{A}_k$ have the mean square order k, for $k = 1, 1.5, 2$. Higher order schemes include Ito multiple stochastic integrals I_α with multi-indexes $\alpha \in \mathcal{B}_k$ or Stratonovich multiple stochastic integrals J_α with multi-indexes $\alpha \in \mathcal{A}_k$, but they are computationally expensive to simulate bounded approximations when $k > 2$.*

5.5 Symplectic schemes for special types of stochastic Hamiltonian systems

5.5.1 SHS with additive noise

First, we consider the special case of SHS with additive noise

$$\begin{aligned} dP_i &= -\frac{\partial H^{(0)}(P,Q)}{\partial Q_i}dt - \sum_{r=1}^{m}\sigma_r \circ dw_t^r, \quad P(t_0)=p, \\ dQ_i &= \frac{\partial H^{(0)}(P,Q)}{\partial P_i}dt + \sum_{r=1}^{m}\tau_r \circ dw_t^r, \quad Q(t_0)=q, \end{aligned} \tag{5.88}$$

where $i = 1,\dots,n$. Notice that $H^{(r)} = \sum_{i=1}^{n}(P_i\tau_r + Q_i\sigma_r)$, where σ_r and τ_r are constants.

To calculate the coefficients of S_ω^1, we replace in (5.43) and get,

$$\begin{aligned} &G^1_{(0,0)} = \sum_{k=1}^{n}\frac{\partial H^{(0)}}{\partial q_k}\frac{\partial H^{(0)}}{\partial P_k}, \quad G^1_{(r_1,0)} = \tau_{r_1}\sum_{k=1}^{n}\frac{\partial H^{(0)}}{\partial q_k}, \quad G^1_{(0,r_1)} = \sigma_{r_1}\sum_{k=1}^{n}\frac{\partial H^{(0)}}{\partial P_k}, \\ &G^1_{(r_1,r_2)} = \sigma_{r_2}\tau_{r_1}, \quad G^1_{(0,r_1,r_2)} = \sigma_{r_2}\sigma_{r_1}\sum_{k_1,k_2=1}^{n}\frac{\partial^2 H^{(0)}}{\partial P_{k_1}\partial P_{k_2}}, \\ &G^1_{(r_1,0,r_2)} = \sigma_{r_2}\tau_{r_1}\sum_{k_1,k_2=1}^{n}\frac{\partial^2 H^{(0)}}{\partial q_{k_1}\partial P_{k_2}}, \quad G^1_{(r_1,r_2,0)} = \tau_{r_2}\tau_{r_1}\sum_{k_1,k_2=1}^{n}\frac{\partial^2 H^{(0)}}{\partial q_{k_1}\partial q_{k_2}}, \\ &G^1_{(r_1,r_2,r_3)} = 0, \quad G^1_{(r_1,r_2,r_3,r_4)} = 0, \end{aligned} \tag{5.89}$$

where $1 \le r_1,\dots,r_4 \le m$. The 1.5 order schemes are obtained by truncating the generating functions to multi-indexes $\alpha \in \mathcal{B}_{1.5}$. Using the approximation of S_ω^1 given in Eq. (5.48), we have the following symplectic implicit scheme of mean square order

1.5:

$$\begin{aligned} P_i(k+1) =& P_i(k) - \frac{\partial H^{(0)}}{\partial Q_i}h - \sum_{r=1}^{m}\Bigg(\sigma_r\sqrt{h}\xi_{hk}^{(r)} + \frac{\partial G^1_{(0,r)}}{\partial Q_i}\bar{I}^h_{(0,r)} + \frac{\partial G^1_{(r,0)}}{\partial Q_i}\bar{I}^h_{(r,0)} \\ &+ \frac{1}{4}\left(2\frac{\partial G^1_{(0,0)}}{\partial Q_i} + \frac{\partial G^1_{(0,r,r)}}{\partial Q_i} + \frac{\partial G^1_{(r,r,0)}}{\partial Q_i}\right)h^2\Bigg) \\ Q_i(k+1) =& Q_i(k) + \frac{\partial H^{(0)}}{\partial P_i}h + \sum_{r=1}^{m}\Bigg(\tau_r\sqrt{h}\xi_{hk}^{(r)} + \frac{\partial G^1_{(0,r)}}{\partial P_i}\bar{I}^h_{(0,r)} + \frac{\partial G^1_{(r,0)}}{\partial P_i}\bar{I}^h_{(r,0)} \\ &+ \frac{1}{4}\left(2\frac{\partial G^1_{(0,0)}}{\partial P_i} + \frac{\partial G^1_{(0,r,r)}}{\partial P_i} + \frac{\partial G^1_{(r,r,0)}}{\partial P_i}\right)h^2\Bigg) \end{aligned} \tag{5.90}$$

where $i = 1, \ldots, n$ and all the functions have $(P(k+1), Q(k))$ as their arguments. Here $\bar{I}^h_{(r,0)} = \frac{h^{\frac{3}{2}}}{2}(\xi_{hk}^{(r)} + \frac{\eta_{hk}^{(r)}}{\sqrt{3}})$ and $\bar{I}^h_{(0,r)} = \xi_{hk}^{(r)}h^{\frac{3}{2}} - \bar{I}^h_{(r,0)}$, where at each time step k, $\xi_{hk}^{(r)}$ and $\eta_{hk}^{(r)}$ are independent bounded random variables as given in (7.20).

Analogously, for S^3_ω, we obtain,

$$\begin{aligned} &G^3_{(0,0)} = 0, \quad G^3_{(r_1,r_2)} = 0, \quad G^3_{(r_1,0)} = -G^3_{(0,r_1)} = \frac{1}{2}T_r^T\nabla H^{(0)}, \\ &G^3_{(r_1,r_2,r_3)} = 0, \quad G^3_{(r_1,r_2,0)} = G^3_{(0,r_1,r_2)} = -G^3_{(r_1,0,r_2)} = \frac{1}{4}T_{r_1}^T\nabla^2 H^{(0)}T_{r_2}, \\ &G^3_{(r_1,r_2,r_3,r_4)} = 0, \end{aligned} \tag{5.91}$$

where $T_r = J^{-1}\nabla H^{(r)} = (-\sigma_r, \ldots, -\sigma_r, \tau_r, \ldots \tau_r)^T$ and $1 \le r_1, \ldots r_4 \le m$. The following 1.5 order scheme is derived based on the truncation of S^3_ω according to multi-indexes $\alpha \in \mathcal{B}_{1.5}$:

$$\begin{aligned} Y_{k+1} =& Y_k + J^{-1}\nabla H^{(0)}(Y_{k+\frac{1}{2}})h + \sum_{r=1}^{m}(T_r\xi_{hk}^{(r)} + J^{-1}\nabla G_{(r,0)}(Y_{k+\frac{1}{2}})(\bar{I}^h_{(r,0)} - \bar{I}^h_{(0,r)}) \\ &+ J^{-1}\nabla G_{(r,r,0)}(Y_{k+\frac{1}{2}})\frac{h^2}{2}) \end{aligned} \tag{5.92}$$

where for each time step k, we have $Y_k = (P_k^T, Q_k^T)^T$ and the arguments are everywhere $Y_{k+\frac{1}{2}} = (Y_{k+1} + Y_k)/2$. The random variables $\bar{I}^h_{(r,0)}$, $\bar{I}^h_{(0,r)}$, $\xi_{hk}^{(r)}$ and $\eta_{hk}^{(r)}$ are the same as for (5.90).

Notice that the 1.5 symplectic methods (5.90) and (5.92) are implicit. These methods have a similar computational complexity as the 1.5 symplectic implicit Runge-Kutta method proposed in [12].

5.5.2 Separable SHS

Let consider the general autonomous SHS (5.1) with separable Hamiltonian functions such that

$$H^{(0)}(P,Q) = V_0(P) + U_0(Q), \quad H^{(r)}(P,Q) = U_r(Q), \quad r = 1,\dots,m \tag{5.93}$$

In this case, the coefficients of S^1_ω become:

$$\begin{aligned}
&G^1_{(r_1,r_2)} = 0, \quad G^1_{(r_1,0)} = 0, \quad G^1_{(0,r1)} = \sum_{k=1}^{n} \frac{\partial U^{(r_1)}}{\partial q_k}\frac{\partial V^{(0)}}{\partial P_k},\\
&G^1_{(0,0)} = \sum_{k=1}^{n} \frac{\partial U^{(0)}}{\partial q_k}\frac{\partial V^{(0)}}{\partial P_k}, \quad G^1_{(r_1,r_2,r_3)} = G^1_{(r_1,r_2,0)} = G^1_{(r_1,0,r_2)} = 0\\
&G^1_{(0,r_1,r_2)} = \sum_{k_1,k_2=1}^{n} \frac{\partial U^{(r_2)}}{\partial q_{k_1}}\frac{\partial U^{(r_1)}}{\partial q_{k_2}}\frac{\partial^2 V^{(0)}}{\partial P_{k_1}\partial P_{k_2}}, \quad G^1_{(r_1,r_2,r_3)} = 0, \quad G^1_{(r_1,r_2,r_3,r_4)} = 0,
\end{aligned} \tag{5.94}$$

where $1 \le r_1,\dots,r_4 \le m$.

The following symplectic first order scheme based on S^1_ω is explicit, and it is different from the two explicit symplectic first mean square order partitioned Runge-Kutta methods presented in [11]:

$$\begin{aligned}
P_i(k+1) =& P_i(k) - \frac{\partial U^{(0)}}{\partial Q_i}(Q(k))h - \sum_{r=1}^{m} \frac{\partial U^{(r)}}{\partial Q_i}(Q(k))\sqrt{h}\xi^{(r)}_{hk}\\
Q_i(k+1) =& Q_i(k) + \frac{\partial V^{(0)}}{\partial P_i}(P(k+1))h,
\end{aligned} \tag{5.95}$$

where $i = 1,\dots,n$. [11] presents an explicit 1.5 mean square order partitioned Runge-Kutta method, however, the symplectic schemes based on the generating function S^1_ω are implicit when the order increases to 1.5 or higher. The 1.5 order scheme derived

from the current approach is provided below:

$$
\begin{aligned}
P_i(k+1) = P_i(k) - \frac{\partial U^{(0)}}{\partial Q_i}(Q(k))h - \sum_{r=1}^{m}\Bigg(\frac{\partial U^{(r)}}{\partial Q_i}(Q(k))\sqrt{h}\xi_{hk}^{(r)} \\
+ \frac{\partial G_{(0,r)}}{\partial Q_i}(P(k+1),Q(k))\bar{I}^h_{(0,r)} + \frac{1}{4}\Bigg(2\frac{\partial G_{(0,0)}}{\partial Q_i}(P(k+1),Q(k)) \\
+ \frac{\partial G_{(0,r,r)}}{\partial Q_i}(P(k+1),Q(k))\Bigg)h^2\Bigg) \qquad (5.96) \\
Q_i(k+1) = Q_i(k) + \frac{\partial V^{(0)}}{\partial P_i}(P(k+1))h + \sum_{r=1}^{m}\Bigg(\frac{\partial G_{(0,r)}}{\partial P_i}(P(k+1),Q(k))\bar{I}^h_{(0,r)} \\
+ \frac{1}{4}\left(2\frac{\partial G_{(0,0)}}{\partial P_i}(P(k+1),Q(k)) + \frac{\partial G_{(0,r,r)}}{\partial P_i}(P(k+1),Q(k))\right)h^2\Bigg)
\end{aligned}
$$

where $i = 1, \ldots, n$ and the random variables are generated following the same procedure as for (5.90)

5.5.3 SHS preserving Hamiltonian functions

Unlike the deterministic cases, in general the SHSs no longer preserve with respect to time for the Hamiltonian functions $H_i, i = 0, \ldots, n$, even when the SHS is autonomous. However, using the chain rule of the Stratonovich stochastic integration, it is easy to verify for the Hamiltonian system (5.1) that the Hamiltonian functions $H^{(i)}, i = 0, \ldots, m$ are invariant (i.e. $dH^{(i)} = 0$), if and only if $\{H^{(i)}, H^{(j)}\} = 0$ for any $i, j = 0, \ldots, m$, where the Poisson bracket is defined as $\{H^{(i)}, H^{(j)}\} = \sum_{k=1}^{n}(\frac{\partial H^{(j)}}{\partial Q_k}\frac{\partial H^{(i)}}{\partial P_k} - \frac{\partial H^{(i)}}{\partial Q_k}\frac{\partial H^{(j)}}{\partial P_k})$.

For systems preserving the Hamiltonian functions, the coefficients G^1_α of S^1_ω are invariant under the permutations on α, when $l(\alpha) = 2$ because for any $r_1, r_2 = 0, \ldots, m$, we have

$$
G^1_{(r_1,r_2)} = G^1_{(r_2,r_1)} = \sum_{k=1}^{n}\frac{\partial H^{(r_1)}}{\partial q_k}\frac{\partial H^{(r_2)}}{\partial P_k}. \qquad (5.97)
$$

Moreover, for $l(\alpha) = 3$, from the formula (5.43) we easily see that $G^1_{(r_1,r_2,r_3)} = G^1_{(r_2,r_1,r_3)}$ for any $r_1, r_2, r_3 = 0, \ldots, m$. Also, since for any $k_1, k_2 = 1, \ldots, n$ and any $r_1, r_2 =$

$0, \ldots, m$, we have

$$\frac{\partial}{\partial q_{k_2}}(\sum_{k_1=1}^{n}\frac{\partial H^{(r_2)}}{\partial q_{k_1}}\frac{\partial H^{(r_3)}}{\partial P_{k_1}}) = \frac{\partial}{\partial q_{k_2}}(\sum_{k_1=1}^{n}\frac{\partial H^{(r_3)}}{\partial q_{k_1}}\frac{\partial H^{(r_2)}}{\partial P_{k_1}}), \tag{5.98}$$

a simple calculation confirms that $G^1_{(r_1,r_2,r_3)} = G^1_{(r_1,r_3,r_2)}$. Hence, G^1_α is also invariant under the permutation on α when $l(\alpha) = 3$.

These properties are helpful not only to reduce the calculations for G^1_α, but the need of using approximation of high-order stochastic multiple integrals in the symplectic schemes based on the generating function S^1_ω is also avoided. For instance, when $m = 1$, we have the second order generating function S^1_ω:

$$\begin{aligned} S^1_\omega = {} & G^1_{(0)}h + G^1_{(1)}\sqrt{h}\xi_h + G^1_{(0,0)}\frac{h^2}{2} + G^1_{(1,1)}\frac{h\xi_h^2}{2} + G^1_{(1,0)}\xi_h h^{\frac{3}{2}} \\ & + G^1_{(1,1,1)}\frac{h^{\frac{3}{2}}\xi_h^3}{6} + G^1_{(1,1,0)}\frac{\xi_h^2 h^2}{2} + G^1_{(1,1,1,1)}\frac{h^2\xi_h^4}{24} \end{aligned} \tag{5.99}$$

where everywhere the arguments are (P_{k+1}, Q_k), and we have used $J_{(0,1)} + J_{(1,0)} = J_{(1)}J_{(0)}$ and $J_{(0,1,1)} + J_{(1,0,1)} + J_{(1,1,0)} = J_{(1,1)}J_{(0)}$ (see the corollary 5.7). Then the second order symplctic scheme is obtained by (5.10).

For the coefficients of S^3_ω, $\{H^{(r_1)}, H^{(r_2)}\} = 0$ for any $0 \le r_1, r_2 \le m$ implies that $G^3_{(r_1,r_2)} = 0$ and $G^3_{(r_1,r_2,r_3,r_4)} = 0$, $r_1, r_2, r_3, r_4 = 1, \ldots, m$. Moreover, a simple computation shows that G^3_α is also invariant under the permutation on α, when $l(\alpha) = 3$. Hence the second order midpoint symplectic scheme when $m = 1$ is given by

$$\begin{aligned} Y_{k+1} = {} & Y_k + J^{-1}\nabla G^3_{(0)}(Y_{k+\frac{1}{2}})h + J^{-1}\nabla G^3_{(1)}(Y_{k+\frac{1}{2}})\sqrt{h}\xi_h \\ & + J^{-1}\nabla G^3_{(1,1,1)}(Y_{k+\frac{1}{2}})\frac{h^{\frac{3}{2}}\xi_h^3}{6} + J^{-1}\nabla G^3_{(1,1,0)}(Y_{k+\frac{1}{2}})\frac{\xi_h^2 h^2}{2} \end{aligned} \tag{5.100}$$

where $Y_{k+\frac{1}{2}} = (Y_{k+1} + Y_k)/2$.

It can be verified that G^3_α is invariant under the permutation on α for any $l(\alpha)$ ([1]), and this property makes the higher order symplectic schemes computationally attractive for the SHS preserving Hamiltonian functions.

5.6 Numerical simulations and conclusion

To validate the high-order symplectic schemes proposed in this study, and to compare the performance with the lower order schemes, we consider three test cases. The cases have been used as the test examples in [12] [11], [5], and the last example is a nonlinear problem which is often used for testing numerical algorithms for stochastic computations [11].

5.6.1 SHS with additive noise

We now consider the following SHS with additive noise:

$$\begin{aligned} dP &= Qdt + \sigma dw_t^1, \quad P(0) = p \\ dQ &= -Pdt + \gamma dw_t^2, \quad Q(0) = q \end{aligned} \tag{5.101}$$

where σ and γ are constant.

The exact solution can be expressed in the following form using the equal-distance time discretization $0 = t_0 < t_1 < \cdots < t_N = T$, where the time-step h ($h = t_{k+1} - t_k$) is a small positive number:

$$X(t_{k+1}) = FX(t_k) + u_k, \quad X(0) = X_0, \quad k = 0, 1, \ldots, N-1 \tag{5.102}$$

where

$$X(t_k) = \begin{bmatrix} P(t_k) \\ Q(t_k) \end{bmatrix}, \quad X_0 = \begin{bmatrix} p \\ q \end{bmatrix}, \quad F = \begin{bmatrix} \cos h & \sin h \\ -\sin h & \cos h \end{bmatrix}, \tag{5.103}$$

$$u_k = \begin{bmatrix} \sigma \int_{t_k}^{t_{k+1}} \cos(t_{k+1} - s) dw_s^1 + \gamma \int_{t_k}^{t_{k+1}} \sin(t_{k+1} - s) dw_s^2 \\ -\sigma \int_{t_k}^{t_{k+1}} \sin(t_{k+1} - s) dw_s^1 + \gamma \int_{t_k}^{t_{k+1}} \cos(t_{k+1} - s) dw_s^2 \end{bmatrix}. \tag{5.104}$$

The mean square order two symplectic scheme based on a truncation of S_ω^1 according to multi-indexes $\alpha \in \mathcal{A}_2$ is given by

$$\begin{bmatrix} 1 + \frac{h^2}{2} & 0 \\ h & 1 \end{bmatrix} X_{k+1} = \begin{bmatrix} 1 & h \\ 0 & 1 + \frac{h^2}{2} \end{bmatrix} X_k + \begin{bmatrix} \sigma J_{(1)} + \gamma J_{(2,0)} \\ \gamma J_{(2)} + \sigma J_{(0,1)} \end{bmatrix}. \tag{5.105}$$

We have the following proposition about the long time error of the symplectic second order scheme.

Proposition 5.18 *If T and h are positive values such that Th^2 and h are sufficiently small, and $E|X_0|^2$ is finite, then the mean square error is bounded by*

$$\sqrt{E|X(t_k) - X_k|^2} \leq K(\sqrt{T}h^2 + \sqrt{T^3h^4}), \quad k = 1, 2, \ldots, N. \tag{5.106}$$

Proof: As in the proof of propositions 6.1 in [12], we can show that if T and h are positive values such that Th^2 and h are sufficiently small, then for $k = 0, 1, \ldots, N$, $T = Nh$, there exists a constant K_1 such that the following inequality holds:

$$||H^k - F^k|| \leq K_1(h^3 + Th^2), \quad H = \begin{bmatrix} 1 + \frac{h^2}{2} & 0 \\ h & 1 \end{bmatrix}^{-1} \begin{bmatrix} 1 & h \\ 0 & 1 + \frac{h^2}{2} \end{bmatrix}. \tag{5.107}$$

The proof then follows from the previous inequality, proceeding as in the proof of propositions 6.2 in [12].

□

The corresponding error for the first-order scheme proposed in [12] is given by $\mathcal{O}(T^{1/2}h + T^{3/2}h^2)$. Clearly, a better performance is expected using the second-order scheme.

In numerical simulations, to guarantee that the exact solution, Euler scheme, first-order and second-order schemes have the same sample paths, eight independent standard normal distributed random variables, $\xi_{1,k}, \xi_{2,k}, \eta_{1,k}, \eta_{2,k}, \zeta_{1,k}, \zeta_{2,k}, \varepsilon_{1,k}, \varepsilon_{2,k}$ are used at every time step k. The random variables in (5.104) and (5.105) are evaluated as:

$$\begin{aligned} &J_{(i)} = \sqrt{h}\xi_{1,k}, \quad \int_{t_k}^{t_{k+1}} \cos(t_{k+1} - s)dw_s^i = \frac{\sin h}{\sqrt{h}}\xi_{i,k} + a_1\eta_{i,k}, \\ &\int_{t_k}^{t_{k+1}} \sin(t_{k+1} - s)dw_s^i = \frac{2}{\sqrt{h}}\sin^2\frac{h}{2}\xi_{i,k} + a_2\eta_{i,k} + a_3\zeta_{i,k}, \\ &J_{(0,i)} = \frac{h^{\frac{3}{2}}}{2}\xi_{i,k} + a_4\eta_{i,k} + a_5\zeta_{i,k} + a_6\varepsilon_{i,k}, \quad J_{(i,0)} = hJ_{(i)} - J_{(0,i)}, \quad i = 1, 2. \end{aligned} \tag{5.108}$$

where

$$a_1 = \sqrt{\frac{h}{2} + \frac{\sin 2h}{4} - \frac{\sin^2 h}{h}}, \quad a_2 = \frac{1}{a_1}(\frac{\sin^2 h}{2} - \frac{2\sin h}{h}\sin^2\frac{h}{2}),$$
$$a_3 = \sqrt{\frac{h}{2} - \frac{\sin 2h}{4} - \frac{4}{h}\sin^4\frac{h}{2} - a_2^2}, \quad a_4 = \frac{1}{a_1}(1 - \cos h - \frac{h\sin h}{2}), \tag{5.109}$$
$$a_5 = \frac{1}{a_3}(h - \sin h - h\sin^2\frac{h}{2} - a_2 a_4), \quad a_6 = \sqrt{\frac{h^3}{12} - a_4^2 - a_5^2}.$$

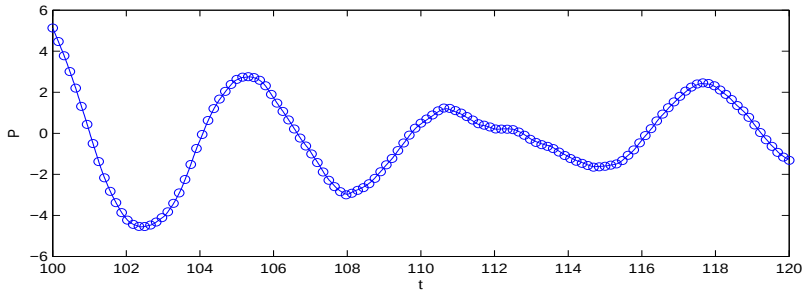

Figure 29: A sample trajectory of the solution to (5.101) for $\sigma = 0$, $\tau = 1$, $p = 1$ and $q = 0$: exact solution (solid line), S^1_ω second order scheme with time step $h = 2^{-6}$ (circle). The circle of different scheme are plotted once per 10 steps.

Fig.29 displays the results obtained using the symplectic schemes for long time simulations. A good agreement with the exact solution is observed when the symplectic scheme is implemented.

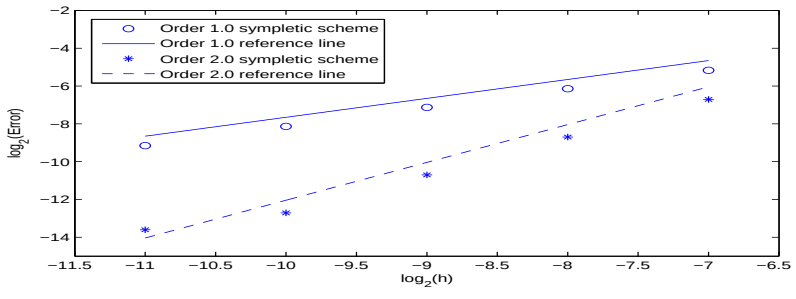

Figure 30: Convergence rate of different order S^1_ω symplectic scheme for (5.101), where error is the maximum error of (P, Q) at $T = 100$.

Fig. 30 presents the estimations of the convergence rate for various order symplectic schemes based on S^1_ω. We notice that the numerical results agree with the prediction based on the theoretical study. So the second order symplectic scheme can provide a more accuracy estimation than the first order scheme with the same time step.

5.6.2 Kubo oscillator

In [11], the following SDEs (the Kubo oscillator) in the sense of Stratonovich are used to demonstrate the advantage of the stochastic symplectic scheme for long time computation.

$$\begin{aligned} dP &= -aQdt - \sigma Q \circ dw_t^1, \quad P(0) = p, \\ dQ &= aPdt + \sigma P \circ dw_t^2, \quad Q(0) = q, \end{aligned} \tag{5.110}$$

where a and σ are constants.

As illustrated in [11], the Hamiltonian functions $H^{(0)}(P(t), Q(t)) = a\frac{P(t)^2+Q(t)^2}{2}$ and $H^{(1)}(P(t), Q(t)) = \sigma\frac{P(t)^2+Q(t)^2}{2}$ are preserved under the phase flow of the systems. This means that the phase trajectory of (5.110) lies on the circle with the center at the origin and the radius $\sqrt{p^2+q^2}$.

Here, we consider the explicit Milstein first order scheme given in (5.85), and five stochastic symplectic schemes: the mean square 0.5, first and second order schemes based on S^1_ω, and the mean square first- and second-order schemes based on S^3_ω. The coefficients G^1_α of S^1_ω for the system (5.110) are given by:

$$\begin{aligned} &G^1_{(0)} = \frac{a}{2}(p^2+q^2), \quad G^1_{(1)} = \frac{\sigma}{2}(p^2+q^2), \quad G^1_{(0,0)} = a^2pq, \quad G^1_{(1,1)} = \sigma^2pq \\ &G^1_{(1,0)} = G^1_{(0,1)} = a\sigma pq, \quad G^1_{(0,0,0)} = a^3(p^2+q^2) \quad G^1_{(1,1,1)} = \sigma^3(p^2+q^2) \\ &G^1_{(1,1,0)} = G^1_{(1,0,1)} = G^1_{(0,1,1)} = a\sigma^2(p^2+q^2), \quad G^1_{(1,1,1,1)} = 5\sigma^4pq. \end{aligned} \tag{5.111}$$

The various order symplectic schemes are obtained by truncating the generating function S^1_ω appropriately.

For S^3_ω, G^3_α for SHSs preserving Hamiltonian functions is zero when $l(\alpha) = 2, 4$.

Thus

$$G^3_{(0)} = \frac{a}{2}(p^2+q^2), \quad G^3_{(1)} = \frac{\sigma}{2}(p^2+q^2), \quad G^3_{(0,0,0)} = \frac{a^3}{4}(p^2+q^2),$$
$$G^3_{(1,1,1)} = \frac{\sigma^3}{4}(p^2+q^2), \quad G^3_{(1,1,0)} = G^3_{(1,0,1)} = G^3_{(0,1,1)} = \frac{a\sigma^2}{4}(p^2+q^2). \tag{5.112}$$

The first-order midpoint scheme was already applied in [11] for the system (5.110) to illustrate the superior performance on the long time intervals compared to the non-symplectic schemes. The second-order midpoint scheme is given in (7.23).

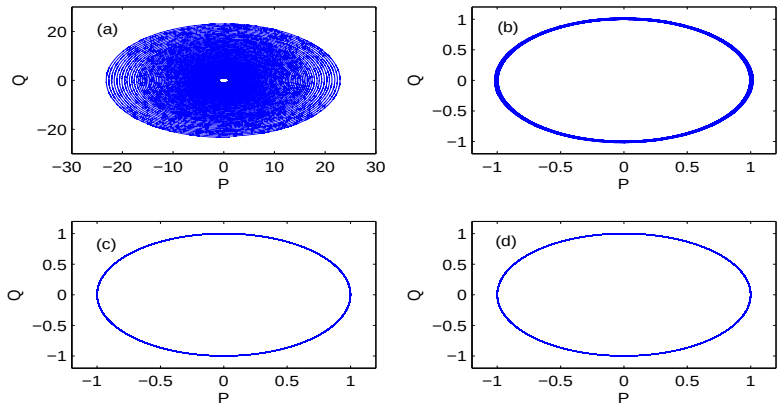

Figure 31: A sample phase trajectory of (5.110) with $a = 2$, $\sigma = 0.3$, $p = 1$ and $q = 0$: The Milstein scheme (a); S^1_ω first-order scheme (b); S^1_ω second-order scheme (c); S^3_ω second-order scheme (d) with time step $h = 2^{-8}$ on the time interval $T \leq 200$

Sample phase trajectories of (5.110) from various numerical scheme are presented in Fig. 31. It can be seen that the phase trajectory of non-symplectic scheme is far away from the circle $P(t)^2 + Q(t)^2 = 1$. However, the symplectic schemes produce accurate numerical solutions.

Figs. 32 and 33 confirm that the symplectic schemes have the expected convergence rate. Hence, the high order symplectic schemes have a more accuracy estimation than the low order symplctic scheme with the same time step.

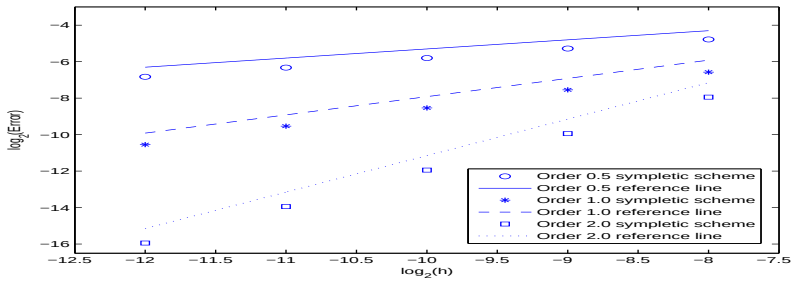

Figure 32: Convergence rate of different order S^1_ω symplectic scheme for (5.110), where error is the maximum error of (P, Q) at $T = 100$.

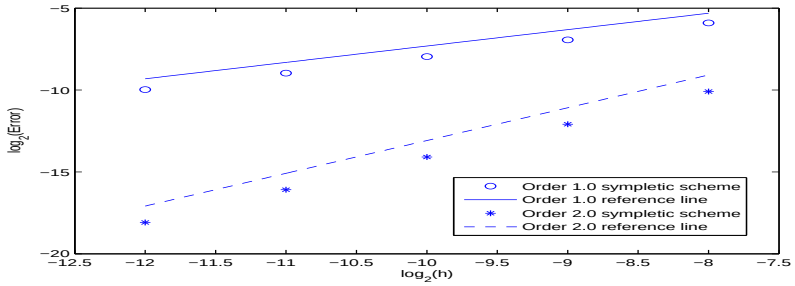

Figure 33: Convergence rate of different order S^3_ω symplectic scheme for (5.110), where error is the maximum error of (P, Q) at $T = 100$.

5.6.3 Synchrotron oscillations

The mathematical model for oscillations of particles in storage rings is given by:

$$\begin{aligned} dP &= -\beta^2 \sin Q dt - \sigma_1 \cos Q \circ dw_t^1 - \sigma_2 \sin Q \circ dw_t^2, \\ dQ &= P dt. \end{aligned} \tag{5.113}$$

We obtain the following formulas for the coefficients G^1_α of S^1_ω

$$\begin{gathered} G^1_{(0)} = \frac{p^2}{2} - \omega^2 \cos q, \quad G^1_{(1)} = \sigma_1 \sin q, \quad G^1_{(2)} = -\sigma_2 \cos q, \quad G^1_{(0,0)} = \omega^2 p \sin q, \\ G^1_{(0,1)} = \sigma_1 p \cos q, \quad G^1_{(0,2)} = \sigma_2 p \sin q, \quad G^1_{(0,1,1)} = \sigma_1^2 \cos^2 q, \quad G^1_{(0,2,2)} = \sigma_2^2 \sin^2 q, \end{gathered} \tag{5.114}$$

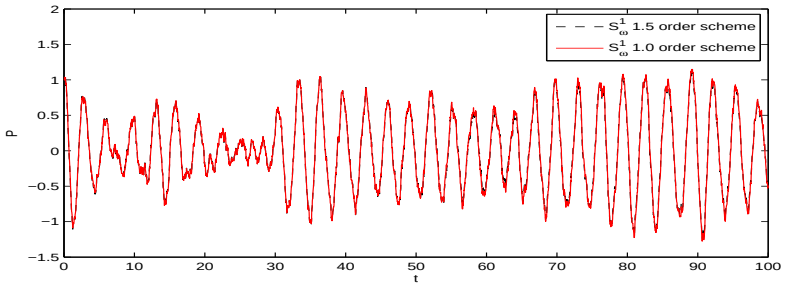

Figure 34: A sample trajectory of (6.26) for $\omega = 2$, $\sigma_1 = 0.2$, $\sigma_2 = 0.1$, and time step $h = 2^{-5}$.

All other G^1_α in (5.48) are zero.

Since the exact solution of the nonlinear SHS (6.26) is not known, it is hard to verify the order of various symplectic schemes. However, using a very fine time step $h = 2^{-8}$, we confirm that the sample trajectories from S^1_ω with first and 1.5 order are almost identical, and this is shown in Fig. 34. Moreover, the results also show that the various order numerical schemes based on S^1_ω are reliable for long time computation.

5.6.4 Conclusions

We present a framework to construct high-order symplectic schemes based on generating functions for stochastic Hamiltonian systems. The theoretical convergence analysis and numerical tests are provided for the proposed numerical methods. In general these symplectic schemes are implicit, and computationally expensive for mean square orders higher than two because they require generating approximations for multiple stochastic integrals of high order. It is also interesting to note that for stochastic Hamiltonian systems preserving Hamiltonian functions, the high order symplectic schemes have simpler forms and include less multiple stochastic integrals than the explicit Taylor expansion schemes.

Bibliography

[1] C. Anton, J. Deng, and Y. S. Wong. Symplectic numerical schemes for stochastic systems preserving hamiltonian functions. *Submitted to International Journal of Numerical Analysis & Modeling*, 2012.

[2] J.-M. Bismut. *Meéanique Aléatoire, Lecture Notes in Mathematics*, volume 866. Springer-Verlag, Berlin-Heidelberg-New York, 1981.

[3] K. Feng. On difference schemes and symplectic geometry. In *Proceedings of the 5-th Intern. Symposium on differential geometry & differential equations*, Beijing, China, 1985. 42-58.

[4] K. Feng, H.M. Wu, M.Z. Qin, and D.L. Wang. Construction of canonical difference schemes for hamiltonian formalism via generating functions. *J. Comp. Math.*, 7:71–96, 1989.

[5] J. Hong, R. Scherer, and L. Wang. Predictorcorrector methods for a linear stochastic oscillator with additive noise. *Mathematical and Computer Modelling*, 46(5–6):738–764, 2007.

[6] P.E. Kloeden and E. Platen. *Numerical solutions of stochastic differential equations*. Springer-Verlag, Berlin, 1992.

[7] H. Kunita. *Stochastic flows and stochastic differential equations*. Cambridge University Press, 1990.

[8] H. Kunita. *Stochastic Flows and Stochastic Differential Equations*. Cambridge University Press, Cambridge ; New York, 1990.

[9] A.H.S. Melbo and D.J. Higham. Numerical simulation of a linear stochastic oscillator with additive noise. *Applied Numerical Mathematics*, 51(1):89–99, 2004.

[10] G. N. Milstein. *Numerical Integration of Stochastic Differential Equations*. Kluwer Academic Publishers, 1995.

[11] G. N. Milstein, M. V. Tretyakov, and Y. M. Repin. Numerical methods for stochastic systems preserving symplectic structure. *SIAM Journal on Numerical Analysis*, 40:1583–1604, 2002.

[12] G. N. Milstein, M. V. Tretyakov, and Y. M. Repin. Symplectic integration of hamiltonian systems with additive noise. *SIAM Journal on Numerical Analysis*, 39:2066–2088, 2002.

[13] R.D. Ruth. A canonical integration technique. *IEEE Trans. Nuclear Science*, (30):2669–2671, 1983.

[14] R. de Vogelaere. Methods of integration which preserve the contact transformation property of the hamiltonian equations. Technical report, Report No. 4, Dept. Math., Univ. of Notre Dame, Notre Dame, Ind., 1956.

[15] L. Wang, J. Hong, R. Scherer, and F. Bai. Dynamics and variational integrators of stochastic hamiltonian systems. *International Journal of Numerical Analysis & Modeling*, 6(4):586–602, 2009.

Chapter 6

Weak Symplectic Schemes for Stochastic Hamiltonian Equations

If the approximation $\bar{X}_k = (\bar{P}, \bar{Q})$, $k = 0, 1, \ldots$, of the solution $X(t_k, \omega) = (P(t_k, \omega), Q(t_k, \omega))$, satisfies

$$|E[F(\bar{X}_k(\omega))] - E[F(X(t_k, \omega)]| \leq Kh^r, \tag{6.1}$$

for F from a sufficiently large class of functions, where $t_k = t_0 + kh \in [t_0, t_0 + T]$, h is the time step, and the constant K does not depend on k and h, then we say that $\bar{X}_k$ approximate the solution $X(t_k)$ of (5.1) in the weak sense [6] with weak order of accuracy m.

In [6], Milstein et.al. have constructed a first-order weak symplectic scheme for the system (5.1). Although several second and third order weak symplectic schemes were proposed for special types of SHS (such as SHSs with additive noise or SHSs with separable Hamiltonians), they conclude that further investigation is needed to obtain higher order symplectic schemes for the general SHS (5.1) with multiplicative noise [6, Remark 4.2].

In this Chapter, we propose a new method to derive symplectic weak schemes, and we construct a second order weak symplectic scheme for the general SHS (5.1). Our approach is a non-trivial extension of the methods based on generating functions from deterministic Hamiltonian systems [1, Chapter 4] to SHS. The generating function method in the stochastic case was applied to obtain strong schemes in [2], [3], but only the low order symplectic schemes with mean square orders up to 3/2 were constructed because of the complexity of the calculations required for finding the coefficients of the

generating function. In previous section, we employ a different formulation, and we obtain a general recursive formula for the coefficients of the generating function. To the best of our knowledge, a systematic approach as presented in this work to construct symplectic weak schemes of any order has not been reported before.

6.1 The weak symplectic schemes

In this section, we present a method to generate weak symplectic numerical schemes for the SHS (5.1) of any given order. From equations (2.34), Chapter 5 in [4], we have the following relationship between the Ito integrals

$$I_\alpha[f(\cdot,\cdot)]_{t_0,t} = \int_{t_0}^{t}\int_{t_0}^{s_l}\cdots\int_{t_0}^{s_2} f(s_1,\cdot)dw_{s_1}^{j_1}\ldots dw_{s_{l-1}}^{j_{l-1}}dw_{s_l}^{j_l}, \quad I_\alpha = I_\alpha[1]_{t_0,t},$$

and the Stratanovich integrals J_α defined in Eq. (5.25): $I_\alpha = J_\alpha$ if $l(\alpha) = 1$ and

$$J_\alpha = I_{(j_l)}\left[J_{\alpha-}\right] + \chi_{\{j_l=j_{l-1}\neq 0\}} I_{(0)}\left[\frac{1}{2}J_{(\alpha-)-}\right], \quad l(\alpha)\geq 2, \tag{6.2}$$

where $\alpha = (j_1, j_2, \ldots, j_l), j_i \in \{0, 1, \ldots, m\}$, χ_A denotes the indicator function of the set A, and f is any appropriate process [4, Chapter 5] .

For $m = 1$, replacing in the previous equation, we get $J_{(0)} = I_{(0)}$, $J_{(1)} = I_{(1)}$, $J_{(0,0)} = I_{(0,0)}$, $J_{(0,1)} = I_{(0,1)}$, $J_{(1,0)} = I_{(1,0)}$, $J_{(1,0,1)} = I_{(1,0,1)}$,

$$\begin{aligned}
&J_{(1,1)} = I_{(1,1)} + \frac{1}{2}I_{(0)}, \quad J_{(1,1,1)} = I_{(1,1,1)} + \frac{1}{2}\left(I_{(1,0)} + I_{(0,1)}\right),\\
&J_{(1,1,0)} = I_{(1,1,0)} + \frac{1}{2}I_{(0,0)}, \quad J_{(0,1,1)} = I_{(0,1,1)} + \frac{1}{2}I_{(0,0)},\\
&J_{(1,1,1,1)} = I_{(1,1,1,1)} + \frac{1}{2}\left(I_{(0,1,1)} + I_{(1,0,1)} + I_{1,1,0}\right) + \frac{1}{4}I_{(0,0)}.
\end{aligned}$$

To obtain a second order weak scheme, we replace in (5.24) the Stratanovich integrals J_α by Ito integrals using the Eq. (6.2), and we truncate the series to include only Ito integrals with multi-indexes α such that $l(\alpha) \leq 2$. Thus, we have the following

approximation for the generating function

$$
\begin{aligned}
S^1_\omega \approx\ & (G^1_{(0)} + \frac{1}{2}G^1_{(1,1)})I_{(0)} + G^1_{(1)}I_{(1)} + \Bigg(G^1_{(0,0)} + \frac{1}{2}(G^1_{(1,1,0)} + G^1_{(0,1,1)}) \\
& + \frac{1}{4}G^1_{(1,1,1,1)}\Bigg)I_{(0,0)} + G^1_{(1,1)}I_{(1,1)} + \left(G^1_{(0,1)} + \frac{1}{2}G^1_{(1,1,1)}\right) I_{(0,1)} \\
& + \left(G^1_{(1,0)} + \frac{1}{2}G^1_{(1,1,1)}\right) I_{(1,0)},
\end{aligned} \tag{6.3}
$$

where everywhere the arguments are (P, q).

Replacing in (5.37), we get the scheme corresponding to the following one step approximation:

$$
\begin{aligned}
\bar{P}_i =\ & p_i - h\frac{\partial G^1_{(0)}}{\partial q_i} - h^{1/2}\xi\frac{\partial G^1_{(1)}}{\partial q_i} - \frac{h^2}{2}\Bigg(\frac{\partial G^1_{(0,0)}}{\partial q_i} + \frac{1}{2}\left(\frac{\partial G^1_{(1,1,0)}}{\partial q_i} + \frac{\partial G^1_{(0,1,1)}}{\partial q_i}\right) \\
& + \frac{1}{4}\frac{\partial G^1_{(1,1,1,1)}}{\partial q_i}\Bigg) - \frac{h\xi^2}{2}\frac{\partial G^1_{(1,1)}}{\partial q_i} - h^{3/2}\epsilon\Bigg(\frac{\partial G^1_{(1,0)}}{\partial q_i} + \frac{1}{2}\frac{\partial G^1_{(1,1,1)}}{\partial q_i}\Bigg) - h^{3/2}(\xi - \epsilon) \\
& \left(\frac{\partial G^1_{(0,1)}}{\partial q_i} + \frac{1}{2}\frac{\partial G^1_{(1,1,1)}}{\partial q_i}\right) \\
\bar{Q}_i =\ & q_i + h\frac{\partial G^1_{(0)}}{\partial \bar{P}_i} + h^{1/2}\xi\frac{\partial G^1_{(1)}}{\partial \bar{P}_i} + \frac{h^2}{2}\Bigg(\frac{\partial G^1_{(0,0)}}{\partial \bar{P}_i} + \frac{1}{4}\frac{\partial G^1_{(1,1,1,1)}}{\partial \bar{P}_i} \\
& + \frac{1}{2}\left(\frac{\partial G^1_{(1,1,0)}}{\partial \bar{P}_i} + \frac{\partial G^1_{(0,1,1)}}{\partial \bar{P}_i}\right)\Bigg) + \frac{h\xi^2}{2}\frac{\partial G^1_{(1,1)}}{\partial \bar{P}_i} + h^{3/2}\epsilon\Bigg(\frac{\partial G^1_{(1,0)}}{\partial \bar{P}_i} + \frac{1}{2}\frac{\partial G^1_{(1,1,1)}}{\partial \bar{P}_i}\Bigg) \\
& + h^{3/2}(\xi - \epsilon)\left(\frac{\partial G^1_{(0,1)}}{\partial \bar{P}_i} + \frac{1}{2}\frac{\partial G^1_{(1,1,1)}}{\partial \bar{P}_i}\right),
\end{aligned}
$$

where $i = 1, \ldots, n$, h is the time step, and everywhere the arguments are $(\bar{P}, q)$. The random variable $\sqrt{h}\xi$ represents the Ito integral $I_{(1)}$, and $h^{3/2}\epsilon$ represents the double Ito integral $I_{(1,0)}$, and we have $\xi \sim N(0,1)$, $\epsilon \sim N(0, 1/3)$ and $E(\xi\epsilon) = 1/2$. Notice that $I_{(0,1)} + I_{(1,0)} = I_{(0)}I_{(1)}$, so $h^{3/2}(\xi - \epsilon)$ represents the double integral $I_{(0,1)}$.

For a weak scheme, we can generate the noise increments more efficiently than for a strong scheme . For example, proceeding as in Section 14.2 of [4], we can avoid the second random variable ϵ and generate a single random variable ζ with the following discrete distribution

$$
P(\zeta = \pm\sqrt{3}) = \frac{1}{6}, \quad P(\zeta = 0) = \frac{2}{3}. \tag{6.4}
$$

The moments of ξ and ζ are equaled up to order 5, and we also replace ϵ by $\frac{1}{2}\zeta$, so we obtain the simplified scheme:

$$\begin{aligned}\bar{P}_i &= p_i - h\frac{\partial G^1_{(0)}}{\partial q_i} - h^{1/2}\zeta\frac{\partial G^1_{(1)}}{\partial q_i} - \frac{h^2}{2}\Bigg(\frac{\partial G^1_{(0,0)}}{\partial q_i} + \frac{1}{4}\frac{\partial G^1_{(1,1,1,1)}}{\partial q_i} \\ &+ \frac{1}{2}\left(\frac{\partial G^1_{(1,1,0)}}{\partial q_i} + \frac{\partial G^1_{(0,1,1)}}{\partial q_i}\right)\Bigg) - \frac{h\zeta^2}{2}\frac{\partial G^1_{(1,1)}}{\partial q_i} - \frac{1}{2}h^{3/2}\zeta\Bigg(\frac{\partial G^1_{(1,0)}}{\partial q_i} + \frac{\partial G^1_{(1,1,1)}}{\partial q_i} \\ &+ \frac{\partial G^1_{(0,1)}}{\partial q_i}\Bigg), \qquad (6.5)\\ \bar{Q}_i &= q_i + h\frac{\partial G^1_{(0)}}{\partial \bar{P}_i} + h^{1/2}\zeta\frac{\partial G^1_{(1)}}{\partial \bar{P}_i} + \frac{h^2}{2}\Bigg(\frac{\partial G^1_{(0,0)}}{\partial \bar{P}_i} + \frac{1}{4}\frac{\partial G^1_{(1,1,1,1)}}{\partial \bar{P}_i} \\ &+ \frac{1}{2}\left(\frac{\partial G^1_{(1,1,0)}}{\partial \bar{P}_i} + \frac{\partial G^1_{(0,1,1)}}{\partial \bar{P}_i}\right)\Bigg) + \frac{h\zeta^2}{2}\frac{\partial G^1_{(1,1)}}{\partial \bar{P}_i} + \frac{1}{2}h^{3/2}\zeta\Bigg(\frac{\partial G^1_{(1,0)}}{\partial \bar{P}_i} + \frac{\partial G^1_{(1,1,1)}}{\partial \bar{P}_i} \\ &+ \frac{\partial G^1_{(0,1)}}{\partial \bar{P}_i}\Bigg), \qquad (6.6)\end{aligned}$$

where $i = 1, \ldots, n$, and everywhere the arguments are $(\bar{P}, q)$.

Lemma 6.1 *The scheme (6.5)-(6.6) is symplectic.*

Proof: By definition the scheme (6.5)-(6.6) is symplectic if it preserves symplectic structure, i.e. if we have $\bar{P} \wedge \bar{Q} = dp \wedge dq$. This can be proved proceeding as in the proof of Theorem 3.1 in [7]. Notice that we can write the scheme (6.5)-(6.6)) as

$$\bar{P}_i = p_i - \frac{\partial \bar{S}_1}{\partial q_i}(\bar{P}, q), \quad \bar{Q}_i = q_i + \frac{\partial \bar{S}_1}{\partial \bar{P}_i}(\bar{P}, q),$$

where

$$\begin{aligned}\bar{S}_1 &= G^1_{(0)}h + G^1_{(1)}\sqrt{h}\zeta + \left(G^1_{(0,0)} + \frac{1}{2}(G^1_{(1,1,0)} + G^1_{(0,1,1)}) + \frac{1}{4}G^1_{(1,1,1,1)}\right)\frac{h^2}{2} \\ &+ G^1_{(1,1)}\frac{h\zeta^2}{2} + \frac{h^{3/2}\zeta}{2}\left(G^1_{(0,1)} + G^1_{(1,1,1)} + G^1_{(1,0)}\right).\end{aligned}$$

□

For the general stochastic Hamiltonian system (5.1) with $d \geq 1$, a second order symplectic scheme can be constructed similarly using the following approximation of

the generating function

$$\bar{S}^1_\omega = \left(G^1_{(0)} + \frac{1}{2}\sum_{k=1}^{d} G^1_{(k,k)} \right) h + \sum_{k=1}^{d} G^1_{(k)} \sqrt{h}\zeta_k + \Bigg(G^1_{(0,0)} + \frac{1}{2}\sum_{k=1}^{d} \Bigg(G^1_{(k,k,0)} + G^1_{(0,k,k)} \Bigg) + \frac{1}{4}\sum_{k,j=1}^{d} G^1_{(k,k,j,j)} \Bigg) \frac{h^2}{2} + \frac{h^{3/2}}{2} \sum_{k=1}^{d} \zeta_k \Bigg(G^1_{(0,k)} + G^1_{(k,0)} + \frac{1}{2}\sum_{j=1}^{d} \left(G^1_{(k,j,j)} + G^1_{(j,j,k)} \right) \Bigg) + \frac{h}{2} \sum_{j,k=1}^{d} G^1_{(j,k)} (\zeta_j \zeta_k + \zeta_{j,k}). \tag{6.7}$$

Here ζ_k, for $k = 1, \ldots, m$ are independent random variables with the distribution given in (6.4) and $\zeta_{j,k}$ are independent, two-point distributed random variables with $\zeta_{j_1,j_1} = -1$,

$$P(\zeta_{j_1,j_2} = \pm 1) = \frac{1}{2}, j_2 = 1, \ldots, j_1 - 1, \quad \zeta_{j_1,j_2} = -\zeta_{j_2,j_1}, j_2 = j_1 + 1, \ldots, d,$$

for $j_1 = 1, \ldots, m$, [4, Chapter 14.2].

It is important to recognize that a symplectic scheme of order m can be constructed in a similar way by replacing the Stratanovich integrals in (5.24) by Ito integrals using the Eq. (6.2) and keeping the Ito integrals I_α with $l(\alpha) \leq r$. Here G^1_α can be determined using (5.43). For example, for order three weak symplectic schemes, we include in the approximation of the generating function S^1_ω all terms containing Ito integral I_α with

$l(\alpha) \le 3$. From (6.2) we have

$$
\begin{aligned}
S^1_\omega \approx & \left(G^1_{(0)} + \frac{1}{2}\sum_{k=1}^{d} G^1_{(k,k)} \right) I_{(0)} + \Big(G^1_{(0,0)} + \frac{1}{2}\sum_{k=1}^{d} (G^1_{(k,k,0)} + G^1_{(0,k,k)}) \\
& + \frac{1}{4}\sum_{k,j=1}^{d} G^1_{(k,k,j,j)} \Big) I_{(0,0)} + \sum_{k=1}^{d} \Bigg(\left(G^1_{(0,k)} + \frac{1}{2}\sum_{j=1}^{d} G^1_{(j,j,k)} \right) I_{(0,k)} \\
& + \left(G^1_{(k,0)} + \sum_{j=1}^{d} \frac{1}{2} G^1_{(k,j,j)} \right) I_{(k,0)} \Bigg) + \sum_{k=1}^{d} G^1_{(k)} I_{(k)} \\
& + \sum_{k,j=1}^{d} G^1_{(k,j)} I_{(k,j)} + \Big(G^1_{(0,0,0)} + \frac{1}{2}\sum_{k=1}^{d} \big(G^1_{(k,k,0,0)} + G^1_{(0,k,k,0)} + G^1_{(0,0,k,k)} \big) \\
& + \frac{1}{4}\sum_{k,j=1}^{d} \big(G^1_{(k,k,j,j,0)} + G^1_{(0,k,k,j,j)} + G^1_{(k,k,0,j,j)} \big) + \frac{1}{8}\sum_{k,j,l=1}^{d} G^1_{(k,k,j,j,l,l)} \Big) I_{(0,0,0)} \\
& + \sum_{k=1}^{d} \Big(G^1_{(0,0,k)} + \frac{1}{2}\sum_{j=1}^{d} \big(G^1_{(j,j,0,k)} + G^1_{(0,j,j,k)} \big) + \frac{1}{4}\sum_{j,l=1}^{d} G^1_{(j,j,l,l,k)} \Big) I_{(0,0,k)} \\
& + \sum_{k=1}^{d} \Big(G^1_{(0,k,0)} + \frac{1}{2}\sum_{j=1}^{d} \big(G^1_{(j,j,k,0)} + G^1_{(0,k,j,j)} \big) + \frac{1}{4}\sum_{j,l=1}^{d} G^1_{(j,j,k,l,l)} \Big) I_{(0,k,0)} \\
& + \sum_{k=1}^{d} \Big(G^1_{(k,0,0)} + \frac{1}{2}\sum_{j=1}^{d} \big(G^1_{(k,j,j,0)} + G^1_{(k,0,j,j)} \big) + \frac{1}{4}\sum_{j,l=1}^{d} G^1_{(k,j,j,l,l)} \Big) I_{(k,0,0)} \\
& + \sum_{k,j=1}^{d} \Bigg(\left(G^1_{(k,j,0)} + \frac{1}{2}\sum_{l=1}^{d} G^1_{(k,j,l,l)} \right) I_{(k,j,0)} + \left(G^1_{(0,k,j)} + \frac{1}{2}\sum_{l=1}^{d} G^1_{(l,l,k,j)} \right) I_{(0,k,j)} \\
& + \left(G^1_{(k,0,j)} + \frac{1}{2}\sum_{l=1}^{d} G^1_{(k,l,l,j)} \right) I_{(k,0,j)} \Bigg) + \sum_{k,j,l=1}^{d} G^1_{(k,j,l)} I_{(k,j,l)},
\end{aligned}
$$

where everywhere the arguments are (P, q). Although it is easier to approximate the multiple Ito integrals I_α for weak schemes than for the strong schemes, it should be noted that weak symplectic schemes with high order (e.g. $r \ge 4$) will involve long formulas for the coefficients G^1_α, including high order partial derivatives of the Hamiltonians $H^{(r)}$, $r = 0, \ldots, m$.

Analogously, using (5.11) and a truncated series for S^2_ω or (5.12) and a truncated series for S^3_ω, we can obtain various weak symplectic schemes for the SHS (5.1). For example, if $m = 1$, we have the following weak second order scheme based on the

truncation of S_ω^3 that includes only the terms containing Ito integrals I_α with multi-indexes α such that $l(\alpha) \leq 2$:

$$\begin{aligned} Y_{k+1} &= Y_k + J^{-1}\nabla H^{(0)}(Y_{k+\frac{1}{2}})h + J^{-1}\nabla H^{(1)}(Y_{k+\frac{1}{2}})h^{1/2}\zeta_k \\ &+ \frac{h^2}{2}J^{-1}\left(\frac{1}{4}\nabla G^3_{(1,1,1,1)}(Y_{k+\frac{1}{2}}) + \frac{1}{2}\big(\nabla G^3_{(1,1,0)}(Y_{k+\frac{1}{2}}) + \nabla G^3_{(0,1,1)}(Y_{k+\frac{1}{2}})\big)\right) \\ &+ \frac{h^{3/2}\zeta_k}{2}J^{-1}\left(\nabla G^3_{(1,0)}(Y_{k+\frac{1}{2}}) + \nabla G^3_{(0,1)}(Y_{k+\frac{1}{2}}) + \nabla G^3_{(1,1,1)}(Y_{k+\frac{1}{2}})\right) \end{aligned} \tag{6.8}$$

where for each time step k, we have $Y_k = (P_k^T, Q_k^T)^T$, and the arguments are everywhere $Y_{k+\frac{1}{2}} = (Y_{k+1} + Y_k)/2$. The random variables ζ_k are the same as for the scheme (6.5)-(6.6), and the coefficients G^3_α can be found using (5.45).

Remark 6.2 *The order 1 scheme presented in [6] (with $\alpha = \beta = 1$) corresponds to the following approximation of the generating function which contains Ito integrals I_α with $l(\alpha) \leq 1$:*

$$\bar{S}_1(P,q) \approx (G^1_{(0)}(P,q) + \frac{1}{2}\sum_{k=1}^{d} G^1_{(k,k)}(P,q))h + \sum_{k=1}^{d} G^1_{(k)}(P,q)\sqrt{h}\eta_k,$$

$P(\eta_k = \pm 1) = 1/2$, and the random variables η_k are mutually independent. The weak order 1 scheme presented in [6] (with $\alpha = \beta = 1/2$) corresponds to the following truncation of the generating function according to indexes α with $l(\alpha) \leq 1$:

$$\bar{S}_3(z) \approx G^3_{(0)}(z)h + \sum_{k=1}^{d} G^3_{(k)}(z)\sqrt{h}\eta_k, \quad P(\eta_k = \pm 1) = \frac{1}{2}, \quad z \in \mathbb{R}^{2n}.$$

and the random variables η_k are mutually independent.

6.2 Convergence study

We study the convergence of the symplectic numerical schemes proposed in the previous section. To keep the notations as simple as possible, we will illustrate the idea of the proof for the scheme (6.5)-(6.6) which corresponds to the system (5.1) with $m = 1$, and to the truncation given in (6.3) of the generating function. The same approach

can be followed in the general case for $m > 1$ and for truncations of the generating function including all Ito integrals I_α with $l(\alpha) \leq r$ with $r > 2$, but the complexity of the calculations in the Taylor expansions increases with m and r.

We assume that the coefficients of (5.1) are smooth enough to satisfy the following global Lipschitz condition

$$\sum_{j=0}^{1} \|\nabla H^{(j)}(P,Q) - \nabla H_j(p,q)\| \leq L_1(\|P-p\| + \|Q-q\|). \tag{6.9}$$

As in [6], we define the class $\mathcal{F}$ to be formed with the functions F defined on $\mathbb{R}^{2n}$ for which there exists constants $K > 0$ and $\chi > 0$, such that

$$|F(x)| \leq K(1+|x|)^\chi,$$

for any $x \in \mathbb{R}^{2n}$. To prove the weak convergence with order 2, we use the general result given in Theorem 4.1 in [6]. We assume that the function F in (6.1) together with its partial derivatives up to order 6 belong to the class $\mathcal{F}$. Moreover, in addition to (6.9), $H^{(0)}$ and $H^{(1)}$ together with their partial derivatives up to order 7 belongs to class $\mathcal{F}$.

Theorem 6.3 *The implicit method (6.5)-(6.6) for the system (5.1) with $m = 1$ is symplectic and of weak order 2.*

Proof: The scheme (6.5)-(6.6) is implicit, so we should first prove that it is well-defined. Using the Lipschitz condition (6.9), the fact that at each step the random variables $|\zeta| \leq \sqrt{3}$, and proceeding as in the proof of lemma 5.3, from the contraction principle we get that there exist constants $K > 0$ and $h_0 > 0$ such that for any $h \leq h_0$, $t_0 \leq t \leq t_0 + T$, $x = (p^T, q^T)^T \in \mathbb{R}^{2n}$, the system (6.5)-(6.6) has a unique solution $\bar{X} = (\bar{P}^T, \bar{Q}^T)^T \in \mathbb{R}^{2n}$ which satisfies the inequality

$$\|\bar{X} - x\| \leq K(1+\|x\|)\sqrt{h}. \tag{6.10}$$

This solution can be found by the method of simple iteration with $x = (p^T, q^T)^T$ as the initial approximation, so the scheme (6.5)-(6.6) is well-defined.

From lemma 6.1, we know that the scheme is symplectic, and to prove the weak convergence with second order, we check the conditions (2) and (4) in Theorem 4.1 in [6]. For $i = 1, \ldots, 2n$, let denote $\bar{\Delta}^i = \bar{X}^i - x^i$ and $\Delta^i = X^i_{t,x}(t+h) - x^i$, where $X_{t,x}(t+h) = (P^T(t+h), Q^T(t+h))^T$ is the solution of the system (5.1) and $X_{t,x}(t) = x$. Then from (6.10) we have

$$E\prod_{j=1}^{6}|\bar{\Delta}^{i_j}| \le K(x)h^3, \quad K \in \mathcal{F}, \quad i_j \in \{1, \ldots, 2n\}, j = 1, \ldots, 6. \tag{6.11}$$

To prove that

$$\left| E\left(\prod_{j=1}^{v}\Delta^{i_j} - \prod_{j=1}^{v}\bar{\Delta}^{i_j}\right)\right| \le k(x)h^3, \quad v = 1, \ldots, 5, \quad k \in \mathcal{F}, \tag{6.12}$$

we compare the scheme (6.5)-(6.6) with the order 2 weak Taylor scheme ([4], pp. 464).

To simplify the notation, let denote

$$\begin{aligned}
f_i(P,Q) &= -\frac{\partial H^{(0)}}{\partial Q_i}(P,Q) + \frac{1}{2}\sum_{j=1}^{n}\Bigg(\frac{\partial H^{(1)}}{\partial Q_j}(P,Q)\frac{\partial^2 H^{(1)}}{\partial P_j \partial Q_i}(P,Q) \\
&\quad - \frac{\partial H^{(1)}}{\partial P_j}(P,Q)\frac{\partial^2 H^{(1)}}{\partial Q_j \partial Q_i}(P,Q)\Bigg) \\
g_i(P,Q) &= \frac{\partial H^{(0)}}{\partial P_i}(P,Q) + \frac{1}{2}\sum_{j=1}^{n}\Bigg(-\frac{\partial H^{(1)}}{\partial Q_j}(P,Q)\frac{\partial^2 H^{(1)}}{\partial P_j \partial P_i}(P,Q) \\
&\quad + \frac{\partial H^{(1)}}{\partial P_j}(P,Q)\frac{\partial^2 H^{(1)}}{\partial P_i \partial Q_j}(P,Q)\Bigg) \\
\sigma_i(P,Q) &= -\frac{\partial H^{(1)}}{\partial Q_i}(P,Q), \quad \gamma_i(P,Q) = \frac{\partial H^{(1)}}{\partial P_i}(P,Q),
\end{aligned}$$

and $f = (f_1, \ldots, f_n)^T$, $g = (g_1, \ldots, g_n)^T$, $\sigma = (\sigma_1, \ldots, \sigma_n)^T$, $\gamma = (\gamma_1, \ldots, \gamma_n)^T$. Using the Ito stochastic integration, we rewrite the equations (5.1) as

$$dP_i = f_i(P,Q)dt + \sigma_i(P,Q)dw_t, \quad P(t_0) = p \tag{6.13}$$

$$dQ_i = g_i(P,Q)dt + \gamma_i(P,Q)dw_t, \quad Q(t_0) = q, \tag{6.14}$$

An order 2 weak Taylor scheme [4, Chapter 14.2] for the Ito system (6.13)-(6.14) is

given in the following equations:

$$\tilde{P} = p + hf + h^{1/2}\zeta\sigma + \frac{h^2}{2}L_0(f) + \frac{h^{3/2}\zeta}{2}(L_0(\sigma) + L_1(f)) + \frac{hL_1(\sigma)}{2}(\zeta^2 - 1), \quad (6.15)$$

$$\tilde{Q} = q + hg + h^{1/2}\zeta\gamma + \frac{h^2}{2}L_0(g) + \frac{h^{3/2}\zeta}{2}(L_0(\gamma) + L_1(g)) + \frac{hL_1(\gamma)}{2}(\zeta^2 - 1), \quad (6.16)$$

where f, g, σ, γ and their derivatives are calculated at (p, q), and the operators L_0 and L_1 are given by

$$L_0 = \sum_{j=1}^{n}\left(f_j\frac{\partial}{\partial P_j} + g_j\frac{\partial}{\partial Q_j}\right) + \frac{1}{2}\sum_{i=1}^{n}\sum_{j=1}^{n}\left(\sigma_i\sigma_j\frac{\partial^2}{\partial P_i P_j} + \gamma_i\gamma_j\frac{\partial^2}{\partial Q_i Q_j} + 2\sigma_i\gamma_j\frac{\partial^2}{\partial P_i Q_j}\right)$$

$$L_1 = \sum_{i=1}^{n}\left(\sigma_i\frac{\partial}{\partial P_i} + \gamma_i\frac{\partial}{\partial Q_i}\right).$$

The random variables ζ are generated independently at each time step according to the discrete distribution given in (6.4).

For $i = 1, \ldots, 2n$ let denote $\tilde{\Delta}^i = \tilde{X}^i - x^i$, where $\tilde{X} = (\tilde{P}^T, \tilde{Q}^T)^T$. Then from [5, Chapter 8] we know that

$$\left| E\left(\prod_{j=1}^{v}\Delta^{i_j} - \prod_{j=1}^{v}\tilde{\Delta}^{i_j}\right)\right| \leq K_0(x)h^3, \quad v = 1, \ldots, 5, \quad K_0 \in \mathcal{F}. \quad (6.17)$$

Let define ρ by

$$\rho_j = \tilde{X}^j - \bar{X}^j = \tilde{\Delta}^j - \bar{\Delta}^j, \quad j = 1, \ldots, 2n.$$

Expanding the terms in the right-hand side of (6.5)-(6.6) around (p, q), we get

$$\Delta^i = \Delta^i_j(p, q) + R_j(\bar{P}, q), \quad |R_j(\bar{P}, q)| \leq F_j h^{\frac{j+1}{2}}, \quad i = 1, \ldots, 2n,$$

where $F_j \in \mathcal{F}$, $j = 1, \ldots, 5$. For example, if $n = 1$, we define recursively

$$\Delta^1_1 = -h^{1/2}\zeta\frac{\partial G_{(1)}}{\partial q}, \quad \Delta^1_2 = -h^{1/2}\zeta\left(\frac{\partial G_{(1)}}{\partial q} + \Delta^1_1\frac{\partial^2 G_{(1)}}{\partial q \partial p}\right) - h\left(\frac{\partial G_{(0)}}{\partial q} + \frac{\zeta^2}{2}\frac{\partial G_{(1,1)}}{\partial q}\right),$$

$$\Delta^1_3 = -h^{1/2}\zeta\left(\frac{\partial G_{(1)}}{\partial q} + \Delta^1_2\frac{\partial^2 G_{(1)}}{\partial q \partial p} + \frac{(\Delta^1_1)^2}{2}\frac{\partial^3 G_{(1)}}{\partial q \partial^2 p}\right) - h\Bigg(\frac{\partial G_{(0)}}{\partial q} + \frac{\zeta^2}{2}\frac{\partial G_{(1,1)}}{\partial q}$$
$$+ \Delta^1_1\frac{\partial}{\partial p}\left(\frac{\partial G_{(0)}}{\partial q} + \frac{\zeta^2}{2}\frac{\partial G_{(1,1)}}{\partial q}\right)\Bigg) - \frac{1}{2}h^{3/2}\zeta\left(\frac{\partial G_{(1,0)}}{\partial q} + \frac{\partial G_{(1,1,1)}}{\partial q} + \frac{\partial G_{(0,1)}}{\partial q}\right),$$

$$\Delta_4^1 = -h^{1/2}\zeta\left(\frac{\partial G_{(1)}}{\partial q} + \Delta_3^1\frac{\partial^2 G_{(1)}}{\partial q\partial p} + \frac{(\Delta_2^1)^2}{2}\frac{\partial^3 G_{(1)}}{\partial q\partial^2 p} + \frac{(\Delta_1^1)^3}{6}\frac{\partial^4 G_{(1)}}{\partial q\partial^3 p}\right) - h\Bigg(\frac{\partial G_{(0)}}{\partial q}$$
$$+ \frac{\zeta^2}{2}\frac{\partial G_{(1,1)}}{\partial q} + \Delta_2^1\frac{\partial}{\partial p}\left(\frac{\partial G_{(0)}}{\partial q} + \frac{\zeta^2}{2}\frac{\partial G_{(1,1)}}{\partial q}\right) + \frac{(\Delta_1^1)^2}{2}\frac{\partial^2}{\partial^2 p}\left(\frac{\partial G_{(0)}}{\partial q} + \frac{\zeta^2}{2}\frac{\partial G_{(1,1)}}{\partial q}\right)\Bigg)$$
$$- \frac{1}{2}h^{3/2}\zeta\Bigg(\frac{\partial G_{(1,0)}}{\partial q} + \frac{\partial G_{(1,1,1)}}{\partial q} + \frac{\partial G_{(0,1)}}{\partial q} + \Delta_1^1\frac{\partial}{\partial p}\left(\frac{\partial G_{(1,0)}}{\partial q} + \frac{\partial G_{(1,1,1)}}{\partial q} + \frac{\partial G_{(0,1)}}{\partial q}\right)\Bigg)$$
$$- \frac{h^2}{2}\Bigg(\frac{\partial G_{(0,0)}}{\partial q} + \frac{1}{4}\frac{\partial G_{(1,1,1,1)}}{\partial q} + \frac{1}{2}\left(\frac{\partial G_{(1,1,0)}}{\partial q} + \frac{\partial G_{(0,1,1)}}{\partial q}\right)\Bigg),$$

$$\Delta_5^1 = -h^{1/2}\zeta\Bigg(\frac{\partial G_{(1)}}{\partial q} + \Delta_4^1\frac{\partial^2 G_{(1)}}{\partial q\partial p} + \frac{(\Delta_3^1)^2}{2}\frac{\partial^3 G_{(1)}}{\partial q\partial^2 p} + \frac{(\Delta_2^1)^3}{6}\frac{\partial^4 G_{(1)}}{\partial q\partial^3 p} + \frac{(\Delta_1^1)^4}{24}\frac{\partial^5 G_{(1)}}{\partial q\partial^4 p}\Bigg)$$
$$- h\Bigg(\frac{\partial G_{(0)}}{\partial q} + \frac{\zeta^2}{2}\frac{\partial G_{(1,1)}}{\partial q} + \Delta_3^1\frac{\partial}{\partial p}\left(\frac{\partial G_{(0)}}{\partial q} + \frac{\zeta^2}{2}\frac{\partial G_{(1,1)}}{\partial q}\right) + \frac{(\Delta_2^1)^2}{2}\frac{\partial^2}{\partial^2 p}\Bigg(\frac{\partial G_{(0)}}{\partial q}$$
$$+ \frac{\zeta^2}{2}\frac{\partial G_{(1,1)}}{\partial q}\Bigg) + \frac{(\Delta_1^1)^3}{6}\frac{\partial^3}{\partial^3 p}\left(\frac{\partial G_{(0)}}{\partial q} + \frac{\zeta^2}{2}\frac{\partial G_{(1,1)}}{\partial q}\right)\Bigg) - \frac{1}{2}h^{3/2}\zeta\Bigg(\frac{\partial G_{(1,0)}}{\partial q} + \frac{\partial G_{(1,1,1)}}{\partial q}$$
$$+ \frac{\partial G_{(0,1)}}{\partial q} + \Delta_2^1\frac{\partial}{\partial p}\Bigg(\frac{\partial G_{(1,0)}}{\partial q} + \frac{\partial G_{(1,1,1)}}{\partial q} + \frac{\partial G_{(0,1)}}{\partial q}\Bigg) + \frac{(\Delta_1^1)^2}{2}\frac{\partial^2}{\partial^2 p}\Bigg(\frac{\partial G_{(1,0)}}{\partial q}$$
$$+ \frac{\partial G_{(1,1,1)}}{\partial q} + \frac{\partial G_{(0,1)}}{\partial q}\Bigg)\Bigg) - \frac{h^2}{2}\Bigg(\frac{\partial G_{(0,0)}}{\partial q} + \frac{1}{4}\frac{\partial G_{(1,1,1,1)}}{\partial q} + \frac{1}{2}\left(\frac{\partial G_{(1,1,0)}}{\partial q} + \frac{\partial G_{(0,1,1)}}{\partial q}\right)$$
$$+ \Delta_1^1\frac{\partial}{\partial p}\Bigg(\frac{\partial G_{(0,0)}}{\partial q} + \frac{1}{4}\frac{\partial G_{(1,1,1,1)}}{\partial q} + \frac{1}{2}\left(\frac{\partial G_{(1,1,0)}}{\partial q} + \frac{\partial G_{(0,1,1)}}{\partial q}\right)\Bigg)\Bigg)$$

Similarly, we define Δ_j^2, $j = 1, \ldots, 5$, starting from $\Delta_1^2 = h^{1/2}\zeta\frac{\partial G_{(1)}}{\partial p}$.

Using MAPLE software for the calculations and using the assumptions on the smoothness and boundedness of $H^{(0)}$ and $H^{(1)}$ and $E(\zeta^l) = 0$, $l = 1, 3, 5$, it is not difficult to verify

$$|\rho_j| \leq K_1(x)h^2, \tag{6.18}$$
$$|E(\rho_j)| = \left|E\left(\tilde{\Delta}^j - \bar{\Delta}^j\right)\right| \leq K_2(x)h^3, \tag{6.19}$$
$$|E(\rho_j\bar{\Delta}^i)| \leq K_3(x)h^3, \quad i, j = 1, \ldots, 2n \tag{6.20}$$

for any $i, j = 1, \ldots, 2n$, where $K_l \in \mathcal{F}$, $l = 1, 2, 3$. Moreover, from (6.10), we get

$$|\bar{\Delta}^j|^l \leq K_4(x)h^{l/2} \quad j = 1, \ldots, 2n, \quad l = 1, 2, \ldots, \quad K_4 \in \mathcal{F}. \tag{6.21}$$

Hence from (6.18)-(6.20), we obtain for $v = 2$

$$|E(\prod_{j=1}^{2} \tilde{\Delta}^{i_j} - \prod_{j=1}^{2} \bar{\Delta}^{i_j})| = |E(\prod_{j=1}^{2} (\bar{\Delta}^{i_j} + \rho_{i_j}) - \prod_{j=1}^{2} \bar{\Delta}^{i_j})| \leq K(x)h^3, \quad K \in \mathcal{F}. \tag{6.22}$$

For $v = 3, 4, 5$, the difference $\prod_{j=1}^{v} \tilde{\Delta}^{i_j} - \prod_{j=1}^{v} \bar{\Delta}^{i_j}$ consists of terms including either a product $\rho_{i_j} \cdots \rho_{i_k}$ with at least 2 factors, or a product $\rho_{i_j} \cdot (\bar{\Delta}^{i_1} \cdots \bar{\Delta}^{i_v})$ with at least three factors. Hence, using (6.18), (6.21) and the Cauchy–Schwarz inequality inequality, we can easily verify that that

$$\left| E\left(\prod_{j=1}^{v} \tilde{\Delta}^{i_j} - \prod_{j=1}^{v} \bar{\Delta}^{i_j} \right) \right| \leq K(x)h^3, \quad v = 3, 4, 5, \quad K \in \mathcal{F}. \tag{6.23}$$

The inequality (6.12) follows from (6.17) and (6.19), (6.22), (6.23).

To conclude the proof, we have to show that for a sufficiently large number m, the moments $E(\|\bar{X}_k\|^r)$ exist and are uniformly bounded with respect to N, where $h = T/N$, and $k = 0, \ldots, N$. Since $E(\zeta) = 0$, expanding the terms in the right-hand side of (6.5)-(6.6) around (p, q), and using the assumptions on smoothness and boundedness of $H^{(0)}$ and $H^{(1)}$, we can show that $|E(\bar{\Delta})| \leq K(1+\|x\|)h$. This inequality and (6.10) ensure the existence and boundedness of the moments $E(\|\bar{X}_k\|^r)$ (see lemma 9.1 in [5]). □

Analogously, we can prove the following result for the midpoint scheme.

Theorem 6.4 *The implicit method (6.8) for the SHS (5.1) is symplectic and of weak order 2.*

The convergence of the symplectic weak scheme of any order m constructed using the generating function S^i_ω, $i = 1, 2, 3$, can be proved in a similar way using Theorem 9.1 in [5] and comparing with the corresponding explicit order m weak Taylor scheme in Chapter 14 in [4].

6.3 Numerical Tests

To validate the performance of the proposed symplectic schemes, we perform numerical simulations. Since we work with weak schemes, for the MCS we only need to simulate uniformly distributed random numbers, and to calculate the expectations, unless we specify otherwise, 100 000 samples were used.

6.3.1 Kubo oscillator

In [7] the Kubo oscillator based on the following SDEs in the sense of Stratonovich is used to demonstrate the advantage of using a stochastic symplectic scheme for long time computations:

$$\begin{aligned} dP &= -aQdt - \sigma Q \circ dw_t, \quad P(0) = p_0, \\ dQ &= aPdt + \sigma P \circ dw_t, \quad Q(0) = q_0, \end{aligned} \tag{6.24}$$

where a and σ are constants.

Here, we consider the Euler weak scheme given in Chapter 14.1 in [4], and four stochastic symplectic weak schemes, namely the first and second order schemes based on S^1_ω and S^3_ω. The coefficients G^1_α of S^1_ω for system (6.24) are given by (see the general formula (5.43)):

$$\begin{aligned} &G^1_{(0)} = \frac{a}{2}(P^2+q^2), \quad G^1_{(1)} = \frac{\sigma}{2}(P^2+q^2), \quad G^1_{(0,0)} = a^2Pq, \quad G^1_{(1,1)} = \sigma^2 Pq \\ &G^1_{(1,0)} = G^1_{(0,1)} = a\sigma Pq, \quad G^1_{(0,0,0)} = a^3(P^2+q^2) \quad G^1_{(1,1,1)} = \sigma^3(P^2+q^2) \\ &G^1_{(1,1,0)} = G^1_{(1,0,1)} = G^1_{(0,1,1)} = a\sigma^2(P^2+q^2), \quad G^1_{(1,1,1,1)} = 5\sigma^4 Pq, \end{aligned}$$

where everywhere the arguments are (P, q). The symplectic schemes of various orders are obtained by truncating the generating function S^1_ω appropriately (see (6.5)-(6.6) for the second order scheme).

For S^3_ω, replacing in the general formula (5.45), we get $G^3_\alpha = 0$ when $l(\alpha) = 2$ and

$G^3_{(1,1,1,1)} = 0$. Thus

$$G^3_{(0)}(p,q) = \frac{a}{2}(p^2+q^2), \quad G^3_{(1)}(p,q) = \frac{\sigma}{2}(p^2+q^2), \quad G^3_{(0,0,0)}(p,q) = \frac{a^3}{4}(p^2+q^2),$$
$$G^3_{(1,1,1)}(p,q) = \frac{\sigma^3}{4}(p^2+q^2), \quad G^3_{(1,1,0)}(p,q) = G^3_{(1,0,1)}(p,q) = G^3_{(0,1,1)}(p,q)$$
$$= \frac{a\sigma^2}{4}(p^2+q^2).$$

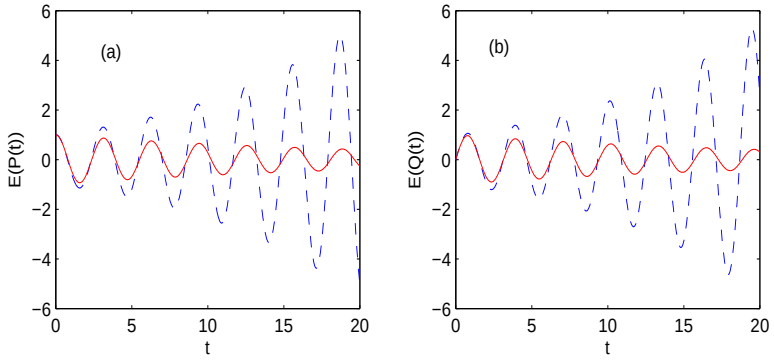

Figure 35: The expected value of $P(t)$ (a) and $Q(t)$ (b) for (6.24) with $a = 2$, $\sigma = 0.2$, $p = 1$, $q = 0$, and time step $h = 2^{-5}$: solid line; second order S^1_ω weak scheme, dashed line; Euler weak scheme

From [7], it is well-known that the Hamiltonian functions $H^{(0)}(P(t),Q(t)) = a\frac{P(t)^2+Q(t)^2}{2}$ and $H^{(1)}(P(t),Q(t)) = \sigma\frac{P(t)^2+Q(t)^2}{2}$ are preserved under the phase flow of the system. Therefore, the expected value of $P(t)^2 + Q(t)^2$ is also invariant with respect to time and we have

$$E(P(t)) = e^{-\frac{\sigma^2 t}{2}}(p\cos(at) - q\sin(at)), \quad E(Q(t)) = e^{-\frac{\sigma^2 t}{2}}(p\sin(at) + q\cos(at)). \tag{6.25}$$

In Fig. 35, we compare the exact values (6.25) with the estimations obtained using the explicit Euler scheme and the second-order weak symplectic scheme (6.5)-(6.6). It is clear that the second-order weak symplectic scheme produces very accurate estimations, while the Euler scheme fails even for a short term simulations.

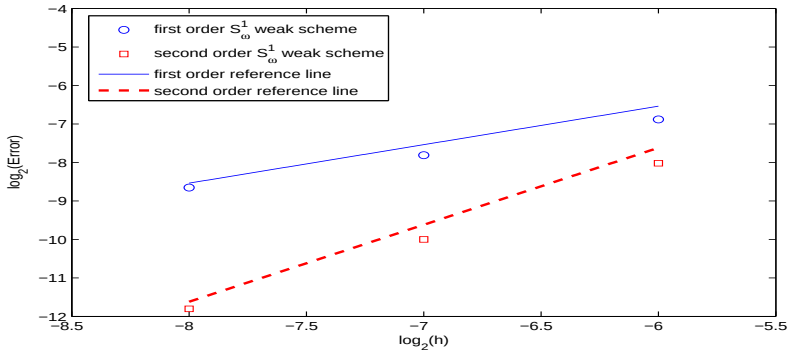

Figure 36: Convergence rate of different order S^1_ω symplectic weak scheme for (6.24)

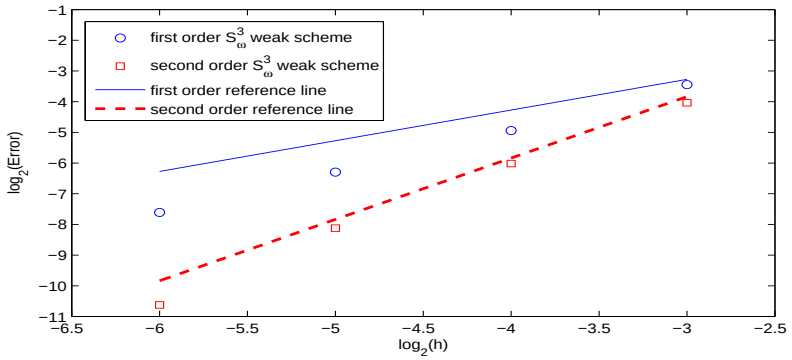

Figure 37: Convergence rate of different order S^3_ω symplectic weak scheme for (6.24).

The convergence rates of various symplectic weak schemes are investigated numerically by comparing the estimations of the expected values of the solutions with the exact value (6.25). Fig. 36 and Fig. 37 both confirm the expected convergence rates of the proposed symplectic schemes. The error is defined as the difference between the estimation of the expected value of solution from the numerical scheme and the exact value (6.25) at $T = 10$.

6.3.2 Synchrotron oscillations

The mathematical model for the oscillations of the particles in storage rings ([7]) is given by:

$$\begin{aligned} dP &= -\beta^2 \sin Q dt - \sigma_1 \cos Q \circ dw_t^1 - \sigma_2 \sin Q \circ dw_t^2, \\ dQ &= P dt. \end{aligned} \tag{6.26}$$

Notice that $H^{(0)}(P,Q) = -\beta^2 cosQ + P^2/2 = U(Q) + V(P)$, $H^{(1)}(P,Q) = \sigma_1 sinQ$, $H^{(2)}(P,Q) = -\sigma_2 cosQ$, so (6.26) is a SHS with separable Hamiltonians. Thus the explicit symplectic schemes in Section 4.2 in [6] can be applied.

Replacing in the general formula (5.43), we obtain the following formulas for the coefficients G_α^1 of S_ω^1

$$\begin{aligned} &G_{(0)}^1 = \frac{P^2}{2} - \beta^2 \cos q, \quad G_{(1)}^1 = \sigma_1 \sin q, \quad G_{(2)}^1 = -\sigma_2 \cos q, \\ &G_{(0,0)}^1 = \beta^2 P \sin q, \quad G_{(0,1)}^1 = \sigma_1 P \cos q, \quad G_{(0,2)}^1 = \sigma_2 P \sin q, \\ &G_{(0,1,1)}^1 = \sigma_1^2 \cos^2 q, \quad G_{(0,2,2)}^1 = \sigma_2^2 \sin^2 q, \end{aligned}$$

where everywhere the arguments are (P,q). All other G_α^1 included in the second order weak symplectic scheme based on the generating function S_ω^1 given in (6.7) are zero, and the first- and second-order symplectic weak schemes based on S_ω^1 are explicit for the SHS (6.26).

The mean energy of the system (6.26) is defined as $E(e(p,q))$, where $e(p,q) = p^2/2 - \beta^2 cos(q)$ ([6]). If $\sigma_1 = \sigma_2$ we have ([6])

$$E(e(P(t;0,p,q),Q(t;0,p,q))) = e(p,q) + \frac{\sigma^2}{2}t. \tag{6.27}$$

To check the accuracy of the proposed symplectic weak schemes, we run MCS and estimate 95% confidence intervals for $E(e(P(t;0,p,q),Q(t;0,p,q)))$ as

$$\bar{e}(t;0,p,q) \pm 1.96 \frac{s_e(t;0,p,q)}{\sqrt{M}}, \tag{6.28}$$

where M is the number of independent realizations in the MCS, $\bar{e}(t;0,p,q)$ is the sample average and $s_e(t;0,p,q)$ is the sample standard deviation (see also formula 7.7

in [6]). In addition to the weak scheme error, we also have the Monte Carlo error, but the margin of error in the confidence intervals (6.28) reflects the Monte Carlo error only.

Table 2: Simulation of $E(e(P(200;0,1,0),Q(200;0,1,0)))$ by the second order weak symplectic scheme based on the generating function S^1_ω given in (6.7)

h	M	$\bar{e}(200;0,1,0)$	$s_e(200;0,1,0)$	95% confidence interval
0.05	10^5	-6.609	0.029	-6.665 to -6.552
0.025	10^5	-6.544	0.029	-6.601 to -6.488
0.01	10^5	-6.497	0.029	-6.553 to -6.44
0.01	$4 \cdot 10^6$	-6.502	0.005	-6.511 to -6.493

The experiments presented in Table 2 demonstrate that the second order weak symplectic scheme based on the generating function S^1_ω given in (6.7) has similar accuracy with the explicit symplectic schemes (7.3) and (7.5) in [6] (see Table 1 in [6]). The values of the parameters used in the simulations are $\sigma_1 = \sigma_2 = 0.3$, $\beta = 4$, the initial values are $P(0) = 1$, $Q(0) = 0$, and $t = 200$. The sample averages $\bar{e}(200;0,1,0)$ displayed in Table 2, corresponding to various time steps h and number of realizations M, are good estimations of the exact solution $E(e(P(200;0,1,0),Q(200;0,1,0))) = -6.5$ obtained from (6.27). This proves the excellent performance for long term simulation of the second order weak symplectic scheme based on the generating function S^1_ω given in (6.7).

6.4 Conclusions

We present a systematic approach based on the generating functions to construct symplectic weak schemes of any order m for a general stochastic Hamiltonian system. For order $m = 1$, the derived weak scheme is the same as that proposed in [6]. However, it should be noted that a different approach is reported in [6], but no detail is provided how to extend this approach to construct symplectic weak scheme of order $m > 1$ for

general SHSs. In this study, we focus on the proposed second order symplectic weak schemes. To our knowledge, this may be the first to present the second order sympletic weak schemes which can be applied to general SHSs. It is important to recognize that higher oder weak schemes can be derived using the same procedure reported in this work.

For the symplectic second order weak schemes, we present a convergence study and validate their accuracy by numerical simulations for two different stochastic Hamiltonian systems. It is known that there are effective explicit methods of weak order 2 for general stochastic differential equations ([4, chapter 14]), but these methods are not symplectic. Compared to the Taylor expansion methods, the proposed symplectic second order weak methods are implicit, but they are comparable in terms of the number and the complexity of the multiple Ito stochastic integrals or the derivatives of the Hamiltonian functions required. Moreover, since for weak schemes we can use bounded discrete random variables to simulate the multiple Ito stochastic integrals, the derived symplectic implicit weak schemes are well defined and they are also computationally efficient.

Constructing weak symplectic schemes with high order (e.g. $m > 4$) is important from a theoretical point of view. Regarding a practical implementation, the Monte-Carlo simulations included in Section 6.3 for the symplectic schemes of weak orders $m = 1$ and $m = 2$ do not require variance reduction methods, but for orders $m > 4$, it is expected that the accuracy of the results will be influenced by the increasing variance. In addition, the weak symplectic schemes with higher order involve high order partial derivatives of the Hamiltonian functions.

Bibliography

[1] E. Hairer. *Geometric numerical integration: structure-preserving algorithms for ordinary differential equations.* Springer, Berlin ; New York, 2006.

[2] J. Hong, L. Wang, and R. Scherer. Simulation of stochastic hamiltonian systems via generating functions. In *Proceedings IEEE 2011 4th ICCSIT*, 2011.

[3] J. Hong, L. Wang, and R. Scherer. Symplectic numerical methods for a linear stochastic oscillator with two additive noises. In *Proceedings of the World Congress on Engineering*, volume I, London, U.K., 2011.

[4] P.E. Kloeden and E. Platen. *Numerical solutions of stochastic differential equations*. Springer-Verlag, Berlin, 1992.

[5] G. N. Milstein. *Numerical Integration of Stochastic Differential Equations*. Kluwer Academic Publishers, 1995.

[6] G. N. Milstein and M. V. Tretyakov. Quasi-symplectic methods for langevin-type equations. *IMA Journal of Numerical Analysis*, (23):593–626, 2003.

[7] G. N. Milstein, M. V. Tretyakov, and Y. M. Repin. Numerical methods for stochastic systems preserving symplectic structure. *SIAM Journal on Numerical Analysis*, 40:1583–1604, 2002.

Chapter 7

Symplectic schemes for stochastic Hamiltonian systems preserving Hamiltonian functions

Unlike the deterministic cases, in general the SHS (5.1) no longer preserves the Hamiltonian functions $H^{(i)}, i = 0, \ldots, n$ with respect to time. However, by the chain rule of the Stratonovich stochastic integration, for any $i = 0, \ldots, m$ we have

$$\begin{aligned} dH^{(i)} &= \sum_{k=1}^{n}(\frac{\partial H^{(i)}}{\partial P_k}dP + \frac{\partial H^{(i)}}{\partial Q_k}dQ) = \sum_{k=1}^{n}(-\frac{\partial H^{(i)}}{\partial P_k}\frac{\partial H^{(0)}}{\partial Q_k} \\ &+ \frac{\partial H^{(i)}}{\partial Q_k}\frac{\partial H^{(0)}}{\partial P_k})dt + \sum_{r=1}^{m}\sum_{k=1}^{n}(-\frac{\partial H^{(i)}}{\partial P_k}\frac{\partial H^{(r)}}{\partial Q_k} + \frac{\partial H^{(i)}}{\partial Q_k}\frac{\partial H^{(r)}}{\partial P_k}) \circ dw_t^r \end{aligned} \tag{7.1}$$

Thus, the Hamiltonian functions $H^{(i)}, i = 0, \ldots, m$ are invariant for the flow of the system (5.1) (i.e. $dH^{(i)} = 0$), if and only if $\{H^{(i)}, H^{(j)}\} = 0$ for $i, j = 0, \ldots, m$, where the Poisson bracket is defined as $\{H^{(i)}, H^{(j)}\} = \sum_{k=1}^{n}(\frac{\partial H^{(j)}}{\partial Q_k}\frac{\partial H^{(i)}}{\partial P_k} - \frac{\partial H^{(i)}}{\partial Q_k}\frac{\partial H^{(j)}}{\partial P_k})$. In this Chapter, we propose symplectic schemes for the special type of SHS preserving the Hamiltonian functions. This type of SHS is a special case of integrable stochastic hamiltonian dynamical systems which has been studied in [2].

The main results are included in section 7.1 where we prove that the coefficients of the generating function are invariant under permutation for this type of systems. That allows us to construct in section 7.2 strong and weak symplectic schemes of order two and three simpler than non-symplectic explicit Taylor expansion schemes with the same order.

7.1 Properties of G_α

In this section we prove an invariance property of the coefficients G^i_α of the generating functions S^i_ω, $i = 1, 2, 3$. For any permutation on $\{1, \ldots, l\}$, $l \geq 1$, and for any multi-index $\alpha = (i_1, \ldots, i_l)$ with $l(\alpha) = l$ let denote by $\pi(\alpha)$ the multi-index defined as $\pi(\alpha) := (i_{\pi(1)}, \ldots, i_{\pi(l)})$.

Based on formula (5.43) we have the following result.

Theorem 7.1 *For SHS preserving the Hamiltonian functions, the coefficients G^1_α of the generating function S^1_ω are invariants under permutations, i.e $G^1_\alpha = G^1_{\pi(\alpha)}$.*

Proof: By induction on the length of the multi-index α, the coefficients G^1_α of S^1_ω are invariant under the permutations on α for systems preserving the Hamiltonian functions, when $l(\alpha) = 2$ because for any $r_1, r_2 = 0, \ldots, m$ we have

$$G^1_{(r_1,r_2)} = \sum_{k=1}^{n} \frac{\partial H^{(r_2)}}{\partial q_k} \frac{\partial H^{(r_1)}}{\partial P_k} = \sum_{k=1}^{n} \frac{\partial H^{(r_1)}}{\partial q_k} \frac{\partial H^{(r_2)}}{\partial P_k} = G^1_{(r_2,r_1)}. \tag{7.2}$$

We assume that $G^1_\alpha = G^1_{\pi(\alpha)}$ for any multi-index α with $l(\alpha) < l$ and any permutation π on $\{1, \ldots, l(\alpha)\}$. Let consider any multi-index α with $l(\alpha) = l$. We suppose that the components of the multi-index α are distinct, otherwise we rename the repeating ones with distinct subscripts. To prove that $G^1_\alpha = G^1_{\pi(\alpha)}$ we analyse several cases, depending on the permutation π on $\{1, \ldots, l\}$

Case 1 Let first consider any permutation π such that $\pi(l) = l$. Then we can write $\alpha = (i_1, \ldots, i_{l-1}, r)$ and $\pi(\alpha) = (i_{\pi(1)}, \ldots, i_{\pi(l-1)}, r)$, with $r = i_l \in \{0, \ldots, m\}$. From (5.43) and $G^1_\beta = G^1_{\pi(\beta)}$ for any multi-index β with $l(\beta) < l$ we get

$$\begin{aligned} G^1_\alpha &= \sum_{i=1}^{l-1} \frac{1}{i!} \sum_{k_1,\ldots,k_i=1}^{n} \frac{\partial^i H^{(r)}}{\partial q_{k_1} \ldots \partial q_{k_i}} \sum_{\substack{l(\alpha_1)+\cdots+l(\alpha_i)=l-1 \\ \alpha - \in \Lambda_{\alpha_1,\ldots,\alpha_i}}} \frac{\partial G^1_{\alpha_1}}{\partial P_{k_1}} \cdots \frac{\partial G^1_{\alpha_i}}{\partial P_{k_i}} \\ &= \sum_{i=1}^{l-1} \frac{1}{i!} \sum_{k_1,\ldots,k_i=1}^{n} \frac{\partial^i H^{(r)}}{\partial q_{k_1} \ldots \partial q_{k_i}} \sum_{\substack{l(\alpha_1)+\cdots+l(\alpha_i)=l-1 \\ \pi(\alpha) - \in \Lambda_{\alpha_1,\ldots,\alpha_i}}} \frac{\partial G^1_{\alpha_1}}{\partial P_{k_1}} \cdots \frac{\partial G^1_{\alpha_i}}{\partial P_{k_i}} = G^1_{\pi(\alpha)}, \end{aligned}$$

Case 2: Let consider any permutation π such that $\pi(l) = l-1$, $\pi(l-1) = l$, $(\alpha-)- = (\pi(\alpha)-)-$ Then we can write $\alpha = (i_1, \dots, i_{l-2}, s, r)$ and $\pi(\alpha) = (i_1, \dots, i_{l-2}, r, s)$, with $r = i_l \in \{0, \dots, m\}$ and $s = i_{l-1} \in \{0, \dots, m\}$. Since $\Lambda_{\alpha_1,\alpha_2} = \Lambda_{\alpha_2,\alpha_1}$ and s is the "largest" number with respect to the partial order $\prec$ on $\alpha-$ we can write

$$
\begin{aligned}
G^1_\alpha &= \sum_{i=1}^{l-1} \frac{1}{i!} \sum_{k_1,\dots,k_i=1}^{n} \frac{\partial^i H^{(r)}}{\partial q_{k_1} \dots \partial q_{k_i}} \sum_{\substack{l(\alpha_1)+\dots+l(\alpha_i)=l-1 \\ \alpha-\in\Lambda_{\alpha_1,\dots,\alpha_i}}} \frac{\partial G^1_{\alpha_1}}{\partial P_{k_1}} \dots \frac{\partial G^1_{\alpha_i}}{\partial P_{k_i}} \\
&= \sum_{k_1=1}^{n} \frac{\partial H^{(r)}}{\partial q_{k_1}} \frac{\partial G^1_{((\alpha-)-)*(s)}}{\partial P_{k_1}} \\
&+ \sum_{i=2}^{l-1} \frac{1}{(i-1)!} \sum_{k_1,\dots,k_i=1}^{n} \frac{\partial^i H^{(r)}}{\partial q_{k_1} \dots \partial q_{k_i}} \frac{\partial H^{(s)}}{\partial P_{k_1}} \sum_{\substack{l(\alpha_2)+\dots+l(\alpha_i)=l-2 \\ (\alpha-)-\in\Lambda_{\alpha_2,\dots,\alpha_i}}} \frac{\partial G^1_{\alpha_2}}{\partial P_{k_2}} \dots \frac{\partial G^1_{\alpha_i}}{\partial P_{k_i}} \\
&+ \sum_{i=2}^{l-2} \frac{1}{i!} \sum_{j=1}^{l-i-1} \sum_{k_1,\dots,k_i=1}^{n} \frac{\partial^i H^{(r)}}{\partial q_{k_1} \dots \partial q_{k_i}} \sum_{\substack{l(\alpha_2)+\dots+l(\alpha_i)=l-2-j, \\ l(\alpha_1)=j, \quad (\alpha-)-\in\Lambda_{\alpha_1,\dots,\alpha_i}}} \frac{\partial G^1_{\alpha_1*(s)}}{\partial P_{k_1}} \dots \frac{\partial G^1_{\alpha_i}}{\partial P_{k_i}}.
\end{aligned}
$$

Using formula (5.43) for the first and the third terms, we get

$$
\begin{aligned}
G^1_\alpha = &\sum_{k_1=1}^{n} \frac{\partial H^{(r)}}{\partial q_{k_1}} \frac{\partial}{\partial P_{k_1}} \Bigg(\sum_{u=1}^{l-2} \frac{1}{u!} \sum_{c_1,\ldots,c_u=1}^{n} \frac{\partial^u H^{(s)}}{\partial q_{c_1} \ldots \partial q_{c_u}} \\
&\sum_{\substack{l(\beta_1)+\cdots+l(\beta_u)=l-2 \\ (\alpha-)-\in\Lambda_{\beta_1,\ldots,\beta_u}}} \frac{\partial G^1_{\beta_1}}{\partial P_{c_1}} \cdots \frac{\partial G^1_{\beta_u}}{\partial P_{c_u}} \Bigg) \\
&+ \sum_{i=2}^{l-1} \frac{1}{(i-1)!} \sum_{k_1,\ldots,k_i=1}^{n} \frac{\partial^i H^{(r)}}{\partial q_{k_1} \ldots \partial q_{k_i}} \frac{\partial H^{(s)}}{\partial P_{k_1}} \\
&\sum_{\substack{l(\alpha_2)+\cdots+l(\alpha_i)=l-2 \\ (\alpha-)-\in\Lambda_{\alpha_2,\ldots,\alpha_i}}} \frac{\partial G^1_{\alpha_2}}{\partial P_{k_2}} \cdots \frac{\partial G^1_{\alpha_i}}{\partial P_{k_i}} \\
&+ \sum_{i=2}^{l-2} \frac{1}{(i-1)!} \sum_{j=1}^{l-i-1} \sum_{k_1,\ldots,k_i=1}^{n} \frac{\partial^i H^{(r)}}{\partial q_{k_1} \ldots \partial q_{k_i}} \\
&\sum_{\substack{l(\alpha_2)+\cdots+l(\alpha_i)=l-2-j, \\ l(\alpha_1)=j, \quad (\alpha-)-\in\Lambda_{\alpha_1,\ldots,\alpha_i}}} \frac{\partial G^1_{\alpha_2}}{\partial P_{k_2}} \cdots \frac{\partial G^1_{\alpha_i}}{\partial P_{k_i}} \\
&\frac{\partial}{\partial P_{k_1}} \Bigg(\sum_{u=1}^{j} \frac{1}{u!} \sum_{c_1,\ldots,c_u=1}^{n} \frac{\partial^u H^{(s)}}{\partial q_{c_1} \ldots \partial q_{c_u}} \sum_{\substack{l(\beta_1)+\cdots+l(\beta_u)=j \\ \alpha_1\in\Lambda_{\beta_1,\ldots,\beta_u}}} \frac{\partial G^1_{\beta_1}}{\partial P_{c_1}} \cdots \frac{\partial G^1_{\beta_u}}{\partial P_{c_u}} \Bigg).
\end{aligned}
\tag{7.3}
$$

By the product rule, we separate G^1_α into two sums denoted by T_1 and T_2 such that T_1 is formed with all terms not including differentiation of the Hamiltonian $H^{(s)}$ with respect to P_i, for any $i = 1, \ldots, n$. Thus $G^1_\alpha = T_1 + T_2$, with

$$
\begin{aligned}
T_1 = &\sum_{u=1}^{l-2} \frac{1}{u!} \sum_{k_1,c_1,\ldots,c_u=1}^{n} \frac{\partial H^{(r)}}{\partial q_{k_1}} \frac{\partial^u H^{(s)}}{\partial q_{c_1} \ldots \partial q_{c_u}} \sum_{\substack{l(\beta_1)+\cdots+l(\beta_u)=l-2 \\ (\alpha-)-\in\Lambda_{\beta_1,\ldots,\beta_u}}} \frac{\partial}{\partial P_{k_1}} \left(\frac{\partial G^1_{\beta_1}}{\partial P_{c_1}} \cdots \frac{\partial G^1_{\beta_u}}{\partial P_{c_u}} \right) \\
&+ \sum_{i=2}^{l-2} \sum_{j=1}^{l-i-1} \sum_{u=1}^{j} \frac{1}{u!(i-1)!} \sum_{\substack{k_1,\ldots,k_i=1 \\ c_1,\ldots,c_u=1}}^{n} \frac{\partial^i H^{(r)}}{\partial q_{k_1} \ldots \partial q_{k_i}} \frac{\partial^u H^{(s)}}{\partial q_{c_1} \ldots \partial q_{c_u}} \\
&\sum_{\substack{l(\alpha_2)+\cdots+l(\alpha_i)=l-2-j, \\ l(\alpha_1)=j, \quad (\alpha-)-\in\Lambda_{\alpha_1,\ldots,\alpha_i}}} \frac{\partial G^1_{\alpha_2}}{\partial P_{k_2}} \cdots \frac{\partial G^1_{\alpha_i}}{\partial P_{k_i}} \sum_{\substack{l(\beta_1)+\cdots+l(\beta_u)=j \\ \alpha_1\in\Lambda_{\beta_1,\ldots,\beta_u}}} \frac{\partial}{\partial P_{k_1}} \left(\frac{\partial G^1_{\beta_1}}{\partial P_{c_1}} \cdots \frac{\partial G^1_{\beta_u}}{\partial P_{c_u}} \right)
\end{aligned}
$$

After some simple manipulations of the summation indexes and $\Lambda_{\alpha_1,\alpha_2} = \Lambda_{\alpha_2,\alpha_1}$, it give

us

$$
\begin{aligned}
T_1 &= \sum_{k_1,c_1=1}^{n} \frac{\partial H^{(r)}}{\partial q_{k_1}} \frac{\partial H^{(s)}}{\partial q_{c_1}} \frac{\partial^2 G^1_{(\alpha-)-}}{\partial P_{k_1} \partial P_{c_1}} \\
&+ \sum_{u=2}^{l-2} \frac{1}{u!} \sum_{k_1,c_1,\dots,c_u=1}^{n} \frac{\partial H^{(r)}}{\partial q_{k_1}} \frac{\partial^u H^{(s)}}{\partial q_{c_1} \dots \partial q_{c_u}} \sum_{\substack{l(\beta_1)+\dots+l(\beta_u)=l-2 \\ (\alpha-)-\in\Lambda_{\beta_1,\dots,\beta_u}}} \frac{\partial}{\partial P_{k_1}} \left(\frac{\partial G^1_{\beta_1}}{\partial P_{c_1}} \dots \frac{\partial G^1_{\beta_u}}{\partial P_{c_u}} \right) \\
&+ \sum_{i=2}^{l-2} \sum_{u=1}^{l-i-1} \frac{1}{(i-1)!u!} \sum_{\substack{k_1,\dots,k_i=1 \\ c_1,\dots,c_u=1}}^{n} \frac{\partial^i H^{(r)}}{\partial q_{k_1} \dots \partial q_{k_i}} \frac{\partial^u H^{(s)}}{\partial q_{c_1} \dots \partial q_{c_u}} \sum_{j=u}^{l-i-1} \sum_{\substack{l(\alpha_2)+\dots+l(\alpha_i)=l-2-j, \\ l(\alpha_1)=j, \quad (\alpha-)-\in\Lambda_{\alpha_1,\dots,\alpha_i}}} \\
&\frac{\partial G^1_{\alpha_2}}{\partial P_{k_2}} \dots \frac{\partial G^1_{\alpha_i}}{\partial P_{k_i}} \sum_{\substack{l(\beta_1)+\dots+l(\beta_u)=j \\ \alpha_1\in\Lambda_{\beta_1,\dots,\beta_u}}} \frac{\partial}{\partial P_{k_1}} \left(\frac{\partial G^1_{\beta_1}}{\partial P_{c_1}} \dots \frac{\partial G^1_{\beta_u}}{\partial P_{c_u}} \right) \\
&= \sum_{k_1,c_1=1}^{n} \frac{\partial H^{(r)}}{\partial q_{k_1}} \frac{\partial H^{(s)}}{\partial q_{c_1}} \frac{\partial^2 G^1_{(\alpha-)-}}{\partial P_{k_1} \partial P_{c_1}} \\
&+ \sum_{u=2}^{l-2} \frac{1}{u!} \sum_{k_1,c_1,\dots,c_u=1}^{n} \frac{\partial H^{(r)}}{\partial q_{k_1}} \frac{\partial^u H^{(s)}}{\partial q_{c_1} \dots \partial q_{c_u}} \sum_{\substack{l(\beta_1)+\dots+l(\beta_u)=l-2 \\ (\alpha-)-\in\Lambda_{\beta_1,\dots,\beta_u}}} \frac{\partial}{\partial P_{k_1}} \left(\frac{\partial G^1_{\beta_1}}{\partial P_{c_1}} \dots \frac{\partial G^1_{\beta_u}}{\partial P_{c_u}} \right) \\
&+ \sum_{i=2}^{l-2} \sum_{u=1}^{l-i-1} \frac{1}{u!(i-1)!} \sum_{\substack{k_1,\dots,k_i=1 \\ c_1,\dots,c_u=1}}^{n} \frac{\partial^i H^{(r)}}{\partial q_{k_1} \dots \partial q_{k_i}} \frac{\partial^u H^{(s)}}{\partial q_{c_1} \dots \partial q_{c_u}} \\
&\sum_{\substack{l(\alpha_2)+\dots+l(\beta_u)=l-2 \\ (\alpha-)-\in\Lambda_{\alpha_2,\dots,\alpha_i,\beta_1,\dots,\beta_u}}} \frac{\partial G^1_{\alpha_2}}{\partial P_{k_2}} \dots \frac{\partial G^1_{\alpha_i}}{\partial P_{k_i}} \frac{\partial}{\partial P_{k_1}} \left(\frac{\partial G^1_{\beta_1}}{\partial P_{c_1}} \dots \frac{\partial G^1_{\beta_u}}{\partial P_{c_u}} \right)
\end{aligned}
$$

Using again the product rule and $\Lambda_{\alpha_1,\alpha_2} = \Lambda_{\alpha_2,\alpha_1}$, we obtain

$$
\begin{aligned}
T_1 = & \sum_{k_1,c_1=1}^{n} \frac{\partial H^{(r)}}{\partial q_{k_1}} \frac{\partial H^{(s)}}{\partial q_{c_1}} \frac{\partial^2 G^1_{(\alpha-)-}}{\partial P_{k_1} \partial P_{c_1}} \\
& + \sum_{u=2}^{l-2} \frac{1}{(u-1)!} \sum_{k_1,c_1,\ldots,c_u=1}^{n} \frac{\partial H^{(r)}}{\partial q_{k_1}} \frac{\partial^u H^{(s)}}{\partial q_{c_1} \ldots \partial q_{c_u}} \sum_{\substack{1 \le l(\beta) \le l-1-u \\ R(\beta) \subseteq R((\alpha-)-)}} \frac{\partial^2 G^1_\beta}{\partial P_{k_1} \partial P_{c_1}} \\
& \sum_{\substack{l(\beta)+l(\gamma_1)\cdots+l(\gamma_{u-1})=l-2 \\ (\alpha-)-\in \Lambda_{\beta,\gamma_1\ldots,\gamma_{u-1}}}} \frac{\partial G^1_{\gamma_1}}{\partial P_{c_2}} \cdots \frac{\partial G^1_{\gamma_{u-1}}}{\partial P_{c_u}} \\
& + \sum_{i=2}^{l-2} \frac{1}{(i-1)!} \sum_{c_1,k_1,\ldots,k_i=1}^{n} \frac{\partial^i H^{(r)}}{\partial q_{k_1} \ldots \partial q_{k_i}} \frac{\partial H^{(s)}}{\partial q_{c_1}} \sum_{\substack{1 \le l(\beta) \le l-1-i \\ R(\beta) \subseteq R((\alpha-)-)}} \frac{\partial^2 G^1_\beta}{\partial P_{k_1} \partial P_{c_1}} \\
& \sum_{\substack{l(\beta)+l(\gamma_1)\cdots+l(\gamma_{i-1})=l-2 \\ (\alpha-)-\in \Lambda_{\beta,\gamma_1\ldots,\gamma_{i-1}}}} \frac{\partial G^1_{\gamma_1}}{\partial P_{k_2}} \cdots \frac{\partial G^1_{\gamma_{i-1}}}{\partial P_{k_i}} \\
& + \sum_{i=2}^{l-3} \sum_{u=2}^{l-i-1} \frac{1}{(i-1)!(u-1)!} \sum_{\substack{k_1,\ldots,k_i=1 \\ c_1,\ldots,c_u=1}}^{n} \frac{\partial^i H^{(r)}}{\partial q_{k_1} \ldots \partial q_{k_i}} \frac{\partial^u H^{(s)}}{\partial q_{c_1} \ldots \partial q_{c_u}} \\
& \sum_{\substack{1 \le l(\beta) \le l-i-u \\ R(\beta) \subseteq R((\alpha-)-)}} \frac{\partial^2 G^1_\beta}{\partial P_{k_1} \partial P_{c_1}} \\
& \sum_{\substack{l(\beta)+l(\gamma_1)+\cdots+l(\gamma_{i+u-2})=l-2 \\ (\alpha-)-\in \Lambda_{\beta,\gamma_1,\ldots,\gamma_{i+u-2}}}} \frac{\partial G^1_{\gamma_1}}{\partial P_{k_2}} \cdots \frac{\partial G^1_{\gamma_{i-1}}}{\partial P_{k_i}} \frac{\partial G^1_{\gamma_i}}{\partial P_{c_2}} \cdots \frac{\partial G^1_{\gamma_{i+u-2}}}{\partial P_{c_u}}
\end{aligned}
\tag{7.4}
$$

Notice that if we sum first with respect to u and next with respect to i, we can rewrite the last term as

$$
\begin{aligned}
& \sum_{u=2}^{l-3} \sum_{i=2}^{l-u-1} \frac{1}{(i-1)!(u-1)!} \sum_{\substack{k_1,\ldots,k_i=1 \\ c_1,\ldots,c_u=1}}^{n} \frac{\partial^i H^{(r)}}{\partial q_{k_1} \ldots \partial q_{k_i}} \frac{\partial^u H^{(s)}}{\partial q_{c_1} \ldots \partial q_{c_u}} \sum_{\substack{1 \le l(\beta) \le l-i-u \\ R(\beta) \subseteq R((\alpha-)-)}} \frac{\partial^2 G^1_\beta}{\partial P_{k_1} \partial P_{c_1}} \\
& \sum_{\substack{l(\beta)+l(\gamma_1)+\cdots+l(\gamma_{i+u-2})=l-2 \\ (\alpha-)-\in \Lambda_{\beta,\gamma_1,\ldots,\gamma_{i+u-2}}}} \frac{\partial G^1_{\gamma_1}}{\partial P_{k_2}} \cdots \frac{\partial G^1_{\gamma_{i-1}}}{\partial P_{k_i}} \frac{\partial G^1_{\gamma_i}}{\partial P_{c_2}} \cdots \frac{\partial G^1_{\gamma_{i+u-2}}}{\partial P_{c_u}}
\end{aligned}
$$

Thus by switching s and r, the formula (7.4) for T_1 does not change, so T_1 is symmetric in s and t.

From Eq. (7.3) and $G^1_\alpha = T_1 + T_2$, we have

$$T_2 = \sum_{i=2}^{l-1} \frac{1}{(i-1)!} \sum_{k_1,\ldots,k_i=1}^{n} \frac{\partial^i H^{(r)}}{\partial q_{k_1} \ldots \partial q_{k_i}} \frac{\partial H^{(s)}}{\partial P_{k_1}} \sum_{\substack{l(\alpha_2)+\cdots+l(\alpha_i)=l-2 \\ (\alpha-)-\in\Lambda_{\alpha_2,\ldots,\alpha_i}}} \frac{\partial G^1_{\alpha_2}}{\partial P_{k_2}} \cdots \frac{\partial G^1_{\alpha_i}}{\partial P_{k_i}}$$

$$+ \sum_{u=1}^{l-2} \frac{1}{u!} \sum_{k_1,c_1,\ldots,c_u=1}^{n} \frac{\partial H^{(r)}}{\partial q_{k_1}} \frac{\partial^{u+1} H^{(s)}}{\partial P_{k_1} \partial q_{c_1} \ldots \partial q_{c_u}} \sum_{\substack{l(\beta_1)+\cdots+l(\beta_u)=l-2 \\ (\alpha-)-\in\Lambda_{\beta_1,\ldots,\beta_u}}} \frac{\partial G^1_{\beta_1}}{\partial P_{c_1}} \cdots \frac{\partial G^1_{\beta_u}}{\partial P_{c_u}}$$

$$+ \sum_{i=2}^{l-2} \sum_{j=1}^{l-i-1} \sum_{u=1}^{j} \frac{1}{(i-1)!u!} \sum_{\substack{k_1,\ldots,k_i=1 \\ c_1,\ldots,c_u=1}}^{n} \frac{\partial^i H^{(r)}}{\partial q_{k_1} \ldots \partial q_{k_i}} \frac{\partial^{u+1} H^{(s)}}{\partial P_{k_1} \partial q_{c_1} \ldots \partial q_{c_u}}$$

$$\sum_{\substack{l(\alpha_2)+\cdots+l(\alpha_i)=l-2-j, \\ l(\alpha_1)=j, \quad (\alpha-)-\in\Lambda_{\alpha_1,\ldots,\alpha_i}}} \frac{\partial G^1_{\alpha_2}}{\partial P_{k_2}} \cdots \frac{\partial G^1_{\alpha_i}}{\partial P_{k_i}} \sum_{\substack{l(\beta_1)+\cdots+l(\beta_u)=j \\ \alpha_1\in\Lambda_{\beta_1,\ldots,\beta_u}}} \frac{\partial G^1_{\beta_1}}{\partial P_{c_1}} \cdots \frac{\partial G^1_{\beta_u}}{\partial P_{c_u}}.$$

Similarly as for T_1, using $\Lambda_{\alpha_1,\alpha_2} = \Lambda_{\alpha_2,\alpha_1}$, we obtain

$$T_2 = \sum_{i=1}^{l-2} \frac{1}{i!} \sum_{k_1,j_1\ldots,j_i=1}^{n} \frac{\partial^{i+1} H^{(r)}}{\partial q_{k_1} q_{j_1} \ldots \partial q_{j_i}} \frac{\partial H^{(s)}}{\partial P_{k_1}} \sum_{\substack{l(\alpha_1)+\cdots+l(\alpha_i)=l-2 \\ (\alpha-)-\in\Lambda_{\alpha_1,\ldots,\alpha_i}}} \frac{\partial G^1_{\alpha_1}}{\partial P_{j_1}} \cdots \frac{\partial G^1_{\alpha_i}}{\partial P_{j_i}}$$

$$+ \sum_{i=1}^{l-2} \frac{1}{i!} \sum_{k_1,j_1\ldots,j_i=1}^{n} \frac{\partial H^{(r)}}{\partial q_{k_1}} \frac{\partial^{i+1} H^{(s)}}{\partial P_{k_1} \partial q_{j_1} \ldots \partial q_{j_i}} \sum_{\substack{l(\beta_1)+\cdots+l(\beta_i)=l-2 \\ (\alpha-)-\in\Lambda_{\beta_1,\ldots,\beta_i}}} \frac{\partial G^1_{\beta_1}}{\partial P_{j_1}} \cdots \frac{\partial G^1_{\beta_i}}{\partial P_{j_i}}$$

$$+ \sum_{i=2}^{l-2} \sum_{u=1}^{l-i-1} \frac{1}{(i-1)!u!} \sum_{\substack{k_1,\ldots,k_i=1 \\ c_1,\ldots,c_u=1}}^{n} \frac{\partial^i H^{(r)}}{\partial q_{k_1} \ldots \partial q_{k_i}} \frac{\partial^{u+1} H^{(s)}}{\partial P_{k_1} \partial q_{c_1} \ldots \partial q_{c_u}}$$

$$\sum_{\substack{l(\alpha_2)+\cdots+l(\beta_u)=l-2 \\ (\alpha-)-\in\Lambda_{\alpha_2,\ldots,\alpha_i,\beta_1,\ldots,\beta_u}}} \frac{\partial G^1_{\alpha_2}}{\partial P_{k_2}} \cdots \frac{\partial G^1_{\alpha_i}}{\partial P_{k_i}} \frac{\partial G^1_{\beta_1}}{\partial P_{c_1}} \cdots \frac{\partial G^1_{\beta_u}}{\partial P_{c_u}}$$

Introducing a new summation index $v = i + u - 1$ for the last term, it gives

$$T_2 = \sum_{i=1}^{l-2} \frac{1}{i!} \sum_{k_1, j_1 \ldots, j_i = 1}^{n} \frac{\partial^{i+1} H^{(r)}}{\partial q_{k_1} q_{j_1} \ldots \partial q_{j_i}} \frac{\partial H^{(s)}}{\partial P_{k_1}} \sum_{\substack{l(\alpha_1)+\cdots+l(\alpha_i)=l-2 \\ (\alpha-)-\in \Lambda_{\alpha_1,\ldots,\alpha_i}}} \frac{\partial G^1_{\alpha_1}}{\partial P_{j_1}} \cdots \frac{\partial G^1_{\alpha_i}}{\partial P_{j_i}}$$

$$+ \sum_{i=1}^{l-2} \frac{1}{i!} \sum_{k_1, j_1 \ldots, j_i = 1}^{n} \frac{\partial H^{(r)}}{\partial q_{k_1}} \frac{\partial^{i+1} H^{(s)}}{\partial P_{k_1} \partial q_{j_1} \ldots \partial q_{j_i}} \sum_{\substack{l(\beta_1)+\cdots+l(\beta_i)=l-2 \\ (\alpha-)-\in \Lambda_{\beta_1,\ldots,\beta_i}}} \frac{\partial G^1_{\beta_1}}{\partial P_{j_1}} \cdots \frac{\partial G^1_{\beta_i}}{\partial P_{j_i}}$$

$$+ \sum_{v=2}^{l-2} \sum_{i=2}^{v} \frac{1}{(i-1)!(v-i+1)!} \sum_{k_1, j_1, \ldots, j_v = 1}^{n} \frac{\partial^{i} H^{(r)}}{\partial q_{k_1} \partial q_{j_1} \ldots \partial q_{j_{i-1}}} \frac{\partial^{v+2-i} H^{(s)}}{\partial P_{k_1} \partial q_{j_i} \ldots \partial q_{j_v}}$$

$$\sum_{\substack{l(\gamma_1)+\cdots+l(\gamma_v)=l-2 \\ (\alpha-)-\in \Lambda_{\gamma_1,\ldots,\gamma_v}}} \frac{\partial G^1_{\gamma_1}}{\partial P_{j_1}} \cdots \frac{\partial G^1_{\gamma_v}}{\partial P_{j_v}}$$

Notice that T_2 can be expressed as follows

$$T_2 = \sum_{v=1}^{l-2} \frac{1}{v!} \sum_{k_1, j_1, \ldots, j_v = 1}^{n} \frac{\partial^{v}}{\partial q_{j_1} \cdots \partial q_{j_v}} \left(\frac{\partial H^{(r)}}{\partial q_{k_1}} \frac{\partial H^{(s)}}{\partial P_{k_1}} \right) \sum_{\substack{l(\gamma_1)+\cdots+l(\gamma_v)=l-2 \\ (\alpha-)-\in \Lambda_{\gamma_1,\ldots,\gamma_v}}} \frac{\partial G^1_{\gamma_1}}{\partial P_{j_1}} \cdots \frac{\partial G^1_{\gamma_v}}{\partial P_{j_v}}. \tag{7.5}$$

Hence T_2 is symmetric with respect to s and r because $\frac{\partial H^{(r)}}{\partial q_{k_1}} \frac{\partial H^{(s)}}{\partial P_{k_1}} = \frac{\partial H^{(r)}}{\partial P_{k_1}} \frac{\partial H^{(s)}}{\partial q_{k_1}}$ for any $k_1 = 1, \ldots, n$.

Thus G^1_α is symmetric with respect to r and s, so we have $G^1_\alpha = G^1_{\pi(\alpha)}$.

Case3: For any arbitrary permutation π on $\{1, \ldots, l\}$ not in any of the previous two cases (i.e. $\pi(l) \neq l$ and either $\pi(l) \neq l-1$ or $\pi(l-1) \neq l$), let consider any multi-index $\alpha = (i_1, \ldots, i_{l-1}, i_l)$, $\pi(\alpha) = (i_{\pi(1)}, \ldots, i_{\pi(l-1)}, i_{\pi(l)})$ and denote $r = i_l$, $s = i_{\pi(l)}$. Since $\pi(l) \neq l$, we have $r \neq s$, and there exists $k \in \{1, \ldots, l-1\}$ such that $i_k = s$. We consider a permutation π_1 on $\{1, \ldots, l\}$ defined by $\pi_1(k) = l-1$, $\pi_1(l-1) = k$, $\pi_1(u) = u$, for $u = 1, \ldots, l$, $u \neq k$, $u \neq l-1$. Thus $\pi_1(\alpha) = (i_{\pi_1(1)}, \ldots, s, r)$, and from cases 1 and 2 we know that $G^1_\alpha = G^1_{\pi_1(\alpha)} = G^1_{\alpha_1}$, where $\alpha_1 = (i_{\pi_1(1)}, \ldots, r, s)$. Notice that $\alpha_1 = (i_1, \ldots, i_{l-1}, \ldots, i_l, s)$, so we can obtain $\pi(\alpha)$ from α_1 applying a permutation π_2 with $\pi_2(l) = l$, and from case 1 we have $G^1_{\alpha_1} = G^1_{\pi_2(\alpha_1)} = G^1_{\pi(\alpha)}$. Thus we get $G^1_\alpha = G^1_{\pi(\alpha)}$.

Putting together the previous three cases, we conclude $G^1_\alpha = G^1_{\pi(\alpha)}$ for any permutation π and any multi-index α with $l(\alpha) = l$ □

Given that the coefficients of the generating function S^2_ω are obtained replacing in the recurrence (5.43) q by p and P by Q, we can easily adapt the previous proof to show that the coefficients of S^2_ω are also invariant under permutations .

A similar result hold also for the coefficients of the generating function S^3_ω and it is based on formula (5.45).

Theorem 7.2 *For SHS preserving the Hamiltonian functions, the coefficients G^3_α of the generating function S^3_ω are invariants to permutations.*

Proof: By induction on the length of the multi-index α, the coefficients G^3_α of S^3_ω are invariant under the permutations on α for systems preserving the Hamiltonian functions, when $l(\alpha) = 2$ because for any $r_1, r_2 = 0, \ldots, m$ we have

$$G^3_{(r_1,r_2)} = \frac{1}{2}\sum_{k=1}^{n}\left(-\frac{\partial H^{(r_2)}}{\partial y_k}\frac{\partial H^{(r_1)}}{\partial y_{k+n}} - \frac{\partial H^{(r_2)}}{\partial y_{k+n}}\frac{\partial H^{(r_1)}}{\partial y_k}\right) = 0 = G^3_{(r_2,r_1)}. \tag{7.6}$$

We assume that $G^3_\alpha = G^3_{\pi(\alpha)}$ for any multi-index α with $l(\alpha) < l$ and any permutation π on $\{1, \ldots, l(\alpha)\}$. Let consider any multi-index α with $l(\alpha) = l$. We suppose that the components of the multi-index α are distinct, otherwise we rename the repeating ones with distinct subscripts. To prove that $G^3_\alpha = G^3_{\pi(\alpha)}$ we analyse the same three cases as in the proof of theorem 7.1. The arguments for Cases 1 and 3 are similar, so we will present the details only for Case 2.

Let consider any permutation π such that $\pi(l) = l-1$, $\pi(l-1) = l$, $(\alpha-)- = (\pi(\alpha)-)-$, and denote $\alpha = (i_1, \ldots, i_{l-2}, s, r)$ and $\pi(\alpha) = (i_1, \ldots, i_{l-2}, r, s)$, with $r, s \in \{0, \ldots, m\}$. Notice that for any $2n$- dimensional vector $v = (v_1, \ldots, v_{2n})^T$ we have $J^{-1}v = (-v_{n+1}, \ldots, v_{2n}, v_1, \ldots, v_n)$.

Since $\Lambda_{\alpha_1,\alpha_2} = \Lambda_{\alpha_2,\alpha_1}$ and s is the "largest" number with respect to the partial order

$\prec$ on $\alpha-$, from formula (5.45) we get

$$G^3_\alpha = \sum_{i=1}^{l-1} \frac{1}{2^i i!} \sum_{k_1,\dots,k_i=1}^{2n} \frac{\partial^i H^{(r)}}{\partial y_{k_1} \dots \partial y_{k_i}} \sum_{\substack{l(\alpha_1)+\dots+l(\alpha_i)=l-1 \\ \alpha-\in\Lambda_{\alpha_1,\dots,\alpha_i}}} (J^{-1}\nabla G^3_{\alpha_1})_{k_1} \dots (J^{-1}\nabla G^3_{\alpha_i})_{k_i}$$

$$= \frac{1}{2} \sum_{k_1=1}^{n} \left(-\frac{\partial H^{(r)}}{\partial y_{k_1}} \frac{\partial G^3_{((\alpha-)-)*(s)}}{\partial y_{k_1+n}} + \frac{\partial H^{(r)}}{\partial y_{k_1+n}} \frac{\partial G^3_{((\alpha-)-)*(s)}}{\partial y_{k_1}} \right)$$

$$+ \sum_{i=2}^{l-1} \frac{1}{2^i (i-1)!} \sum_{k1=1}^{n} \sum_{k_2,\dots,k_i=1}^{2n} \left(-\frac{\partial^i H^{(r)}}{\partial y_{k_1} \dots \partial y_{k_i}} \frac{\partial H^{(s)}}{\partial y_{k_1+n}} + \frac{\partial^i H^{(r)}}{\partial y_{k_1+n} \dots \partial y_{k_i}} \frac{\partial H^{(s)}}{\partial y_{k_1}} \right)$$

$$\sum_{\substack{l(\alpha_2)+\dots+l(\alpha_i)=l-2 \\ (\alpha-)-\in\Lambda_{\alpha_2,\dots,\alpha_i}}} (J^{-1}\nabla G^3_{\alpha_2})_{k_2} \dots (J^{-1}\nabla G^3_{\alpha_i})_{k_i}$$

$$+ \sum_{i=2}^{l-2} \frac{1}{2^i i!} \sum_{j=1}^{l-i-1} \sum_{k_1=1}^{n} \sum_{k_2,\dots,k_i=1}^{2n} \sum_{\substack{l(\alpha_2)+\dots+l(\alpha_i)=l-2-j, \\ l(\alpha_1)=j, \quad (\alpha-)-\in\Lambda_{\alpha_1,\dots,\alpha_i}}} (J^{-1}\nabla G^3_{\alpha_2})_{k_2} \dots (J^{-1}\nabla G^3_{\alpha_i})_{k_i}$$

$$\left(-\frac{\partial^i H^{(r)}}{\partial y_{k_1} \dots \partial q_{k_i}} \frac{\partial G^3_{\alpha_1*(s)}}{\partial y_{k_1+n}} + \frac{\partial^i H^{(r)}}{\partial y_{k_1+n} \dots \partial q_{k_i}} \frac{\partial G^3_{\alpha_1*(s)}}{\partial y_{k_1}} \right)$$

Using formula (5.45) for the first and the third terms, we obtain

$$G^3_\alpha = \frac{1}{2}\sum_{k_1=1}^{n}\sum_{u=1}^{l-2}\frac{1}{2^u u!}\Bigg(-\frac{\partial H^{(r)}}{\partial y_{k_1}}\frac{\partial}{\partial y_{k_1+n}}\Bigg(\sum_{c_1,\dots,c_u=1}^{2n}\frac{\partial^u H^{(s)}}{\partial y_{c_1}\dots\partial y_{c_u}}$$

$$\sum_{\substack{l(\beta_1)+\dots+l(\beta_u)=l-2\\(\alpha-)-\in\Lambda_{\beta_1,\dots,\beta_u}}}(J^{-1}\nabla G^3_{\beta_1})_{c_1}\dots(J^{-1}\nabla G^3_{\beta_i})_{c_i}\Bigg)+\frac{\partial H^{(r)}}{\partial y_{k_1+n}}$$

$$\frac{\partial}{\partial y_{k_1}}\Bigg(\sum_{c_1,\dots,c_u=1}^{2n}\frac{\partial^u H^{(s)}}{\partial y_{c_1}\dots\partial y_{c_u}}\sum_{\substack{l(\beta_1)+\dots+l(\beta_u)=l-2\\(\alpha-)-\in\Lambda_{\beta_1,\dots,\beta_u}}}(J^{-1}\nabla G^3_{\beta_1})_{c_1}\dots(J^{-1}\nabla G^3_{\beta_i})_{c_i}\Bigg)\Bigg)$$

$$+\sum_{i=2}^{l-1}\frac{1}{2^i(i-1)!}\sum_{k1=1}^{n}\sum_{k_2,\dots,k_i=1}^{2n}\Bigg(-\frac{\partial^i H^{(r)}}{\partial y_{k_1}\dots\partial y_{k_i}}\frac{\partial H^{(s)}}{\partial y_{k_1+n}}+\frac{\partial^i H^{(r)}}{\partial y_{k_1+n}\dots\partial y_{k_i}}\frac{\partial H^{(s)}}{\partial y_{k_1}}\Bigg)$$

$$\sum_{\substack{l(\alpha_2)+\dots+l(\alpha_i)=l-2\\(\alpha-)-\in\Lambda_{\alpha_2,\dots,\alpha_i}}}(J^{-1}\nabla G^3_{\alpha_2})_{k_2}\dots(J^{-1}\nabla G^3_{\alpha_i})_{k_i}$$

$$+\sum_{i=2}^{l-2}\frac{1}{2^i(i-1)!}\sum_{j=1}^{l-i-1}\sum_{u=1}^{j}\frac{1}{2^u u!}\sum_{k_1=1}^{n}\sum_{k_2,\dots,k_i=1}^{2n}\sum_{\substack{l(\alpha_2)+\dots+l(\alpha_i)=l-2-j,\\ l(\alpha_1)=j,\quad(\alpha-)-\in\Lambda_{\alpha_1,\dots,\alpha_i}}}(J^{-1}\nabla G^3_{\alpha_2})_{k_2}\dots$$

$$(J^{-1}\nabla G^3_{\alpha_i})_{k_i}\Bigg(-\frac{\partial^i H^{(r)}}{\partial y_{k_1}\dots\partial q_{k_i}}\frac{\partial}{\partial y_{k_1+n}}\Bigg(\sum_{c_1,\dots,c_u=1}^{2n}\frac{\partial^u H^{(s)}}{\partial y_{c_1}\dots\partial y_{c_u}}$$

$$\sum_{\substack{l(\beta_1)+\dots+l(\beta_u)=j\\ \alpha_1\in\Lambda_{\beta_1,\dots,\beta_u}}}(J^{-1}\nabla G^3_{\beta_1})_{c_1}\dots(J^{-1}\nabla G^3_{\beta_u})_{c_u}\Bigg)+\frac{\partial^i H^{(r)}}{\partial y_{k_1+n}\dots\partial q_{k_i}}\frac{\partial}{\partial y_{k_1}}\Bigg(\sum_{c_1,\dots,c_u=1}^{2n}\frac{\partial^u H^{(s)}}{\partial y_{c_1}\dots\partial y_{c_u}}$$

$$\sum_{\substack{l(\beta_1)+\dots+l(\beta_u)=j\\ \alpha_1\in\Lambda_{\beta_1,\dots,\beta_u}}}(J^{-1}\nabla G^3_{\beta_1})_{c_1}\dots(J^{-1}\nabla G^3_{\beta_u})_{c_u}\Bigg)\Bigg)$$

As in the proof of theorem 7.1 we separate into $G^3_\alpha = T_1 + T_2$ with

$$
\begin{aligned}
T_1 = &\sum_{u=1}^{l-2} \frac{1}{2^{u+1}u!} \sum_{k_1=1}^{n} \sum_{c_1,\dots,c_u=1}^{2n} \frac{\partial^u H^{(s)}}{\partial y_{c_1} \dots \partial y_{c_u}} \\
&\sum_{\substack{l(\beta_1)+\dots+l(\beta_u)=l-2 \\ (\alpha-)-\in\Lambda_{\beta_1,\dots,\beta_u}}} \Bigg(-\frac{\partial H^{(r)}}{\partial y_{k_1}} \frac{\partial}{\partial y_{k_1+n}} \left((J^{-1}\nabla G^3_{\beta_1})_{c_1} \dots (J^{-1}\nabla G^3_{\beta_u})_{c_u} \right) \\
&+ \frac{\partial H^{(r)}}{\partial y_{k_1+n}} \frac{\partial}{\partial y_{k_1}} \left((J^{-1}\nabla G^3_{\beta_1})_{c_1} \dots (J^{-1}\nabla G^3_{\beta_u})_{c_u} \right) \Bigg) \\
&+ \sum_{i=2}^{l-2} \sum_{j=1}^{l-i-1} \sum_{u=1}^{j} \frac{1}{2^{u+i}u!(i-1)!} \sum_{k_1=1}^{n} \sum_{\substack{k_2,\dots,k_i=1 \\ c_1,\dots,c_u=1}}^{2n} \frac{\partial^u H^{(s)}}{\partial y_{c_1} \dots \partial y_{c_u}} \\
&\sum_{\substack{l(\alpha_2)+\dots+l(\alpha_i)=l-2-j, \\ l(\alpha_1)=j, \quad (\alpha-)-\in\Lambda_{\alpha_1,\dots,\alpha_i}}} (J^{-1}\nabla G^3_{\alpha_2})_{k_2} \dots (J^{-1}\nabla G^3_{\alpha_i})_{k_i} \\
&\sum_{\substack{l(\beta_1)+\dots+l(\beta_u)=j \\ \alpha_1\in\Lambda_{\beta_1,\dots,\beta_u}}} \Bigg(-\frac{\partial^i H^{(r)}}{\partial y_{k_1} \dots \partial y_{k_i}} \frac{\partial}{\partial y_{k_1+n}} \Bigg((J^{-1}\nabla G^3_{\beta_1})_{c_1} \dots (J^{-1}\nabla G^3_{\beta_u})_{c_u} \Bigg) \\
&+ \frac{\partial^i H^{(r)}}{\partial y_{k_1+n} \dots \partial y_{k_i}} \frac{\partial}{\partial y_{k_1}} \Bigg((J^{-1}\nabla G^3_{\beta_1})_{c_1} \dots (J^{-1}\nabla G^3_{\beta_u})_{c_u} \Bigg) \Bigg)
\end{aligned}
$$

After simple manipulations of the summation indexes and $\Lambda_{\alpha_1,\alpha_2} = \Lambda_{\alpha_2,\alpha_1}$, it gives

$$
\begin{aligned}
T_1 = {} & \frac{1}{2^2} \sum_{k_1=1}^{n} \sum_{c_1=1}^{2n} \frac{\partial H^{(s)}}{\partial y_{c_1}} \left(-\frac{\partial H^{(r)}}{\partial y_{k_1}} \frac{\partial (J^{-1} \nabla G^3_{(\alpha-)_-})_{c_1}}{\partial y_{k_1+n}} + \frac{\partial H^{(r)}}{\partial y_{k_1+n}} \frac{\partial (J^{-1} \nabla G^3_{(\alpha-)_-})_{c_1}}{\partial y_{k_1}} \right) \\
& + \sum_{u=2}^{l-2} \frac{1}{2^{u+1} u!} \sum_{k_1=1}^{n} \sum_{c_1,\ldots,c_u=1}^{2n} \frac{\partial^u H^{(s)}}{\partial y_{c_1} \ldots \partial y_{c_u}} \\
& \sum_{\substack{l(\beta_1)+\cdots+l(\beta_u)=l-2 \\ (\alpha-)-\in \Lambda_{\beta_1,\ldots,\beta_u}}} \left(-\frac{\partial H^{(r)}}{\partial y_{k_1}} \frac{\partial}{\partial y_{k_1+n}} \left((J^{-1} \nabla G^3_{\beta_1})_{c_1} \ldots (J^{-1} \nabla G^3_{\beta_u})_{c_u} \right) \right. \\
& \left. + \frac{\partial H^{(r)}}{\partial y_{k_1+n}} \frac{\partial}{\partial y_{k_1}} \left((J^{-1} \nabla G^3_{\beta_1})_{c_1} \ldots (J^{-1} \nabla G^3_{\beta_u})_{c_u} \right) \right) \\
& + \sum_{i=2}^{l-2} \sum_{u=1}^{l-i-1} \frac{1}{2^{u+i} u! (i-1)!} \sum_{k_1=1}^{n} \sum_{\substack{k_2,\ldots,k_i=1 \\ c_1,\ldots,c_u=1}}^{2n} \frac{\partial^u H^{(s)}}{\partial y_{c_1} \ldots \partial y_{c_u}} \\
& \sum_{\substack{l(\alpha_2)+\cdots+l(\beta_u)=l-2 \\ (\alpha-)-\in \Lambda_{\alpha_2,\ldots,\alpha_i,\beta_1,\ldots,\beta_u}}} (J^{-1} \nabla G^3_{\alpha_2})_{k_2} \ldots (J^{-1} \nabla G^3_{\alpha_i})_{k_i} \\
& \left(-\frac{\partial^i H^{(r)}}{\partial y_{k_1} \ldots \partial y_{k_i}} \frac{\partial}{\partial y_{k_1+n}} \left((J^{-1} \nabla G^3_{\beta_1})_{c_1} \ldots (J^{-1} \nabla G^3_{\beta_u})_{c_u} \right) \right. \\
& \left. + \frac{\partial^i H^{(r)}}{\partial y_{k_1+n} \ldots \partial y_{k_i}} \frac{\partial}{\partial y_{k_1}} \left((J^{-1} \nabla G^3_{\beta_1})_{c_1} \ldots (J^{-1} \nabla G^3_{\beta_u})_{c_u} \right) \right)
\end{aligned}
$$

Using again $\Lambda_{\alpha_1,\alpha_2} = \Lambda_{\alpha_2,\alpha_1}$ and the product rule, we obtain

$$
\begin{aligned}
T_1 = \frac{1}{2^2} \sum_{k_1,c_1=1}^{n} \Bigg(& \frac{\partial H^{(r)}}{\partial y_{k_1}} \frac{\partial H^{(s)}}{\partial y_{c_1}} \frac{\partial^2 G^3_{(\alpha-)-}}{\partial y_{k_1+n} \partial y_{c_1+n}} + \frac{\partial H^{(r)}}{\partial y_{k_1+n}} \frac{\partial H^{(s)}}{\partial y_{c_1+n}} \frac{\partial^2 G^3_{(\alpha-)-}}{\partial y_{k_1} \partial y_{c_1}} \\
& - \frac{\partial H^{(r)}}{\partial y_{k_1}} \frac{\partial H^{(s)}}{\partial y_{c_1+n}} \frac{\partial^2 G^3_{(\alpha-)-}}{\partial y_{k_1+n} \partial y_{c_1}} - \frac{\partial H^{(r)}}{\partial y_{k_1+n}} \frac{\partial H^{(s)}}{\partial y_{c_1}} \frac{\partial^2 G^3_{(\alpha-)-}}{\partial y_{k_1} \partial y_{c_1+n}} \Bigg) \\
& + \sum_{u=2}^{l-2} \frac{1}{2^{u+1}(u-1)!} \sum_{k_1,c_1=1}^{n} \sum_{c_2,\ldots,c_u=1}^{2n} \sum_{\substack{1 \le l(\beta) \le l-1-u \\ R(\beta) \subseteq R((\alpha-)-)}} \Bigg(\frac{\partial H^{(r)}}{\partial y_{k_1}} \frac{\partial^u H^{(s)}}{\partial y_{c_1} \ldots \partial y_{c_u}} \frac{\partial^2 G^3_\beta}{\partial y_{k_1+n} \partial y_{c_1+n}} \\
& + \frac{\partial H^{(r)}}{\partial y_{k_1+n}} \frac{\partial^u H^{(s)}}{\partial y_{c_1+n} \ldots \partial y_{c_u}} \frac{\partial^2 G^3_\beta}{\partial y_{k_1} \partial y_{c_1}} - \frac{\partial H^{(r)}}{\partial y_{k_1+n}} \frac{\partial^u H^{(s)}}{\partial y_{c_1} \ldots \partial y_{c_u}} \frac{\partial^2 G^3_\beta}{\partial y_{k_1} \partial y_{c_1+n}} \\
& - \frac{\partial H^{(r)}}{\partial y_{k_1}} \frac{\partial^u H^{(s)}}{\partial y_{c_1+n} \ldots \partial y_{c_u}} \frac{\partial^2 G^3_\beta}{\partial y_{k_1+n} \partial y_{c_1}} \Bigg) \sum_{\substack{l(\beta)+l(\gamma_1)\cdots+l(\gamma_{u-1})=l-2 \\ (\alpha-)-\in \Lambda_{\beta,\gamma_1\ldots,\gamma_{u-1}}}} (J^{-1}\nabla G^3_{\gamma_1})_{c_2} \ldots (J^{-1}\nabla G^3_{\gamma_{u-1}})_{c_u} \\
& + \sum_{i=2}^{l-2} \frac{1}{2^{i+1}(i-1)!} \sum_{k_1,c_1=1}^{n} \sum_{k_2,\ldots,k_i=1}^{2n} \sum_{\substack{1 \le l(\beta) \le l-1-i \\ R(\beta) \subseteq R((\alpha-)-)}} \Bigg(\frac{\partial^i H^{(r)}}{\partial y_{k_1} \ldots \partial y_{k_i}} \frac{\partial H^{(s)}}{\partial y_{c_1}} \frac{\partial^2 G^3_\beta}{\partial y_{k_1+n} \partial y_{c_1+n}} \\
& + \frac{\partial^i H^{(r)}}{\partial y_{k_1+n} \ldots \partial y_{k_i}} \frac{\partial H^{(s)}}{\partial y_{c_1+n}} \frac{\partial^2 G^3_\beta}{\partial y_{k_1} \partial y_{c_1}} - \frac{\partial^i H^{(r)}}{\partial y_{k_1+n} \ldots \partial y_{k_i}} \frac{\partial H^{(s)}}{\partial y_{c_1}} \frac{\partial^2 G^3_\beta}{\partial y_{k_1} \partial y_{c_1+n}} \\
& - \frac{\partial^i H^{(r)}}{\partial y_{k_1} \ldots \partial y_{k_i}} \frac{\partial H^{(s)}}{\partial y_{c_1+n}} \frac{\partial^2 G^3_\beta}{\partial y_{k_1+n} \partial y_{c_1}} \Bigg) \sum_{\substack{l(\beta)+l(\gamma_1)\cdots+l(\gamma_{i-1})=l-2 \\ (\alpha-)-\in \Lambda_{\beta,\gamma_1\ldots,\gamma_{i-1}}}} (J^{-1}\nabla G^3_{\gamma_1})_{k_2} \ldots (J^{-1}\nabla G^3_{\gamma_{i-1}})_{k_i} \\
& + \sum_{i=2}^{l-3} \sum_{u=2}^{l-i-1} \frac{1}{2^{u+i}(i-1)!(u-1)!} \sum_{k_1,c_1=1}^{n} \sum_{\substack{k_2,\ldots,k_i=1 \\ c_2,\ldots,c_u=1}}^{2n} \sum_{\substack{1 \le l(\beta) \le l-i-u \\ R(\beta) \subseteq R((\alpha-)-)}} \Bigg(\frac{\partial^i H^{(r)}}{\partial y_{k_1} \ldots \partial y_{k_i}} \frac{\partial^u H^{(s)}}{\partial y_{c_1} \ldots \partial q_{c_u}} \\
& \frac{\partial^2 G^3_\beta}{\partial y_{k_1+n} \partial y_{c_1+n}} + \frac{\partial^i H^{(r)}}{\partial y_{k_1+n} \ldots \partial y_{k_i}} \frac{\partial^u H^{(s)}}{\partial y_{c_1+n} \ldots \partial y_{c_u}} \frac{\partial^2 G^3_\beta}{\partial y_{k_1} \partial y_{c_1}} \\
& - \frac{\partial^i H^{(r)}}{\partial y_{k_1} \ldots \partial y_{k_i}} \frac{\partial^u H^{(s)}}{\partial y_{c_1+n} \ldots \partial y_{c_u}} \frac{\partial^2 G^3_\beta}{\partial y_{k_1+n} \partial y_{c_1}} - \frac{\partial^i H^{(r)}}{\partial y_{k_1+n} \ldots \partial y_{k_i}} \frac{\partial^u H^{(s)}}{\partial y_{c_1} \ldots \partial y_{c_u}} \frac{\partial^2 G^3_\beta}{\partial y_{k_1} \partial y_{c_1+n}} \Bigg) \\
& \sum_{\substack{l(\beta)+l(\gamma_1)+\cdots+l(\gamma_{i+u-2})=l-2 \\ (\alpha-)-\in \Lambda_{\beta,\gamma_1,\ldots,\gamma_{i+u-2}}}} (J^{-1}\nabla G^3_{\gamma_1})_{k_2} \cdots (J^{-1}\nabla G^3_{\gamma_{i-1}})_{k_i} (J^{-1}\nabla G^3_{\gamma_i})_{c_2} \cdots (J^{-1}\nabla G^3_{\gamma_{i+u-2}})_{c_u}
\end{aligned}
$$

Notice that the previous formula does not change by switching r and s, so T_1 is symmetric in r and s.

The difference $T_2 = G^3_\alpha - T_1$ is given by

$$T_2 = \sum_{i=2}^{l-1} \frac{1}{2^i (i-1)!} \sum_{k1=1}^{n} \sum_{k_2,\ldots,k_i=1}^{2n} \left(-\frac{\partial^i H^{(r)}}{\partial y_{k_1} \ldots \partial y_{k_i}} \frac{\partial H^{(s)}}{\partial y_{k_1+n}} + \frac{\partial^i H^{(r)}}{\partial y_{k_1+n} \ldots \partial y_{k_i}} \frac{\partial H^{(s)}}{\partial y_{k_1}} \right)$$

$$\sum_{\substack{l(\alpha_2)+\cdots+l(\alpha_i)=l-2 \\ (\alpha-)-\in\Lambda_{\alpha_2,\ldots,\alpha_i}}} (J^{-1}\nabla G^3_{\alpha_2})_{k_2} \ldots (J^{-1}\nabla G^3_{\alpha_i})_{k_i}$$

$$+ \sum_{u=1}^{l-2} \frac{1}{2^{u+1} u!} \sum_{k_1=1}^{n} \sum_{c_1,\ldots,c_u=1}^{n} \left(-\frac{\partial H^{(r)}}{\partial y_{k_1}} \frac{\partial^{u+1} H^{(s)}}{\partial y_{k_1+n} \partial y_{c_1} \ldots \partial y_{c_u}} + \frac{\partial H^{(r)}}{\partial y_{k_1+n}} \frac{\partial^{u+1} H^{(s)}}{\partial y_{k_1} \partial y_{c_1} \ldots \partial y_{c_u}} \right)$$

$$\sum_{\substack{l(\beta_1)+\cdots+l(\beta_u)=l-2 \\ (\alpha-)-\in\Lambda_{\beta_1,\ldots,\beta_u}}} (J^{-1}\nabla G^3_{\beta_1})_{c_1} \ldots (J^{-1}\nabla G^3_{\beta_u})_{c_u}$$

$$+ \sum_{i=2}^{l-2} \sum_{j=1}^{l-i-1} \sum_{u=1}^{j} \frac{1}{2^{u+i}(i-1)! u!} \sum_{k_1=1}^{n} \sum_{\substack{k_2,\ldots,k_i=1 \\ c_1,\ldots,c_u=1}}^{n} \left(-\frac{\partial^i H^{(r)}}{\partial y_{k_1} \ldots \partial y_{k_i}} \frac{\partial^{u+1} H^{(s)}}{\partial y_{k_1+n} \partial y_{c_1} \ldots \partial y_{c_u}} \right.$$

$$\left. + \frac{\partial^i H^{(r)}}{\partial y_{k_1+n} \ldots \partial y_{k_i}} \frac{\partial^{u+1} H^{(s)}}{\partial y_{k_1} \partial y_{c_1} \ldots \partial y_{c_u}} \right) \sum_{\substack{l(\alpha_2)+\cdots+l(\alpha_i)=l-2-j, \\ l(\alpha_1)=j, \quad (\alpha-)-\in\Lambda_{\alpha_1,\ldots,\alpha_i}}} (J^{-1}\nabla G^3_{\alpha_2})_{k_2} \ldots (J^{-1}\nabla G^3_{\alpha_i})_{k_i}$$

$$\sum_{\substack{l(\beta_1)+\cdots+l(\beta_u)=j \\ \alpha_1\in\Lambda_{\beta_1,\ldots,\beta_u}}} (J^{-1}\nabla G^3_{\beta_1})_{c_1} \ldots (J^{-1}\nabla G^3_{\beta_u})_{c_u}$$

Introducing new summation indexes $j = i - 1$ for the first term, and $v = i + u - 1$ for

the last term and using $\Lambda_{\alpha_1,\alpha_2} = \Lambda_{\alpha_2,\alpha_1}$, we obtain

$$T_2 = \sum_{j=1}^{l-2} \frac{1}{2^{j+1} j!} \sum_{k1=1}^{n} \sum_{c_1,\ldots,c_j=1}^{2n} \left(-\frac{\partial^j H^{(r)}}{\partial y_{k_1} \ldots \partial y_{c_j}} \frac{\partial H^{(s)}}{\partial y_{k_1+n}} + \frac{\partial^j H^{(r)}}{\partial y_{k_1+n} \ldots \partial y_{c_j}} \frac{\partial H^{(s)}}{\partial y_{k_1}} \right)$$

$$\sum_{\substack{l(\alpha_1)+\cdots+l(\alpha_j)=l-2 \\ (\alpha-)-\in\Lambda_{\alpha_1,\ldots,\alpha_j}}} (J^{-1}\nabla G^3_{\alpha_1})_{c_1} \ldots (J^{-1}\nabla G^3_{\alpha_j})_{c_j}$$

$$+ \sum_{u=1}^{l-2} \frac{1}{2^{u+1} u!} \sum_{k_1=1}^{n} \sum_{c_1,\ldots,c_u=1}^{n} \left(-\frac{\partial H^{(r)}}{\partial y_{k_1}} \frac{\partial^{u+1} H^{(s)}}{\partial y_{k_1+n} \partial y_{c_1} \ldots \partial y_{c_u}} + \frac{\partial H^{(r)}}{\partial y_{k_1+n}} \frac{\partial^{u+1} H^{(s)}}{\partial y_{k_1} \partial y_{c_1} \ldots \partial y_{c_u}} \right)$$

$$\sum_{\substack{l(\beta_1)+\cdots+l(\beta_u)=l-2 \\ (\alpha-)-\in\Lambda_{\beta_1,\ldots,\beta_u}}} (J^{-1}\nabla G^3_{\beta_1})_{c_1} \ldots (J^{-1}\nabla G^3_{\beta_u})_{c_u}$$

$$+ \sum_{v=2}^{l-2} \sum_{i=2}^{v} \frac{1}{2^{v+1}(i-1)!(v-i+1)!} \sum_{k_1=1}^{n} \sum_{j_1,\ldots,j_v=1}^{2n} \left(-\frac{\partial^i H^{(r)}}{\partial y_{k_1} \partial y_{j_1} \ldots \partial y_{j_{i-1}}} \frac{\partial^{v+2-i} H^{(s)}}{\partial y_{k_1+n} \partial y_{j_i} \ldots \partial y_{j_v}} \right.$$

$$\left. + \frac{\partial^i H^{(r)}}{\partial y_{k_1+n} \partial y_{j_1} \ldots \partial y_{j_{i-1}}} \frac{\partial^{v+2-i} H^{(s)}}{\partial y_{k_1} \partial y_{j_i} \ldots \partial y_{j_v}} \right) \sum_{\substack{l(\gamma_1)+\cdots+l(\gamma_v)=l-2 \\ (\alpha-)-\in\Lambda_{\gamma_1,\ldots,\gamma_v}}} (J^{-1}\nabla G^3_{\gamma_1})_{j_1} \cdots (J^{-1}\nabla G^3_{\gamma_v})_{j_v}$$

Notice that $T_2 = 0$ because $\frac{\partial H^{(r)}}{\partial y_{k_1}} \frac{\partial H^{(s)}}{\partial y_{k_1+n}} = \frac{\partial H^{(r)}}{\partial y_{k_1+n}} \frac{\partial H^{(s)}}{\partial y_{k_1}}$ for any $k_1 = 1, \ldots, n$ and T_2 can be expressed as follows

$$T_2 = \sum_{v=1}^{l-2} \frac{1}{2^{v+1} v!} \sum_{k_1=1}^{n} \sum_{j_1,\ldots,j_v=1}^{2n} \frac{\partial^v}{\partial y_{j_1} \cdots \partial y_{j_v}} \left(-\frac{\partial H^{(r)}}{\partial y_{k_1}} \frac{\partial H^{(s)}}{\partial y_{k_1+n}} + \frac{\partial H^{(r)}}{\partial y_{k_1+n}} \frac{\partial H^{(s)}}{\partial y_{k_1}} \right)$$

$$\sum_{\substack{l(\gamma_1)+\cdots+l(\gamma_v)=l-2 \\ (\alpha-)-\in\Lambda_{\gamma_1,\ldots,\gamma_v}}} (J^{-1}\nabla G^3_{\gamma_1})_{j_1} \cdots (J^{-1}\nabla G^3_{\gamma_v})_{j_v}$$

Thus $G^3_\alpha = T_1$ is symmetric with respect to s and r □

7.2 Symplectic schemes

We now use the generating function method and the special properties of the coefficients G^i_α, $i = 1, 2, 3$ to construct symplectic schemes for SHS preserving the Hamiltonian functions. Taking advantage of the invariance under permutations of the coefficients G^i_α, $i = 1, 2, 3$, we propose strong and weak symplectic schemes of relatively high order that are still computationally attractive.

7.2.1 Symplectic strong schemes

Let define $\mathcal{A}_\gamma = \{\alpha : l(\alpha) + n(\alpha) \leq 2\gamma\}$, where $n(\alpha)$ is the number of zero components of the multi-index α. Symplectic schemes that have mean square order of convergence k can be build using the equations (5.10)-(5.12) and truncations of the appropriate generating functions S^i_ω, $i = 1, 2, 3$, according to the indexes $\alpha \in \mathcal{A}_{2k}$. Since these schemes are implicit, the Stratonovich stochastic integrals should be approximated by bounded random variables ([5]).

In Chapter 6, we propose first order schemes for the SHS (5.1) based on truncations of the generating function S^i_ω, $i = 1, 3$, according to $\mathcal{A}_2$. To construct second order schemes, we use the following truncations according to $\mathcal{A}_4$:

$$\begin{aligned} S^i_\omega \approx\ & G^i_{(0)} J_{(0)} + \sum_{r=1}^{m} \left(G^i_{(r)} J_{(r)} + G^i_{(0,r)} J_{(0,r)} + G^i_{(r,0)} J_{(r,0)} \right) + G^i_{(0,0)} J_{(0,0)} \\ & + \sum_{r,j=1}^{m} G^i_{(r,j)} J_{(r,j)} + \sum_{r,j,k=1}^{m} G^i_{(r,j,k)} J_{(r,j,k)} + \sum_{r,j,k,s=1}^{m} G^i_{(r,j,k,s)} J_{(r,j,k,s)} \\ & + \sum_{r,j=1}^{m} \left(G^i_{(r,j,0)} J_{(r,j,0)} + G^i_{(0,r,j)} J_{(0,r,j)} + G^i_{(r,0,j)} J_{(r,0,j)} \right), \end{aligned} \tag{7.7}$$

for any $i = 1, 2, 3$.

Using (5.34) we obtain

$$J_{(0)}J_{(r)} = \sum_{\beta\in\Lambda_{(0),(r)}} J_\beta = J_{(0,r)} + J_{(r,0)} \tag{7.8}$$

$$J_{(0)}J_{(r,r)} = \sum_{\beta\in\Lambda_{(0),(r,r)}} J_\beta = J_{(0,r,r)} + J_{(r,r,0)} + J_{(r,0,r)} \tag{7.9}$$

$$J_{(0)}J_{(r)}J_{(j)} = \sum_{\beta\in\Lambda_{(0),(r),(j)}} J_\beta = J_{(0,r,j)} + \ldots + J_{(j,r,0)} \tag{7.10}$$

$$J_{(r)}J_{(j)} = \sum_{\beta\in\Lambda_{(r),(j)}} J_\beta = J_{(r,j)} + J_{(j,r)} \tag{7.11}$$

$$J_{(j)}J_{(r,r)} = \sum_{\beta\in\Lambda_{(j),(r,r)}} J_\beta = J_{(j,r,r)} + J_{(r,r,j)} + J_{(r,j,r)} \tag{7.12}$$

$$J_{(j)}J_{(0,0)} = \sum_{\beta\in\Lambda_{(j),(r,r)}} J_\beta = J_{(j,0,0)} + J_{(0,0,j)} + J_{(0,j,0)} \tag{7.13}$$

$$J_{(r,r)}J_{(j,j)} = \sum_{\beta\in\Lambda_{(r,r),(j,j)}} J_\beta = J_{(r,r,j,j)} + \ldots + J_{(j,j,r,r)} \tag{7.14}$$

$$J_{(j)}J_{(r,r,r)} = \sum_{\beta\in\Lambda_{(j),(r,r,r)}} J_\beta = J_{(j,r,r,r)} + J_{(r,r,j,r)} + J_{(r,j,r,r)} + J_{(r,r,r,j)} \tag{7.15}$$

$$J_{(k)}J_{(r)}J_{(j)} = \sum_{\beta\in\Lambda_{(k),(r),(j)}} J_\beta = J_{(k,r,j)} + \ldots + J_{(j,r,k)} \tag{7.16}$$

$$J_{(k)}J_{(j)}J_{(r,r)} = \sum_{\beta\in\Lambda_{(k),(j),(r,r)}} J_\beta = J_{(k,j,r,r)} + \ldots + J_{(r,j,k,r)} \tag{7.17}$$

$$J_{(s)}J_{(k)}J_{(r)}J_{(j)} = \sum_{\beta\in\Lambda_{(s),(k),(r),(j)}} J_\beta = J_{(s,k,r,j)} + \ldots + J_{(j,r,k,s)}, \tag{7.18}$$

for any distinct positive integers r, j, k, $s = 1, \ldots, m$. The previous equations and Propositions 7.1 and 7.2 give us the following truncations of the genrating functions

S^i_ω, $i = 1, 2, 3$:

$$
\begin{aligned}
S^i_\omega \approx\ & G^i_{(0)} J_{(0)} + \sum_{r=1}^{m} \left(G^i_{(r)} J_{(r)} + G^i_{(r,r)} J_{(r,r)} + G^i_{(0,r)} J_{(0)} J_{(r)} \right) \\
& + G^i_{(0,0)} J_{(0,0)} + \sum_{r=1}^{m} \left(G^i_{(r,r,0)} J_{(r,r)} J_{(0)} + G^i_{(r,r,r)} J_{(r,r,r)} + G^i_{(r,r,r,r)} J_{(r,r,r,r)} \right) \\
& + \sum_{r=1}^{m-1} \sum_{j=r+1}^{m} \left(G^i_{(r,j)} J_{(r)} J_{(j)} + G^i_{(r,r,j,j)} J_{(r,r,)} J_{(j,j)} + G^i_{(0,r,j)} J_{(0)} J_{(r)} J_{(j)} \right) \\
& + \sum_{r,j=1, r\neq j}^{m} \left(G^i_{(r,r,j)} J_{(r,r)} J_{(j)} + G^i_{(r,r,r,j)} J_{(r,r,r)} J_{(j)} \right) \\
& + \sum_{r=1}^{m-2} \sum_{j=r+1}^{m-1} \sum_{k=j+1}^{m} G^i_{(r,j,k)} J_{(r)} J_{(j)} J_{(k)} \\
& + \sum_{k=1}^{m-1} \sum_{j=k+1}^{m} \sum_{\substack{r=1, \\ r\neq k, r\neq j}}^{m} G^i_{(r,r,j,k)} J_{(r,r)} J_{(j)} J_{(k)} \\
& + \sum_{r=1}^{m-3} \sum_{j=r+1}^{m-2} \sum_{k=j+1}^{m-1} \sum_{s=k+1}^{m} G^i_{(r,j,k,s)} J_{(r)} J_{(j)} J_{(k)} J_{(s)}.
\end{aligned}
\tag{7.19}
$$

Notice that for SHS preserving Hamiltonian functions to construct second order symplectic schemes, we need to generate only the stochastic integrals $J_{(0)}$, $J_{(0,0)}$, $J_{(r)}$, $J_{(r,r)}$, $J_{(r,r,r)}$, and $J_{(r,r,r,r)}$, $r = 1, \ldots, m$. To ensure that these implicit schemes are well-defined, we proceed as in [5], and to generate the stochastic integrals , instead of the independent random variables $\xi(r) \sim N(0, 1)$, $r = 1, \ldots, m$, we use the bounded random variables $\xi_h(r)$:

$$
\xi_h(r) = \begin{cases} -\hat{A}_h & \text{if } \xi < -\hat{A}_h \\ \xi(r) & \text{if } |\xi| \leq \hat{A}_h \\ \hat{A}_h & \text{if } \xi > \hat{A}_h, \end{cases}
\tag{7.20}
$$

where $0 < h < 1$ is a small time step and $\hat{A}_h = 2\sqrt{2|\ln h|}$. Hence we use the following approximations for the stochastic integrals:

$$
\begin{aligned}
& J_{(0)} = h, \quad J_{(0,0)} = \frac{h^2}{2}, \quad J_{(r)} = \sqrt{h}\xi_h(r), \\
& J_{(r,r)} = \frac{h\xi_h^2(r)}{2}, \quad J_{(r,r,r)} = \frac{h^{3/2}\xi_h^3(r)}{6}, \quad J_{(r,r,r,r)} = \frac{h^2\xi_h^4(r)}{24}.
\end{aligned}
\tag{7.21}
$$

For example, for $m = 1$ (i.e. the SHS with one noise), using (5.10) and (7.19) we construct the symplectic mean square second-order scheme based on the truncation of the generating function S^1_ω:

$$\begin{aligned} P_i(k+1) &= P_i(k) - \Bigg(\frac{\partial G^1_{(0)}}{\partial Q_i} h + \frac{\partial G^1_{(1)}}{\partial Q_i} \sqrt{h}\xi_h + \frac{\partial G^1_{(0,0)}}{\partial Q_i} \frac{h^2}{2} + \frac{\partial G^1_{(1,1)}}{\partial Q_i} \frac{h\xi_h^2}{2} \\ &+ \frac{\partial G^1_{(1,0)}}{\partial Q_i} \xi_h h^{\frac{3}{2}} + \frac{\partial G^1_{(1,1,1)}}{\partial Q_i} \frac{h^{\frac{3}{2}}\xi_h^3}{6} + \frac{\partial G^1_{(1,1,0)}}{\partial Q_i} \frac{\xi_h^2 h^2}{2} + \frac{\partial G^1_{(1,1,1,1)}}{\partial Q_i} \frac{h^2\xi_h^4}{24} \Bigg) \\ Q_i(k+1) &= Q_i(k) + \Bigg(\frac{\partial G^1_{(0)}}{\partial P_i} h + \frac{\partial G^1_{(1)}}{\partial P_i} \sqrt{h}\xi_h + \frac{\partial G^1_{(0,0)}}{\partial P_i} \frac{h^2}{2} + \frac{\partial G^1_{(1,1)}}{\partial P_i} \frac{h\xi_h^2}{2} \\ &+ \frac{\partial G^1_{(1,0)}}{\partial P_i} \xi_h h^{\frac{3}{2}} + \frac{\partial G^1_{(1,1,1)}}{\partial P_i} \frac{h^{\frac{3}{2}}\xi_h^3}{6} + \frac{\partial G^1_{(1,1,0)}}{\partial P_i} \frac{\xi_h^2 h^2}{2} + \frac{\partial G^1_{(1,1,1,1)}}{\partial P_i} \frac{h^2\xi_h^4}{24} \Bigg), \end{aligned} \tag{7.22}$$

where everywhere the arguments are $(P(k+1), Q(k))$, and the random variables ξ_h are generated independently at each step k according to (7.20).

For the coefficients of S^3_ω, a simple calculation shows that $G^3_{(r_1,r_2)} = 0$ for any $r_1, r_2 = 0, 1$ and $G^3_{(1,1,1,1)} = 0$. Hence using (5.12), when $m = 1$ the second order midpoint symplectic scheme is given by

$$\begin{aligned} Y_{k+1} &= Y_k + J^{-1}\nabla G^3_{(0)}(Y_{k+\frac{1}{2}})h + J^{-1}\nabla G^3_{(1)}(Y_{k+\frac{1}{2}})\sqrt{h}\xi_h \\ &+ J^{-1}\nabla G^3_{(1,1,1)}(Y_{k+\frac{1}{2}})\frac{h^{\frac{3}{2}}\xi_h^3}{6} + J^{-1}\nabla G^3_{(1,1,0)}(Y_{k+\frac{1}{2}})\frac{\xi_h^2 h^2}{2} \end{aligned} \tag{7.23}$$

where $Y_{k+\frac{1}{2}} = (Y_{k+1} + Y_k)/2$, and the random variables ξ_h are generated independently at each step k according to (7.20).

Since the schemes (7.22) and (7.23) are based on generating functions, we can easily proved that they are symplectic (see also the proof of Theorem 3.1 in [5]). Analogously with Theorem 5.16 in Chapter 5, the convergence with mean square order two can be proved under appropriate conditions using repeated Taylor expansions and Theorem 1.1 in [3].

7.2.2 Weak schemes

To obtain an k order symplectic weak scheme, we replace in (5.24) the Stratonovich integrals J_α by Ito integrals using the Eq. (6.2), and we truncate the series to include

only Ito integrals with multi-indexes α such that $l(\alpha) \leq k$, $k = 1, 2, 3$. Replacing in (6.2) we get $J_{(0)} = I_{(0)}$, $J_{(i)} = I_{(i)}$, $J_{(0,0)} = I_{(0,0)}$, $J_{(0,i)} = I_{(0,i)}$, $J_{(i,0)} = I_{(i,0)}$, $J_{(i,0,j)} = I_{(i,0,j)}$, $J_{(i,0,i)} = I_{(i,0,i)}$, $J_{(i,j)} = I_{(i,j)}$, $J_{(k,0,0)} = I_{(k,0,0)}$, $J_{(0,k,0)} = I_{(0,k,0)}$, $J_{(0,0,k)} = I_{(0,0,k)}$, $J_{(i,j,i)} = I_{(i,j,i)}$

$$\begin{aligned}
&J_{(i,i)} = I_{(i,i)} + \frac{1}{2} I_{(0)}, \quad J_{(i,i,j)} = I_{(i,i,j)} + \frac{1}{2} I_{(0,j)} \\
&J_{(j,i,i)} = I_{j,i,i)} + \frac{1}{2} I_{(j,0)}, \quad J_{(i,i,0)} = I_{(i,i,0)} + \frac{1}{2} I_{(0,0)}, \\
&J_{(0,i,i)} = I_{(0,i,i)} + \frac{1}{2} I_{(0,0)}, \quad J_{(i,i,i)} = I_{(i,i,i)} + \frac{1}{2} \left(I_{(0,i)} + I_{(i,0)} \right) \\
&J_{(i,i,j,j)} = I_{(i,i,j,j)} + \frac{1}{2} \left(I_{(0,j,j)} + I_{(i,i,0)} \right) + \frac{1}{4} I_{(0,0)}, \\
&J_{(i,i,i,i)} = I_{(i,i,i,i)} + \frac{1}{2} \left(I_{(0,i,i)} + I_{(i,0,i)} + I_{(i,i,0)} \right) + \frac{1}{4} I_{(0,0)},
\end{aligned} \tag{7.24}$$

for any $i \neq j$, $i, j = 1, \ldots, d$. Thus, for a second order weak scheme we use the following approximation for the generating functions S^i_ω, $i = 1, 2, 3$:

$$\begin{aligned}
\bar{S}^i_\omega = &\left(G^i_{(0)} + \frac{1}{2} \sum_{k=1}^{d} G^i_{(k,k)} \right) I_{(0)} + \sum_{k=1}^{d} G^i_{(k)} I_{(k)} \\
&+ \left(G^i_{(0,0)} + \frac{1}{2} \sum_{k=1}^{d} (G^i_{(k,k,0)} + G^i_{(0,k,k)}) + \frac{1}{4} \sum_{k,j=1}^{d} G^i_{(k,k,j,j)} \right) I_{(0,0)} \\
&+ \sum_{k=1}^{d} \left(\left(G^i_{(0,k)} + \frac{1}{2} \sum_{j=1}^{d} G^i_{(j,j,k)} \right) I_{(0,k)} + \left(G^i_{(k,0)} + \frac{1}{2} \sum_{j=1}^{d} G^i_{(k,j,j)} \right) I_{(k,0)} \right) \\
&+ \sum_{j,k=1}^{d} G^i_{(j,k)} I_{(j,k)}.
\end{aligned} \tag{7.25}$$

Using Propositions 7.1 and 7.2 and equations (7.8), (7.11), we get:

$$\begin{aligned}
\bar{S}^i_\omega = &\left(G^i_{(0)} + \frac{1}{2} \sum_{k=1}^{m} G^i_{(k,k)} \right) I_{(0)} + \sum_{k=1}^{m} G^i_{(k)} I_{(k)} \\
&+ \left(G^i_{(0,0)} + \sum_{k=1}^{m} \left(G^i_{(k,k,0)} + \frac{1}{4} G^i_{(k,k,k,k)} \right) + \frac{1}{2} \sum_{k=1}^{m} \sum_{j=k+1}^{m} G^i_{(k,k,j,j)} \right) I_{(0,0)} \\
&+ \sum_{k=1}^{m} \left(G^i_{(0,k)} + \frac{1}{2} \sum_{j=1}^{m} G^i_{(j,j,k)} \right) I_{(0)} I_{(k)} + \sum_{k=1}^{m} G^i_{(k,k)} I_{(k,k)} \\
&+ \sum_{k=1}^{m} \sum_{j=k+1}^{m} G^i_{(k,j)} I_{(k)} I_{(j)}.
\end{aligned} \tag{7.26}$$

For a weak scheme, we can generate the noise increments more efficiently than for a strong scheme. Hence proceeding as in section 14.2 of [1] to simulate the stochastic integrals $I_{(k)}$, $k = 1, \ldots, d$, at each time step, we generate independent random variable $\sqrt{h}\zeta_k$, $k = 1, \ldots, d$, with the following discrete distribution

$$P(\zeta_k = \pm\sqrt{3}) = \frac{1}{6}, \quad P(\zeta_k = 0) = \frac{2}{3}. \tag{7.27}$$

The moments of ζ_k are equal up to order 5 with the moments of the normal distribution $N(0,1)$, so we obtain the scheme based on S^1_ω:

$$\begin{aligned}
\bar{P}_i &= p_i - h\frac{\partial G^1_{(0)}}{\partial q_i} - h^{1/2}\sum_{k=1}^m \zeta_k \frac{\partial G^1_{(k)}}{\partial q_i} - \frac{h^2}{2}\Bigg(\frac{\partial G^1_{(0,0)}}{\partial q_i} \\
&+ \sum_{k=1}^m \left(\frac{\partial G^1_{(k,k,0)}}{\partial q_i} + \frac{1}{4}\frac{\partial G^1_{(k,k,k,k)}}{\partial q_i}\right) + \frac{1}{2}\sum_{k=1}^{m-1}\sum_{j=k+1}^m \frac{\partial G^1_{(k,k,j,j)}}{\partial q_i}\Bigg) \\
&- \frac{h}{2}\sum_{k=1}^m \zeta_k^2 \frac{\partial G^1_{(k,k)}}{\partial q_i} - \frac{h}{2}\sum_{k=1}^m\sum_{j=k+1}^m \frac{\partial G^1_{(k,j)}}{\partial q_i}\zeta_k\zeta_j \\
&- h^{3/2}\sum_{k=1}^m \zeta_k\left(\frac{\partial G^1_{(0,k)}}{\partial q_i} + \frac{1}{2}\sum_{j=1}^m \frac{\partial G^1_{(j,j,k)}}{\partial q_i}\right), \\
\bar{Q}_i &= q_i + h\frac{\partial G^1_{(0)}}{\partial p_i} + h^{1/2}\sum_{k=1}^m \zeta_k \frac{\partial G^1_{(k)}}{\partial p_i} + \frac{h^2}{2}\Bigg(\frac{\partial G^1_{(0,0)}}{\partial p_i} \\
&+ \sum_{k=1}^m \left(\frac{\partial G^1_{(k,k,0)}}{\partial p_i} + \frac{1}{4}\frac{\partial G^1_{(k,k,k,k)}}{\partial p_i}\right) + \frac{1}{2}\sum_{k=1}^{m-1}\sum_{j=k+1}^m \frac{\partial G^1_{(k,k,j,j)}}{\partial p_i}\Bigg) \\
&+ \frac{h}{2}\sum_{k=1}^m \zeta_k^2 \frac{\partial G^1_{(k,k)}}{\partial p_i} + \frac{h}{2}\sum_{k=1}^m\sum_{j=k+1}^m \frac{\partial G^1_{(k,j)}}{\partial p_i}\zeta_k\zeta_j \\
&+ h^{3/2}\sum_{k=1}^m \zeta_k\left(\frac{\partial G^1_{(0,k)}}{\partial p_i} + \frac{1}{2}\sum_{j=1}^m \frac{\partial G^1_{(j,j,k)}}{\partial p_i}\right),
\end{aligned} \tag{7.28}$$

where $i = 1, \ldots, n$, and everywhere the arguments are $(\bar{P}, q)$. In Theorem 6.3 in Chapter 6 we prove that the scheme based on the one step approximation (7.28) is symplectic and of weak order two.

Similarly we can construct symplectic schemes of weak order three based on the

following approximations of the generating functions S^i_ω, $i = 1, 2, 3$:

$$
\begin{aligned}
S^i_\omega \approx & \left(G^i_{(0)} + \frac{1}{2}\sum_{k=1}^{m} G^i_{(k,k)} \right) I_{(0)} + \Bigg(G^i_{(0,0)} + \frac{1}{2}\sum_{k=1}^{m} (G^i_{(k,k,0)} + G^i_{(0,k,k)}) \\
& + \frac{1}{4}\sum_{k,j=1}^{m} G^i_{(k,k,j,j)} \Bigg) I_{(0,0)} + \sum_{k=1}^{m} \Bigg(\left(G^i_{(0,k)} + \frac{1}{2}\sum_{j=1}^{m} G^i_{(j,j,k)} \right) I_{(0,k)} \\
& + \left(G^i_{(k,0)} + \sum_{j=1}^{m} \frac{1}{2} G^i_{(k,j,j)} \right) I_{(k,0)} \Bigg) + \sum_{k=1}^{m} G^i_{(k)} I_{(k)} \\
& + \sum_{k,j=1}^{m} G^i_{(k,j)} I_{(k,j)} + \Bigg(G^i_{(0,0,0)} + \frac{1}{2}\sum_{k=1}^{m} \left(G^i_{(k,k,0,0)} + G^i_{(0,k,k,0)} + G^i_{(0,0,k,k)} \right) \\
& + \frac{1}{4}\sum_{k,j=1}^{m} \left(G^i_{(k,k,j,j,0)} + G^i_{(0,k,k,j,j)} + G^i_{(k,k,0,j,j)} \right) + \frac{1}{8}\sum_{k,j,l=1}^{m} G^i_{(k,k,j,j,l,l)} \Bigg) I_{(0,0,0)} \\
& + \sum_{k=1}^{m} \Bigg(G^i_{(0,0,k)} + \frac{1}{2}\sum_{j=1}^{m} \left(G^i_{(j,j,0,k)} + G^i_{(0,j,j,k)} \right) + \frac{1}{4}\sum_{j,l=1}^{m} G^i_{(j,j,l,l,k)} \Bigg) I_{(0,0,k)} \\
& + \sum_{k=1}^{m} \Bigg(G^i_{(0,k,0)} + \frac{1}{2}\sum_{j=1}^{m} \left(G^i_{(j,j,k,0)} + G^i_{(0,k,j,j)} \right) + \frac{1}{4}\sum_{j,l=1}^{m} G^i_{(j,j,k,l,l)} \Bigg) I_{(0,k,0)} \\
& + \sum_{k=1}^{m} \Bigg(G^i_{(k,0,0)} + \frac{1}{2}\sum_{j=1}^{m} \left(G^i_{(k,j,j,0)} + G^i_{(k,0,j,j)} \right) + \frac{1}{4}\sum_{j,l=1}^{m} G^i_{(k,j,j,l,l)} \Bigg) I_{(k,0,0)} \\
& + \sum_{k,j=1}^{m} \Bigg(\left(G^i_{(k,j,0)} + \frac{1}{2}\sum_{l=1}^{m} G^i_{(k,j,l,l)} \right) I_{(k,j,0)} + \left(G^i_{(0,k,j)} + \frac{1}{2}\sum_{l=1}^{m} G^i_{(l,l,k,j)} \right) I_{(0,k,j)} \\
& + \left(G^i_{(k,0,j)} + \frac{1}{2}\sum_{l=1}^{m} G^i_{(k,l,l,j)} \right) I_{(k,0,j)} \Bigg) + \sum_{k,j,l=1}^{m} G^i_{(k,j,l)} I_{(k,j,l)},
\end{aligned}
$$

where everywhere the arguments are (P, q). Using Propositions 7.1 and 7.2, equations

(7.8)- (7.13), (7.16) and (7.24), the previous approximation becomes

$$
\begin{aligned}
\bar{S}^i_\omega \approx & \left(G^i_{(0)} + \frac{1}{2}\sum_{k=1}^m G^i_{(k,k)} \right) I_{(0)} + \sum_{k=1}^m G^i_{(k)} I_{(k)} \\
& + \left(G^i_{(0,0)} + \sum_{k=1}^m \left(G^i_{(k,k,0)} + \frac{1}{4} G^i_{(k,k,k,k)} \right) + \frac{1}{2}\sum_{k=1}^m \sum_{j=k+1}^m G^i_{(k,k,j,j)} \right) I_{(0,0)} \\
& + \sum_{k=1}^m \left(G^i_{(0,k)} + \frac{1}{2}\sum_{j=1}^m G^i_{(j,j,k)} \right) I_{(0)} I_{(k)} + \sum_{k=1}^m G^i_{(k,k)} I_{(k,k)} \\
& + \sum_{k=1}^m \sum_{j=k+1}^m G^i_{(k,j)} I_{(k)} I_{(j)} + \left(G^i_{(0,0,0)} + \frac{3}{2}\sum_{k=1}^m G^i_{(k,k,0,0)} \right. \\
& \left. + \frac{3}{4}\sum_{k,j=1}^m G^i_{(k,k,j,j,0)} + \frac{1}{8}\sum_{k,j,l=1}^m G^i_{(k,k,j,j,l,l)} \right) I_{(0,0,0)} \\
& + \sum_{k=1}^m \left(G^i_{(0,0,k)} + \sum_{j=1}^m G^i_{(j,j,0,k)} + \frac{1}{4}\sum_{j,l=1}^m G^i_{(j,j,l,l,k)} \right) I_{(0,0)} I_{(k)} \\
& + \sum_{k=1}^{m-1} \sum_{j=k+1}^m \left(G^i_{(k,j,0)} + \frac{1}{2}\sum_{l=1}^m G^i_{(k,j,l,l)} \right) I_{(k)} I_{(j)} I_{(0)} \\
& + \sum_{k=1}^m \left(G^i_{(k,k,0)} + \frac{1}{2}\sum_{l=1}^m G^i_{(k,k,l,l)} \right) \left(I_{(k,k)} I_{(0)} + I_{(0,0)} \right) \\
& + \sum_{k=1}^{m-2} \sum_{j=k+1}^{m-1} \sum_{l=j+1}^m G^i_{(k,j,l)} I_{(k)} I_{(j)} I_{(l)} + \sum_{k=1}^m G^i_{(k,k,k)} I_{(k,k,k)} \\
& + \sum_{k=1}^{m-1} \sum_{j=k+1}^m G^i_{(k,k,j)} \left(I_{(k,k)} I_{(j)} + \frac{1}{2} I_{(k)} I_{(j)} \right).
\end{aligned}
\tag{7.29}
$$

We can obtain third order symplectic weak schemes based on one of the equations (5.10)-(5.12) and the approximation (7.29) of the corresponding generating functions S^i_ω, $i = 1, 2, 3$. At each time step, we generate the stochastic integrals $I_{(k)}$, $k = 1, \ldots, m$, as independent random variable $\sqrt{h}\xi_k$, $k = 1, \ldots, m$, with the following discrete distribution (see the scheme (10.36) in [3])

$$
P(\xi_k = 0) = \frac{1}{3}, \quad P(\xi_k = \pm 1) = \frac{3}{10}, \quad P(\xi_k = \pm\sqrt{6}) = \frac{1}{30}, \tag{7.30}
$$

$I_{(k,k)}$, as $h\xi_k^2/2$, and $I_{(k,k,k)}$, as $h\sqrt{h}\xi_k^3/6$, $k = 1, \ldots, m$. Under appropriate assumptions regarding the functions $H^{(r)}$, $r = 0, \ldots, r$ we can prove the convergence of the schemes

with weak order three proceeding as in Theorem 6.3, using Theorem 4.1 in [4] and repeated Taylor expansions.

7.3 Numerical simulation

Consider the Kubo oscillator as follows

$$\begin{aligned} dP &= -aQdt - \sigma Q \circ dw_t^1, \quad P(0) = p, \\ dQ &= aPdt + \sigma P \circ dw_t^2, \quad Q(0) = q. \end{aligned} \tag{7.31}$$

As the Poisson bracket of the Hamiltonian functions $H^{(0)}$ and $H^{(1)}$ vanish, $H^{(0)}$ and $H^{(1)}$ conserve along the phase flow of the systems. Because the superior performance of symplectic schemes on long term simulation is shown in previous chapter, we only consider five types of stochastic strong symplectic schemes, such as the mean square 0.5, first and second order schemes based on S_ω^1, and the mean square first- and second-order schemes based on S_ω^3, and we compare that efficiency.

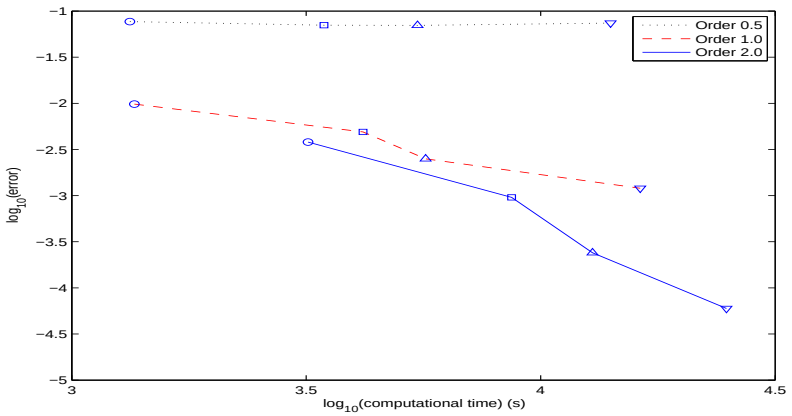

Figure 38: Computing time v.s. error for different types of symplectic strong S_ω^1 scheme with various time step for $T = 100$ with 10^5 samples, ◯: $h = 0.004$; □: $h = 0.002$; △: $h = 0.001$, ▽: $h = 0.0005$.

Fig. 38 and Fig. 39 show that the higher order strong schemes are more efficient than the lower ones. The computing time takes about 4180 seconds to complete the

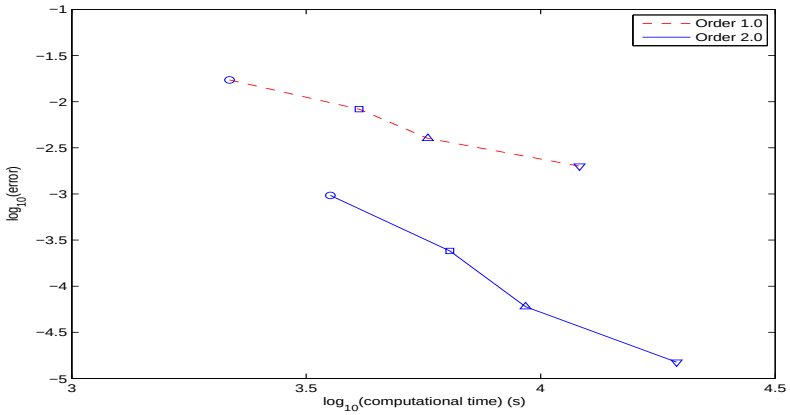

Figure 39: Computing time v.s. Error for different types of symplectic strong S^3_ω scheme with various time step for $T = 100$ with 10^5 samples, ◯: $h = 0.004$; □: $h = 0.002$; △: $h = 0.001$, ▽: $h = 0.0005$

first order S^1_ω schemes simulation for $h = 0.002$. The computing time for the second order S^1_ω schemes with time step $h = 0.004$ is about 3200 seconds. However, the error of second order S^1_ω schemes is 0.0038, compared to 0.0049, the error of first order S^1_ω scheme.

Bibliography

[1] P.E. Kloeden and E. Platen. *Numerical solutions of stochastic differential equations*. Springer-Verlag, Berlin, 1992.

[2] Joan-Andreu Lázaro-Camí and Juan-Pablo Ortega. Stochastic hamiltonian dynamical systems. *Reports on Mathematical Physics*, 61(1):65 – 122, 2008.

[3] G. N. Milstein. *Numerical Integration of Stochastic Differential Equations*. Kluwer Academic Publishers, 1995.

[4] G. N. Milstein and M. V. Tretyakov. Quasi-symplectic methods for langevin-type equations. *IMA Journal of Numerical Analysis*, (23):593–626, 2003.

[5] G. N. Milstein, M. V. Tretyakov, and Y. M. Repin. Numerical methods for stochastic systems preserving symplectic structure. *SIAM Journal on Numerical Analysis*, 40:1583–1604, 2002.

Chapter 8

Summary and Conclusion

In this thesis, the effect of noise on dynamical systems is considered. In the first part of this study, we investigate the effect of uncertainties in the parameters of an aeroelastic system. The stochastic normal form is applied to study the aeroelastic system with uncertainties in the bifurcation parameter and the non-linear coefficients in the plunge and pitch. The stochastic normal form is capable of capturing the behavior of the limit cycle oscillation, and predict the influence of the noise with small intensity on the amplitudes and frequencies of the limit cycle oscillation. Moreover, unlike the deterministic case, the stochastic bifurcation analysis shows that a noise with small intensity and weak structural non-linearities may lead to divergent solutions.

As the stochastic normal form is a technique used to investigate the dynamical system with small random perturbation, another method, a stochastic collocation method, is proposed to study the behavior of aeroelastic system with noise with larger intensity. The stochastic collocation method is presented with particular attention given to the nonlinear phenomena in the Hopf and the secondary bifurcations in an aeroelastic system. Various types of interpolation schemes are examined to demonstrate the advantage of high order interpolation on the stochastic collocation method. A sparse grid and a dimension adaptive strategy are considered for the aeroelastic system with multidimensional random variables. The numerical results shows that the stochastic collocation method can provide an accurate prediction of the effect of uncertainties parameters on aeroelastic systems.

In the second part, we study the construction of symplectic schemes for stochastic Hamiltonian systems. First, a framework to derive high-order strong symplectic

schemes based on generating functions for stochastic Hamiltonian systems is proposed, and then, it is extended to derive the weak symplectic schemes. The theoretical convergence analysis is presented. Systemic construction of the stochastic symplectic schemes with arbitrary high order is important from the theoretical point of view. Regarding a practical implementation, for the high order (≥ 4) weak symplectic scheme, it is expected that the accuracy of the results will be influenced by the increasing variance. It is interesting to notice that for stochastic Hamiltonian systems preserving Hamiltonian functions, the high order symplectic schemes turn out to have simpler forms and without requiring the approximation of more multiple stochastic integrals than the explicit Taylor expansion schemes. Numerical simulations are also reported, and they confirm the the superior performance of the symplectic schemes for long time simulation.

The superior performance of the symplecitc schemes has been reported for some non-Hamiltonian systems. In the future, it will be interest to investigate the application of stochastic symplectic schemes for the aeroelastic system with stochastic noise.